

DISS. ETH Nr. 26005

*Innovative strategies for the immunotherapy  
of liquid and solid tumors*

a thesis submitted to attain the degree of

DOCTOR OF SCIENCES of ETH Zurich

(Dr. sc. ETH Zurich)

presented by

*CORNELIA DEBORAH HUTMACHER-BERNDT*

*MSc Pharmaceutical Sciences, ETH Zurich*

born March 12, 1991

Citizen of Biberist (SO)

accepted on the recommendation of

*Prof. Dr. Dario Neri, examiner*

*Prof. Dr. Cornelia Halin, co-examiner*

2019



*To my beloved family*





## Index

<b>1. Summary</b>	<b>1</b>
<b>2. Zusammenfassung</b>	<b>3</b>
<b>3. Introduction</b>	<b>5</b>
<b>3.1. Antibody based tumor targeting</b>	<b>5</b>
3.1.1. Antibodies	5
3.1.1.1. Overview	5
3.1.1.2. Engineering antibodies for cancer therapy	5
3.1.1.3. Antibody structures and formats	8
3.1.1.4. Therapeutic antibodies and their mechanism of action	9
3.1.1.4.1. Naked antibodies	9
3.1.1.4.2. Armed antibodies	11
3.1.2. Immunocytokines	13
3.1.2.1. From cytokines to antibody-cytokine fusion proteins	14
3.1.2.2. Immunocytokine formats and molecular targets	16
3.1.2.3. Cytokine payloads for cancer therapy	20
3.1.2.4. Factors influencing the tumor targeting properties of immunocytokine products	21
3.1.2.5. Immunocytokines with promising preclinical results	23
3.1.2.6. Opportunities for combination therapy	33
3.1.2.7. Immunocytokines in clinical trials	36
3.1.2.8. Potential drawbacks of immunocytokines and possible strategies to minimize them	43
<b>3.2. Acute Myeloid Leukemia</b>	<b>45</b>
3.2.1. Leukemia overview	45
3.2.1.1. Disease and classification of AML	47
3.2.1.2. Treatment of AML	50
3.2.1.2.1. Induction therapy	51
3.2.1.2.2. Post-remission strategy	51
3.2.1.2.3. Alternative strategies and novel therapeutics	52
3.2.1.3. CD123 as a novel target for the treatment of AML	54
<b>3.3. Aim of the thesis</b>	<b>55</b>
<b>4. Results</b>	<b>58</b>
<b>4.1. F8-IL2 in combination with immune-check-point inhibitors</b>	<b>58</b>
4.1.1. Product characterization	58
4.1.2. Therapy experiments	59
4.1.3. Mechanistic studies	62
<b>4.2. Development of a novel fully-human anti-CD123 antibody to target acute myeloid leukemia</b>	<b>71</b>
4.2.1. Generation, affinity maturation and reformatting of fully-human antibodies against CD123	71
4.2.2. <i>In vitro</i> characterization of anti-leukemic activity of H9- and CSL362-based therapeutics	74
4.2.3. <i>In vitro</i> analysis of BiTE biocidal activity	78
<b>5. Discussion</b>	<b>80</b>
<b>5.1. F8-IL2 in combination with immune-check-point inhibitors</b>	<b>80</b>
<b>6.1. Development of a novel fully-human anti-CD123 antibody to target acute myeloid leukemia</b>	<b>84</b>
<b>7. Conclusions and outlook</b>	<b>86</b>
<b>8. Materials and methods</b>	<b>91</b>

<b>8.1.</b>	<b>F8-IL2 in combination with immune-check-point inhibitors .....</b>	<b>91</b>
8.1.1.	Cell lines, animals, and tumor models .....	91
8.1.2.	Antibodies for therapy experiments.....	92
8.1.3.	<i>In vitro</i> characterization of F8-IL2 .....	92
8.1.4.	Quantitative biodistribution study .....	93
8.1.5.	Therapy study and <i>in vivo</i> depletion of NK cells and CD4+ and CD8+ T cells .....	93
8.1.6.	Tumor re-challenge.....	94
8.1.7.	Immunohistochemical analysis of EDA expression in CT26 and MC38 tumors .....	94
8.1.8.	Flow cytometry .....	94
8.1.9.	Statistical analysis of murine tumor, lymph node, and spleen datasets .....	95
<b>8.2.</b>	<b>Development of a novel fully-human anti-CD123 antibody to target acute myeloid leukemia.....</b>	<b>96</b>
8.2.1.	Cell lines .....	96
8.2.2.	Cloning and expression of recombinant CD123.....	96
8.2.3.	Generation of a stable CD123 monoclonal cell line.....	96
8.2.4.	Selection of antibodies from the ETH-2 Gold library by phage display and affinity maturation ..	97
8.2.5.	Cloning of BiTE(H9/OKT3), BiTE (CSL362/OKT3) and the CSL362 antibody .....	97
8.2.6.	Expression of antibodies and antibody fragments .....	97
8.2.7.	Epitope mapping using peptide array.....	97
8.2.8.	Flow cytometry-based binding of H9 and CSL362 to stable CD123 monoclonal cell line.....	98
8.2.9.	Surface Plasmon Resonance .....	98
8.2.10.	ADCC potentiation .....	98
8.2.11.	Isolation of human peripheral blood mononuclear cells (PBMCs) .....	98
8.2.12.	ADCC assay on human cell lines.....	99
8.2.13.	ADCC assay on AML blasts .....	99
8.2.14.	<i>In vitro</i> BiTE-mediated T-cell killing of primary AML blast .....	100
<b>10.</b>	<b>Copyright.....</b>	<b>101</b>
<b>11.</b>	<b>List of abbreviations.....</b>	<b>102</b>
<b>12.</b>	<b>References.....</b>	<b>105</b>
<b>13.</b>	<b>Supplementary Information .....</b>	<b>150</b>
<b>13.1.</b>	<b>F8-IL2 in combination with immune check-point inhibitors .....</b>	<b>150</b>
13.1.1.	Microscopic analysis of EDA expression (green) on CT26 colon carcinoma .....	150
13.1.2.	Rechallenge tumor studies.....	151
13.1.3.	Multiparameter flowcytometric analysis of CT26 tumor immune cell infiltrates.....	152
13.1.4.	Multiparameter flowcytometric analysis of lymph nodes and intrasplenic immune cell infiltrates of CT26 colon carcinoma bearing mice.....	153
13.1.5.	Multiparameter flowcytometric analysis of MC38 tumor immune cell infiltrates .....	155
13.1.6.	Multiparameter flowcytometric analysis of lymph node immune cell infiltrates of MC38 colon carcinoma bearing mice .....	157
13.1.7.	Antibody clone list .....	159
<b>13.2.</b>	<b>Development of a novel fully-human anti-CD123 antibody to target acute myeloid leukemia.....</b>	<b>160</b>
13.2.1.	Expression and characterization of IgG1(CSL362), IgG1 <sup>pot</sup> (CSL362) and BiTE(CSL362/OKT3) .....	160
13.2.2.	Sequences of the parental anti CD123 scFv with the highest ELISA signal derived from phage display, the affinity matured scFv(H9), the IgG1(H9) and the IgG1 <sup>pot</sup> (H9) heavy and light chains .....	161
<b>14.</b>	<b>Acknowledgments .....</b>	<b>163</b>
<b>15.</b>	<b>Curriculum vitae .....</b>	<b>164</b>



## 1. Summary

Recombinant interleukin 2 (IL2) was the first cancer immunotherapeutic product approved by the FDA. IL2 can induce durable complete responses in patients with melanoma and renal cell carcinoma. The systemic administration of high dose IL2, however, may cause substantial toxicity which limits the use to a small cohort of patients. Antibody-IL2 fusion proteins may therefore be particularly attractive, as the selective localization of the cytokine at the site of disease leads to an increased therapeutic index. Our group has recently described F8-IL2, an antibody-IL2 fusion protein that targets the alternatively spliced extra-domain A (EDA) of fibronectin that is overexpressed in the majority of solid tumors and lymphoma and absent from healthy tissue. Recombinant IL2 has been studied in clinical trials in combination with a check-point inhibitor (ipilimumab) for the treatment of metastatic melanoma with encouraging results. Check-point inhibitors are foundational drugs that provide a clear benefit to patients, but cancer cures are still rare. In this thesis, we explored whether the targeted delivery of IL2 can boost the anticancer activity of immune check-point inhibitors in immunocompetent mouse models of cancer. The combination of F8-IL2 with CTLA-4 and PD-1 blockade was efficacious in the mouse, leading to cancer cures and protective immunity against subsequent tumor re-challenges. The combination with PD-L1 blockade was less efficacious. The results may depend, at least in part, on the choice of antibodies that were used. Additionally, we performed detailed high-parametric single-cell analysis of the tumor leukocyte composition in CT26 and MC38 models which revealed that the selective delivery of IL2 to the tumor resulted in profound changes in T and natural killer (NK) cell features in the tumor bed, without collateral immune activation in the systemic immune compartment. Lymphocyte depletion studies revealed the strict requirement for NK and CD8+ T cell activity, in order to achieve maximal therapeutic performance. The results support the use of targeted IL2 in combination with check-point inhibitors for cancer therapy in the clinics.

In spite of progress in the treatment of acute myeloid leukemia (AML), this cancer type remains potentially lethal for patients who are not eligible for or do not benefit from intensive chemotherapy or allogeneic hematopoietic stem cell transplantation (allo-HSCT). There is an urgent need to develop new therapeutic agents. Within this thesis, we have described the

generation and characterization of a fully-human monoclonal antibody specific to CD123, a surface marker which is overexpressed in a variety of hematological disorders, including acute myeloid leukemia. The antibody was affinity-matured and the Fc portion was engineered to display enhanced antibody-dependent cell-mediated cytotoxicity (ADCC). The antibody [termed IgG1<sup>pot</sup>(H9)] was slightly more potent for the selective killing of leukemic cells *in vitro* ADCC assays using cell lines, compared to a previously-described anti-CD123 antibody [IgG1<sup>pot</sup>(CSL362)]. The two antibodies recognize different epitopes on the surface of CD123. IgG1(CSL362) has an apparent K<sub>d</sub> of approximately 20 pM which is approximately 10-fold higher than the one of IgG1(H9). Both IgG1<sup>pot</sup>(H9) and IgG1<sup>pot</sup>(CSL362) were able to kill patient-derived AML blasts using purified allogeneic NK cells. Further, the two antibodies were reformatted as bispecific BiTE reagents by fusion with the anti-CD3 scFv(OKT3) antibody fragment. BiTE(CSL362/OKT3) exhibited a 10-fold higher potency in killing AML blasts compared to BiTE(H9/OKT3).

In summary, we have generated novel anti-CD123 biopharmaceuticals which have shown promising *in vitro* results that may be useful in the future for the treatment of AML. Moreover, we have shown that tumor targeting antibody-IL2 fusions may nicely synergize with immune check-point inhibitors.

## 2. Zusammenfassung

Rekombinantes Interleukin 2 (IL2) war das erste immunotheapeutische Produkt, welches von der FDA zugelassen wurde. IL2 kann vollständige Remissionen erzielen bei Patienten mit Melanoma und Nierenzellkarzinoma. Die systemische Administration von hoch dosiertem IL2 kann aber auch beträchtliche Nebenwirkungen haben, was den Gebrauch von IL2 auf eine kleine Patientenzahl beschränkt. Daher erscheinen Antikörper-IL2 Fusionsproteine attraktiv, weil die selektive Lokalisation von dem Zytokin am Ort der Erkrankung den therapeutischen Index erhöhen kann. Unsere Gruppe hat kürzlich F8-IL2 beschrieben, ein Antikörper-IL2 Fusionsprotein, welches eine alternative Spleissvariante von Fibronektion, die Extradomäne A (EDA), bindet. EDA ist überexprimiert in der Mehrheit von festen Tumoren und Lymphomen während es gleichzeitig im gesunden Gewebe nicht vorkommt. Rekombinantes IL2 wurde in Kombination mit Immun-Checkpoint-Inhibitoren in klinischen Studien untersucht bei Patienten mit metastasierendem Melanom – mit erfolgsversprechenden Resultaten. Checkpoint-Inhibitoren sind grundlegende Krebsmedikamente, von denen die Patienten klar profitieren. Allerdings ist die vollständige Krebsheilung noch immer selten. In dieser Arbeit haben wir in immunkompetenten Mäusen untersucht, ob die zielgerichtete Administration von IL2 die krebshemmende Wirkung von Immun-Checkpoint-Inhibitoren erhöhen kann. Die Kombination von F8-IL2 mit CTLA-4 und PD-1 Inhibitoren in Mäusen war effizient und führte zu anhaltender Heilung und einer protektiven Immunität gegenüber einer erneuten Tumorinjektion. Die Kombination mit einem PD-L1 Inhibitor hingegen war weniger erfolgreich. Die Resultate hängen mit hoher Wahrscheinlichkeit davon ab, welcher Antikörper gebraucht wurde. Zusätzlich haben wir eine detaillierte Multiparameter Einzelzellanalyse von intratumoralen Leukozyten gemacht. Dies hat ergeben, dass die zielgerichtete Administration von IL2 im Tumor zu tiefgründigen Veränderungen von T und natürlichen Killerzellen (NK) führte, ohne dass das systemische Immunsystem aktiviert wurde. Aus einer Studie mit Mäusen, in welchen selektiv Lymphozyten erschöpft wurden, geht hervor, dass NK und T Zellen für die maximale Wirkung der Kombination absolut notwendig sind. Die Resultate unterstützen den Gebrauch von zielgerichtetem IL2 in Kombination mit Checkpoint-Inhibitoren in der klinischen Krebstherapie.

Trotz dem Fortschritt in der Behandlung von akuter myeloischer Leukämie (AML) bleibt dieser Krebstyp potentiell tödlich für diejenigen Patienten, welche nicht für intensive Chemotherapie oder eine allogene Stammzelltransplantation in Frage kommen oder nicht davon profitieren. Die Entwicklung neuer Medikamente ist daher von grosser Bedeutung. In dieser Arbeit haben wir die Entwicklung und die Charakterisation von einem vollständig humanen Antikörper beschrieben, welcher spezifisch gegen CD123 gerichtet ist. CD123 ist ein Zelloberflächenmarker, der in einer Vielzahl von hämatologischen Erkrankungen inklusive AML überexprimiert ist. Die Affinität vom Antikörper wurde maturiert und das kristallisierbare Fragment so mutiert, dass es eine erhöhte antikörperabhängige zellvermittelte Zytotoxizität auslöst. Dieser Antikörper [nachfolgend genannt als IgG1<sup>pot</sup>(H9)] war ein bisschen potenter als ein zuvor beschriebener anti-CD123 Antikörper [IgG1<sup>pot</sup>(CSL362)] in der selektiven Tötung von Leukämie Zelllinien *in vitro*. Die zwei Antikörper erkennen zwei verschiedene Epitope von CD123. IgG1<sup>pot</sup>(CSL362) hat einen apparenten Dissoziationskonstanten von ungefähr 20 pM, was etwa 10-Mal höher ist als der von IgG1(H9). Beide Antikörper, IgG1<sup>pot</sup>(CSL362) und IgG1<sup>pot</sup>(H9), konnten die von Patienten stammende AML Blasten zerstören mithilfe von allogenen NK Zellen. Die zwei Antikörper wurden neu auch als bispezifische T-Zellen Antikörper (BiTE) formatiert mittels Fusion mit dem anti-CD3 einkettigen Antikörperfragment (OKT3). BiTE(CSL362/OKT3) war 10-Mal potenter in der Tötung von AML Blasten.

Zusammenfassend haben wir neue anti-CD123 biopharmazeutische Produkte entwickelt, die vielversprechende Resultate in *in vitro* zeigten und daher womöglich in der zukünftigen Behandlung von AML nützlich sein könnten. Ausserdem haben wir gezeigt, dass tumorspezifische Antikörper-IL2 Fusionsproteine möglicherweise sehr gut mit Immun-Checkpoint-Inhibitoren korrespondieren.

## 3. Introduction

### 3.1. Antibody based tumor targeting

#### 3.1.1. Antibodies

##### 3.1.1.1. Overview

Monoclonal antibodies are the most important class of biopharmaceuticals for the treatment of cancer and autoimmune diseases in terms of sales and numbers of products in development [1]. They can be raised against almost any antigen of interest and have been hailed as “magic bullets” for their high specificity [2]. Most approved antibodies correspond to intact immunoglobulin molecules. However, using genetic engineering, a variety of different antibody formats and conjugates have been designed, in order to tailor the product’s characteristics to the specific pharmaceutical need.

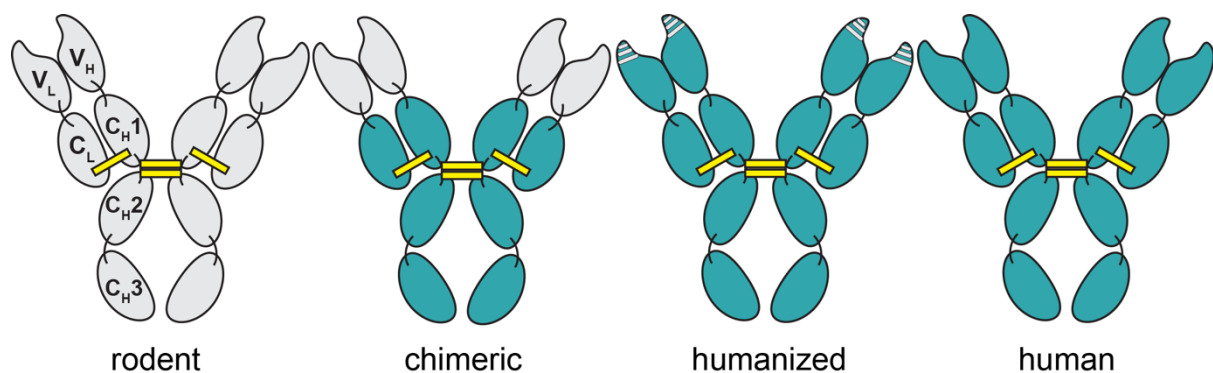
##### 3.1.1.2. Engineering antibodies for cancer therapy

The production of monoclonal antibodies with pre-defined specificity (mAb) roots in the hybridoma technology invented by Georges Köhler and César Milstein in 1975 [3]. Before 1975, it was impossible to produce monoclonal antibodies specific to an antigen of interest. Hybridoma technology involves the fusion of murine B cell clones with myeloma cells that have infinite proliferative capacity [3]. For the production of murine B cell clones, mice are immunized with an antigen of interest, their splenocytes extracted and immortalized through the fusion with myeloma cells [3]. After *in vitro* culturing, a selection is performed to yield those hybridoma clones with the highest selectivity and affinity [3]. This technology resulted in the approval of the first therapeutic mAb (an anti CD3 mAb, called muromonab) for preventing acute kidney transplant rejection by the FDA [4]. Although hybridoma technology revolutionized the field, the use of rodent antibodies in humans was hampered by immunogenicity. Mouse antibodies are recognized as non-self by the humane immune system which triggers the formation of human-anti-mouse antibodies (HAMAs) [5]. HAMAs can neutralize the therapeutic mAb and lead to the rapid clearance of the therapeutic mAb, thus narrowing their therapeutic window. More importantly, HAMAs can also stimulate the immune system which potentially results in anaphylactic reactions and serum sickness [6].



Moreover, human complement and Fc receptors do not bind the Fc part of murine IgGs thus murine IgGs cannot elicit Fc-dependent effector immune responses [7].

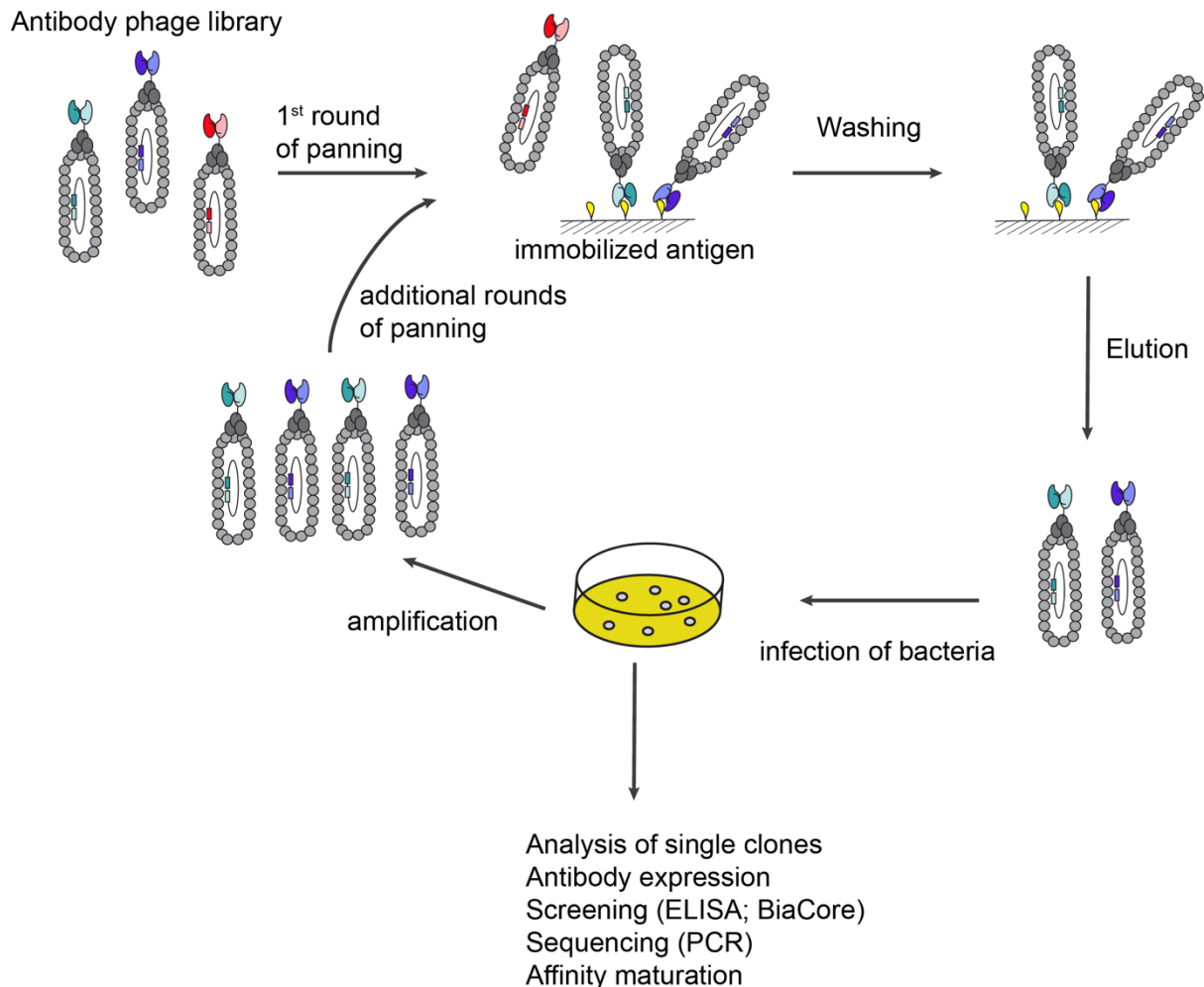
The clinical application of murine IgGs is limited and newer technologies aimed at reducing the immunogenicity of antibody products. Advances in genetic engineering led to the production of “chimeric antibodies”, which consist of human constant domains and mouse variable regions [Figure 1][8].



**Figure 1:** Humanization of monoclonal antibodies. Rodent domains are depicted in grey and human proteins in green. Chimeric mAbs consist of human constant domains ( $C_L$ ,  $C_{H1}$ ,  $C_{H2}$ ,  $C_{H3}$ ) and rodent variable regions ( $V_L$ ,  $V_H$ ). Humanized mAbs only contain the hypervariable regions that are of rodent origin whereas the rest is human.

Several chimeric antibodies have been approved by the FDA for the treatment of cancer and rheumatology diseases and are routinely used in the clinic [e.g., Rituximab (Rituxan<sup>®</sup>), Cetuximab (Erbix<sup>®</sup>)]. Although chimeric antibodies are less immunogenic than fully murine antibodies, human anti-chimeric antibody responses can also be observed [9–11]. Humanization of antibodies was achieved by grafting the antigen-specific complementarity determining regions (CDRs) of animal origin onto a human antibody scaffold [12]. CDR grafting technology was invented by Sir Gregory Winter and colleagues and led to the generation of many successful antibodies that are clinically used (e.g., Trastuzumab (Herceptin<sup>®</sup>), Alemtuzumab (Campath-1H<sup>®</sup>)). The development of antibody-phage display technology and transgenic mice that express human immunoglobulin genes (e.g., XenoMouse, UltiMAb, TC Mouse and KM-Mouse platform) finally allowed the production of fully-human antibodies [13–15]. The first human antibody ever approved by the FDA (adalimumab, an anti-TNF antibody) was generated by phage display technology. In phage display technology, a large

repertoire of human antigen-binding fragments are expressed on the surface of filamentous phages and screened for binding an antigen of interest [Figure 2]. The genetic information of the displayed antibody is encoded within the phages genome and can therefore be easily obtained. The best clones can then also be affinity matured [16,17].



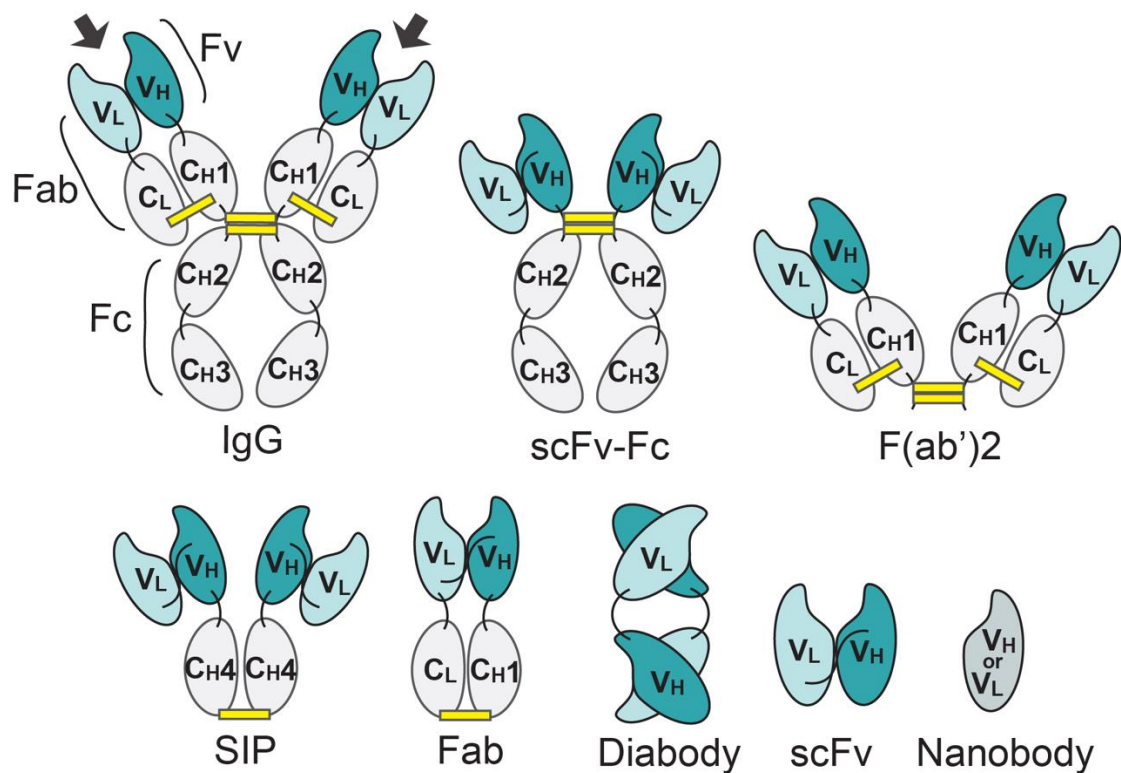
**Figure 2:** Workflow of Phage Display. Phage display relies on the possibility to display human antigen-binding fragments on the surface of filamentous phages. Large antibody phage libraries can be used to screen against virtually any antigen of interest (peptide/ protein). After washing, potential binders can be eluted and used to infect bacteria. Single clones can be picked and antibodies screened for their affinity. The best binders can be sequenced and affinity matured. Phages can also be amplified for additional rounds of panning.

Transgenic mice are immunized with the antigen of interest, their B cells harvested and used in traditional hybridoma technology (i.e., fused with an immortal myeloma cell line and screened subsequently). The first antibody generated with transgenic mice and approved by

the FDA, is Panitumumab (Vectibix®), an epidermal growth factor specific mAb for wild-type KRAS colorectal cancer [14].

### 3.1.1.3. Antibody structures and formats

An IgG molecule consists of two heavy and two light chains and forms a Y-shaped structure stabilized by disulfide bridges and non-covalent interactions [**Figure 3**][18]. The heavy chain is composed of 3 constant protein domains ( $C_{H1}$ ,  $C_{H2}$ ,  $C_{H3}$ ) and 1 variable domain ( $V_H$ ) whereas the light chain is composed of 1 constant domain ( $C_L$ ) only and 1 variable domain ( $V_L$ ). Each variable domain has 3 complementary determining regions (CDRs)[18]. The 3 CDRs of the light chain and the 3 CDRs of the heavy chain shape the antigen binding site (paratope)[18]. The fragment crystallizable (Fc) region of an IgG is formed by the constant domains of the heavy chains ( $2 \times C_{H2}-C_{H3}$ )[18]. The Fc region is not involved in antigen binding, but is responsible for the effector mechanisms of an IgG such as the antibody-cell-mediated cytotoxicity (ADCC) or the activation of the complement cascade that will be discussed in chapter 3.1.1.4.1 [18]. Additionally, the Fc region confers the long circulatory half-life to an IgG (in the range of ~21 days) by binding to the neonatal Fc receptor on endothelial cells and in the liver, rescuing the antibody from degradation [19]. For biotechnological applications, this long half-life of antibody products is not always desirable and antibody fragments can be designed that lack the Fc portion [such as the  $F(ab)_2$ , diabody, scFv, nanobody]. The smallest antibody format is the monomeric nanobody (i.e., a camel-derived single domain antibody). Smaller antibody fragments typically have a shorter half-life, but at the same time penetrate the tissue better than full IgGs [20]. Even though tissue penetration of small antibody fragments may be increased compared to intact immunoglobulins, rapid clearance and insufficient affinity may lead to a lower tumor uptake compared to full IgG molecules [21]. Especially diabodies display favorable properties. These bivalent products retain the avidity and long tumor residence time of the parental full IgG counterpart but are cleared more rapidly from the blood.



**Figure 3:** Schematic representation of antibody formats. *V<sub>H</sub>*: heavy chain variable domain. *V<sub>L</sub>*: light chain variable domain. *C*: constant domain of the heavy (*C<sub>H1-4</sub>*) and the light chain (*C<sub>L</sub>*). *SIP*: small immune protein that uses the  $\epsilon$ *CH<sub>4</sub>* domain of an IgE antibody. Minibodies (or SIPs) can also be constructed with the *CH<sub>3</sub>* domain of an IgG. Arrows indicate the site of antigen binding. Yellow bars: disulfide bridges. *Fc*: fragment crystallizable, *Fv*: fragment variable, *SIP*: small immunoprotein *Fab*: Fragment antigen binding. *scFv*: single chain variable fragment.

#### 3.1.1.4. Therapeutic antibodies and their mechanism of action

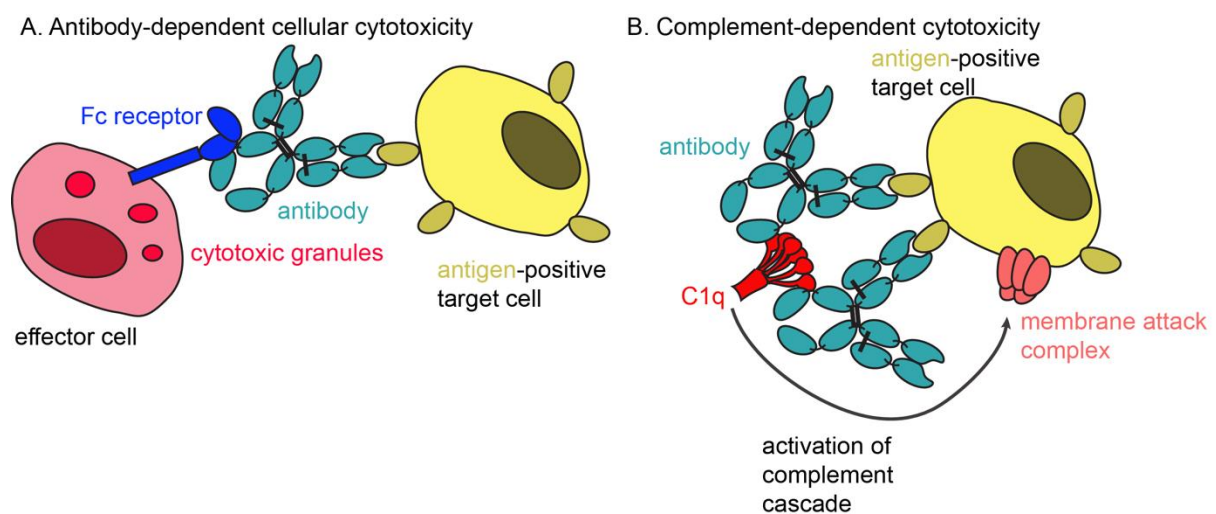
Therapeutic antibodies can be divided into “naked” and “armed” monoclonal antibodies. “Armed” antibodies are conjugated to other functional moieties whereas “naked” antibodies are solely composed of the antibody scaffold.

##### 3.1.1.4.1. Naked antibodies

“Naked” antibody products have a variety of functions. Firstly, they can be used to neutralize the activity of a target antigen. For example, Adalimumab (Humira) is an antibody that binds to tumor necrosis factor  $\alpha$  (TNF)[22]. Adalimumab dampens the immune response in a

variety of autoimmune disorders including rheumatoid arthritis. Secondly, antibodies can be designed to induce or inhibit a signaling event. Ipilimumab (Yervoy) binds to cytotoxic T-lymphocyte-associated protein 4 (CTLA-4, CD152), an inhibitory protein on the surface of T cells [23]. This interaction prevents binding of CD80 or CD86 on antigen-presenting cells to CTLA-4 which dampens the immune response[23]. Ipilimumab is used to activate the immune system in melanoma and renal cell carcinoma.

Antibodies can also be used to promote tumor cell killing by ADCC and CDC [Figure 4]. ADCC is triggered when natural killer cells (NK cells) or macrophages are recruited to an IgG-coated target cell by interaction of the antibody Fc portion with cognate Fc-gamma receptors [24]. This interaction triggers the NK cell to release perforin and granzymes which results in the death of the target cell [18]. The complement cascade may be activated, when C1q recognizes a high-local density of IgG molecules on a cell surface [18].



**Figure 4:** **A** Antibody-dependent cellular cytotoxicity. Effector cells such as NK cells bind to the Fc region of an antibody which coat the surface of an antigen-positive target cell. This triggers the effector cell to release cytotoxic granules that contain perforins and granzymes which result in the lysis of the target cell. **B** Complement-dependent cytotoxicity. The Fc portion of antibodies that coat the surface of an antigen-positive cell can also be recognized by proteins of the innate immune system (C1q). The binding activates the complement cascade that results in the formation of the cell-killing membrane attack complex.

The complement cascade promotes local inflammation and causes cell lysis [18]. Rituximab (Rituxan) is a monoclonal antibody that targets CD20 on the surface of B cells. Treatment with Rituximab results in the killing of B cells by ADCC, CDC and induction of apoptosis by CD20 cross-linking [25]. Rituximab is approved for the treatment of various B-cell non-Hodgkin's lymphomas, chronic lymphocytic leukemia, as well as certain autoimmune disorders, such as rheumatoid arthritis.

#### 3.1.1.4.2. Armed antibodies

Antibodies are ideal "vehicles" for the selective delivery of bioactive payloads to the tumor site sparing normal tissues. They can be used for the pharmacodelivery of radionuclides [Antibody Radionuclides conjugates (ARCs)], cytotoxic drugs [Antibody drug conjugates (ADCs)] and cytokines (Immunocytokines).

ARCs have a unique potential to be used simultaneously as imaging tools and therapeutics depending on the isotope. These products have been extensively studied and their limitations and potential explored. An attractive characteristic of ARCs is represented by the crossfire effect (i.e. the ability to damage cells adjacent to the target cell). In hematological malignancies, the use of radioimmunoconjugates has been successful and led to the approval of <sup>90</sup>Y-labelled ibritumomab-tiuxetan (Zevalin) and <sup>131</sup>I-labelled tositumomab (Bexxar) for the treatment of relapsed or refractory non-Hodgkin's lymphoma [26]. Typically, solid cancers have a higher intrinsic radio sensitivity than hematological cancers and many radioimmunoconjugates have failed to show success [27]. One major challenge is the large molecular size of an intact IgG that results in a long half-life and poor tumor-uptake [28]. In turn, the use of small antibody fragments with improved pharmacokinetics and enhanced tumor penetration is limited due to their short tumor residence time and suboptimal tumor uptake [28]. Moreover, an elevated interstitial fluid pressure and hypoxia of the tumor stroma as well as heterogenous antigen expression may hinder the successful delivery of the ARC [28]. In order to optimize the delivery of ARC, various biological modifiers are being used such as IL-2, TNF, VEGF and Platelet-derived growth factor inhibitors [28]. Biological modifiers have an impact on the tumor structure, blood flow, vascular permeability or tumor interstitial pressure. Another strategy to improve the delivery of ARC and to reduce systemic toxicity is to use pre-targeting antibodies. In pre-targeting, typically a bispecific antibody is injected and

allowed to localize to the tumor associated antigen for a sufficient amount of time and to be cleared from all other tissues [29]. Afterwards, a radiolabeled small molecule is injected which is captured by the bispecific antibody [29]. With pre-targeting, higher radiation doses can be administered, side effects reduced and higher tumor: normal tissue ratios achieved [29]. Encouraging results from human clinical studies have been reported [29,30].

Antibody drug conjugates can deliver highly potent cytotoxic drugs to the tumor site. Ideally, the drug should be stably conjugated to the antibody and only released when the product reaches the tumor site (e.g. by internalization and subsequent lysosomal degradation). Four ADCs are currently approved by the FDA [Gemtuzumab ozogamicin (Mylotarg), Brentuximab vedotin (Adcetris), Trastuzumab emtansine (Kadcyla), Inotuzumab ozogamicin (Besponsa)], but many other ADCs are undergoing clinical evaluation [31]. The first ADC to receive marketing approval was Gemtuzumab ozogamicin (Mylotarg). Mylotarg is a CD33-directed antibody used to treat AML. It was approved 2001 but voluntarily withdrawn from the market 2010 because of safety and efficacy concerns. However potential benefits might have been covered by suboptimal dosing schemes and lack of patient subgroup analysis [32]. In 2017, Mylotarg was reintroduced based on data from a meta-analysis that demonstrated a favorable risk: benefit profile [33,34]. Serious side effects of ADCs can be caused by linker instability problems and off-target toxicities [32]. For this reason, a substantial amount of research efforts has been devoted to the optimization of linker stability. One such construct with optimized linker technology has been developed by Seattle Genetics (SGN-CD33A). Despite improved linker stability, a phase 3 clinical study in patients with acute myeloid leukemia has been stopped due to a higher mortality rate in the SGN-CD33A verum group [35]. Enhanced linker stability is no guarantee for better safety and each new construct has to be carefully tested.

Bispecific antibodies represent one of the most promising classes of biopharmaceutical products, which are attracting substantial investments. Bispecific antibodies are a special class of armed antibodies as they bring a second antibody moiety to the target site. Indeed, bispecific antibodies simultaneously recognize two different epitopes. The epitopes can be located on two different proteins. Such products can be used to maximize the antibody concentration on the tumor site (e.g., if antigens are low expressed), to increase the

therapeutic potency (e.g., blocking two cytokines in autoimmune diseases is better than only one), or to minimize the development of resistance in cancer [36,37]. The epitopes can also be located on two different binding sites on the same target antigen for enhanced binding, or on two different cells in order to bring them in close proximity. In particular, the latter strategy is currently being pursued for cancer immunotherapy applications. The importance of cytotoxic CD8+ T cells in tumor cell eradication has been demonstrated in a large number of studies. However, T cells do not express Fc $\gamma$  receptors and cannot participate in effector mechanisms, such as ADCC, provoked by the Fc portion of an IgG. The engineering of antibodies that form an immunological synapse between a CD8+ T cell and a tumor cell represents an elegant strategy to recruit and to enhance tumor cell eradication by CD8+ T cells. The only two bispecific antibodies that have been approved by the FDA are based on this principle. Catumaxomab (Removab) is a trifunctional bispecific antibody that consists of mouse fragments against CD3 on T cells, rat fragments against endothelial cell adhesion molecule (EpCAM) on tumor cells and an Fc region that binds Fc $\gamma$  receptors on macrophages and NK cells [36]. This bispecific antibody may lead to the tumor cell eradication by ADCC, phagocytosis, cytokine cytotoxicity or T-cell cytotoxicity [36]. Catumaxomab was approved for the treatment of malignant ascites but withdrawn from the market due to commercial reasons [38]. The other bispecific antibody which has reached marketing authorization by the FDA is composed of a scFv against the CD19 antigen and is called Blincyto (Blinatumumab). It is approved for the treatment of patients with Philadelphia chromosome-negative relapsed or refractory B cell precursor acute lymphoblastic leukemia (ALL), and minimal residual disease (MRD)-positive B-cell precursor ALL.

Immunocytokines consist of antibodies armed with cytokines. They will be discussed in more detail in chapter 3.1.2.

### 3.1.2. Immunocytokines

Parts of this chapter have been adapted from:

Hutmacher and Neri, **Antibody-cytokine fusion proteins: Biopharmaceuticals with immunomodulatory properties for cancer therapy**, *Advanced Drug Delivery Reviews* (2018), *in press*



### 3.1.2.1. From cytokines to antibody-cytokine fusion proteins

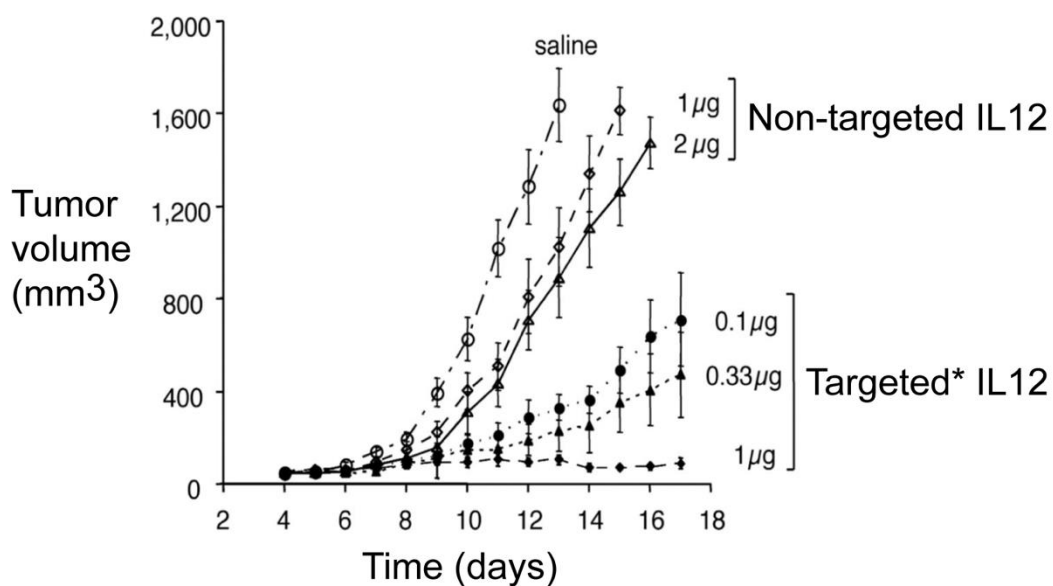
Harnessing components of the immune system for therapeutic applications (“immunotherapy”) is steadily gaining importance for the therapy of cancer, also thanks to the clinical success associated with the use of immune check-point inhibitors [39]. Various approaches to modulate the activity of the immune system against neoplastic cells have been considered over the years. Among them, the use of cytokines for therapeutic applications continues to draw attention and R&D investments.

Cytokines are proteins which modulate the activity of immune cells by binding to their cognate receptors and by triggering subsequent signaling events [18]. A number of cytokine products have gained marketing authorization and are routinely used in clinical practice. The most widely used cytokine products include G-CSF (Neupogen®) and GM-CSF (Leukine®) for the treatment of congenital and acquired neutropenia (e.g., induced by radiation), as well as interferon-alpha for the treatment of certain viral conditions (Pegasys®) and interferon-beta for the treatment of multiple sclerosis (Betaseron®, Avonex®, Plegridy®)[40]. However, various forms of interferon-alpha are also used for oncological applications, such as the treatment of hairy cell leukemia, chronic myelogenous leukemia, lymphoma, advanced or metastatic renal cell carcinoma, malignant melanoma and AIDS-related Kaposi’s sarcoma (Intron A®, Roferon A®). Despite recent progress with immune check-point inhibitors, interleukin 2 (IL2, Proleukin®) is still used for the treatment of metastatic renal-cell carcinoma and melanoma, as a small portion of treated patients can be cured with this modality [41–43]. Moreover, tumor necrosis factor (TNF, Beromun®) has received marketing authorization for the treatment of unresectable soft tissue sarcoma in combination with melphalan [44,45].

The systemic administration of pro-inflammatory cytokines is often associated with severe dose-limiting toxicities (e.g., flu-like symptoms or vascular leak syndrome that causes hypotension and reduced organ perfusion), which may prevent dose escalation to therapeutically active regimens. These limitations underline the need and opportunity to generate novel cytokine-based products, which retain a potent immunostimulatory activity against tumor cells but display reduced side effects. Striking preclinical results were achieved by the intra- or peritumoral application of cytokines, intratumoral implantation of cytokine-producing cells or cytokine gene transfection of cancer cells before implantation without

significant toxicities [46–50]. Although these settings are rarely applicable in the clinic and not suited for treating disseminated tumors, these experiments show that cytokines can mediate cancer cures, provided that sufficiently high concentration of product can be localized within the tumor microenvironment.

Antibodies that are specific to accessible tumor-associated antigens represent ideal “vehicles” for the selective delivery of therapeutic payloads to the tumor environment, helping spare healthy tissues. In principle, the antibody-based targeted delivery of cytokines should lead to a more potent therapeutic benefit with reduced side effects. Indeed, antibody-cytokine fusion proteins (“immunocytokines”) based on certain immunostimulatory payloads have shown impressive activity and selectivity in mouse models of cancer. The very first immunocytokine to enter clinical trials (Hu14.18-IL2) was based on remarkable preclinical findings with the murine analog of the immunocytokine ch.14.18-IL2. Not only was ch14.18-IL2 able to eradicate metastatic melanoma and neuroblastoma in immunocompetent mice, the immunocytokine also induced protective tumor-specific long-term immunity [51,52]. Moreover, in our own experience, the antibody-based delivery of murine interleukin 12 (IL12) to the tumor neo-vasculature exhibited potent activity in various immunocompetent mouse models of cancer, at a dose which was at least 20-fold lower compared to recombinant murine IL12 used as a “non-targeted” drug [53] [Figure 5].



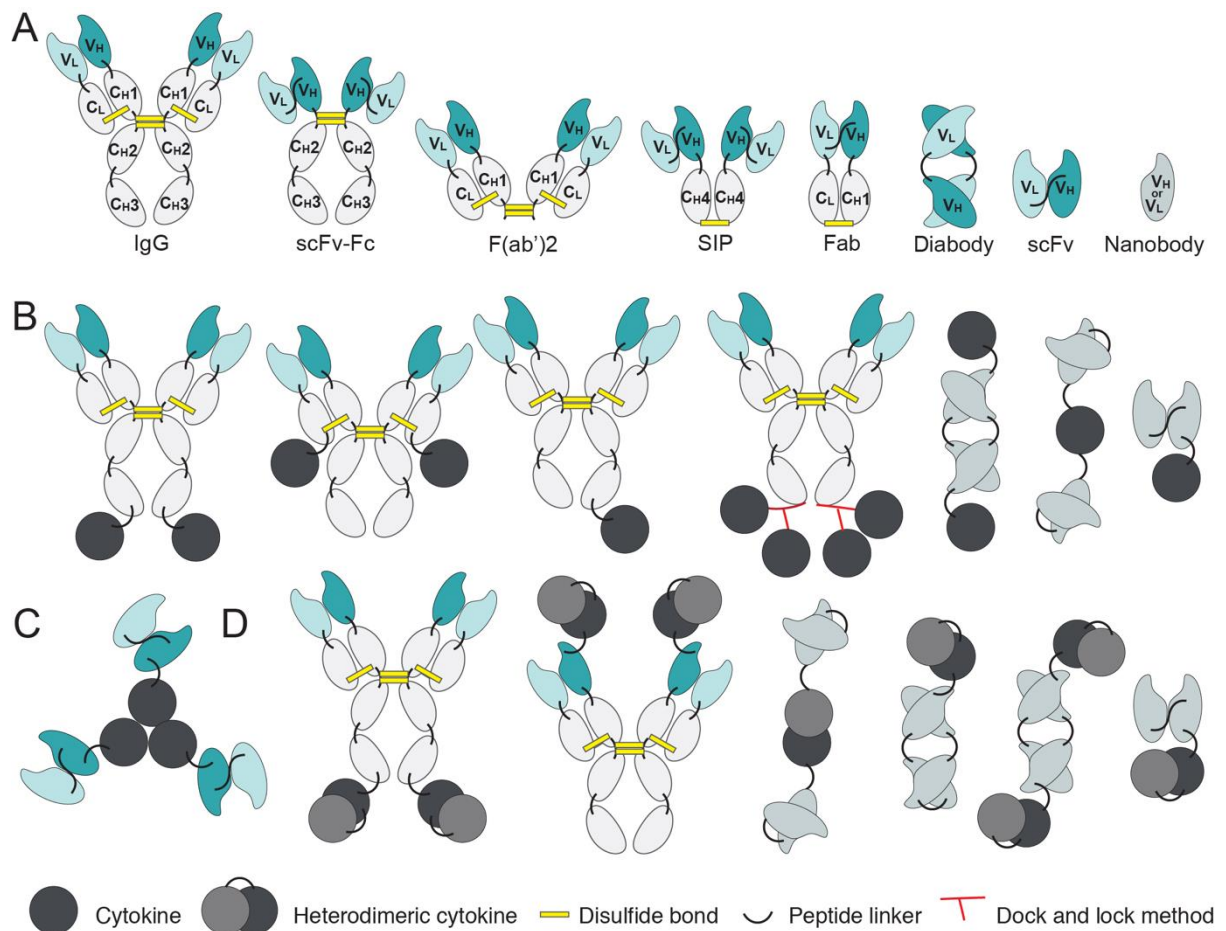
**Figure 5:** Immunocompetent mice bearing F9 tumors were treated with non-targeted IL12 or targeted IL12. A clear dose response is visible as well as a markedly better therapeutic benefit

*of targeted IL12 over untargeted IL12. The indicated IL12-L19 doses are stated as IL-12 equivalents (1 µg IL-12 equivalent corresponds to 1.4 µg IL12-L19). \*IL12 was fused to L19, an antibody against the alternatively-spliced domain B of fibronectin. Adapted from Ref. [53].*

Success in immunocytokine development for pharmaceutical applications may depend on several factors. Besides the choice of the cytokine payload and of the antibody target, the engineering of structural features of the fusion protein greatly contributes to pharmacokinetic and pharmacodynamic properties. The next chapters cover basic concepts associated with immunocytokine design and development, surveys preclinical findings for anti-cancer immunocytokines and discusses recent results published for clinical-stage products.

#### 3.1.2.2. Immunocytokine formats and molecular targets

Various types of antibody formats can be used to design antibody-cytokine fusion proteins [Figure 6]. The antibody moiety can range from a nanobody (MW ~ 14 kDa) to a full-sized immunoglobulin (IgG, MW ~ 150 kDa). The architecture of the antibody portion can have a profound impact on the *in vivo* targeting performance with differences in blood clearance, extravasation, tissue penetration, diffusion and *in vivo* binding properties [54].



**Figure 6:** (A) Schematic representation of antibody formats. *V<sub>H</sub>*: heavy chain variable domain. *V<sub>L</sub>*: light chain variable domain. *C*: constant domain of the heavy (*C<sub>H1-4</sub>*) and the light chain (*C<sub>L</sub>*). *SIP*: small immune protein that uses the  $\epsilon$ *CH*<sub>4</sub> domain of an IgE antibody. Minibodies (or *SIPs*) can also be constructed with the *CH*<sub>3</sub> domain of an IgG. *Fab*: Fragment antigen binding. *scFv*: single chain variable fragment. (B) – (D): Common immunocytokine formats used for the generation of monomeric (B), trimeric (C) and heterodimeric (D) cytokines. Cytokine payloads can be fused to practically any site of the antibody moiety (variable or constant domain of heavy or light chain). In certain *scFv* or *diabody* fusion structures, the colors for *V<sub>H</sub>* and *V<sub>L</sub>* are not indicated (and depicted in grey), since different *V<sub>H</sub>-V<sub>L</sub>* or *V<sub>L</sub>-V<sub>H</sub>* arrangements can be considered. The dock and lock method has been described by Rossi and colleagues that features the separate expression of both the antibody domain containing an AD2 peptide and the cytokine fused to a docking and dimerization domain (DDD2)[55–57]. When the two proteins are incubated under specific conditions, the DD2 domain binds to AD2 and disulfide bridges are formed which stabilize the construct [55–57].

Immunocytokines based on full-size IgGs are bivalent in nature, leading to a high binding avidity. The extravasation and tumor penetration tend to be rather inefficient for intact immunoglobulins and their derivatives. However, higher tumor uptake compared to small antibody fragments can still be observed [58], resulting from a long circulatory half-life in blood [18]. The fragment crystallizable (Fc) region of an IgG can bind to cognate neonatal Fc receptors (FcRn) on endothelial cells and in the liver, rescuing the antibody product from degradation and thus leading to half-life prolongation [59,60]. In principle, the Fc portion could mediate the delivery of cytokine moieties to non-tumoral cells (e.g., leukocytes) and activate the immune system. Antibody-dependent-cell-mediated cytotoxicity (ADCC) is triggered when natural killer cells (NK cells) or macrophages are recruited to an IgG-coated target cell by interaction of the antibody Fc portion with cognate Fc-gamma receptors [24]. Moreover, the complement cascade may be activated, when C1q recognizes a high-local density of IgG molecules on a cell surface [18]. In order to minimize these potential problems, Roche has adopted a combination of glyco-engineering and amino acid mutagenesis at key positions in order to abrogate the interaction of IgG-based immunocytokines with immune system components [61–64].

Immunocytokines based on small antibody fragments display a rapid clearance from circulation, thus contributing to a more favorable tolerability profile [21]. The smallest antibody format that can be used to generate antibody-cytokine fusion proteins is the monomeric nanobody (i.e., a camel-derived single domain antibody). Even though tissue penetration of small antibody fragments may be increased compared to intact immunoglobulins, rapid clearance and insufficient affinity may lead to a lower tumor uptake compared to full IgG molecules [21]. Favorable tumor-to-organ ratios can be observed with certain immunocytokines that are based on noncovalent single-chain variable fragments and form homodimers (“diabodies”)[65,66]. These bivalent products retain the avidity and long tumor residence time of the parental full IgG counterpart. Good *in vivo* selectivity profiles (i.e., tumor: organ ratios) have been reported for numerous diabody-based products [65,67].

The spatial arrangement of the antibody and cytokine moieties can have a profound influence on the *in vivo* performance of the corresponding product. In principle, the cytokine payload can be fused to any site of the antibody. For IgGs, the carboxy-terminus of the heavy chain is

the most commonly used position, that typically results in full conservation of cytokine activity [68]. However, other configurations can be considered. For example, the fusion of an IL2 moiety at the C-terminus of the light chain (rather than the heavy chain) was shown to decrease the affinity to the “intermediate-affinity IL2 receptor” (IL2R $\beta\gamma$ ) while retaining full affinity for the “high-affinity IL2 receptor” (IL2R $\alpha\beta\gamma$ )[69]. This feature may be advantageous *in vivo* for retaining full IL2 activity but less toxicity. Heterodimeric payloads, such as IL12, allow for even more flexibility in product design [Figure 6D].

Immunocytokines should ideally target specific antigens that are abundantly expressed in neoplastic tissues but absent from normal tissue. The tumor microenvironment is a unique niche that emerges during the formation and progression of a tumor. Tissue remodeling and neo-angiogenesis can be observed in aggressive malignancies to guarantee an adequate supply of nutrients [70]. Antigens located on new blood vessels or in surrounding extracellular matrix (ECM) structures are particularly attractive for pharmacodelivery applications. The alternatively-spliced extra domains A (EDA) and B (EDB) of fibronectin and the A1 domain of tenascin-C (TnC A1)[70,71] are strongly expressed in the majority of aggressive solid tumors and lymphomas but are absent from normal tissue, except for the female reproductive system during the proliferative phase (i.e., placenta, endometrium and ovarian vessels)[72,73]. Monoclonal antibodies directed against ECM components, such as F8, L19 and F16 [74–80], have shown promising biodistribution profiles in animal models and in patients.

A number of cellular targets have been considered for antibody-based pharmacodelivery activities, including integrins ( $\alpha_v\beta_3$ ), annexin A<sub>1</sub>, prostate-specific membrane antigen (PSMA), vascular endothelial growth factors (VEGF) and their receptors, endoglin (CD105), CD44 isoforms and alanyl aminopeptidase (CD13)[71]. The A33 and the carcinoembryonic (CEA) antigen are particularly attractive for the targeting of colorectal cancer [81–85], while carbonic anhydrase IX is one of the best markers of clear-cell renal cell carcinoma [86]. EpCAM, disialoganglioside 2 (GD2) and the fibroblast activation protein (FAP) have been proposed as targets, which are expressed by multiple tumor types [87–89]. Immunocytokine programs against these targets are currently at the preclinical or clinical investigation stage [Table 1].

### 3.1.2.3. Cytokine payloads for cancer therapy

A large number of cytokines have been tested as immunocytokine payloads during the last few years. A summary of all the immunocytokines that have been investigated in animal tumor models can be found in **Table 1** in chapter 3.1.2.5. Interleukin-2 (IL2) represents the most commonly studied cytokine payload for anti-cancer applications.

Cytokines are mediators of physiological processes that exert their function in an autocrine or paracrine fashion [18]. Thus, immunocytokines which are specific for tumor associated antigens on the surface of neoplastic cells can bridge tumor cells to certain leukocytes bearing the corresponding cytokine receptor and trigger specific responses. Indeed, an IL2 fusion protein was shown to mediate an immune synapse between a tumor cell and an NK cell that promoted NK cell mediated killing of the tumor cell [90]. Immunocytokines specific for tumor-associated extracellular matrix components were shown to increase the density of leukocytes (especially NK cells and T cells) in the tumor niche [91–94]. Moreover, some cytokines such as IL2 and TNF are able to activate the endothelium at the tumor site thus favoring an increased uptake of therapeutics into the neoplastic tissue [95–97].

Our laboratory has worked with many cytokine payloads and the most promising anticancer results have so far been achieved with products based on IL2, IL12 or TNF. These payloads exhibit different mechanisms of action. Interleukin-2 acts as a mitogen and activator of both NK cell and T cell function [98]. The antibody-based delivery of IL2 to the tumor leads to an increased cellular infiltrate within the neoplastic mass, thus leading to a gain in therapeutic index [99–101]. The mechanism of action for TNF-based pharmaceuticals is unique, as they can trigger a rapid hemorrhagic necrosis of the tumor mass. At a later stage, tumor reactive CD8+ T cells and NK may facilitate the eradication of minimal residual disease [102]. TNF was originally identified as an endotoxin-induced serum factor that caused the necrosis of certain murine tumors *in vivo* [103]. Tumor-homing antibody products, such as L19-TNF, can turn a cancer mass into a black scab [102,104]. IL12 is a cytokine which potently activates certain leukocytes (e.g., CD8+ T cells and NK cells), but which also displays anti-angiogenic activity, by upregulation of CXCL10 [105]. IL12 also regulates the balance between type 1 (Th1) and

type 2 (Th2) subsets of T helper cells and promotes the differentiation of naïve T cells into IFN $\gamma$ - producing Th1 cells [106]. High local concentration of IFN $\gamma$  may promote a tumor infiltration of CD4+ T cells and a decrease in T regulatory (Treg) cells [107–110].

#### 3.1.2.4. Factors influencing the tumor targeting properties of immunocytokine products

In order to learn about factors which influence the tumor targeting properties of antibody fusions, it is convenient to compare a sufficiently large number of different products based on the same antibody moiety. Our laboratory has fused many different cytokine payloads to antibodies of proven *in vivo* tumor targeting performance (e.g., F8 and L19) and has characterized the corresponding biodistribution properties in tumor-bearing mice, using radioiodinated protein preparations [**Table 1**]. These studies have shed light on certain parameters which can influence the tumor homing properties of antibody-cytokine fusions. These investigations were facilitated by the fact that antibodies directed against splice variants of fibronectin exhibited similar tumor targeting performance (measured as percent of injected dose per gram of tumor, or as tumor:organ ratios) over a broad range of administered doses (e.g., between 0.1  $\mu$ g and 150  $\mu$ g of antibody fusions; Ref. [77], references of Table 1 [53,94,95,101,111–138] and unpublished observations).

The majority of cytokine payloads, when fused to the L19 or to the F8 antibody, can efficiently be delivered to solid tumors in mice, after intravenous administration in the 5 – 20  $\mu$ g dose range. In that case, the tumor uptake and tissue selectivity of immunocytokines are typically similar or even better than the ones of the parental antibodies. Cytokine fusions with favorable tumor targeting profiles include products based on IL2, IL3, IL4, IL6, IL10, IL12, IL22, TNF, IFN $\alpha$  and G-CSF [53,93,109,110,115,129,139–141].

Certain payloads, however, exhibited a dose-dependent tumor-targeting performance and other cytokines completely abrogated the tumor homing properties of the parental antibodies. These observations have allowed us to identify molecular parameters which are crucially important for a successful delivery to the tumor. Trapping of the cytokine payload by abundant receptors expressed in normal tissues may compromise the targeting



performance of certain fusion proteins. For instance, antibody fusions with IFN $\gamma$  were shown to selectively localize to neoplastic lesions only if IFN $\gamma$  receptor knockout mice were used for the experiment, or if a large amount of unlabeled antibody-cytokine fusion protein had been pre-administered to wild-type tumor-bearing mice [142,143]. Similar dose-dependent biodistribution profiles were observed for IL7, IL15 and GM-CSF, suggesting the presence of “titratable” receptors, which could hinder pharmacodelivery applications at low doses [144,145].

The isoelectric point of antibody fusions may also have a negative impact on biodistribution results. For example, the fusion of calmodulin (with high negative charge) or the coupling of Tat peptides (with high positive charge) completely abrogated the tumor homing properties of the parental L19 antibody, even though the products were fully immunoreactive *in vitro* and well-behaved in biochemical assays (e.g., in SDS-PAGE and gel-filtration analysis)[146,147]. Interestingly, L19 fusions to murine VEGF-120 efficiently targeted tumors, while the larger and positively-charged VEGF-164 payload prevented targeting [148].





Glycosylation and excessive molecular mass may also prevent efficient tumor targeting *in vivo*. Certain heavily glycosylated payloads (e.g., murine B7.2) were rapidly cleared via the hepatobiliary route and did not efficiently localized to tumors [149]. Interestingly, when similar payloads were fused to an antibody in IgG format, selective tumor uptake and tumor growth retardation was observed [150,151]. L19-IL12 and L19-TNF efficiently localized to solid tumors in mice. However, when murine IL12 and TNF were simultaneously fused to the L19 antibody, the resulting fusion protein (with a molecular mass of approximately 120 kDa) had poor biodistribution properties, while being completely immunoreactive in *in vitro* assays [95]. Additionally, protein production methods can influence antibody glycosylation and, as a consequence, biodistribution results. For example, production of the F8-IL9 fusion protein with different set-ups (transient gene expression or stable gene expression) reproducibly led to protein preparations of similar biochemical properties (SDS-PAGE, gel filtration, BIAcore analysis) but completely different tumor homing performances. Subtle differences in glycosylation patterns had a major impact on the biodistribution profile [152] and preparations with higher proportions of terminal sialic acid residues tended to perform better.






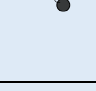




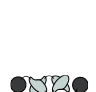

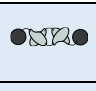

Biodistribution studies, performed with fusions of the F8 antibody to various members of the TNF superfamily, have surprisingly revealed big differences in pharmacokinetic and tumor uptake properties, even if the products had similar molecular formats and biochemical properties. TNF and proteins of the TNF superfamily are non-covalent homotrimers, which may, however, differ in terms of thermodynamic stability [153]. TNF is a potently vasoactive payload, which exhibited excellent biodistribution profiles, when fused either to L19 or to F8 [95,134,154]. However, antibody fusions with CD40L, FasL, TRAIL, truncated versions of TRAIL, VEGI, truncated versions of VEGL, LIGHT and various lymphotoxin combinations exhibited biodistribution results which were, to a varying extent, worse compared to the ones of L19-TNF and F8-TNF [155]. Recent research results of Roland Kontermann and collaborators have shown that members of the TNF superfamily may benefit from being expressed as a single polypeptide, connecting the three monomeric units, instead of being expressed as monomeric units that form non-covalent homotrimers [153,156].



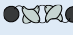




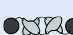







### 3.1.2.5. Immunocytokines with promising preclinical results



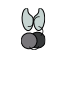


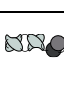






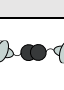



A large number of immunocytokines has been investigated in preclinical mouse models of cancer. **Table 1** presents a summary of fusion proteins which have been proposed for therapeutic applications. For many of them, quantitative biodistribution studies and therapy results in tumor-bearing mice have been reported. The table also displays the molecular arrangement of the antibodies (or antibody fragments) and cytokine payloads.
















**Table 1:** List of antibody-cytokine fusion proteins and their characterization



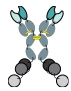











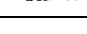





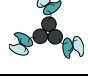
Compound	Format	Antigen	<i>In vivo</i> targeting	Tumor Model	Efficacy	Lit.
<b>G-CSF</b>						
GCSF-F8		EDA	+	F9 s.c.	F9 s.c.: I ≈ P	[139]
<b>GM-CSF</b>						
Anti-HER2/ <i>neu</i> IgG3-GMCSF		HER2/ <i>neu</i>	+	CT26 s.c., CT26 HER+ s.c.	CT26 HER+: I > NC	[157–160]
CLL1-GMCSF		MHCII	+	ARH-77	n.a.	[114]
L19-GMCSF		EDB	+(d.d.)	F9 s.c., i.v.	F9 s.c.: I > NC,	[145]



















				C51 s.c., i.v.	C51 s.c./i.v., F9 i.v.: I > P	
<b>Interleukin 1<math>\beta</math></b>						
F8-IL1 $\beta$ , IL1 $\beta$ -F8		EDA	+	F9 s.c.	F9 s.c.: I > NC	[140]
<b>Interleukin 2</b>						
2aG4-IL2		PS	n.a.	4T1 i.v.	Vaccination: I > NC	[161]
Anti-CEA-IL2		CEA	+	MC-38 s.c. MC38-CEA s.c.	MC38-CEA: I > NC	[111]
Anti HER2/ <i>neu</i> IgG3-IL2		HER2/ <i>neu</i>	n.a.	CT26-HER2	CT26-HER2: I > NC	[158– 160,162 –164]
CEA-IL2v		CEA	+	MC38-CEA i.s., PancO2-CEA i.Pc., A549 i.v., Ls174t i.s., N87 s.c., KPL-4 m.f.p.	MC38-CEA i.s., PancO2-CEA i.Pc.: I > P A549 i.v., Ls174t i.s., N87 s.c., KPL-4 m.f.p.: combo therapies: I > P	[112,16 5]
ch14.18-IL2		GD2	+	M21 i.v., i.s., s.c., B16-GD2 i.v., i.s., SK-N-AS i.s., NX2S i.v., s.c., s.m.	M21, i.v., B16-GD2, SK-N-AS, NX2S i.v., s.m., s.c.: I > NC	[51,99,1 13,166– 168]
ch225-IL2		EGF	n.a.	M24met i.s.	M24met i.s.: I > NC	[166,16 9]
CLL1-IL2		MHCII	+	ARH-77	n.a.	[114]
Di-Leu16-IL2		CD20	n.a.	Daudi i.v.	Daudi i.v.: I > NC	[170]
F8-IL2		EDA	+	Caki-1 s.c., C1498 s.c., NB4 s.c., WM1552/5 s.c., A375M i.v., K1735M2 s.c., F9 s.c., WEHI-163 s.c.	Caki s.c.: I > NC, C1498 s.c.: I i.v. > NC, I i.t. $\approx$ P, NB4 s.c.: I > NC, WM1552/5 s.c.: I $\approx$ NC, A375M i.v.: I $\approx$ NC, K1735M s.c.: I > NC, F9 s.c.: I i.v., i.t. > P, WEHI-163 s.c.: I i.t. $\approx$ P, LLC s.c.: i.t. I > P,	[93,101, 109,115 ,122,17 1–173]
F16-IL2		Tnc A1	+	MDA-MB-231 s.c, U87MG s.c., i.c.	MDA-MB-231 s.c.: I > NC U87MG s.c., i.v.: I > P	[116,11 7]
FAP-IL2v		FAP	n.a.	MC-38-FAP s.c.	MC-38-FAP: I > NC	[165,17 4,175]
FUMK1-IL2		EpCAM	+	MKN-74 s.c.	MKN-74 s.c.: I > NC	[118]
IL2-FuP		EGFR	+	BLM s.c.	BLM s.c.: I > FuP naked	[119]

IL2-MOV19		αFR	+	CT26-αFR i.v., s.c.	CT26-αFR s.c.: I > NC	[120]
KS-IL2		EpCAM	+	CT26-KSA i.s., i.v., s.c., PC-3.MM2 i.v., 4T1-KSA s.c., i.v., LLC-KSA s.c.	CT26.KSA: i.v., i.s., s.c., PC-3.MM2 i.v., 4T1-KSA s.c., LLC-KSA: I > NC	[121,176,177]
L19-IL2		EDB	+	F9 s.c., C51 s.c., N52 s.c., Ramos s.c., i.v., A20 s.c., DoHH-2 s.c., CT26 s.c., N2A s.c., NIE-115 s.c., K1735M2 s.c., J558L s.c., DanG i.Pc., MiaPaca i.Pc., MiaPaca-A2 i.Pc.,	F9 s.c., C51 s.c., N52 s.c., Ramos s.c., i.v., Do-HH-2 s.c., CT26 s.c., K1735M2 s.c., J558L s.c., DanG i.Pc., MiaPaca i.Pc.: I > NC, N2A s.c.: I > P, NIE-115 s.c.: I in combo > P	[72,94,122,178-181]
NHS-IL2LT		Histone	+	NX2S i.v., LCC i.v.	NX2S i.v., LLC i.v.: I > NC	[123]
Ta99-IL2		A33	+	B16F10 s.c.	B16F10 s.c.: I > NC	[124]
sm3E-IL2		CEA	+	B16F10 s.c.	B16F10 s.c.: I > NC	[124]
<b>Interleukin 3</b>						
F8-IL3		EDA	+	F9 s.c.	F9 s.c.: I ≈ P	[139]
<b>Interleukin 4</b>						
F8-IL4		EDA	+	F9 s.c., CT26 s.c., A20 s.c.	F9 s.c., CT26 s.c., A20 s.c.: I > NC	[93]
F8-IL4-F8		EDA	+	F9 s.c.	F9 s.c.: I > P	[139]
<b>Interleukin 6</b>						
F8-IL6, IL6-F8		EDA	+	F9 s.c.	F9 s.c.: I > NC	[140]
<b>Interleukin 7</b>						
F8-IL7		EDA	+	F9 s.c.	F9 s.c.: I > NC	[144]
F8-IL7-F8		EDA	+	F9 s.c.	F9 s.c.: I > NC	[144]
<b>Interleukin 9</b>						
F8-IL9		EDA	+	n.a.	n.a.	[152]
<b>Interleukin 12</b>						
BC1-IL12		EDB	+	PC3mm2 i.v., s.c., A431 s.c., HT29 s.c.	pC3 i.v., PC3 s.c., HT9 s.c.: I > NC A431 s.c.: I ≈ NC	[110,182]
chTNT3-IL12; NHS-IL12		DNA	+	LS147T s.c., DU145 s.c., LLC s.c., MC38 s.c., B16 s.c., MC38/MUC1+ s.c., Panc02/MUC1+ s.c., Renca s.c., Panc02 s.c., MB49 s.c.	DU145 s.c., LLC s.c., MC38 s.c., B16 s.c.; I > NC, MC38/MUC1+ s.c., Panc02/MUC1+ s.c., MB49 s.c; I in combo > P, Renca s.c., Panc02 s.c.: I > P	[125,183,184]

KS-IL12		EpCAM	n.a.	DU145 i.v., CT26-EP21 i.v.	DU145 i.v., CT26-EP21 i.v.: I > NC	[185]
mscIL12-her2.IgG3		Her2/ <i>neu</i>	n.a.	CT26-HER2 s.c., i.v., CT26 i.v.	CT26-HER2: s.c., i.v, CT26 i.v.: I ≈ NC	[186,187]
IL12-L19(scFv)		EDB	+	F9 s.c.: C51 s.c., i.v.	F9 s.c., C51 s.c., i.v.: I > NC,	[92,95,126]
IL12-L19(SIP)		EDB	+	F9 s.c.	n.a.	[126]
L19-p35/p40-L19		EDB	+	F9 s.c.	F9 s.c.: I > NC	[126]
F8-p35/p40-F8		EDA	+	F9 s.c.	n.a.	[127]
IL12-F8-F8		EDA	+	F9 s.c., CT26 s.c., A20 s.c.	F9 s.c.: I > NC, CT26 s.c., A20 s.c.: I > P	[109]
IL12-SSI		MSLN	n.a.	NCI-H226 i.p.	NCI-H226 i.p.: I > P	[188]
HRS3scFv-IL12 and HRS3scFv-Fc-IL12		CD30	+	n.a.	n.a.	[128]
<b>Interleukin 13</b>						
F8-IL13		EDA	+	Wehi-164 s.c.	Wehi-164: I > NC	[189]
<b>Interleukin 15</b>						
L19-IL15, IL15-L19		EDB	+	F9 s.c., i.v. C51 s.c., i.v.	F9 s.c.: I > NC, C51 s.c./i.v., F9 i.v.: I > P	[145]
Anti-GD2-RLI (IL15)		GD2	n.a.	EL4 s.c., NXS2 i.v.,	EL4 s.c., NXS2 i.v.: I > NC	[190]
scFv-RD-IL15		FAP	+	B16-FAP i.v.	B16-FAP i.v.: I > NC	[191,192]
<b>Interleukin 17</b>						
F8-IL17/IL17-F8		EDA	+	F9 s.c.	F9 s.c.: I ≈ P	[193]
<b>Interleukin 18</b>						
F8-IL18		EDA	+(d.d.)	F9 s.c.	F9 s.c.: I ≈ P	[194]
<b>Interleukin 21</b>						
Anti-CD20-IL21		CD20	n.a.	A20-huCD20 s.c.	A20-huCD20 s.c.: I > NC	[195,196]
<b>Interferon α</b>						

F8-IFN $\alpha$		EDA	+	F9 s.c., Cloudman S91 s.c.	F9 s.c., Cloudman S91 s.c.: I $\approx$ NC	[197]
CD20IgG3-IFN $\alpha$		CD20	n.a.	38C13-CD20 s.c., Daudi s.c.	38C13-CD20 s.c., Daudi s.c.: I > NC	[198]
AntiHER2/ <i>neu</i> -IFN $\alpha$		Her2/ <i>neu</i>	n.a.	38C13-HER2+ s.c.	38C13-HER2+ s.c.: I > NC	[198,199]
C2-2b-2b		HLA-DR	n.a.	Daudi i.v., CAG i.v.	Daudi i.v., CAG i.v.: I > NC	[200]
20-2b		CD20	n.a.	Daudi i.v., Raji i.v., NAMALWA i.v.	Daudi i.v., Raji i.v., NAMALWA i.v.: I > NC	[55]
<b>Interferon <math>\gamma</math></b>						
L19-IFN $\gamma$		EDB	+	F9 s.c., i.v., C51 s.c., i.v., CT26 s.c.	F9 s.c., i.v.: I > NC, C51 s.c., i.v., CT26 s.c.: I $\approx$ P	[142]
TNT3-IFN $\gamma$		DNA	+	LS174T s.c., MAD109 s.c., RENCA i.v.	RENCA: I > NC	[136,201]
<b>TNF</b>						
F8-TNF		EDA	+	WEHI-164 s.c., Sarcoma 180 s.c.	WEHI-164 s.c., Sarcoma 180 s.c.: I > P	[102,154]
FAP-TNF		FAP	n.a.	HT1080-FAP+ s.c.	HT1080-FAP+ s.c.: I > NC	[202]
G250-TNF		CAIX	+	NU-12 s.c., SK-RC17/52 s.c.	SK-RC17/52 s.c.: I > NC	[130]
scFvMEL-TNF		gp240	+	A375 s.c.	A375 s.c.: I > NC	[132,133]
L19-TNF		EDB	+	F9 s.c., WEHI-164 s.c., C51 s.c., N2A s.c., NIE-115 s.c., K1735M2 s.c., J558L s.c.	F9 s.c., WEHI-164 s.c., C51 s.c., K1735M2 s.c., J558L s.c.: I > NC, N2A s.c. I > P, NIE-115 s.c.: I in combo > P	[95,122,134,178-180,203]
MFE23-TNF		CEA	+	LS174T s.c.	n.a.	[135]
TNF-TNT3		DNA	+	LS174T s.c.	n.a.	[136]
TNF-FuP		EGFR	+	BLM s.c.	BLM s.c.: I > NC	[119]

TNF-B1		LeY	n.a.	MCF-7 s.c.	MCF-7 s.c.: I > NC	[204]
ZME/TNF		gp240	+	A375 s.c.	A375 s.c.: I > NC	[137]
<b>heterodimeric cytokines</b>						
KS-IL12/IL2		EpCAM	n.a.	LLC-EpCAM+ i.v., i.t.	LLC-EpCAM+ i.v., i.t.: I > NC	[205]
HRS3scFv-IL12-Fc-IL2		CD30	n.a.	9G10-HRS3A+ s.c.	9G10-HRS3A+ s.c.: I > P	[128]
IL2-F8-TNFmut		EDA	+	WEHI-164 s.c., CT26 s.c., C1498 s.c., F9 s.c.	WEHI-164 s.c.: I > NC CT26 s.c., C1498 s.c., F9 s.c.: I > P	[138]
IL4L-Ab-GMCSF and IL4H-Ab-GMCSF		EpCAM	n.a.	n.a.	n.a.	[205]
IL12-IgG3-IL2		Her2/ <i>neu</i>	n.a.	TUBO s.c.	Vaccine adjuvant: I > P	[160]
IL12-IgG3-GMCSF		Her2/ <i>neu</i>	n.a.	TUBO s.c.	Vaccine adjuvant: I > P	[160]
<b>Chemokines</b>						
CCL5-F8		EDA	n.a.	n.a.	n.a.	[206]
CCL17-F8		EDA	n.a.	n.a.	n.a.	[206]
CCL19-F8		EDA	+	n.a.	n.a.	[206]
CCL20-F8		EDA	+	n.a.	n.a.	[206]
CCL21-F8		EDA	+	n.a.	n.a.	[206]
CXCL4-F8		EDA	n.a.	n.a.	n.a.	[206]
CXCL9-F8		EDA	n.a.	n.a.	n.a.	[206]
CXCL10-F8		EDA	+	F9 s.c.	F9 s.c.: I > P	[206]
CXCL111-F8		EDA	n.a.	n.a.	n.a.	[206]
F8-ITIP		EDA	n.a.	n.a.	n.a.	[206]
<b>TNF superfamily members</b>						
F8-TRAIL		EDA	+	n.a.	n.a.	[155]
F8-TRAILtrunc		EDA	+	n.a.	n.a.	[155]
F8-CD40L		EDA	+	n.a.	n.a.	[155]

scFv-OX40L		END	n.a.	n.a.	n.a.	[207]
F8-FasL		EDA	+	n.a.	n.a.	[155]
LIGHT-F8		EDA	+	n.a.	n.a.	[155]
scFv-LIGHT		END	n.a.	n.a.	n.a.	[207]
F8-VEGI		EDA	+	n.a.	n.a.	[155]
F8-VEGItrunc		EDA	+	n.a.	n.a.	[155]
F8-LTA		EDA	+	n.a.	n.a.	[155]
scFv36-4-1BBL		FAP	n.a.	n.a.	n.a.	[208]
scFv-4-1BBL		END	+	B16-FAP i.v.	B16-FAP i.v.: in combo I > P	[207]
F8-LTβ		EDA	+	n.a.	n.a.	[155]
F8-LTα/β2		EDA	+	n.a.	n.a.	[155]
scFv-TNC-GITRL		END	n.a.	n.a.	n.a.	[207]
<b>other payloads</b>						
B7.1Db		FAP	n.a.	B16 i.v	B16 i.v: in combo I > P	[207]
B7.2Db		FAP	+	n.a.	n.a.	[207,209]
F8-B7.2		EDA	+	n.a.	n.a.	[149]
scFv(19)-tTF		EDB	+	C51 s.c., F9 s.c., FE8 s.c.	C51 s.c., F9 s.c., FE8 s.c.: I > NC	[210]
L19- VEGF-A <sup>164</sup>		EDB	+	n.a.	n.a.	[148]
L19-VEGF-A <sup>120</sup>		EDB	+	n.a.	n.a.	[148]

**Legend Table 1:** Summary of immunocytokines that have been tested in animal models. In vivo targeting was assessed by biodistribution studies. Efficacy was defined as tumor growth retardation (“I >” the immunocytokine performed better, “I ≈” the immunocytokine performed



equally) compared with a saline group (P) or negative control group (NC, untargeted cytokine or cytokine fused to an antibody of irrelevant specificity). The format of the immunocytokine is depicted according to the color code of **Figure 6** with the exception of the C<sub>H1</sub>-C<sub>H3</sub> and C<sub>H1</sub> domains which are depicted in blue. In the structure of dual cytokine fusion proteins, the additional cytokine payload is illustrated with a grey circle. The red domain in the structure of scFv-RD-IL15 illustrates the ILR $\alpha$  domain. Blue shading: immunocytokines in clinical trials

Abbreviations: +: biodistribution results published, n.a.: biodistribution data not available. i.v.: intravenous, s.c.: subcutaneous, i.s.: intrasplenic, i.Pc.: intrapancreatic, i.c.: intracranial, i.t.: intratumoural, m.f.p: mammary fat pad, s.m.: spontaneous metastasis, I.: Immunocytokine, DD: dose dependence, combo: in combination with a second anti-cancer therapeutic. G-CSF: Granulocyte colony-stimulating factor, GM-CSF: Granulocyte-macrophage colony-stimulating factor. EDA: alternatively-spliced extradomain A of fibronectin, EDB: alternatively-spliced extradomain B of fibronectin, HER2/neu: human epidermal growth factor receptor 2, MHCII: major histocompatibility complex class II, PS: phosphatidylserine, CEA: carcinoembryonic antigen, GD2: disialoganglioside, Tnc A1: alternatively spliced A1 domain of tenascin-C, FAP: fibroblast-activating protein, EpCAM: epithelial cell adhesion molecule, EGF: epidermal growth factor, EGFR: epidermal growth factor receptor,  $\alpha$ FR: alpha folate receptor, MSLN: mesothelin, HLA-DR: human leukocyte antigen DR, CAIX: carbonic anhydrase IX, LeY: Lewis Y antigen

The most promising therapy results have so far been achieved with immunocytokine products based on IL2, IL12 or TNF as payloads [51,53,65,94,95,99,101,102,110–113,115–121,123–128,130,132,133,135,137,138,154,160,162,167–169,174,175,177,185,186,188,202,204,205,211–217]. Not surprisingly, these cytokines are not only important anti-cancer weapons from an immunological viewpoint, but also exhibit favorable tumor homing properties in biodistribution studies [53,94,95,101,111–138], when fused to suitable antibodies. Some fusion proteins based on IL2, IL12 or TNF have progressed to clinical trials, as described in chapter 8.

**Figure 5** illustrates the benefit which can be achieved by the targeted delivery of a cytokine payload to the tumor site. In this case, murine IL12 displayed a much more potent anti-cancer activity in immunocompetent mice bearing F9 murine tumors when fused to the L19

antibody, compared to the non-targeted recombinant murine IL12 counterpart [53]. Therapeutic activity was clearly dose-dependent.

The groups of Reisfeld and Gillies have previously reported that IgG fusions, featuring IL2 as a payload, exhibited strong anti-cancer activity in various mouse models of cancer, including metastatic melanoma, neuroblastoma, prostate carcinoma, colon adenocarcinoma, non-small cell lung carcinoma and lymphoma [51,52,61,90,99,113,123,166–168,177,212,213,218,219]. The fusion proteins were typically not able to cure tumor-bearing mice, but durable complete responses were reported for melanoma, neuroblastoma and lymphoma bearing mice [51,113,166–168,213].

The groups of Morrison and Penichet showed that anti-HER-2/*neu* antibody fusion proteins based on IL2 [158–160,162,164,220], IL12 [186,221] and GM-CSF [157–160], IFN $\alpha$  [198,199] can elicit potent antitumor responses against anti-HER-2/*neu* or CEA expressing murine tumors or lymphomas. Immunocytokines based on IL2 or GM-CSF were not only potent in inhibiting tumor growth, but also in preventing tumor growth in mice when used in combination with vaccines [158,160].

Dafne Müller and colleagues have extensively studied antibody-cytokine fusion proteins that are composed of antibodies in the diabody or the scFv format linked to members of the TNF superfamily [207–209]. Recently, the group of Müller has described an antibody fusion protein based on an antibody moiety targeting the fibroblast activation protein, interleukin 15 (IL15) and a fragment of the IL-15R $\alpha$  chain. This IL15 fusion protein should mimic physiologic *trans*-presentation of the cytokine payload [191]. IL15 normally acts in a membrane-bound form bound to the IL-15R $\alpha$  expressed on monocytes and dendritic cells [222]. IL15/IL15R $\alpha$  can then bind to the heterodimeric intermediate affinity receptor IL2/IL15R $\beta\gamma$  on NK or CD8+ T cells and trigger subsequent signaling events [222]. The domain of IL15R $\alpha$  involved in the binding of IL15 has been identified [223]. The Müller group reported the successful generation of a fusion protein that consists of the IL15 and an extended IL15R $\alpha$  domain which displayed a superior antitumor activity compared to the untargeted or the receptor domain missing forms [191]. The group also described a trifunctional fusion protein

consisting of a tumor homing antibody, IL15 linked to the IL15R $\alpha$  fragment and the extracellular domain of 4-1BBL [192]. This trifunctional fusion protein was even more potent in a mouse model of melanoma than the corresponding bifunctional molecules [192].

The fusion proteins L19-IL2 and F8-IL2 have exhibited favorable biodistribution results in tumor-bearing mice and a potent tumor growth inhibitory activity in various models of cancer [72,93,94,101,115,122,178]. Single-agent cancer cures were rare, but certain models (e.g., BALB/c mice bearing CT26 colon carcinoma or C57BL/6 mice bearing TIB49 acute myeloid leukemia) typically responded better than other models (e.g., C57BL/6 mice bearing Lewis Lung Carcinoma), for reasons that are still not fully understood [101,178].

Interleukin-12 is a promising payload, as it can activate NK cells and CD8<sup>+</sup> T cells, while also favoring a Th1 polarization of CD4<sup>+</sup> T cell response [105,106]. Both tumor homing properties and therapeutic performance crucially depend on the molecular arrangement chosen for the antibody moiety and the heterodimeric IL12 payload [126]. A format based on a single polypeptide, connecting the two IL12 subunits with the F8 antibody in single-chain diabody format, is easier to express compared to other molecular arrangements [109,126,127] and performs well *in vivo*. This format may thus represent the best candidate for future clinical development programs.

TNF is a homotrimeric cytokine, which can conveniently be fused to antibodies in scFv format, leading to a stable non-covalent homotrimeric product [96,129,134,135,224]. In our experience, murine TNF was the only cytokine payload (among many that we have tested) capable of promoting a rapid hemorrhagic necrosis of the tumor mass in preclinical models [102]. Neoplastic lesions can be converted into necrotic scabs within few hours and this process correlates with therapeutic performance [102]. In most cases, TNF-based immunocytokines cannot cure tumor-bearing mice when used as single agents, since a rim of residual tumor cells survives and may eventually regrow. However, TNF-based products may be ideally suited for debulking strategies or as combination partners with other modalities, as discussed in a later chapter.

### 3.1.2.6. Opportunities for combination therapy

Immunocytokines based on pro-inflammatory cytokines may be ideal combination partners for various anti-cancer therapeutic agents. Besides boosting the immune system, pro-inflammatory cytokines can activate the endothelium and increase vascular permeability [95–97], thus favoring the accumulation of other drugs at the tumor site. Various combination partners have been tested in preclinical experiments, including (cytotoxic) drugs [101,115–117,134,154,172,183], small molecule drug conjugates (SMDC)[225], intact antibodies [72,112,124,183], bispecific antibodies [207,209], radiation [183,226–228], radiofrequency ablation [218], immune check-point inhibitors [95,138,175,184,229], antibody-drug conjugates (ADC)[214,230], vaccination strategies [158,160] and even other immunocytokine products [93,95,109,112,128,138,160,173,178,192,205].

Tumor surgery and conventional chemotherapy are often the first-line treatment given to cancer patients. However, chemotherapy often is accompanied by serious side effects (e.g., nausea, myelotoxicity) that prevents dose escalation to therapeutically active regimens. Immunocytokines appear to synergize well with some, but not all, cytotoxic drugs. In addition to increasing drug uptake within the tumor mass [97,134], certain immunocytokines can exploit the immune reaction against tumor cells, initially promoted by drug-related immunogenic cell death [172]. In addition to the beneficial effects on tumor immunogenicity, certain drugs could in principle also antagonize the effects of immunotherapy (especially when used at high doses), as cytotoxic agents may be myelotoxic and kill the very same leukocytes needed to fight cancer. In this context, dose and schedule appear to be crucially important. For example, melanoma cures were observed when an IL2-based product was administered *after* paclitaxel chemotherapy in a mouse model of the disease, while the reverse schedule did not exhibit any additive benefit [172].

The administration of pro-inflammatory cytokines activates the endothelium (potentially leading to hypotension, which may be dose-limiting) and triggers flu-like symptoms [41,97]. These side effects often do not overlap with those of chemotherapy (e.g., myelotoxicity) and, for these reasons, it is often possible to combine the two regimens at the recommended dose, without a forced reduction in the administered quantities. Another strategy is to use antibody-drug conjugates (ADC) which can deliver highly potent cytotoxic drugs to the tumor

site sparing normal tissues. In an immunocompetent mouse model of AML, the combination of an ADC and an immunocytokine based on IL2 achieved significantly better results than the ADC or the immunocytokine alone [214]. A trifunctional antibody-drug-cytokine conjugate (consisting of IL2 and a maytansinoid DM1 microtubular inhibitor fused to an antibody moiety) showed selective tumor-homing performance and potent anticancer activity in two mouse models, further encouraging this combinatorial approach [230]. Small molecule-drug conjugates may offer additional benefits compared to ADCs in terms of rapid diffusion into the tumor [231], immunogenicity [232] and lower cost-of-goods [233]. The activity of a non-internalizing small molecule-drug conjugate was recently shown to be enhanced in combination with L19-IL2 [225].

The combination of intact IgGs and immunocytokines has also shown promising preclinical results [72,112,124,183]. Products that mediate an increased density and activity of NK cells within the tumor mass are likely to potentiate antibody-dependent cell cytotoxicity (ADCC)[72,112].

There is a considerable therapeutic potential associated with the combination of pairs of judiciously chosen immunocytokine products. Immune reactions are often boosted by the simultaneous presence of two or more stimuli [18]. A synergistic effect has been reported for the combined use of L19-IL2 and L19-TNF, both in a preclinical and clinical setting [122,173,178,180,234,235]. In a mouse model of neuroblastoma, treatment with the combination of L19-IL2 and L19-TNF resulted in a 70 % complete cure rate compared to the 30 % cure rates observed for the respective monotherapies [235]. Moreover, total splenocytes from cured mice were able to fully protect naïve mice against a homologous tumor mediated predominantly by CD8+ T cells, thus suggesting a vaccination effect. Also in a myeloma model, the combined administration of L19-IL2/ L19-TNF was significantly better than the monotherapies [180]. In a different syngeneic immunocompetent mouse model of cancer, a single intratumoral injection of L19-IL2 combined with L19-TNF resulted in complete remission whereas the two components administered separately did not lead to cures [178]. These results were confirmed in two additional mouse models of cancer in an independent study (K1735M2 melanoma, WEHI-163 sarcoma)[122]. Other examples of immunocytokine combinations leading to potent anticancer activity include products based on the pairs

IL2/IL12 [128,160,205], IL12/TNF [95] and IL4/IL12 [93]. The latter combination was surprising considering that IL4 and IL12 are technically antagonistic in polarizing different fates of CD4+ T cell development [18].

The combination of multiple immunocytokine products is attractive from an immunological perspective, but difficult to implement in pharmaceutical development, as it requires more than one product and involves double the amount of studies and regulatory approvals. For this reason, it may be attractive to generate a novel class of biopharmaceutical agent featuring multiple cytokine payloads. This approach would lead to single products for industrial development (thus reducing development time and costs), but presents certain challenges. Not all payloads can be combined into the same molecular entity whilst retaining an adequate tumor targeting performance [95]. Moreover, different cytokine payloads may be active at different doses.

Gillies et al. have generated a series of dual cytokine fusion proteins which are composed of IL2, IL12 and the anti-EpCAM antibody (KS-1/4)[205]. Cytokine activity was preserved in those constructs where the cytokines were fused to the C-terminus of the heavy or light chain domain, or where one cytokine was linked to the C-terminus of the heavy chain while the other payload was linked to the N-terminus of the heavy or light chain variable region [205]. These KS-IL2/ IL12 fusion proteins showed remarkable anti-tumor activity in a mouse model of Lewis Lung carcinoma [205].

Our group has recently reported the successful generation of a “potency-matched” dual cytokine fusion protein[138]. This novel fusion protein consists of the tumor targeting antibody F8 linked to IL2 and TNF [138]. A single point mutation of TNF was enough to match its potency with IL2 (IL2-F8-TNF<sup>mut</sup>)[138]. IL2-F8-TNF<sup>mut</sup> eradicated soft tissue sarcomas that are typically not responsive to the individual cytokine fusion proteins or the standard treatment with doxorubicin [138]. Also, in other mouse models of cancer (CT26, C1498, F9), the dual cytokine fusion protein mediated a potent therapeutic activity [138].

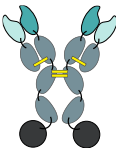
Antibodies against immune check-point inhibitors (such as the cytotoxic T-lymphocyte-associated protein 4 (CTLA-4), programmed cell death 1 (PD-1) or programmed cell death


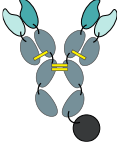
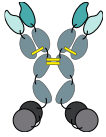
ligand 1 (PD-L1)) are rapidly gaining importance for the treatment of various forms of cancer [236]. Marketed products include ipilimumab (directed against CTLA-4), nivolumab and pembrolizumab (directed against PD-1) and atezolizumab, durvalumab and avelumab (all directed against PD-L1). Ipilimumab was the first immune check-point inhibitor that was approved by the FDA. The CTLA-4 blocker is approved for the treatment of melanoma and is undergoing numerous clinical trials for including amongst others: the treatment of non-small cell lung carcinoma (NSLC), small cell lung cancer, bladder cancer and prostate cancer. Check-point inhibitors provide a clear benefit to a proportion of treated patients, but cancer cures are still rare for many indications. It has been argued (and shown preclinically) that certain cytokine combinations (e.g., featuring the use of PEGylated products [237,238] or antibody fusions [180]) may turn “cold” tumors “hot” and may be used to potentiate immune-oncology drugs. L19-IL2 has been shown to effectively synergize with CTLA-4 blockade in mice with CT26 colon carcinoma [100]. Cured mice were able to reject subsequent rechallenge with the same tumor model which means that a protective long-term immunity was achieved. These experiments provide a first rationale for the clinical use of targeted cytokines with immune check-point inhibitors.

### 3.1.2.7. Immunocytokines in clinical trials

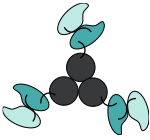
Many immunocytokines have been studied in mouse models of cancer, but relatively few products have entered clinical trials for oncological applications. Those products feature IL2, TNF or IL12 as immunomodulatory payloads. A list of clinical-stage antibody-cytokine fusions is shown in **Table 2**. Selected examples are described more closely in this section.

**Table 2:** List of immunocytokines in clinical trials

Compound	Generic Name	Antibody format	Antigen	Indications	Clinical trial identifier	Company	Literature
<b>Interleukin 2</b>							
Hu14.18-IL2	EMD 273063; APN301		GD2	Neuroblastoma, malignant melanoma	<b>Phase I:</b> NCT03209869, NCT00003750 <b>Phase II:</b> NCT00590824, NCT00109863, NCT00082758, NCT01334515	Merck KGaA	[239–241]

NHS-IL2LT	Selectikine; EMD 521873; MSB0010445		DNA/ Histone complex	Lung cancer, NSCL carcinoma, Non-Hodgkin lymphoma, melanoma	<b>Phase I:</b> NCT00879866, NCT01032681 <b>Phase II:</b> NCT01973608	Merck KGaA	[226,242]
huKS-IL2	Tucotuzumab celmoleukin; EMD 273066		EpCAM	Ovarian cancer, colorectal cancer, NSCL carcinoma, prostate cancer	<b>Phase I:</b> NCT00132522, NCT00016237	Merck KGaA	[243–246]
anti-CD20-IL2	DI-Leu16-IL2		CD20	Lymphoma	<b>Phase I:</b> NCT00720135 <b>Phase I/II:</b> NCT01874288 NCT02151903	Alopexx Oncology, LLC	[247–249]
L19-IL2	Darleukin		EDB	Solid tumors, lymphoma, melanoma, pancreas cancer, DLBCL	<b>Phase I:</b> NCT02086721, NCT01198522 <b>Phase I/II:</b> NCT02957019, NCT02076646, NCT01058538 <b>Phase II:</b> NCT02076633, NCT02735850, NCT01253096, NCT01055522 <b>Phase III:</b> NCT02938299	Philogen	[180,234,25 0–255]
F16-IL2	Teleukin		Tnc A1	AML, lung cancer	<b>Phase I:</b> NCT02957032, NCT03207191 <b>Phase I/II:</b> NCT01131364, NCT01134250 <b>Phase II:</b> NCT02054884	Philogen	[101,256– 259]
anti-CEA-IL2v	Cergutuzumab amunaleukin; RO6895882		CEA	Solid CEA+ cancers	<b>Phase I:</b> NCT02004106 NCT02350673	Roche Glycart	[260–264]
anti-FAP-IL2v	RO6874281; RG7461		FAP	Renal cell carcinoma, solid tumors, breast cancer, cancer of head and neck	<b>Phase I:</b> NCT03063762, NCT02627274 <b>Phase II:</b> NCT03386721	Roche Glycart	[261]
<b>Interleukin 12</b>							
NHS-IL12	M-9241		DNA/ Histone complex	Advanced solid tumors, malignant, epithelial tumors, malignant mesenchymal tumors	<b>Phase I:</b> NCT02994953, NCT01417546	Merck KGaA	[265]



BC1-IL12	AS1409		FN D7	Metastatic melanoma, metastatic renal cell carcinoma	<b>Phase I:</b> NCT00625768	Antisoma	[110,266–268]
<b>TNF</b>							
L19-TNF	Fibromun		EDB	Malignant melanoma, unresectable or metastatic soft tissue sarcoma	<b>Phase II:</b> NCT02076633, NCT03420014 <b>Phase III:</b> NCT02938299	Philogen	[44,45,234,253,254]

**Legend Table 2:** Clinical stage products. The format of the immunocytokine is depicted according to the color code of **Figure 6** with the exception of the  $C_H1-C_H3$  and  $C_HL$  domains which are depicted in blue. The indications for each biopharmaceutical are given as well as the clinicaltrial.gov identifier number. Abbreviations: GD2: disialoganglioside, EpCAM: epithelial cell adhesion molecule, EDB of fibronectin: alternatively-spliced extradomain B of fibronectin, Tnc A1: alternatively-spliced A1 domain of tenascin-C, CEA: carcinoembryonic antigen, FAP: fibroblast-activating protein, FN D7: domain 7 of fibronectin.

The only TNF-based immunocytokine in clinical development is L19-TNF (Fibromun). Fibromun is composed of the L19 antibody in scFv format specific for the EDB domain of fibronectin and human TNF [134,203]. TNF naturally forms a stable homotrimer and hence L19-TNF arranges into a trivalent antibody-cytokine fusion protein. Murine TNF fused to L19 has shown remarkable tumor targeting *in vivo* in preclinical experiments in mice with a tumor to blood ration of 100:1 (24 hours postinjection) and superior antitumor effects relative to untargeted TNF in various mouse models of cancer [95,122,134,178,203,235]. Fibromun is currently being studied in Phase III clinical trials for the *i.v.* treatment of patients with metastatic soft-tissue sarcoma in combination with doxorubicin (EudraCT number 2016-003239-38). Moreover, the product is being tested in a Phase III clinical trial in combination with L19-IL2 (Darleukin) for the intralesional administration to patients with fully-resectable stage IIIB/C melanoma (clinicaltrial.gov identifier NCT02938299, EudraCT number 2015-002549-72)[253,254].

When used as monotherapy in a Phase I/II clinical study, L19-TNF was well tolerated as up to 1 mg doses per patient and the maximum tolerated dose (MTD) was not reached [44]. Tumor stabilizations were recorded but no objective tumor responses were observed [44]. The same

product, when used in isolated limb perfusion in combination with melphalan in patients with locally advanced extremity melanoma, induced objective responses in 89 % of the patients [269] at a dose which was more than ten times lower compared to the one of recombinant TNF used for similar procedures [270]. An *ex vivo* immunohistochemical analysis of tumor lesions confirmed a preferential localization of L19-TNF to the tumor neo-vasculature [269].

The clinical development of L19-TNF in combination with doxorubicin for the treatment of soft-tissue sarcoma is motivated by the high sensitivity of sarcoma lesions to TNF [271] and by the observation of cancer cures in immunocompetent mouse models of the disease [102,154]. Interestingly, mechanistic studies in mice revealed the upregulation of cytotoxic CD8+ T cell specific for a common endogenous retroviral antigen AH1 (derived from the gp70 envelope protein of the murine leukemia virus) upon treatment with F8-TNF and doxorubicin [102]. Such retroviral sequences have been found in the genome of all vertebrate species and their expression has been associated with autoimmune diseases and chronic infection [272–274] as well as with cancer [275,276]. Furthermore, cytolytic CD8+ T cells specific for retroviral antigens, which potently lysed melanoma cells, have already been detected in patients [277]. These facts raise the question if, similar to the mouse model, specific CD8+ T cells against retroviral antigens could also be increased in patients after L19-TNF treatment, which could then contribute to tumor eradication.

When used in combination with L19-IL2, the intralesional administration of L19-TNF showed potent therapeutic activity [234]. A potent anticancer activity was seen not only in injected lesions, but also in a high proportions of non-injected lesions, suggesting that the product may be able to induce a systemic anti-cancer protective immunity [234].

DI-Leu16-IL2 (an immunocytokine specific to the CD20 antigen expressed on B cells and on certain B cell malignancies) showed remarkable superior anticancer activity compared to 25-fold higher doses of an anti CD20 immunocytokine combined with untargeted IL2 in mouse model of human B lymphoma [213]. When tested in B cell lymphoma patients, 5 out of 13 patients showed a partial response (PR, 2/13) or a complete response (CR, 3/13)[247]. Hu14.18-IL2, a product with similar molecular format (IgG-IL2 fusion) but specific to GD2 (a disialoganglioside which is abundantly expressed on tumors of neuroectodermal origin and

normally found only in the cerebellum and peripheral nerves), was studied in a Phase II clinical trial for children with relapsed or refractory neuroblastoma. No responses were detected in 13 children with bulky disease, but 5 out of 23 children with less prominent but still evaluable disease showed a CR [239].

Roche has focused on antibody-IL2 fusions based on intact IgG formats, but the company has preferred to use mutated versions of IL2, which display reduced binding affinity to the alpha subunit of the IL2 receptor (CD25)[112,174,175,278]. This choice was motivated by the fact that CD25 is highly expressed on regulatory T cells (T<sub>reg</sub>). Preferential binding of IL2 fusions to those cells could result in immunosuppressive effects, as suggested by the clinical experience with low-dose IL2 in patients with graft-vs-host responses [279]. In order to generate products with a single cytokine payload, researchers at Roche employed “knob-into-hole” technology [280], favoring heterodimer formation between one antibody heavy chain devoid of IL2 and a second antibody heavy chain, fused to the cytokine payload [Table 2]. Two products, targeting the CEA in colorectal cancer (CEA-IL2v) or FAP (FAP-IL2v) in various types of malignancies, are currently being investigated in clinical trials, alone or in combination with atezolizumab (anti PD-L1 antibody, clinicaltrial.gov identifier: NCT02350673, NCT03063762, NCT03386721), trastuzumab (anti HER-2 antibody, clinicaltrial.gov identifier: NCT02627274), or cetuximab (anti EGFR antibody, clinicaltrial.gov identifier: NCT02627274).

Merck KGaA has also developed a fusion protein (NHS-IL2LT) in IgG format, featuring two mutant IL2 payloads at the C-terminal end. A single mutation (D20T) in the IL2 domain was introduced in order to decrease vascular toxicity by eliminating the toxin motif that binds endothelial cells [123]. Interestingly, this mutation also increased the specificity for activating the high-affinity IL2 receptor thus preferentially binding to activated T cells [123,281]. However, Tregs (which bear the high-affinity receptor) are also activated and thus the potential problem of stimulating more Tregs than antitumor effector cells remains. NHS-IL2LT binds to DNA-histone complexes, which become exposed and accessible in necrotic tissues (a characteristic feature of many rapidly-growing solid tumors)[123,282]. In a Phase I clinical trial with patients bearing localized or metastatic refractory solid tumors, NHS-IL2LT mediated a prolonged disease stabilization in a proportion of patients, but no objective tumor responses were reported [226].

L19-IL2 is an antibody-IL2 fusion in diabody format, which has been studied in various clinical trials, both as monotherapy or in combination with other modalities. The tumor-homing properties of the fusion protein were characterized by quantitative biodistribution studies with radiolabeled protein preparations [94]. Moreover, the parental L19 antibody has been used to image more than 100 patients with different types of malignancies [76,80,283]. In preclinical studies, L19-IL2 strongly reduced tumor growth in various mouse models of cancer [94,122,181,229,235], but was rarely able to completely eradicate cancer when used as single agent. A microscopic analysis of tumor lesions revealed a rich infiltrate of NK cells and T cells within the neoplastic mass, which was clearly different from the one observed with recombinant IL2 or with IL2 fusions with antibodies of irrelevant specificity in the mouse [94]. In a monotherapy study in patients with renal cell carcinoma, stable disease was observed in 83 % patients after 2 cycles (total 6 infusions) of L19-IL2 [250]. Treatment was well tolerated with manageable toxicities that resolved within hours or days after L19-IL2 administration.

L19-IL2 has also been used in combination with other modalities, including L19-TNF (as described above). The combination of L19-IL2 with dacarbazine has led to encouraging results for the treatment of patients with stage IV melanoma [251]. On the basis of those results, a controlled Phase II trial has been initiated (EudraCT number 2012-004495-19). Preclinical findings have shown that L19-IL2 was able to potentiate the therapeutic activity of external beam radiation, promoting an abscopal effect [227]. A clinical study, featuring the administration of L19-IL2 after stereotactic ablative radiotherapy, has recently begun, in the frame of the European Union IMMUNOSABR project. A potent synergistic effect has also been observed when combining L19-IL2 with the anti-CD20 antibody rituximab [72]. A high local concentration of IL2 within the tumor mass promotes the influx and activation of certain leukocytes, including NK cells (which are crucially important for antibody-dependent cell cytotoxicity). A Phase Ib clinical trial (clinicaltrials.gov identifier NCT02957019), featuring the administration of L19-IL2 and rituximab to patients with relapsed or refractory diffuse large B-cell lymphoma, has recently started.

F16-IL2 is a fusion protein with a format, which is similar to the one of L19-IL2. The immunocytokine consists of a diabody fused to two IL2 moieties which targets the

alternatively spliced A1 domain of tenascin-C [116]. This antigen is overexpressed in many cancer types but virtually undetectable in normal tissue [284,285]. The F16 antibody selectively accumulates at neo-vascular tumor sites in animal models and most human breast, lung, and head/neck cancers [116,117,284–286]. In a xenograft model of human breast cancer in mice, F16-IL2 showed potent therapeutic activity alone as well as in combination with doxorubicin and paclitaxel [116]. In combination with temozolomide, F16-IL2 exhibited a strong antitumor activity in subcutaneous and intracranial glioblastoma xenografts [117]. F16-IL2 is now extensively being studied in several clinical trials. F16-IL2 is being investigated in combination with doxorubicin (clinicaltrial.gov identifier NCT01131364) or paclitaxel (clinicaltrial.gov identifier NCT02054884, NCT01134250, EudraCT number 2012-004018-33) in patients with solid tumors or metastatic breast cancer [256,258,259], with low dose cytarabine (clinicaltrial.gov identifier NCT02957032) or with BI 836858 (an anti CD33 antibody, clinicaltrial.gov identifier NCT03207191) in AML [101,257] and with nivolumab (anti PD-1 inhibitor)[255] in non-small cell lung carcinoma patients.

The only two products in clinical trials based on IL-12 are NHS-IL12 and BC1-IL12. NHS-IL12 [183,184] is specific for DNA-histone H1 complex exposed in necrotic tumors. In a preclinical experiment, NHS-IL12 was able to achieve a partial response in 2 out of 11 canines with spontaneously occurring solid tumors by a single injection [265]. In order to determine the maximum tolerated dose in humans, NHS-IL12 is now being investigated in Phase I clinical trials, alone (clinicaltrial.gov identifier NCT01417546) or in combination with the immune check-point inhibitor avelumab (clinical trial identifier NCT02994953)[265].

BC1-IL12 targets a cryptic epitope on domain 7 of fibronectin, which becomes exposed in the presence of the alternatively-spliced EDB domain [110,285,287]. The BC1 antibody is a humanized version of the parental murine BC1 product that has been used for immunoscintigraphy to image tumors in glioblastoma patients [268]. The tumor-homing properties of the humanized BC1 antibody in full IgG format, linked to the dimeric IL12 at the C-terminus of the heavy chain, have been characterized in tumor-bearing mice, using quantitative biodistribution studies [182]. In a Phase I clinical trial, BC1-IL12 induced a disease stabilization for at least 4 months in 6 out of 11 patients with malignant melanoma [266]. Only one patient had achieved a sustained partial response 17 months later [266]. The

product was well tolerated [266], with pyrexia (85 %), fatigue (92 %), chills (62%), nausea (50 %), vomiting (62 %) and transient liver function abnormalities (77 %) as main toxicities being observed in the majority of patients. IFN- $\gamma$  and CXCL10 concentrations were elevated in the serum of all patients, thus indicating a cell-mediated immune response, which is in line with previous preclinical observations [205].

#### 3.1.2.8. Potential drawbacks of immunocytokines and possible strategies to minimize them

Immunocytokines are promising biopharmaceuticals but, like cytokine products, can cause side effects in patients. These side effects may vary, to a certain extent, from cytokine to cytokine, due to differences in mode of action. Pro-inflammatory agents are typically active on the vasculature and it is not surprising that hypotension was reported as one of the limiting toxicities for clinical-stage antibody-cytokine fusions [239]. Similarly, cytokine payloads may cause flu-like symptoms, nausea and vomit [242,266,288].

There are substantial differences in the way recombinant cytokines were used and current procedures for antibody-based fusions. For example, the high-dose IL2 regimen of Rosenberg and colleagues features the administration of up to 800 million international units (Mio IU) of IL2 in one week which is repeated after one week of rest [289,290]. By contrast, various antibody-IL2 fusions have been administered at weekly doses in the 67.5-110-Mio IU/m<sup>2</sup> range for more than 6 months [239,250].

The side effects of immunocytokines are influenced not only by the pharmacokinetic properties of the product, but also by the administration schedule and by the animal species. For example, different mouse strains exhibit variations in the maximal tolerated dose. In general, side effects are associated with peak concentrations of the product in blood. It is therefore tempting to hypothesize that immunocytokines may display a non-linear toxicity profile and that the products may be better tolerated when administered with slow infusion procedures. There is initial clinical evidence in support of this hypothesis. For example, the maximal tolerated dose (MTD) of L19-IL2 was found to be 22.5 Million International Units of IL2 equivalents in clinical trials with 1 hour infusion regimens [250], while three-fold higher

doses could be safely administered to patients, using a 3-hour infusion protocol (unpublished results).

Immunocytokine products based on antibody fragments (e.g., L19-IL2, L19-TNF, F16-IL2) were found to be not immunogenic in clinical trials [250,251,256,291]. Interestingly, a small set of patients who developed a low human antibody titer against the fusion proteins subsequently lost this reactivity upon continuation of the treatment at later cycles, possibly pointing to an induction of tolerance [291]. These findings are robust, as they were confirmed both by sandwich ELISA and by BIAcore. A similar immunogenicity study has been performed on hu14.18-IL2, an immunocytokine product based in IgG format. In this case, anti-immuncytokine antibodies were found in most patients, but they did not induce allergic reactions or increase toxicity [292].

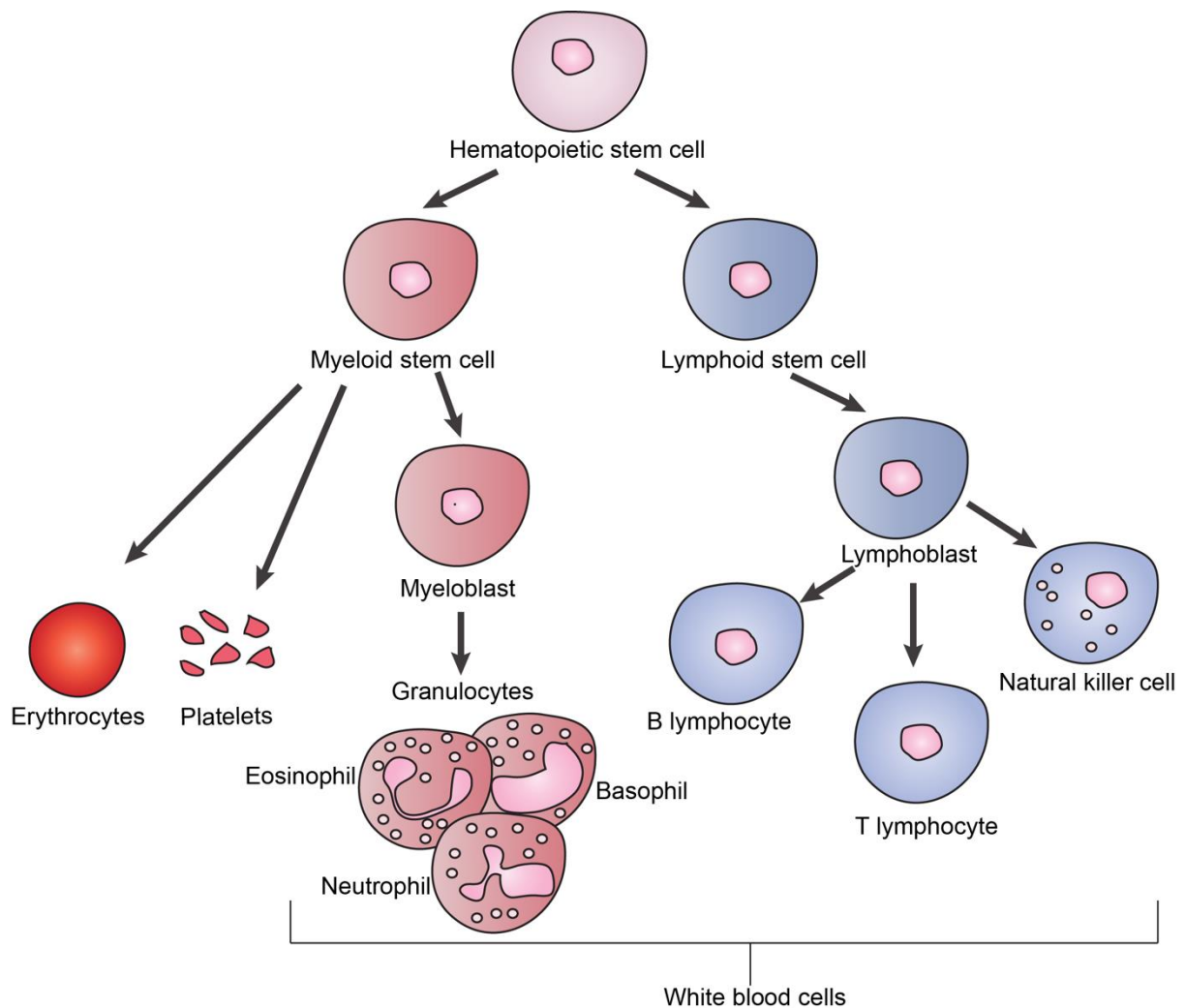
Looking at the future, strategies that provide “activity-on-demand” for immunocytokine products may be particularly attractive. Ideally, antibody fusions would gain activity at the site of disease, upon antigen binding. Strategies that have been proposed include the use of “split cytokine” payloads [293] and allosteric modulation of cytokine activity upon antigen binding [69]. It is also possible that combination treatments may allow the use of immunocytokine products at doses which are well below the MTD.

## 3.2. Acute Myeloid Leukemia

### 3.2.1. Leukemia overview

Leukemia (greek for λευκος= white and αιμα= blood) is a group of cancer that is characterized by an abnormal increase of white blood cells [294,295]. It forms in the blood-forming tissues such as the bone marrow [294]. A broad classification of leukemia is based on the cell of origin (e.g., myeloid or lymphoid) and the rate of disease progression (e.g. acute or chronic)[296]. With this rough classification, acute lymphoid leukemia (ALL), chronic lymphoid leukemia (CLL), acute myeloid leukemia (AML) and chronic myeloid leukemia (CML) can be distinguished from each other. Lymphoid leukemia is formed by cell types of the lymphoid blood lineage whereas myeloid leukemia is formed by cells of the myeloid blood lineage. A blood stem cell may become a myeloid stem cell that gives rise to red blood cells, platelets and granulocytes (eosinophils, basophils, neutrophils) or a lymphoid stem cell that eventually forms B or T lymphocytes or natural killer (NK) cells **[Figure 7]**[297].



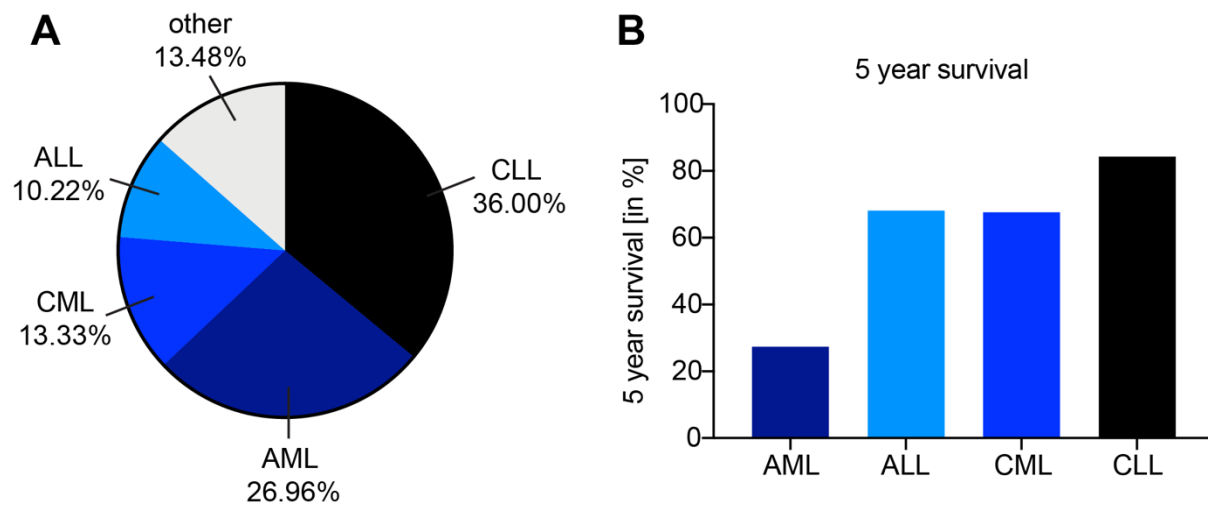


**Figure 7:** The development of the blood cells. A hematopoietic stem cell may become a myeloid or lymphoid stem cell. The myeloid cell lineage results in the production of erythrocytes, platelets and granulocytes. The lymphoid cell lineage yields B and T lymphocytes and natural killer cells (adapted from [297]).

Acute forms of leukemia progress rapidly. Symptoms of acute leukemia appear relatively quickly since it involves immature cells that are aberrant. Chronic leukemia is usually caused by more mature cell types that may still carry out some of their normal functions. Chronic leukemia develops over a longer time than acute leukemia and the disease and symptoms get worse at a slower rate.

The relative incidence rate [Figure 8A] shows that CLL is the most prevalent form (36 %) of leukemia followed by AML (27 %). Although CLL is the most prevalent form of leukemia, it has

also the highest 5-year survival rate (84.2%). In contrast, AML is not only the second most prevalent form of leukemia, it has also the lowest 5-year survival rate (27.4%) [Figure 8B].

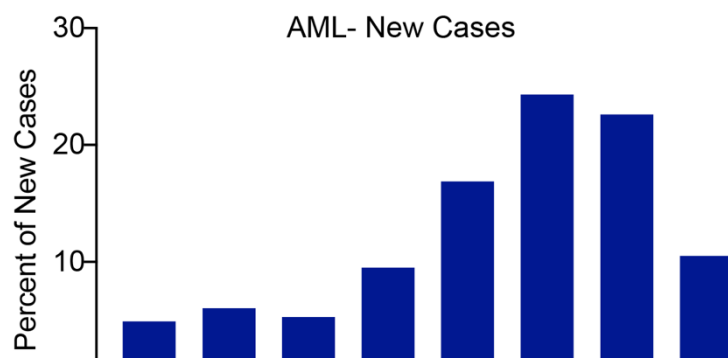


**Figure 8:** Leukemia statistics. **A** The relative incidence rates (in %) indicate that CLL is the most prevalent form of leukemia followed by AML. **B** The 5 year survival (in %) shows that AML has the worst 5 year survival of the four leukemia forms (AML, ALL, CML, CLL).[298].

While the most common leukemia diagnosed in adults are CLL and AML, ALL is most common in children and adolescents [299].

### 3.2.1.1. Disease and classification of AML

Acute myeloid leukemia (AML) is a group of hematopoietic neoplasms which are formed from progenitor cells committed to the myeloid lineage. With an incidence of 4.3 per 100'000 men and women (age-adjusted to the 2000 US standard population) AML accounts for 1.8 % of all cancer deaths [298]. AML can occur at any age but the incidence rises with increasing age



**Figure 9:** The incidence of AML rises with increasing age (adapted from [298])

[Figure 9] and it is most frequently diagnosed among people aged 65-74 with a median age at diagnosis of 68 [298]. The incidence of AML is slightly higher in males (5.2 per 100'000 persons) than females (3.6 per 100'000)[298].

AML is diagnosed if more than 20 % myeloid blasts can be identified in the bone marrow and/or peripheral blood [300]. Two systems have been used to classify AML into subtypes. The older, the French-American-British (FAB) classification uses the cell morphology and the degree of differentiation to group acute leukemias [Table 3][301].

**Table 3:** The French-American-British classification groups acute leukemias according to the morphology and the degree of differentiation (adapted from [301]).

FAB subtype	Name
M0	Undifferentiated acute myeloblastic
M1	Acute myeloblastic leukemia with minimal maturation
M2	Acute myeloblastic leukemia with maturation
M3	Acute promyelocytic leukemia
M4	Acute myelomonocytic leukemia
M4 eos	Acute myelomonocytic leukemia with eosinophilia
M5	Acute monocytic leukemia
M6	Acute erythroid leukemia
M7	Acute megakaryoblastic leukemia

A newer system is based on the World Health Organization (WHO) classification of 2008 which considers molecular genetics, morphological, cytogenetics and immunological markers with the additional aim to deliver a prognostic value [Table 4] [302].

**Table 4:** The WHO classification of AML adapted from [302]. *t* = translocation, *inv*= inversion

<p><b>AML with recurrent genetic abnormalities:</b></p> <ul style="list-style-type: none"> <li>• AML with t(8;21), <i>RUNX1-RUNXT1</i></li> <li>• AML with inv(16)(p13.1q22) or t(16;16)(p13.1;q22); <i>CBFB-MYH11</i></li> <li>• APL with t(15;17)(q22;q23); <i>PML-RARA</i></li> <li>• AML with t(9;11)(p22;q23); <i>MLLT3-MLL</i></li> <li>• AML with t(6;9)(p23;q34); <i>DEK-NUP214</i></li> </ul>
--

- AML with inv(3)(q21q26.2) or t(3;3)(q21;q26.2); *RPN1-EVI1*
- AML (megakaryoblastic) with t(1;22)(p13;q13); *RBM15-MKL1*
- Provisional entity: AML with mutated *NPM1*
- Provisional entity: AML with mutated *CEBPA*

**Acute myeloid leukemia with myelodysplasia-related changes**

**Therapy-related myeloid neoplasms** (patients that previously had chemotherapy and/or radiation)

**Acute myeloid leukemia, not otherwise specified** (this group includes cases of AML that do not fall into one of the above mentioned classes and it is similar to the FAB classification):

- AML without maturation (M0)
- AML with minimal differentiation (M1)
- AML with maturation (M2)
- Acute myelomonocytic leukemia (M4)
- Acute monoblastic/monocytic leukemia (M5)
- Acute erythroid leukemia (Pure erythroid leukemia/ Erythroleukemia) (M6)
- Acute megakaryoblastic leukemia (M7)
- Acute basophilic leukemia
- Acute panmyelosis with myelofibrosis

**Myeloid sarcoma** (chloromas)

**Myeloid proliferations related to Down syndrome**

**Acute leukemias of ambiguous lineage** (these leukemias contain both lymphocytic and myeloid characteristics)

Prognostic factors, such as chromosomal abnormalities and gene mutations, are used to determine the risk of disease recurrence. For example, a patient carrying a translocation between chromosome 8 and 21 usually has a good prognosis whereas a patient with an internal tandem duplication of the *FLT3* gene has a higher relapse rate [303]. Cytogenetic and molecular genetic data can be used to define 4 general risk groups (favorable, intermediate-I, intermediate-II, adverse) [Table 5].

**Table 5:** Cytogenetic and molecular genetic data allows the classification of AML into 4 general risk groups (adapted from [304]). \* = AML with normal karyotype, t(a;b) = translocation between chromosome a and b, inv(a) = inversion of chromosome a, ITD= internal tandem duplication

Genetic group	Subsets
---------------	---------

<b>Favorable</b>	t(8;21)(q22;q22); <i>RUNX1-RUNX1T1</i> inv(16)(p13.1q22) or t(16;16)(p13.1;q22); <i>CBFB-MYH11</i> Mutated <i>NPM1</i> without <i>FLT3-ITD</i> * Mutated <i>CEBPA</i> *
<b>Intermediate-I</b>	Mutated <i>NPM1</i> and <i>FLT3-ITD</i> * Wild-type <i>NPM1</i> and <i>FLT3-ITD</i> * Wild-type <i>NPM1</i> without <i>FLT3-ITD</i> *
<b>Intermediate-II</b>	t(9;11)(p22;q23); <i>MLLT3-MLL</i> cytogenetic abnormalities not classified as favorable or adverse
<b>Adverse</b>	inv(3)q(21q26.2) or t(3;3)(q21;q26.2); <i>RPN1-EVI1</i> t(6;9)(p23;q34); <i>DEK-NUP214</i> t(v;11)(v;q23); <i>MLL</i> rearranged -5 or del(5q); -7; abn(17p); complex karyotype

Other factors that have an adverse prognosis include higher age (remission rates are inversely related to age), markers of the cells (such as the progenitor cell antigen CD34), increased white blood cell count ( $>100,000/m^3$ ), systemic infections at diagnosis, leukemia cells which have spread into the central nervous system and a history of myelodysplastic syndrome [303,304].

Symptoms of AML are caused by a shortage of normal blood cells (e.g., shortness of breath, pale skin), reduced platelet count (e.g., prolonged bleeding or easy bruising), low neutrophil counts (frequent infections) and high number of leukemia cells (e.g., bone and/or joint pain, splenomegaly, hepatomegaly) [305]. Unspecific symptoms include night sweat, fatigue, loss of appetite and weight [305].

#### 3.2.1.2. Treatment of AML

The standard pharmacotherapy regimen for AML patients is typically composed of an “induction phase” to achieve a complete remission (usually defined when the bone marrow blasts  $< 5\%$ , absence of extramedullary disease, absolute neutrophil count  $> 1000/\mu l$ , platelet count  $> 100000/\mu l$ ), followed by a “consolidation phase” to maintain this response [304].

#### 3.2.1.2.1. Induction therapy

The standard induction therapy consists of 3 days of an anthracycline (e.g., daunorubicin 45-60 mg/m<sup>2</sup>, or an alternative anthracycline at equivalent dose such as idarubicin) followed by 7 days of cytarabine (100-200 mg/m<sup>2</sup> continuous IV). This is called the “3+7 regimen”, which is routinely adapted since 1973 [304,306]. Complete response (CR) is achieved in 60- 80% of younger adults (age 18- 60) and in 50% of older adults (age 60- 74). In younger adults, no other induction therapy has been shown to be better so far [304]. Only the use of higher dose of daunorubicin (60 mg/m<sup>2</sup>) results in a higher rate of complete remission (age group 17-60: 70 % vs 57% and in age group 60-83: 64 % vs 54 %) and improved overall survival (age group 17-60: 23.7 vs 15.7 months, age group 60-83: no significant difference) compared to the standard dose of the drug without a higher rate of serious adverse events [307,308]. For patients older than 75 years of age, the chances of a cure with the “3+7 regimen” is estimated to be less than 10% [309]. Older patients (60 years +) typically exhibit more comorbidities and therapeutic resistance (probably due to differential chemotherapy metabolism) than younger patients [309]. They often display a higher incidence of unfavorable chromosomal abnormalities and suffer more often from treatment-related death (up to 25%) [304]. In the elderly population, patient-specific fitness is an important criteria in the decision for the treatment. Alternative therapies should be considered for patients which are not fit for the intensive standard therapy. However in a randomized trial, low-dose cytarabine (20 mg twice daily, s.c for 10 days) was still better than hydroxyurea (18 % vs 1 %) and supportive care in achieving CR in this patient group [310].

#### 3.2.1.2.2. Post-remission strategy

Various post-remission strategies have been tested including high-dose cytarabine (HiDAC,  $\geq 1000$  mg/m<sup>2</sup>), prolonged maintenance chemotherapy and high dose chemotherapy followed by autologous or allogeneic hematopoietic stem cell transplantation (allo-HSCT) [300,304]. Allo-HSCT is associated with the lowest relapse rate in patients younger than 60 years and induces a significant better overall survival in patients with intermediate- and high-risk AML compared to alternative post-remission strategies [304]. Treatment-related mortality for allo-HSCT is high (varies between 15% to 50%) and the decision to perform a allogeneic HSCT has to be carefully considered, taking cytogenetics, fitness and comorbidities into account [304]. Patients with favorable-risk AML (according to cytogenetic and molecular

genetic risk criteria mentioned in **Table 5**) are usually not subjected to allogeneic HSCT unless the transplant risk is low [304]. Instead, a common post-remission therapy that consist of repetitive cycles of HiDAC is pursued.

#### 3.2.1.2.3. Alternative strategies and novel therapeutics

In spite of progress in the treatment of AML, this cancer type remains potentially lethal for patients who do not benefit from a successful bone marrow transplant or for the elderly population, which cannot receive a bone marrow (BM) allograft [311]. There is an urgent need to develop new therapeutic agents that display a biocidal activity against AML cells, while sparing normal tissues, as conventional chemotherapeutic agents are often unable to promote durable complete remissions [312]. Several strategies are being explored including FLT3 inhibitors (e.g., sorafenib, midastaurin, quizartinib), hypomethylating agents, and checkpoint inhibitors [**Table 6**] [300]. Monoclonal antibodies have also been considered as biopharmaceuticals for the treatment of AML. For example, immunoglobulins directed against CD33, CD117 or CD123 have been investigated for antibody-dependent cell-mediated cytotoxicity (ADCC) applications, in spite of the fact that those surface antigens are also found on the surface of hematopoietic stem cells [311]. Moreover, products based on “armed” antibody have been developed for AML treatment, including antibody-drug conjugates (ADCs), bispecific antibodies and Chimeric Antigen Receptor-T cells (CAR-Ts) [311]. For instance, Mylotarg<sup>®</sup> is an ADC product which has been approved for the treatment of relapsed or refractory CD33-positive AML, while several other antibody therapeutics are currently being studied in clinical trials in AML patients.

**Table 6:** *Potential targets and selected therapeutics for the treatment of AML ([300,313,314]).*  
*PD-1: programmed cell death 1, PD-L1: programmed cell death ligand 1, LAG-3: lymphocyte-activation gene 3, IDH: isocitrate dehydrogenase, MDM2: mouse double minute 2 homolog, MLL: mixed lineage leukemia, CXCR4: C-X-C chemokine receptor type 4, DOT1L: DOT1-like histone H3 methyltransferase, BET: bromodomain and extraterminal domain family, PI3K, phosphoinositide 3-kinase; MEK: mitogen/ extracellular signal-regulated kinase, TET2: Tet*

*methylcytosine dioxygenase 2, FLT3: fms-related tyrosine kinase 3, DNMT3A: DNA-methyltransferase 3 alpha*

Target	Therapeutic	Strategy
CD25	ACDT-301	Antibody drug conjugate
CD27	CDX-1127	Naked IgG
CD33	BI 836858	Naked IgG
	Gemtuzumab ozagomicin	Antibody drug conjugate
	SGN-33	Naked IgG
	SGN-33A	Antibody drug conjugate
	<sup>90</sup> Y/ <sup>213</sup> Bi/ <sup>225</sup> Ac-SGN-33	Radioimmunoconjugates
	IMGN779	Antibody drug conjugate
CD45	BC8	Radioimmunoconjugate
CD56	IMGN770	Antibody drug conjugate
CD70	ARGX-110	Naked IgG
CD98	IGN523	Naked IgG
CD123	CSL362	Naked IgG
	SL-401	Cytokine toxin fusion protein
	KHK2823	Naked IgG
	SGN-CD123A	Antibody drug conjugate
	IMGN632	Antibody drug conjugate
	XmAB14045	Bispecific antibody
	MGD006	Bispecific antibody
	JNJ63709178	Bispecific antibody
	UCART123	CAR-T cell
	MB-102	CAR-T cell
CD152 (CTLA-4)	Ipilimumab, tremelimumab	Check-point inhibitor
CD274 (PD-L1)	Durvalumab, atezolizumab, avelumab	Check-point inhibitor
CD279 (PD-1)	Nivolumab, pembrolizumab	Check-point inhibitor
CXCR4	BL-8040	Peptide
DNMT3a	Decitabine	Hypomethylating agent
	5-azacytidine	Hypomethylating agent
FLT3	Sorafenib	Small molecule kinase inhibitor
	Midostaurin	Small molecule kinase inhibitor
	Quizartinib	Small molecule kinase inhibitor
	Crenolanib	Small molecule kinase inhibitor
IDH1	AG-120	Small molecule



IDH2	Venetoclax	Small molecule
	AG-221	Small molecule
LAG3	Check-point inhibitor	Naked IgG
MDM2	RG7388	Small molecule
	RG7112	Small molecule
MEK	MEK162	Small molecule kinase inhibitor
	Trametinib	Small molecule kinase inhibitor
MLL	DOT1L inhibitor	Small molecule
	BET inhibitors	Small molecule
PI3K	BYL719	Small molecule
RAS	Trametinib	Small molecule kinase inhibitor
TET2	5-azacytidine	Hypomethylating agents

### 3.2.1.3. CD123 as a novel target for the treatment of AML

The  $\alpha$  chain of interleukin 3 receptor (IL3RA or CD123) is overexpressed in a variety of hematological disorders including AML, chronic myeloid leukemia, B-lymphoid leukemia, blastic plasmacytoid dendritic neoplasms and hairy cell leukemia [315]. CD123 was first reported as unique surface marker for CD34+CD38- acute myelogenous leukemia stem cells (LSCs) [316] and was later shown to be also overexpressed on AML blasts compared to normal HSCs and myeloid progenitors [317,318]. High levels of CD123 correlate with an adverse prognosis [319,320]. For these reasons, pharmaceutical companies have considered CD123 as a target for the development of biopharmaceuticals. Clinical-stage ADCs directed against CD123 include SGN-CD123A and IMG632 [314]. In addition, bispecific antibody products (e.g., XmAB14045, MGD006, JNJ63709178)[321–323], CAR-T cells (e.g., MB-102, UCART123)[324,325], as well as “naked” IgGs with enhanced ADCC activity (CSL362, KHK2823) have started clinical development programs [314]. CSL362 (Talacotuzumab) was the first anti-CD123 antibody to be tested in patients. CSL362 is derived from a parental murine monoclonal antibody, that has been humanized, affinity-matured and ADCC-potentiated by the insertion of S293D and I332E substitutions in the Fc region [326]. The industrial development of CSL362 has been discontinued, because of unfavorable risk/ benefit profiles *in vivo* [327].

### 3.3. Aim of the thesis

Within this thesis, two independent research projects were performed. In a first project, an existing therapeutic, namely F8-IL2, was studied in combination with immune check-point inhibitors in tumor-bearing mice. In a second project, a new therapeutic was developed for the treatment of AML.

#### Project 1: F8-IL2 in combination with immune-check-point inhibitors

Systemic high-dose IL2 is able to elicit complete responses in patients suffering from metastatic melanoma [328]. However, the majority of patients cannot receive the whole treatment dose due to severe toxicities [41,329]. Other approved drugs such as chemotherapeutics [330] and immune check-point inhibitors [331,332] also provide a clear benefit to patients, but cancer cures are still rare. Therefore, targeting IL2 to the site of disease represents a promising strategy to circumvent its toxicity and maximize efficacy.

Our laboratory has previously described two fusion proteins (F8-IL2 and L19-IL2), featuring antibodies in diabody format fused to IL2 and expressed in mammalian cells [94,115,172], which recognize the alternatively-spliced EDA and EDB domains of fibronectin, respectively. These extra-domains of 91 amino acids are conserved from mouse to human [333] and are expressed in the majority of aggressive solid tumors and lymphomas while being undetectable in normal tissue, with the exception of the female reproductive system (placenta, endometrium, and some ovarian vessels) [334]. Both F8-IL2 and L19-IL2 have shown single-agent activity in various immunocompetent mouse models of cancer [94,101,115,178], and these products can potently synergize with certain cytotoxic agents [101,172], external beam radiation [227], intact immunoglobulins working through ADCC mechanisms [72], as well as other antibody-cytokine fusions [93,178,179]. The disease-homing properties of the parental L19 and F8 antibodies have been extensively characterized in mouse models and in patients using nuclear medicine procedures [76,77,101,115,283,335].

The aim of the first part of the thesis was to study the anti-cancer activity of F8-IL2 in combination with antibodies directed against murine PD-1, PD-L1, and CTLA-4 in

immunocompetent mice bearing syngeneic tumors. The immune checkpoint inhibitors against the PD-1/ PD-L1 (nivolumab, pembrolizumab, atezolizumab, durvalumab, avelumab) or CTLA-4 (ipilimumab, tremelimumab) pathway served as murine surrogates for successful biopharmaceuticals, which are increasingly being used for the treatment of patients with various types of malignancies [236].

The work was published in:

Hutmacher and Neri, **Targeted Interleukin 2 and synergy with immune check-point inhibitors [abstract]**; *Cancer Res* (2018),78(13 Suppl): Abstract nr 3811

Hutmacher and Nuñez et al., **Targeted Delivery of IL2 to the Tumor Stroma Potentiates the Action of Immune Checkpoint Inhibitors by Preferential Activation of NK and CD8+ T Cells**, *Cancer Immunol Res* (2019), *In Press*

Project 2: New therapeutics for the treatment of AML

In spite of progress in the treatment of acute myeloid leukemia (AML), this cancer type remains potentially lethal for patients who do not benefit from bone marrow (BM) transplantation or for the elderly population, which cannot tolerate high-dose chemotherapy nor receive allogeneic BM graft [336]. Moreover, conventional chemotherapeutic agents are often unable to promote durable complete remissions [312]. Therefore, there is an urgent need to develop new therapeutic agents that display a biocidal activity against AML cells, while sparing hematopoietic stem cells (HSCs).

Our laboratory has performed a surface proteome analysis of myeloid leukemia cell lines and presented an atlas of potential targets for the treatment of AML [337]. One of the identified antigens, CD123, was already known to be overexpressed in AML and to be correlated with a worse prognosis based on literature research [317–320]. Several pharmaceutical companies have developed biopharmaceuticals that target CD123 including intact immunoglobulins [314], bispecific antibodies [321–323], CAR-T cells [324,325], and ADCs [314]. The aim of this project was to produce and characterize a new and fully-human anti-CD123 antibody for the treatment of AML.

The work has recently been submitted for publication:

Hutmacher et al., **Development of a novel fully-human anti-CD123 antibody to target acute myeloid leukemia**, *submitted*

## 4. Results

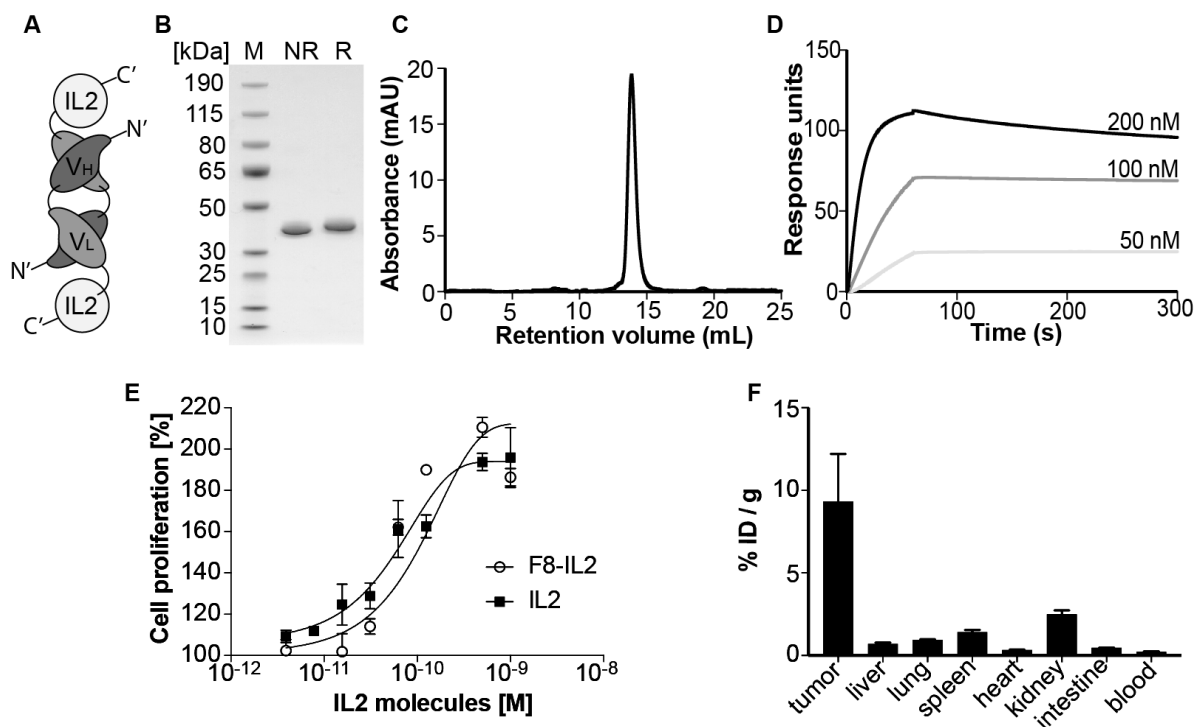
### 4.1. F8-IL2 in combination with immune-check-point inhibitors

This chapter has been adapted from

Hutmacher and Nuñez et al., **Targeted Delivery of IL2 to the Tumor Stroma Potentiates the Action of Immune Checkpoint Inhibitors by Preferential Activation of NK and CD8+ T Cells**, *Cancer Immunol Res* (2019), *In Press*

#### 4.1.1. Product characterization

The fusion protein composed of the F8 antibody specific to the extra-domain A of fibronectin and human IL2 in diabody format (F8-IL2) was produced as previously described by our group [115] and purified to homogeneity. **Figure 10A** shows a schematic illustration of the non-covalent homodimer, formed by the antibody-IL2 fusion in diabody format.



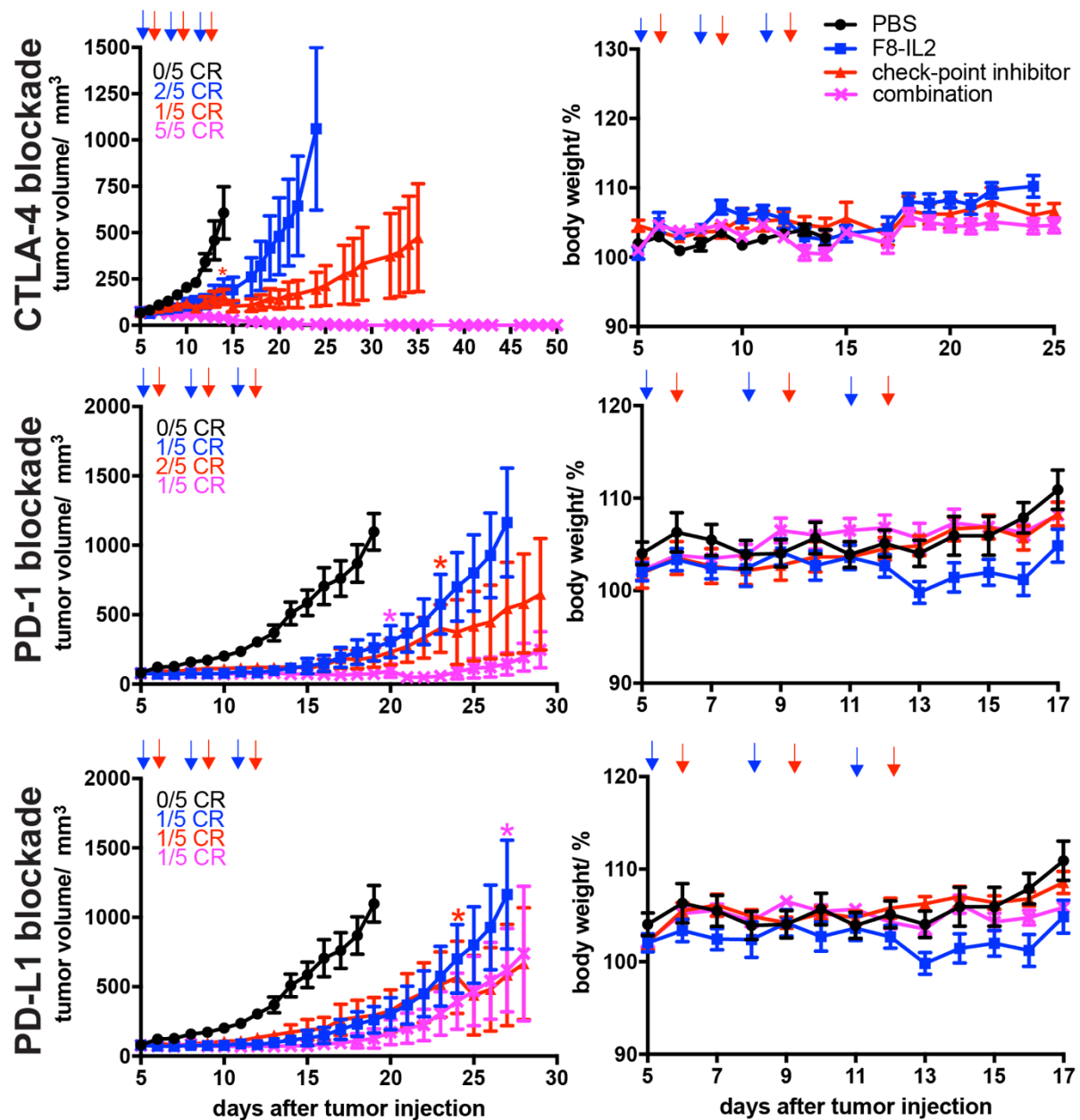
**Figure 10: In vitro and in vivo characterization of F8-IL2.** (A) Schematic domain assembly of the F8-IL2 in diabody format. (B) SDS-PAGE analysis of purified F8-IL2 under nonreducing (NR) and reducing (R) conditions. M = Marker. (C) Size-exclusion chromatography profile. (D) BIAcore analysis of F8-IL2 on EDA-coated chip. (E) CTLL2 cell proliferation assay. The biological

activity of the IL2 moiety was assessed by its capability to stimulate proliferation of CTLL2 cells. Starved CTLL2 cells were seeded in triplicates in 96-well plates in culture medium supplemented with different concentrations of F8-IL2 or recombinant IL2. Shown is the mean  $\pm$  SEM of triplicates. (F) Biodistribution study of F8-IL2 in F9 teratocarcinoma bearing mice. Mice were injected with 0.86  $\mu$ g radio-iodinated F8-IL2, sacrificed after 24 hours, organs excised, and the radioactivity counted. The radioactivity of each organ is expressed as injected dose per gram of tissue (% ID/g  $\pm$  SE).

The product was homogeneous and had the estimated molecular size of approximately 42 kDa in SDS-PAGE and gel-filtration analysis [Figure 10B,C], bound avidly to the cognate antigen EDA of fibronectin [Figure 10D], and retained the same *in vitro* activity as commercial human recombinant IL2 in a proliferation assay of murine T lymphocytes [Figure 10E]. A radio-iodinated preparation of F8-IL2 selectively localized in solid tumor lesions of F9 teratocarcinomas compared with liver, lung, spleen, kidney, heart, intestine, and blood 24 hours after intravenous administration. At that time point, a mean of  $9.3 \pm 2.9$  percent injected dose per gram of tumor (% ID/g) was observed, with a tumor:blood ratio of 42.5 [Figure 10F]. The F8 antibody stained the stroma of CT26 and MC38 tumors, whereas the KSF antibody (directed against hen egg lysozyme and serving as negative control) did not exhibit a specific staining. CD31 was used as the target for staining blood vessels to have a better understanding of the tumor structure [Suppl. Figure 1A,B]. Collectively, our findings showed that the F8-IL2 construct retained the activity of recombinant IL2, bound with high affinity to the cognate EDA antigen, and selectively localized to tumors *in vivo*.

#### 4.1.2. Therapy experiments

For therapy studies, we used immunocompetent mice bearing subcutaneous CT26 carcinomas. These tumors had previously been reported to respond to immune checkpoint inhibitors (directed against murine PD-1, PD-L1, and CTLA-4) when used as monotherapy [338,339]. Mice bearing subcutaneously grafted CT26 tumors were treated when lesions had reached approximately 80 mm<sup>3</sup>. F8-IL2 was administered on days 5, 8, and 11 at a dose of 45  $\mu$ g, whereas immune checkpoint inhibitors were given on days 6, 9, and 12 at a dose of 200  $\mu$ g [Figure 11].



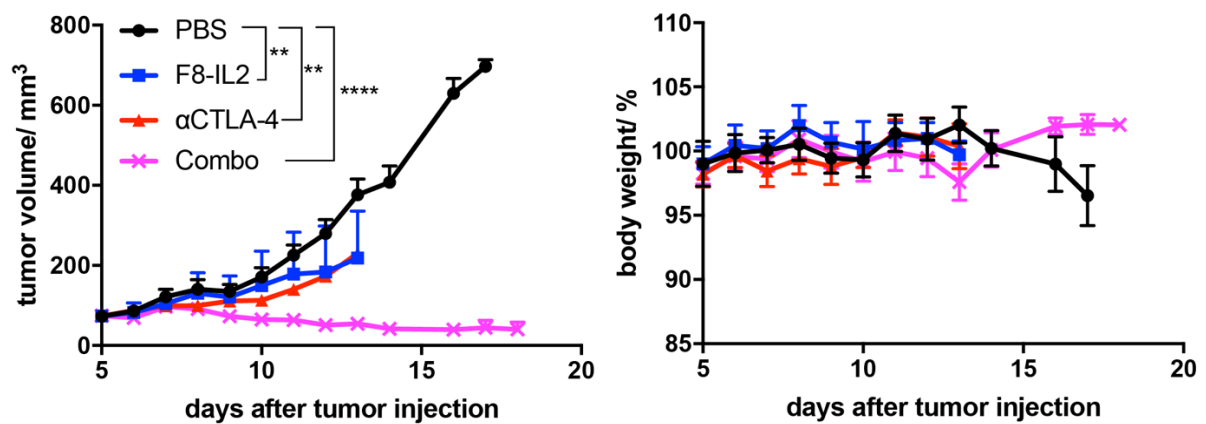
**Figure 11: Therapeutic performance of F8-IL2 and checkpoint inhibitors in immunocompetent BALB/c mice bearing subcutaneous CT26 colon carcinoma.** Mice received intravenous injections of either 45  $\mu$ g F8-IL2 (blue squares), 200  $\mu$ g of a checkpoint inhibitor (anti-CTLA-4, anti-PD-1 or anti-PD-L1, red triangles), 45  $\mu$ g F8-IL2 followed by 200  $\mu$ g of a checkpoint inhibitor (pink x) or PBS (black circles). The left column depicts tumor volume versus time. The right column shows the corresponding body weight changes over time. Data represent tumor volume  $\pm$  SEM or body weight change (%)  $\pm$  SEM.  $n = 5$  mice per group. CR = complete response. Arrows indicate the day of injection of F8-IL2 (blue arrows) and checkpoint inhibitors (red arrows). Colored stars indicate days on which a mouse of the corresponding group with the same color code had to be euthanized according to the termination criteria. A

*regular two-way ANOVA test with the Bonferroni post-test was performed to determine the statistical significance between the groups (\*,  $p < 0.05$ , \*\*,  $p < 0.01$ ; \*\*\*\*,  $p < 0.0001$ ). For the CTLA-4 study on day 14: PBS vs each treatment group  $p = ***$ , F8-IL2 vs CTLA-4 non-significant, F8-IL2 vs Combo  $p = ***$ , Combo vs CTLA-4  $p = ***$ . For the PD-1 study on day 19: PBS vs each treatment group  $p = ***$ , F8-IL2 vs PD-1 non-significant, F8-IL2 vs Combo  $p = *$ , PD-1 vs Combo non-significant. For the PD-L1 study on day 19: PBS vs each treatment group  $p = ***$ , the difference between the treatment groups is non-significant ( $p > 0.05$ ).*

F8-IL2 displayed a potent tumor growth inhibition compared to the saline control, but complete remission was observed only in a small proportion of treated mice. Similarly, antibodies directed against CTLA-4, PD-1, and PD-L1 had single-agent activity, but also only rarely led to complete tumor control [Figure 11]. The combination of F8-IL2 with CTLA-4 blockade led to complete and durable responses in all treated animals. A potent activity was also observed for the combination with anti-PD-1 antibodies, even though most tumors eventually regrew. The lowest therapeutic activity was observed for the PD-L1 combination. All treatments were very well tolerated, as evidenced by the absence of body weight loss [Figure 11].

To determine whether the combination of F8-IL2 in combination with CTLA-4 blockade would also be effective in a second tumor model, we treated immunocompetent mice bearing MC38 colon carcinomas. This model had previously been reported to be associated with an immunosuppressive phenotype and does not respond well to immune checkpoint inhibitors used as a monotherapy [338]. Mice bearing subcutaneously grafted MC38 colon carcinomas were treated when lesions had reached approximately 75 mm<sup>3</sup>. F8-IL2 was administered on days 5, 8, and 11 at a dose of 30 µg, and anti-CTLA-4 was given on days 6, 9, and 12 at a dose of 200 µg. The combination of CTLA-4 blockade with F8-IL2 substantially reduced the tumor growth, whereas the individual agents were significantly less potent ( $p < 0.0001$ ) [Figure 12].





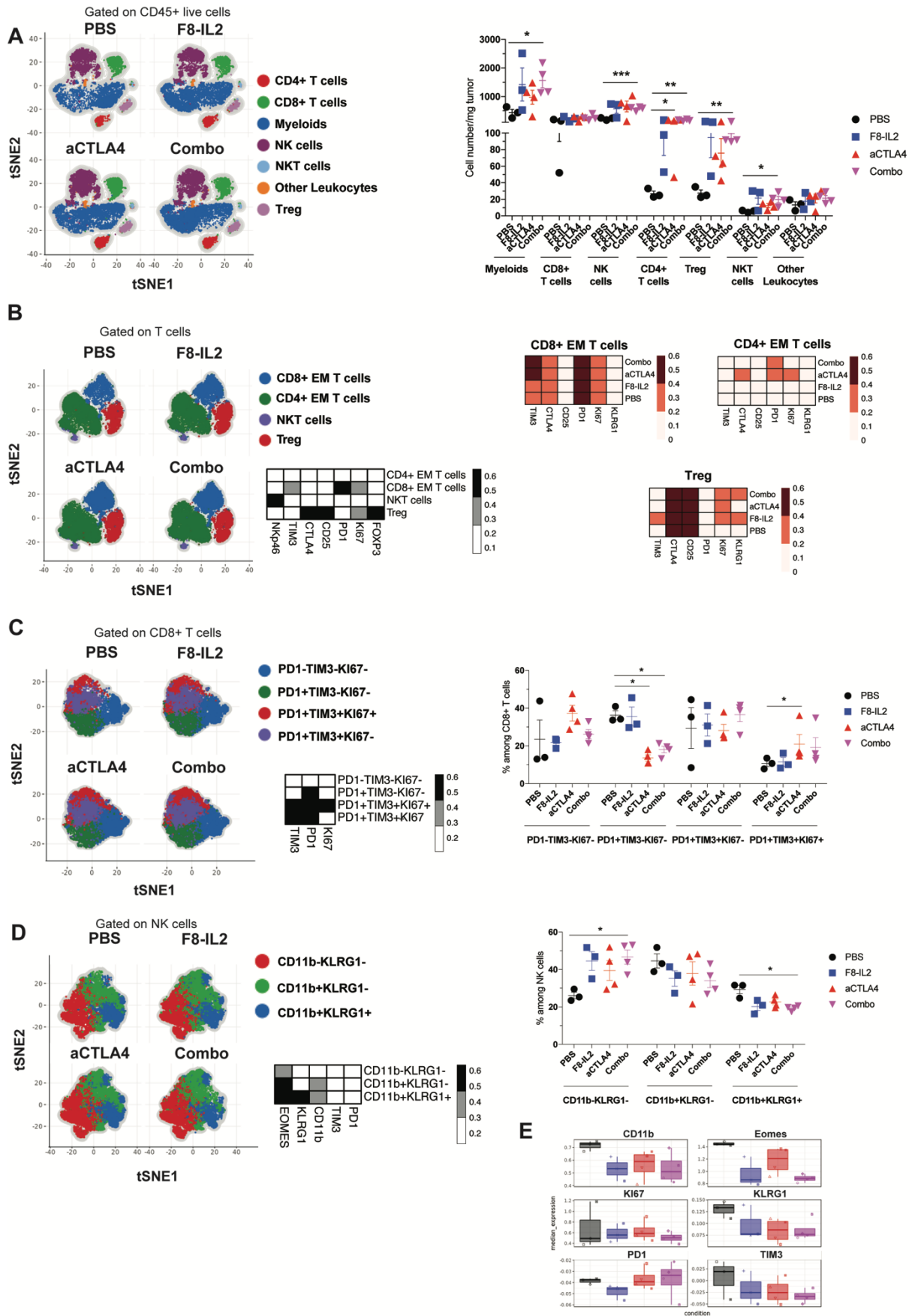
**Figure 12: Therapeutic activity of the F8-IL2/CTLA-4 blockade combination against subcutaneous MC38 colon carcinoma.** Mice were challenged with  $1 \times 10^6$  MC38 colon carcinoma cells, and treatment was started when tumors reached a size of approximately  $75 \text{ mm}^3$ . Mice received intravenous injection of either  $45 \mu\text{g}$  F8-IL2 (blue squares, on day 5, 8, and 11 after tumor cell implantation),  $200 \mu\text{g}$  of an anti-CTLA-4 (red triangles, on day 6, 9, and 12), or  $30 \mu\text{g}$  F8-IL2 followed 24 hours later by  $200 \mu\text{g}$  of the checkpoint inhibitor (pink x, on day 5, 8, and 11) or PBS (black circles, on day 5, 6, 8, 9, 11, and 12). The left graph depicts tumor volume versus time, and the right graph displays the body weight change versus time. Data represent tumor volume or body weight change  $\pm$  SEM.  $n = 4$  mice per group. \*\*,  $p < 0.01$ ; \*\*\*\*,  $p < 0.0001$  (regular two-way ANOVA with the Bonferroni post-test).

Mice without measurable tumor masses at day 62 or day 60 after the tumor implantation were re-challenged with CT26 or MC38 cells. In all cases, the tumors did not grow back [Suppl. Figure 2], indicative of protective anti-cancer immunity and immune memory, presumably directed against the AH1 antigen [339–343].

#### 4.1.3. Mechanistic studies

To gain mechanistic insights on the anti-cancer activity played by different types of leukocytes, we performed a multiparameter flow-cytometric characterization of leukocytes using a panel of 23 fluorochromes [Suppl. Table 1]. We analyzed the leukocyte populations present in tumors, spleens, and draining lymph nodes in CT26 tumor-bearing mice at day 13 after tumor implantation (i.e., 24 hours after the last injection) [Figure 13-Figure 14, Suppl. Figure 3-Suppl. Figure 4]. Figure 13 shows the phenotype of the tumor-infiltrating leukocytes

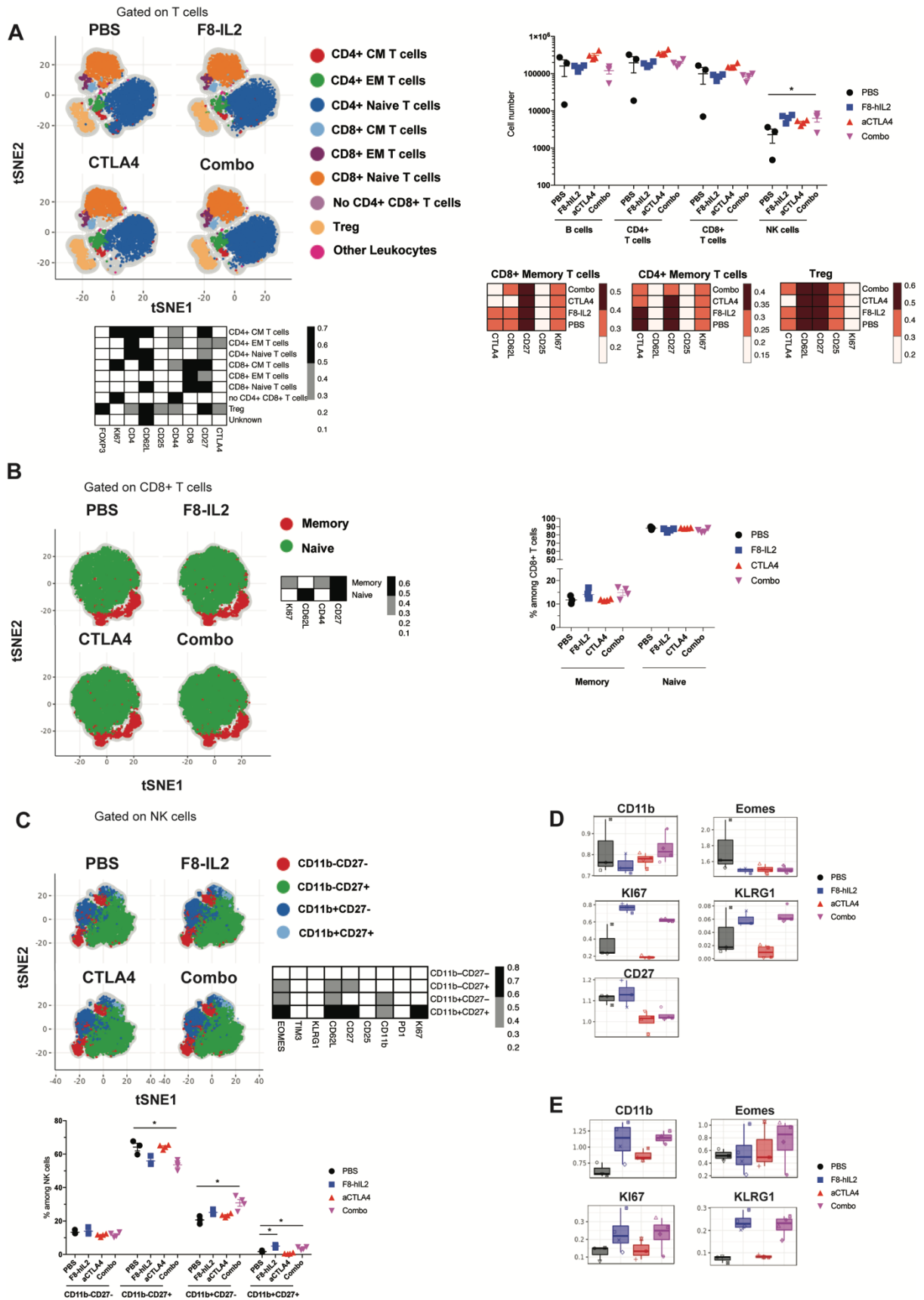
from all treated groups, defined as saline (PBS), F8-IL2, anti-CTLA-4 (aCTLA-4), and combination (Combo) treatment. For an unbiased analysis, we reduced the high-dimensional dataset into two dimensions through t-distributed stochastic neighbor embedding (t-SNE) that stochastically displayed CD45<sup>+</sup> cells from the 4 groups [Figure 13, Suppl. Figure 3A] in combination with FlowSOM meta-clustering. Heatmaps show the normalized marker expression of each population (black and white) or each condition (red) in the tumor [Figure 13]. We identified 7 main clusters with this approach [Figure 13A]. An increased density (cell number/ mg tumor) of myeloid, NK cells, and CD4<sup>+</sup> T cells in tumors from mice that received F8-IL2 or anti-CTLA-4 (alone or in combination) was observed [Figure 13A]. All these treatments also doubled the density of CD8<sup>+</sup> T cells and increased Tregs approximately three fold [Figure 13A]. Differences in CTLA-4, KLRG1, PD-1, and Ki67 positivity in Tregs were observed in the Combo group compared with PBS-treated mice [Figure 13B, Suppl. Figure 3B]. A finer analysis of T-cell marker expression in different treatment groups revealed that CTLA-4 blockade (alone or in combination) led to increased PD-1 positivity in CD4<sup>+</sup> T cells [Figure 13B]. In those cells, CD25 was upregulated in all treatment groups compared to saline [Suppl. Figure 3B]. Analysis of CD8<sup>+</sup> T cells showed that CTLA-4 treatment (alone or in combination) was the most efficient in triggering the expression for TIM-3 [Figure 13B]. Unbiased analysis of the CD8<sup>+</sup> T-cell compartment (using FlowSOM and Citrus) displayed a lower frequency of PD1<sup>+</sup>TIM3<sup>-</sup>Ki67<sup>-</sup>CD8<sup>+</sup> T cells in mice treated with CTLA-4 blockade (alone or in combination with F8-IL2) [Figure 13C, Suppl. Figure 3C]. However, in those mice, the frequency and the expression for PD-1, TIM-3, and Ki67 were increased, suggesting local T-cell activation and expansion [Figure 13C, Suppl. Figure 3C]. Further analysis (using FlowSOM and Citrus) of the NK cell compartment showed an increased frequency and expression for KLRG1, CD11b, and EOMES in the PBS-treated group, corresponding to a more mature phenotype and a slower *in vivo* turnover rate [344] [Figure 13D,E, Suppl. Figure 3D].



**Figure 13: Multiparameter flow cytometric analysis of tumor immune cell infiltrates.** Single-cell suspensions from CT26 tumors (PBS n=3, F8-IL2 n=3, CTLA-4 n=4, Combo n=4 tumors per group) were stained with fluorochrome-conjugated antibodies. (A) t-SNE map showing the FlowSOM-guided meta-clustering (left) and quantification (cell number/ mg tumor) of live intratumoral CD45<sup>+</sup> cell clusters in the different treatment groups (right). Each color represents a meta-cluster and is associated with a different immune population (left). (B) t-SNE map showing the FlowSOM-guided meta-clustering gated on TCRβ<sup>+</sup> cells from live CD45<sup>+</sup> cells (left), heatmap showing the median marker expression (value range: 0-1) for each defined population (middle; black and white), and among each T-cell subpopulation in the different conditions (right; red). (C) t-SNE map showing the FlowSOM-guided meta-clustering gated on CD8<sup>+</sup> T cells from live CD45<sup>+</sup>, TCRβ<sup>+</sup> cells (left), heatmap showing the median marker expression for each defined population (middle; black and white), and frequencies of the four CD8<sup>+</sup> T-cell subclusters among total CD8<sup>+</sup> T cells within the different conditions (right). (D) t-SNE map showing the FlowSOM-guided meta-clustering gated on NK cells from live CD45<sup>+</sup>, TCRβ<sup>-</sup>, NKp46<sup>+</sup> cells (left), heatmap showing the median marker expression (value range: 0-1) for each defined population (middle), and frequencies of the three NK cell subclusters among total NK cells within the different conditions. (E) Median expression of selected cell markers shown for all intratumoral NK cells for each treatment. The experiment was performed once. Shown is the mean ± SEM. The Mann Whitney test was used to assess the statistical significance. \*, p<0.05; \*\*, p<0.01; \*\*\*, p<0.001

Similarly, a detailed analysis of T cells and NK cells in tumor-draining lymph nodes was also performed based on t-SNE (displaying randomly cells from the 4 groups) in combination with FLOW SOM meta-clustering [Figure 14, Suppl. Figure 4A-E]. The differences in the NK cell population were the most significant. We observed an increase in the frequency of NK cells in all treated groups compared with saline-treated mice [Figure 14A]. As expected, the majority of CD8<sup>+</sup> and CD4<sup>+</sup> T cells had a naïve phenotype [Figure 14B, Suppl. Figure 4C,D]. However, the percentage of CD8<sup>+</sup> effector-memory T cells was higher in mice treated with F8-IL2 (alone or in combination) although not significant [Figure 14B, Suppl. Figure 4C,D]. NK cells had an activated phenotype in mice treated with F8-IL2 (alone or in combination), as revealed by their CD11b<sup>+</sup>CD27<sup>+</sup> status [Figure 14C, Suppl. Figure 4E] Treatment with F8-IL2

(alone or in combination) led to an increase in proliferation (Ki67 positivity) [**Figure 14D**, **Suppl. Figure 4E**]. By contrast, NK cells in the anti-CTLA-4 monotherapy and saline groups exhibited a similar phenotype [**Figure 14C,D**].



**Figure 14: Multiparameter flow cytometric analysis of lymph node immune cell infiltrates.** Single-cell suspensions from CT26 tumor draining lymph nodes (PBS  $n=3$ , F8-IL2  $n=4$ , CTLA-4

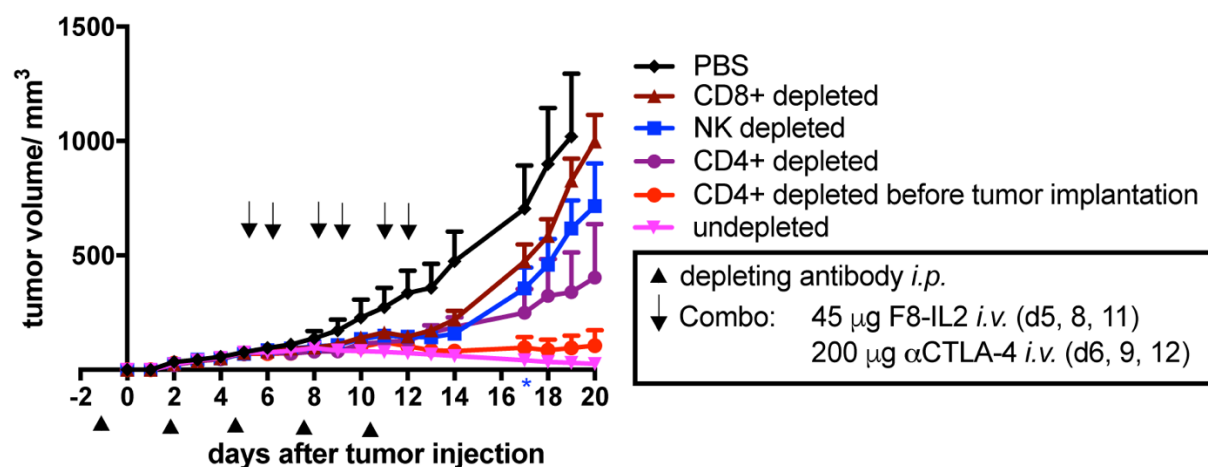
*n=4, Combo n=4 draining lymph nodes per group) were stained with fluorochrome-conjugated antibodies. (A) t-SNE map showing the FlowSOM-guided meta-clustering and heatmap showing the median marker expression (value range: 0-1, black and white) for each defined population (left). Quantification (cell number) of TCR $\beta^+$  cell and heatmap showing the median marker expression in the different treated groups (right). Each color (left) represents a meta-cluster and is associated with a different immune population. Gating was performed on live CD45 $^+$ , TCR $\beta^+$  cells. (B) t-SNE map showing the FlowSOM-guided meta-clustering gated on CD8 $^+$  T cells from live CD45 $^+$ , TCR $\beta^+$  cells (left), heatmap showing the median marker expression (value range: 0-1) for each defined population (middle) and frequencies of the four CD8 $^+$  T-cell subclusters among total CD8 T cells within the different conditions. (C) t-SNE map showing the FlowSOM-guided meta-clustering gated on NK cells (live CD45 $^+$ , TCR $\beta^-$ , NKp46 $^+$  cells, left), heatmap showing the median marker expression for each defined population (middle, black and white), and frequencies of the four NK cell subclusters among total NK cells within the different conditions (bottom). (D) Median expression of selected cell markers shown for all NK cells for each treatment. (E) Splenocytes (PBS n=3, F8-IL2 n=4, CTLA-4 n=4, Combo n=4 spleen per group) from mice bearing CT26 tumors were stained with fluorochrome-conjugated antibodies. Median expression of selected cell markers is shown for all NK cells for each treatment. The experiment was performed once. Shown is the mean  $\pm$  SEM. The Mann Whitney test was used to determine the statistics. \*,  $p < 0.05$ ; \*\*,  $p < 0.01$ ; \*\*\*,  $p < 0.001$*

For the splenocytes, we observed similar results to what was detected in the lymph nodes [Figure 14E, Suppl. Figure 4F,G]. Mice treated with F8-IL2 (alone or in combination) showed increased Ki67, CD11b, and KLRG1 staining of NK cells, whereas the NK cells in the PBS- and CTLA-4-treated mice behaved similarly [Figure 14E].

We also performed a multiparameter flow-cytometric characterization of leukocytes present in tumors and draining lymph nodes of MC38 bearing mice [Suppl. Figure 5A-D, Suppl. Figure 6A-D]. Because the combination was very effective and almost led to a total regression in MC38 tumors, we could obtain only a few tumors for the flow-cytometric analysis. An increase of granzyme B (GZMB $^+$ ) and Ki67 staining within the CD8 $^+$  T and NK cell population was observed after F8-IL2 treatment in the tumors and draining lymph nodes [Suppl. Figure 5B-D, Suppl. Figure 6C,D]. We observed a similar high frequency of GZMB $^+$ CD8 $^+$  T and GZMB $^+$

NK cells in the tumors of the combination group compared to F8-IL2 alone, but a decrease in the Treg frequency [Suppl. Figure 5A-D]. In the draining lymph nodes, the frequency of Tregs was the highest when the mice were treated with F8-IL2 in combination with CTLA-4 blockade [Suppl. Figure 6B]. Leukocytes present in the neoplastic masses and lymph nodes after CTLA-4 blockade displayed a phenotype similar to the one of leukocytes from saline-treated mice [Suppl. Figure 5A-D, Suppl. Figure 6A-D].

Single-cell analysis of the leukocyte composition within the tumors and secondary lymphoid organs among the treatment groups suggested that alterations in the CD8<sup>+</sup> and CD4<sup>+</sup> T- and NK cell frequencies and phenotypes may influence the therapeutic outcome. To determine the relevant therapeutic cellular target, we depleted either CD4<sup>+</sup>, CD8<sup>+</sup>, or NK cells during therapy in CT26 colon carcinoma bearing mice. The *in vivo* depletion of either NK or CD8<sup>+</sup> T cells completely abolished the therapeutic activity of F8-IL2 in combination with CTLA-4 blockade (CR in both groups 0/5) [Figure 15]. CD4<sup>+</sup> T-cell depletion before (CR 3/5) or after (CR 2/5) tumor implantation only had a minor influence on the therapeutic result.



**Figure 15: *In vivo* depletion study.** CT26 colon carcinoma bearing mice received a total of three injections of 45  $\mu\text{g}$  F8-IL2 followed by 200  $\mu\text{g}$  anti-CTLA-4 24 hours later. Depletion antibodies were injected intraperitoneally on days -1, 2, 5, 8, or 11 (black arrowheads). CD8<sup>+</sup> T cell-depleted mice (250  $\mu\text{g}$  are depicted in brown triangles, NK cell-depleted mice in blue squares, and CD4<sup>+</sup> T cell-depleted in purple circles). A group in which CD4<sup>+</sup> T cells were depleted before tumor implantation is shown in red circles. A saline-treated, undepleted negative control was included (black circles), as well as an undepleted positive control group that received F8-IL2 and anti CTLA-4 inhibitor (pink x). Black arrows indicate the day of injection of



*the therapeutic agents. Data represent mean tumor volume  $\pm$  SEM. n = 5 mice per group (for NK cell depleted group, n = 4 from day 17 as indicated by a blue star due to the termination criteria). A regular two-way ANOVA test with the Bonferroni post-test was performed to determine the statistical significance between the groups (ns, non-significant  $p > 0.05$ , \*,  $p < 0.05$ , \*\*,  $p < 0.01$ ; \*\*\*\*,  $p < 0.0001$ )*

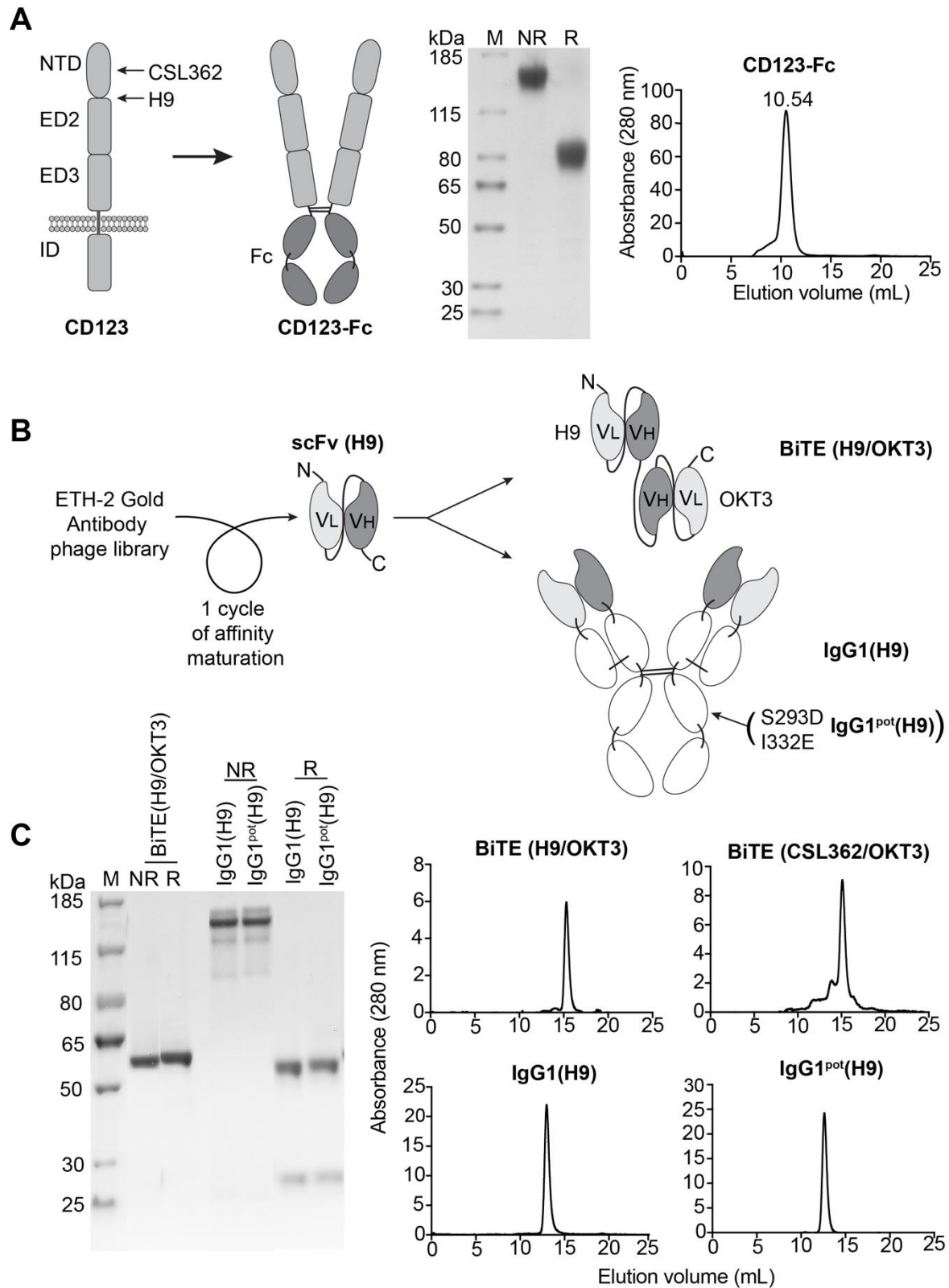
## 4.2. Development of a novel fully-human anti-CD123 antibody to target acute myeloid leukemia

This chapter has recently been submitted for publication:

Hutmacher et al., **Development of a novel fully-human anti-CD123 antibody to target acute myeloid leukemia**, *submitted*

### 4.2.1. Generation, affinity maturation and reformatting of fully-human antibodies against CD123

A fusion protein consisting of the extracellular domains of human CD123 (NTD, ED2 and ED3) and a human Fragment crystallizable (Fc) tag (CD123-Fc) was cloned, expressed in mammalian cells and purified to homogeneity [**Figure 16A**]. The protein was glycosylated and migrated as a disulfide-linked homodimer in SDS-PAGE analysis performed in non-reducing conditions, while a monomeric band of the expected size was visible in reducing conditions [**Figure 16A**]. Size-exclusion chromatography analysis confirmed that CD123-Fc was eluted at a volume consistent with a disulfide-linked structure [**Figure 16A**].



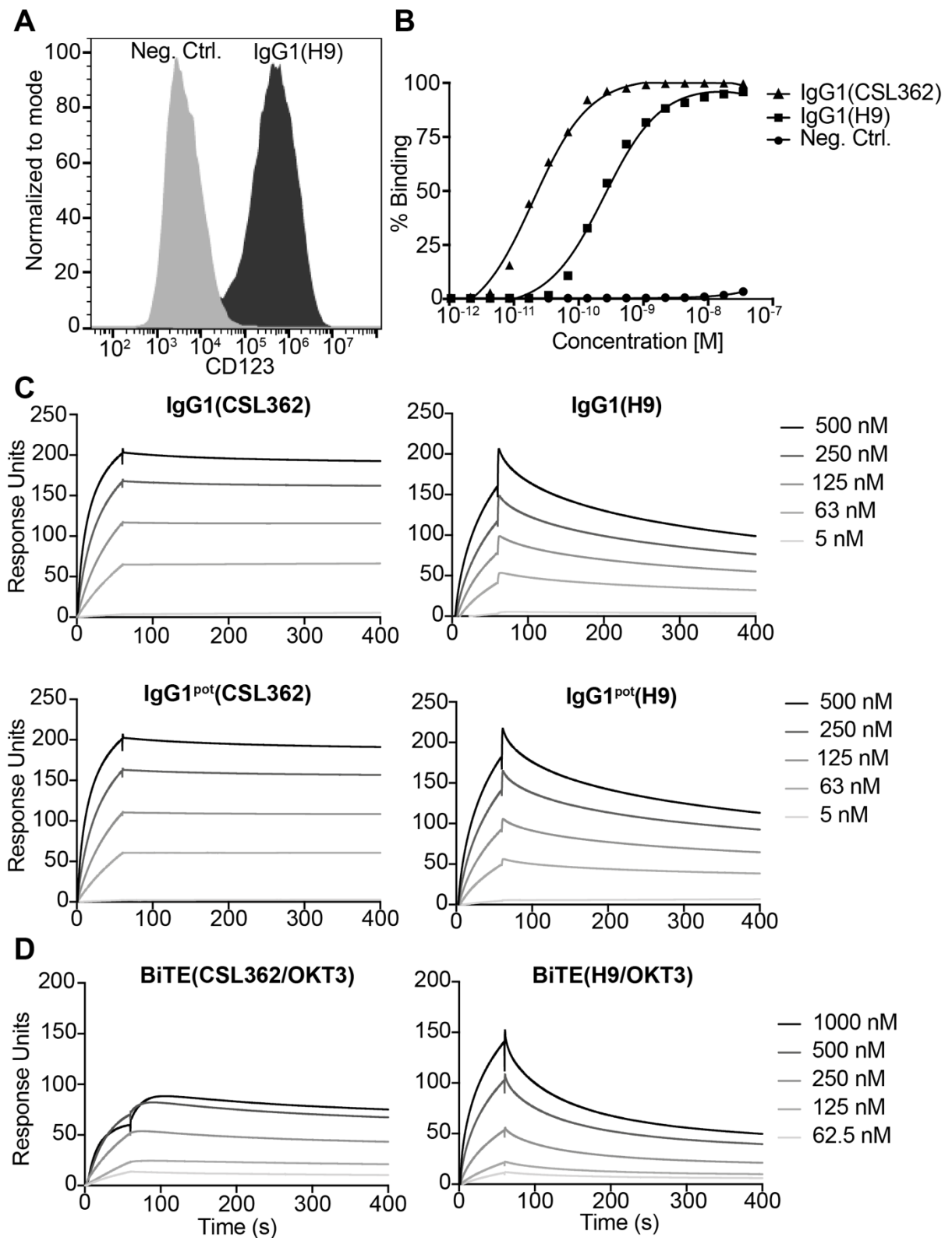
**Figure 16: Generation and expression of fully-human antibodies against CD123.** (A) CD123 is composed of three extracellular domains: the N-terminal domain (NTD) and extracellular domains 2 and 3 (ED2 and ED3). ED3 is followed by a transmembrane domain and an intracellular domain (ID). CSL362 and H9 bind to different epitopes on NTD. The extracellular

domains of CD123 were fused to a Fc tag, expressed in mammalian cells and analyzed using SDS-PAGE and size exclusion chromatography. (B) Schematic illustration of the workflow to generate anti CD123 therapeutics. A large synthetic human antibody library was used to isolate anti-CD123 antibodies. The clone in scFv format with the best signal in the ELISA was selected and affinity matured to yield the scFv(H9). The VL and VH domains of H9 were used to generate a BiTE(H9/OKT3) and a full IgG (H9). Point mutations were inserted into the Fc domain to obtain ADCC potentiated mutants. (C) SDS-PAGE analysis under non-reducing (NR) and reducing (R) conditions and (D) size exclusion chromatography profile of BiTE(H9/OKT3), BiTE (CSL362/OKT3), IgG1(H9) and IgG1<sup>pot</sup>(H9). M= Marker. The SDS-PAGE analysis and size exclusion profile of IgG1(CSL362), IgG1<sup>pot</sup>(CSL362) and BiTE(CSL362/OKT3) can be found in **Suppl. Figure 7**.

The fusion protein CD123-Fc was used to isolate a first low-affinity anti-CD123 antibody from a large synthetic human antibody library (ETH-2 Gold library) using established protocols [Figure 16B] [78,345]. In order to affinity-mature this clone, we generated and screened a phage display library of 6 million antibody variants, obtained by combinatorial mutagenesis of 6 residues in the CDR1 loop of the VH and VL domains, using previously described procedures [Figure 16B] [17]. The antibody clone (termed “H9”) which gave the strongest ELISA signal was further characterized and used for reformatting activities. The VL and VH domains of H9 were used to clone a BiTE(H9/OKT3) and a full IgG1(H9) [Figure 16B]. Moreover, two amino acid mutations (S239D and I332E) were introduced into the Fc region in order to enhance ADCC activity, as previously described for IgG1(CSL362) [326]. Similar IgG1 and BiTE products were generated for CSL362, starting from a synthetic gene of the antibody sequence [326,347]. The resulting proteins were expressed in mammalian cells and characterized using standard biochemical assays, such as SDS-PAGE analysis and size exclusion chromatography [Figure 16C and Suppl. Figure 7]. The complete amino acid sequence of these constructs can be found in **Suppl. Figure 8**.

#### 4.2.2. *In vitro* characterization of anti-leukemic activity of H9- and CSL362-based therapeutics

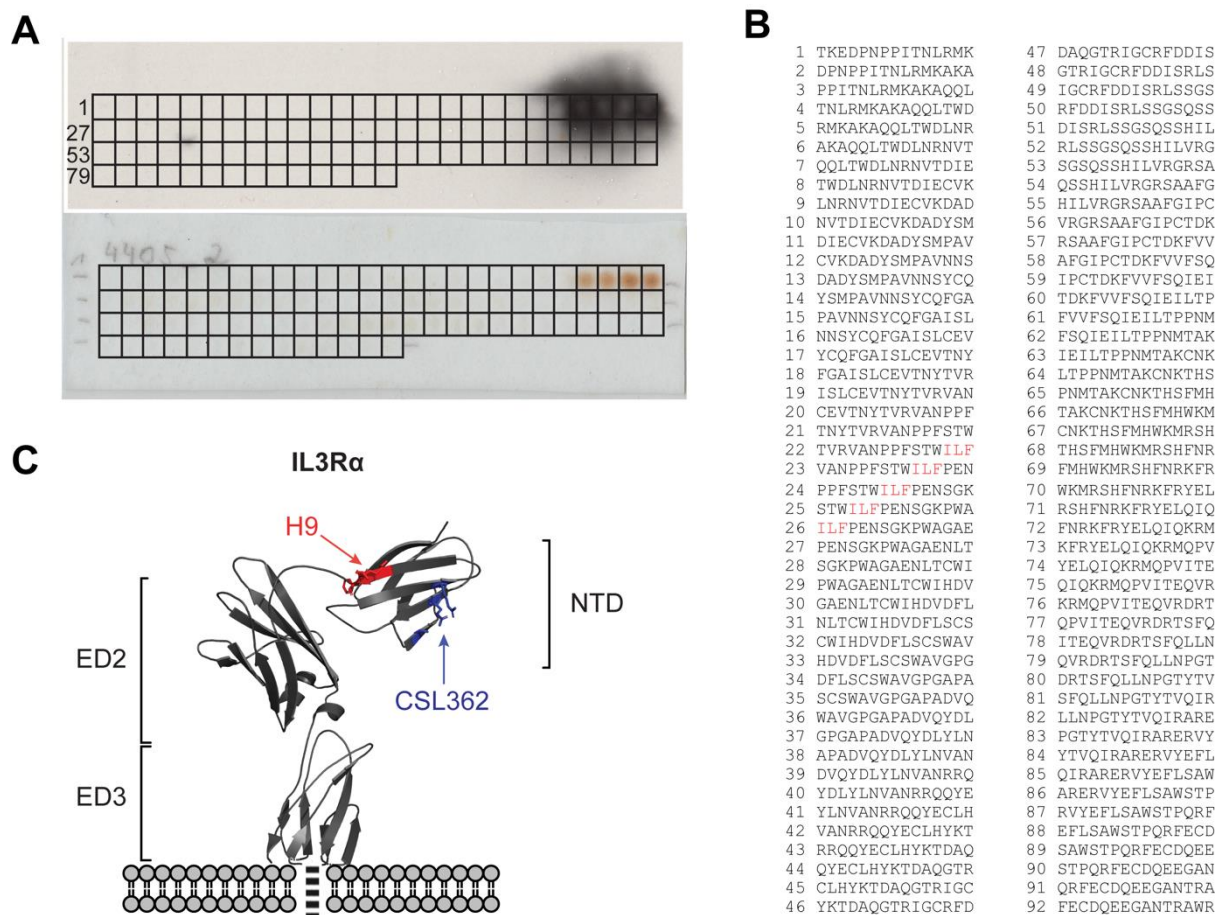
First, we generated a stable CD123 expressing CHO-S cell line, which was used to analyze the binding affinity of the antibody products. IgG1(H9) exhibited a large shift in FACS analysis, compared to an antibody of irrelevant specificity in this setting [IgG1(L19), an anti-EDB antibody[348]], which was used as negative control [**Figure 17A**]. Analysis of a titration series for the FACS experiment revealed that IgG1(CSL362) exhibited a high functional affinity ( $K_d^{\text{app}} = 20 \text{ pM}$ ), which was  $\sim 10$ -fold higher than the one of IgG1(H9) ( $K_d^{\text{app}} = 250 \text{ pM}$ ) [**Figure 17B**]. Next, we analyzed the kinetic binding properties of the two antibodies in different formats. As expected, IgG1(CSL362) exhibited an extremely low kinetic dissociation profile from the antigen coated on a BIAcore microsensor chip, while a measurable kinetic dissociation profile was visible for IgG1(H9) [**Figure 17C**]. Similarly, BiTE(CSL362/OKT3), featuring a monovalent binding to the cognate CD123 antigen, displayed a flat dissociation profile from the antigen, while BiTE(H9/OKT3) exhibited a  $k_{\text{off}}$  value of  $2 \times 10^{-3} \text{ s}^{-1}$  [**Figure 17D**].



**Figure 17: Binding analysis.** (A) Representative histogram display of IgG1(H9) (black shaded) and a negative control (neg. Ctrl.) antibody IgG1(L19) to visualize binding of CD123 on CD123+ CHO-S cells. (B) Dose titration of IgG1(CSL362), IgG1(H9), and a negative control IgG (neg. Ctrl.) IgG1(L19) to determine the binding affinity of the antibodies to CD123 expressing CHO-

S cells. (C) and (D) Surface plasmon resonance analysis of IgG1(CSL362), IgG1<sup>pot</sup>(CSL362), IgG1(H9), IgG1<sup>pot</sup>(H9), BiTE(CSL362/OKT3), and BiTE(H9/OKT3) on a CD123-Fc coated CM-5 chip.

The binding site of CSL362 on the N-terminal domain of CD123 has previously been characterized by X-ray crystallography [349]. In order to identify the binding site of H9 on the surface of CD123, we used SPOT technology [350] and immunodetection of antibody binding events to peptides spanning the antigen sequence, synthesized on cellulose. **Figure 18** shows that CSL362 and H9 recognize different epitopes, located on opposite faces of the N-terminal domain of CD123.

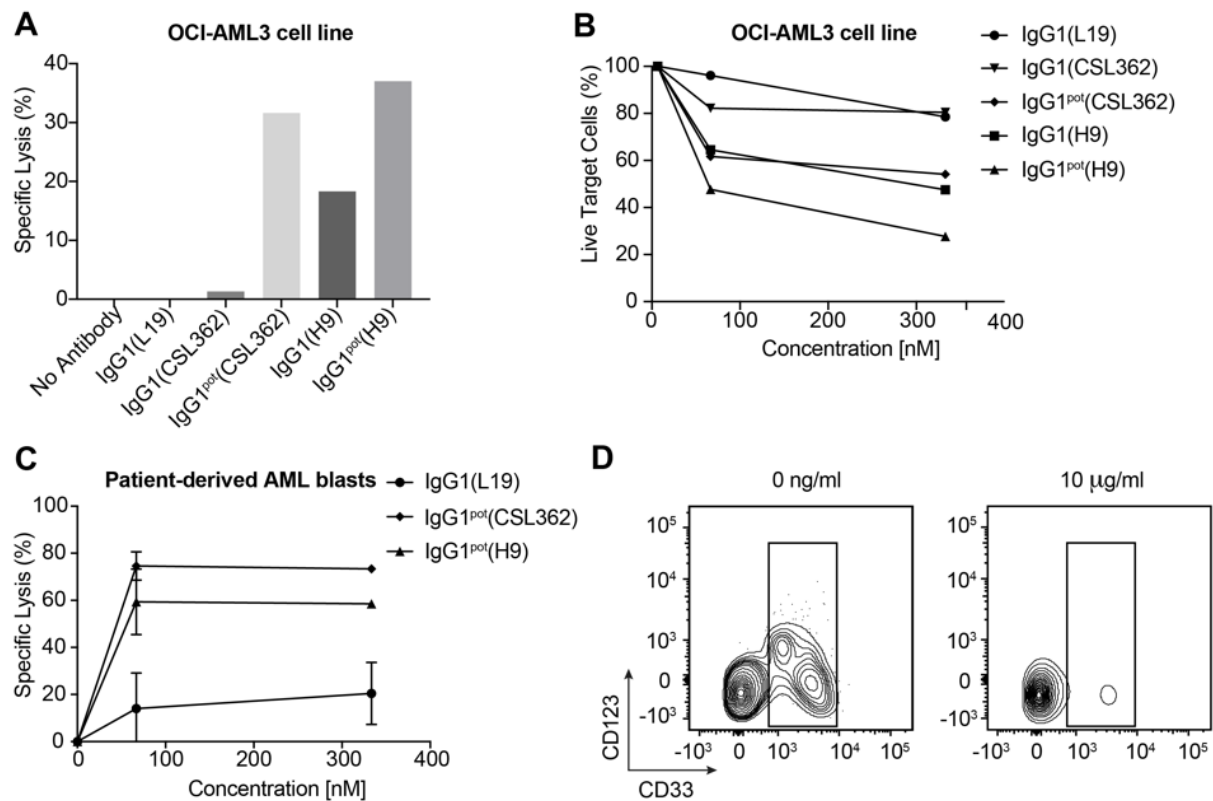


**Figure 18:** Epitope mapping of antibody binding to the NTD of CD123. (A) Autoradiographic results of the SPOT analysis performed using the H9 antibody. Portions of the extracellular domain of CD123 were synthesized as a consecutive series of 15 amino acid-long peptides [listed in (B)], spanning the protein sequence with 3 residues shift each. (C) Three dimensional model of CD123, indicating both the binding sites of H9 (red) and of CSL362 (blue), was built

on the basis of the 4JZJ pdb file [349]. The binding sites of IgG(H9) and of IgG(CSL362) both lie on the NTD domain. The epitope of H9 is centered around the I94-L95-F96 sequence, while the epitope of CSL362 is centered around E51, S59, and R84 [351].

We then tested the antibodies in conventional IgG1 format and in the corresponding ADCC-potentiated version (IgG1<sup>pot</sup>) for their ability to mediate ADCC against a human AML cell line *in vitro*. In this assay, both ADCC-potentiated antibodies induced ~30% specific lysis of the OCI-AML3 cell line when used at 10 µg/ml, in keeping with previously published reports for CSL362 [326] [Figure 19A]. We repeated the ADCC assay using three different concentrations, confirming that IgG1<sup>pot</sup>(H9) was the product with the most potent ADCC activity [Figure 19B]. Similar experiments, performed using patient-derived AML blasts and purified allogeneic NK cells at an effector to target (E:T) ratio of 10:1, confirmed the ability of the two antibodies to selectively kill leukemic cells *in vitro* [Figure 19C]. Over 75% of CD45<sup>dim</sup> CD33<sup>+</sup> AML blasts were efficiently depleted by 10 µg/ml IgG1<sup>pot</sup>(CSL362) after 24 hours of co-culture with allogeneic NK cells [Figure 19D]. Interestingly, also CD45<sup>dim</sup>CD33<sup>+</sup>CD123<sup>low</sup> AML blasts were killed in this assay.



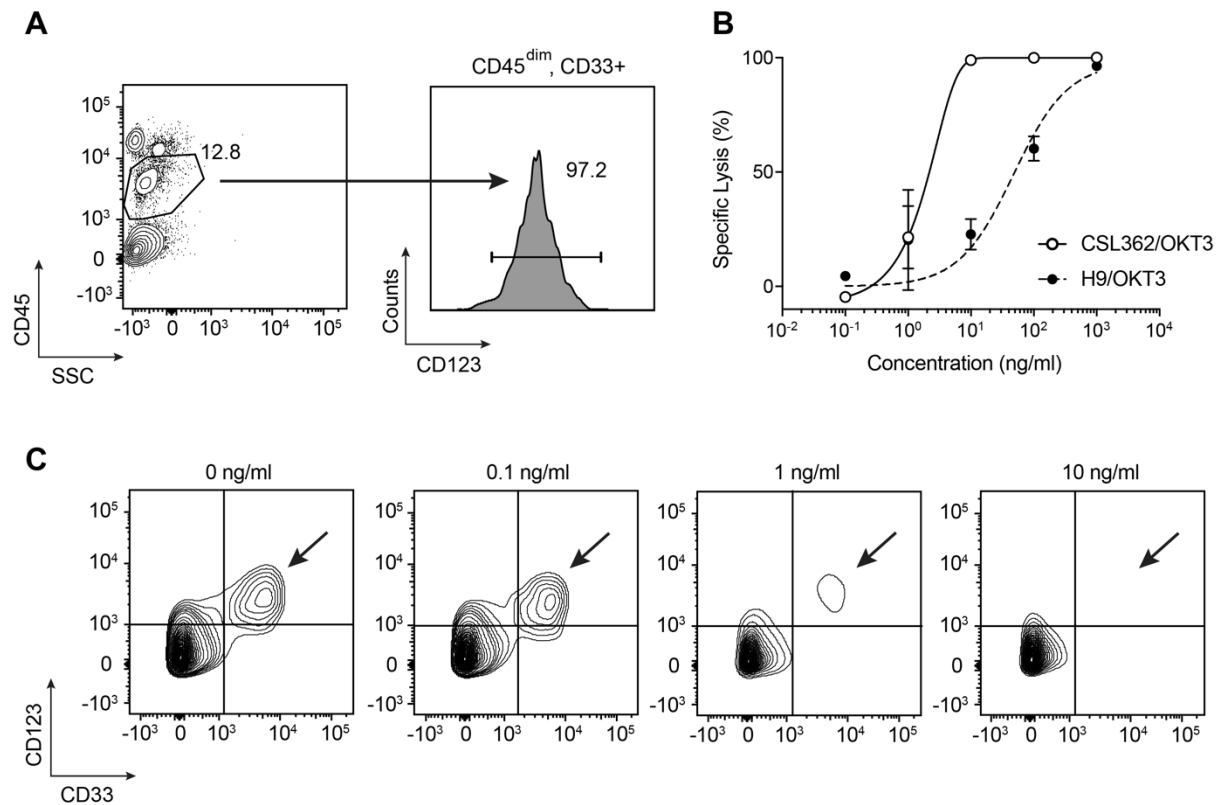


**Figure 19:** *In vitro* ADCC killing of human AML cell lines and of primary AML blast cells. (A) Percentage of specific lysis of OCI-AML3 cells 24 hours after co-culture with healthy donor PBMCs only or with PBMCs and 10 µg/ml of either anti-EDB IgG(L19), anti-CD123 IgG(CSL362), IgG<sup>pot</sup>(CSL362), IgG(H9) or IgG<sup>pot</sup>(H9) antibodies. The anti-EDB IgG1(L19) antibody was used as negative control. (B) The percentage live target cells (OCI-AML3 cells) after 24 hours of co-culture with healthy donor PBMCs only or with PBMCs and with indicated concentrations of either IgG(L19), IgG(CSL362), IgG<sup>pot</sup>(CSL362), IgG(H9) or IgG<sup>pot</sup>(H9) antibodies. (C) Percentage specific lysis of CD45<sup>dim</sup> CD33<sup>+</sup> AML blast cells after 24 hours of co-culture with purified healthy donor NK cells and either anti-EDB IgG(L19) IgG<sup>pot</sup>(CSL362) or IgG<sup>pot</sup>(H9) antibodies at the indicated concentrations. The effector to target ratio was set to 10:1. (D) Representative flow cytometry plots of CD45<sup>dim</sup> CD33<sup>+</sup> AML blast cells incubated with healthy donor NK cells and different concentration of IgG<sup>pot</sup>(CSL362) after 24 hours.

#### 4.2.3. *In vitro* analysis of BiTE biocidal activity

**Figure 20A** shows a FACS gating analysis of patient-derived AML blasts (left panel) prior to *in vitro* cytotoxicity assay and evaluation (right panel). Virtually all leukemic blasts exhibited CD123 cell surface expression in the CD45<sup>dim</sup> CD33<sup>+</sup> cell population. We tested the anti-leukemic activity of BiTE(H9/OKT3) and of BiTE(CSL362/OKT3) in an *in vitro* assay, using

patient's derived AML blasts and autologous T cells as effectors. Using an E:T ratio of 10:1, we observed a concentration-dependent AML killing. BiTE(CSL362/OKT3), with an IC<sub>50</sub> value of 4 ng/ml (corresponding to 7.3 pM), was approximately 10-times more potent than BiTE(H9/OKT3) [Figure 20B,C].



**Figure 20:** *In vitro* BiTE mediated depletion of primary AML blast cells. (A) Flow cytometry plot showing the percentage of CD45<sup>dim</sup> AML blast cells from a CD3/CD19 depleted AML patient bone marrow sample (left panel). Almost all CD45<sup>dim</sup> CD33<sup>+</sup> AML blast cells (97.2%) were also positive for CD123 (right panel). (B) Specific lysis of CD123<sup>+</sup> CD45<sup>dim</sup> CD33<sup>+</sup> AML blast cells after 24 hours of co-culture with autologous T cells (E:T = 10:1), at the indicated concentrations of CSL/OKT3 or H9/OKT3 BiTEs. (C) Representative flow cytometry plots of patient-derived CD45<sup>dim</sup> CD33<sup>+</sup> CD123<sup>+</sup> AML blast cells after treatment with various concentrations of CSL/OKT3 BiTE with autologous T cells (E:T = 10:1). The arrow indicates the population of AML blasts that disappears as a result of the activity of the bispecific antibody.

## 5. Discussion

### 5.1. F8-IL2 in combination with immune-check-point inhibitors

This chapter has been adapted from

Hutmacher and Nuñez et al., **Targeted Delivery of IL2 to the Tumor Stroma Potentiates the Action of Immune Checkpoint Inhibitors by Preferential Activation of NK and CD8+ T Cells**, *Cancer Immunol Res* (2019), *In Press*

In this study, we explored the therapeutic potential of immune checkpoint inhibitors in combination with F8-IL2, a tumor-targeting antibody-IL2 fusion protein. The combination of F8-IL2 with CTLA-4 and PD-1 blockade was extremely potent in immunocompetent mice bearing subcutaneous CT26 tumors, whereas the combination with PD-L1 blockade was less efficacious. The results may depend, in part, on the choice of antibodies that were used for the study. We based our investigations (i.e., antibody clone and dose) on a previous report by MedImmune, which extensively explored the performance and mechanism of action of 9D9 anti-CTLA-4 and 10F.9G2 anti-PD-L1 in various immunocompetent mouse models of cancer [338].

Recombinant IL2 has been studied in clinical trials in combination with ipilimumab for the treatment of metastatic melanoma with encouraging results (clinicaltrial.gov identifier: NCT00058279, NCT01856023) [352,353]. NKTR-214 (a pro-drug version of IL2, that regains activity over time upon loss of polyethyleneglycol chains) [237] has shown promising preclinical and clinical results in combination with immune checkpoint inhibitors, thus, stimulating additional investigations with engineered forms of IL2. In this context, antibody-IL2 fusion proteins may be particularly attractive, as a selective localization of the cytokine payload at the site of disease leads to a considerable increase in therapeutic index in immunocompetent animals [92,94,101]. IL2-based products may be ideally suited for combination with immune checkpoint inhibitors because IL2 can increase the activity not only of T cells, but also of NK cells.

All mice treated with a combination of F8-IL2 and CTLA-4 blockade exhibited a complete tumor remission and rejected subsequent challenges with CT26 tumors. A multiparameter

FACS analysis of leukocytes in tumors, draining lymph nodes, and spleen provided insights on the relative contribution of individual therapeutic agents. The most significant effect of F8-IL2 (alone or in combination) was on the intratumoral density of NK cells. These leukocytes displayed an activated and more immature phenotype, as revealed by their low KLRG1, Eomes, and CD11b expression. CTLA-4 blockade (alone or in combination) was associated with a characteristic increase of CD8<sup>+</sup> T cells in the tumor mass. These lymphocytes were PD1<sup>+</sup> and TIM-3<sup>+</sup> (revealing an exhausted phenotype), but also stained for Ki67 (indicating a proliferative potential). In the CD4<sup>+</sup> T-cell population, CTLA-4 blockade (alone or in combination) led to PD-1 upregulation. Most probably, a fine balance between activation and inhibition signals determines the antitumor activity of these lymphocytes. The features of lymphocytes in secondary lymphoid organs were substantially different compared to tumor-infiltrating lymphocytes (TILs), in keeping with recent reports published with other therapeutic modalities [342,354]. In line with the targeting result, the most significant effects of F8-IL2 on the leukocytes were seen in the TILs rather than the draining lymph nodes and spleen.

Single-cell analysis of the leukocyte composition within the tumor and secondary lymphoid organs between the treatment groups suggested that changes in the CD4<sup>+</sup> and CD8<sup>+</sup> T- and NK cell frequencies and phenotypes may influence the therapeutic outcome. The initial tumor regression was caused by both CD8<sup>+</sup> T cells and NK cells, as evidenced by leukocyte depletion experiments. CD4<sup>+</sup> T cells did not play a crucial role. Similar findings, showing an absolute requirement for CD8<sup>+</sup> T-cell and NK cell activity have previously been reported for other antibody-cytokine fusions (including products based on IL12, IL4, TNF, IL15, GM-CSF) in various immunocompetent mouse models of cancer [93,101,172,227,343].

CT26 carcinomas have often been considered to be immunologically “hot tumors”, whereas other models (such as 4T1, B16F10, LL/2, and MC38) are characterized by a sparse T-cell infiltration and, thus, associated with a “cold” phenotype [338]. The combination treatment with F8-IL2 and a checkpoint inhibitor against CTLA-4 was also efficacious in the MC38 model, whereas the individual agents displayed little activity when used in monotherapy. The combination treatment was associated with a rich leukocyte infiltrate in the tumor, with enhanced functional properties (e.g., cytolytic activity, as revealed by GZMB staining).

IL2-based therapeutics are complicated in cancer therapy because the antineoplastic activity could, in principle, be potentially mitigated by the potentiation of Treg activity [98]. Indeed, recombinant human IL2 at ultra-low dose has shown encouraging effects for the treatment of host-versus-graft disease [279]. The therapeutic activity of IL2 is likely to be context- and dose-dependent. In our setting, thanks to the antibody-based delivery to the tumor, the density of Tregs did not substantially vary between the treatment group in the CT26 colon carcinoma model. Similar observations have been reported in the bone marrow of patients with acute myeloid leukemia, treated with the F16-IL2 fusion protein directed against the alternatively-spliced A1 domain of tenascin-C [257].

We found that the treatment with the anti-CTLA-4 did not lead to the depletion of intratumoral Treg cells in the CT26 colon carcinoma model. Most probably, this is caused by the tumor model itself and the antibody that was chosen. Sergio Quezada and colleagues had previously shown that other anti-CTLA-4 antibodies (e.g., 9H10, IgG1<sub>SDALIE</sub> a mutated antibody with high binding affinity to CD16a) may be more effective than 4F10 and 9D9 in eradicating Tregs via an antibody-dependent cell-cytotoxicity mechanism [355,356]. In general, IgG2a isotypes in the mouse are thought to be better depleting antibodies than IgG2b isotypes (such as 9D9)[357]. Low levels of intratumoral antigen-presenting cells displaying cytotoxic Fc receptors may contribute to the poor depletion activity observed. We chose to use the 9D9 clone for our study because the impact of this antibody in many immunocompetent mouse models of cancer has been described in detail [338].

Immune checkpoint inhibitors have become foundational drugs for cancer therapy [236]. In the clinic, PD-1 blockade appears to be more active and better tolerated than CTLA-4 blockade, possibly because approved products (nivolumab, pembrolizumab) may interfere with the negative regulation of T cells at the site of disease, rather than in secondary lymphoid organs [358]. In the mouse, however, CTLA-4 blockade has often shown more potent anti-cancer activity compared to PD-1 and PD-L1 blockers [178,338,359].

Various antibody-IL2 fusions are currently being investigated in clinical trials [360]. In addition to F8-IL2, we contributed to the development of L19-IL2 [72,94,179]. Although the F8 antibody recognizes the alternatively-spliced EDA domain of fibronectin, L19 is specific to the

EDB domain of fibronectin [348]. L19-IL2 has been used for the treatment of patients with various types of malignancies both as monotherapy [250,361] and in combination with other modalities [234]. The product is currently being studied in Phase III clinical trials in combination with L19-TNF for the treatment of patients with fully resectable stage IIIB,C melanoma (clinicaltrial.gov identifier NCT02938299) [234]. Other companies have preferred to use IL2 fusions based on antibodies in full IgG format [241,246,248], sometimes with mutations on the IL2 moiety that reduce the affinity to the CD25 receptor [112].

The results of our study provide a rationale for the combined use of engineered IL2 therapeutics with immune checkpoint inhibitors for cancer therapy. The emerging notion that tumors, which do not respond to immune checkpoint inhibitors, still contain a large number of tumor-rejection antigens (e.g., neoepitopes) and of cognate T cells [362,363] provides a motivation to expand and stimulate these T-cell populations with experimental therapeutics.

## 6.1. Development of a novel fully-human anti-CD123 antibody to target acute myeloid leukemia

This chapter has recently been submitted for publication:

Hutmacher et al., **Development of a novel fully-human anti-CD123 antibody to target acute myeloid leukemia**, *submitted*

We have reported the generation of a novel fully-human anti-CD123 antibody (named H9) and we have compared its properties to the ones of a previously described clinical-stage antibody (named CSL362). The two antibodies recognized different epitopes on the same domain of CD123, allowing an initial comparison of anti-cancer activity for different types of therapeutic products. CD123 has been considered for many years as a target for antibody-based anti-AML approaches [315] and its differential expression on AML cell, compared to normal leukocytes and hematopoietic stem cells, has been studied by FACS [364] and by surface proteomics methodologies [365,366].

The use of Fc-engineered antibodies in IgG1 format led to the best anti-AML activity results in *in vitro* ADCC assays. The simultaneous substitution of two amino acid residues in the C<sub>H</sub>2 domain of the heavy chain (S293D and I332E) led to a potentiation of ADCC activity. These mutations have previously been shown to increase Fc binding to human V158 and F158 FcγRIIIa receptors of several antibodies such as trastuzumab, rituximab and cetuximab [347]. Other antibodies harboring the S293D-I332E amino acid modifications have previously displayed a substantial improvement of ADCC activity *in vitro* compared to their native IgG molecules. MOR208, an anti-CD19 antibody, carries the same amino acid mutations and is currently tested in clinical studies in Non-Hodgkin lymphoma, large B cell lymphoma, chronic lymphocytic leukemia and adult acute lymphoblastic leukemia (clinicaltrials.gov identifier: NCT02763319, NCT01161511, NCT01685021, NCT01685008, NCT02639910, NCT02399085, NCT02005289) [367].

It is likely that the therapeutic activity of Fc-potentiated anti-CD123 products may be enhanced by combination with certain antibody-cytokine fusions. We have previously reported that rituximab completely eradicated human B-cell lymphoma xenografts in

combination with the tumor targeting immunocytokine L19-IL2 [72]. Additionally, we have shown that the antibody-based delivery of interleukin-2 (IL-2) to the tumor neovasculature potentially increased the activity of the chemotherapeutic cytarabine [101]. Scientists at Roche have used glycoengineering to improve ADCC activity and reported the successful generation of an anti-CD20 antibody (Obinutuzumab) [368]. The anti-CD20 antibody was glycoengineered which improved ADCC activity substantially. A clinical trial, featuring the combination of the F16-IL2 fusion protein [116] with an Fc-engineered anti-CD33 antibody in patients with AML is currently on-going (clinicaltrials.gov identifier: NCT03207191).

The anti-CD123 antibodies exhibited promising results also when reformatted as bispecific antibodies. BiTE(CSL362/OKT3) was superior to BiTE(H9/OKT3) for the *in vitro* killing of patient-derived AML blasts in an autologous setting, but both products were able to kill AML cell lines at concentrations in the picomolar range. There have been recent research reports on the fact that epitopes closer to the cell membrane may lead to more efficient tumor cell killing with bispecific antibodies [369]. In this context, it may be attractive in the future to study novel antibody therapeutics, which recognize epitopes on CD123 which are closer to the lipid bilayer.

In summary, we have generated novel anti-CD123 antibodies and biopharmaceuticals, which have shown initial signs of activity in *in vitro* models of AML. IgG1<sup>pot</sup>(H9) may be the most promising product for ADCC applications, while BiTE(CSL362/OKT3) would be a good candidate for bispecific antibody-based therapeutic purposes. More than 15 formats have been described for the engineering of bispecific antibodies [370]. While the only bispecific antibody on the market (Blinatumomab, approved for patients with B-cell precursor acute lymphoblastic leukemia) is in BiTE format, it is still not clear whether biopharmaceuticals with a longer circulatory half-life may be preferable. In all cases, the antibodies described in this article may represent useful tools for the implementation of novel anti-AML strategies. We do not know, at this moment in time, whether selective tumor cell killing can be achieved while sparing hematopoietic stem cells.



## 7. Conclusions and outlook

There is a considerable interest in modern cancer research in making “cold tumors hot”, so that the full therapeutic potential of immune check-point inhibitors can be harnessed. This thesis describes how the selective antibody-mediated targeted delivery of interleukin-2 to the tumor stroma potentiates the anti-cancer activity of immune check-point inhibitors in preclinical models of cancer. The targeted delivery of IL2 (e.g., by means of F8-IL2) mediated a very strong anti-cancer effect in the mouse, with excellent tolerability. The combination with CTLA-4 blockade and PD-1 blockade was particularly active (leading to cancer cures), while a lower activity was observed in combination with anti-PD-L1 antibodies. Detailed mechanistic investigations, based on a high-parametric single cell analysis of leukocytes within the tumor masses and in secondary lymphoid organs, revealed that the selective delivery of IL2 to the tumor resulted in profound changes in T cell and NK cell features in the tumor bed, without collateral immune activation in the systemic immune compartment. Moreover, depletion of NK cells and cytotoxic T lymphocytes completely abolished the clinical efficacy providing the mechanistic insights into the therapeutic effect of this combination therapy. Furthermore, cured mice were able to reject subsequent tumors, which is indicative for the acquisition of a protective immunity.

Our group has recently published mechanistic studies in mice in which cytotoxic CD8<sup>+</sup> T cell specific for a common endogenous retroviral antigen AH1 (derived from the gp70 envelope protein of the murine leukemia virus) were upregulated upon treatment with F8-TNF and doxorubicin [102]. Such retroviral sequences have been found in the genome of all vertebrate species and their expression has been associated with autoimmune diseases and chronic infection [272–274] as well as with cancer [275,276]. Furthermore, cytolytic CD8<sup>+</sup> T cells specific for retroviral antigens, which potently lysed melanoma cells, have already been detected in patients [277]. Our group has shown, that as much as 50% of CD8<sup>+</sup> T cells in tumors implanted in BALB/c mice are specific to the AH1 peptide of retroviral origin (which acts as immunodominant tumor rejection antigen), while the frequency of AH1-specific T cells is much lower in secondary lymphoid organs, including tumor-draining lymph nodes [371]. It will be important to study if and to which extent such specific cytotoxic CD8<sup>+</sup> T cells against retroviral antigens are upregulated after treatment with check-point inhibitors, F8-IL2 and

the combination. Researchers at Bristol-Myers Squibb have shown that AH1-specific CD8+ T cells were expanded in the spleens of CT26 tumor bearing mice upon treatment with a combination of PD-1 and CTLA-4 antibodies [342]. These AH1 specific CD8+ T cells increased from 1 % to approximately 15.6 % [342]. Within the tumors, the frequency of AH1 specific CD8+ T cells did not vary substantially between the treatment groups and the control [342]. These lymphocytes represented about 15 % of total tumor infiltrating leukocyte [342]. Our group has shown that treatment with the F8-TNF immunocytokine was able to expand the AH1 specific intratumoral CD8+ T cells from 29 to 40 %. It will be interesting to study if this could also be achieved after the administration of F8-IL2. If specific CD8+ T cells against retroviral antigens can be detected in mouse models using F8-IL2 alone or in combination with check-point inhibitors, it would be important to learn whether such T cells could also be increased in humans. The detailed multiparametric analysis of leukocytes within the tumor mass in different treatment groups may serve as a reference for future therapeutic studies, which may employ IL2-based therapeutics or immune checkpoint inhibitors, perhaps in combination with other agents.

The work of this thesis may have translational value, as immune check-point inhibitors represent foundational drugs for modern cancer therapy and since a growing number of engineered IL2 products is being investigated in clinical trials. Our results provide a rationale for the evaluation of IL-2 based products in combination with check-point inhibitors in humans.

The second part of this thesis describes the generation and *in vitro* characterization of novel human antibodies against CD123, a surface marker which is overexpressed in a variety of hematological disorders including acute myeloid leukemia. Current treatment options for AML patients are suboptimal, especially for young patients who do not benefit from allo-HSCT or for the elderly, not eligible for intensive chemotherapy and allo-HSCT. Thus, there is a need to provide them with better and safer treatment strategies. Novel immunotherapeutic strategies for AML include the use of intact immunoglobulins, ADCs, CAR-Ts, and bispecific T-cell engagers. The most challenging aspect of treating AML is associated to the fact that all known target antigens (such as CD33, CD123, or cKIT) are not only expressed on leukemic

stem cells, but also on normal stem cells. For the different immunotherapeutics mentioned above, this limitation may have more or less serious consequences. In particular, the use of CAR-Ts for the treatment of AML appears to be problematic, because of high risks of myeloablation. At the moment, it is extremely difficult to switch CAR-T cells off. This problem aggravates the use of CAR-T cells in AML, because whenever new stem cells are transplanted (which are vital), they get killed by the long-lived CAR-Ts. Promising preclinical and clinical results have been achieved with ADCs, as illustrated by Mylotarg, the first ADC to receive marketing authorization. Seattle Genetics has developed an ADC that targets CD123 (SGN-CD123A)[372]. It was the first anti CD123 based ADC to start clinical investigation, but phase I clinical trials have already been stopped due to patients death (clinicaltrial.gov identifier: NCT02848248).

In this thesis, we have developed a new fully-human antibody IgG1(H9) by means of phage display technology that specifically recognized the cognate antigen in standard biochemical assays. The antibody has been affinity matured and engineered for enhanced antibody dependent cellular cytotoxicity IgG1(H9)<sup>pot</sup>. IgG1(H9)<sup>pot</sup> was benchmarked against a previously described anti-CD123 antibody (CSL362) that was the first anti-CD123 antibody to be tested in humans. IgG1(H9) exhibited an approximately 10-fold lower functional affinity than IgG1(CSL362)( $K_d^{app} = 250$  pM versus  $K_d^{app} = 20$  pM). The two antibodies recognized different epitopes on the N-terminal domains of CD123. IgG1(H9)<sup>pot</sup> was slightly more potent than IgG1(CSL362)<sup>pot</sup> *in vitro* ADCC assays using cell lines. Moreover, both antibodies were able to selectively kill patients' blasts *in vitro*. At this stage, however, it is unclear whether *in vivo* selective tumor cell killing can be achieved while sparing hematopoietic stem cells. A next experimental step in mice could be to test the *in vivo* targeting performance of the antibody by a quantitative biodistribution study in mice bearing subcutaneous AML xenografts. The efficacy of the new product should also be tested in acute myeloid leukaemia xenografts. AML xenograft cells can be injected intravenously into severe combined immunodeficiency mice and allowed to engraft. After successful engraftment, the antibody can be administered and the levels of human AML cells monitored by means of flow cytometry of peripheral blood. Another interesting experiment would be to perform a thorough characterization of CD123 expression in healthy tissue and AML specimens (e.g., diseased bone marrow and chloroma lesions). A first insight into protein expression is given by Human Protein Atlas

([www.proteinatlas.org](http://www.proteinatlas.org)). For most cancers and organs, the Atlas shows a moderate intracellular staining for CD123 with additional membrane positivity. This feature may represent an antibody-related staining artefact and may therefore be misleading. Obviously, any intracellular CD123 molecule would not be accessible to an intravenously administered antibody product.

The anti-CD123 antibodies were reformatted as bispecific antibodies (BiTE(CSL362/OKT3), BiTE(H9/OKT3)) and yielded promising *in vitro* results. Both antibodies induced the selective killing of patient-derived AML blasts in the picomolar range, although BiTE(CSL362/OKT3) was 10-fold more potent. BiTEs are attractive biopharmaceuticals which can recruit effector cells to the side of disease and induce tumor cell killing. They do not have an Fc portion, thus potentially decreasing “off-target” toxicity. In general, however, BiTEs have a short half-life and the monovalent binding of the target antigen may result in poor targeting results. Strategies to prolong the half-life include those based on an increase of the hydrodynamic radius (e.g., by PEGylation or PASylation or the use of recombinant polypeptides) or the use of fusion proteins which bind to and are recycled by the neonatal Fc receptor (e.g., Fc or albumin tags)[373–375]. BiTEs with low affinity for one of the target antigen, such as BiTE(H9/OKT3), can also be reformatted into formats that consist of a single chain diabody (scDb; e.g. against CD123) fused to the anti-CD3 scFv. Ideally, the tumor-targeting performance and the activity of the BiTEs should be tested in animal models. This is usually difficult to implement for hematological malignancies, as target antigens are typically not conserved from mice to humans. To test a BiTE, human tumors are normally implanted in immunocompromised mice followed by the administration of human hematopoietic stem cells. This is a very artificial setting and a complicated procedure. Alternatively, one could consider the use of mice which are transgenic for the human  $\epsilon$  chain of the CD3 complex and a mouse tumor cell line that is stably transfected with the human tumor antigen. This approach has been successfully implemented by scientists at Regeneron.

It remains to be investigated, which leukemia antigen is the best candidate for biopharmaceuticals and which strategy gives the best results. It could be, that the simultaneous targeting of two antigens (e.g., CD33 and CD123) by the DuoBody technology (GenMab) or a Tribody yields the best therapeutic index.

In summary, the results of this thesis support the use of IL-2 based products in combination with check-point inhibitors in the clinics and provide novel fully-human antibodies for the future treatment and AML research.

## 8. Materials and methods

### 8.1. F8-IL2 in combination with immune-check-point inhibitors

This chapter has been adapted from

Hutmacher and Nuñez et al., **Targeted Delivery of IL2 to the Tumor Stroma Potentiates the Action of Immune Checkpoint Inhibitors by Preferential Activation of NK and CD8+ T Cells**, *Cancer Immunol Res* (2019), *In Press*

#### 8.1.1. Cell lines, animals, and tumor models

The CT26 colon carcinoma (CRL-2638), the F9 teratocarcinoma (CRL-170), and the CTLL-2 (TIB-214) cell lines were obtained from ATCC, expanded, and stored as cryopreserved aliquots in liquid nitrogen. The MC38 cell line was a kind gift of Prof. Onur Boyman. Cells were grown according to the supplier's protocol and kept in culture for no longer than 2 weeks. The CT26 colon carcinoma cells were expanded and cultured in RPMI1640 (Gibco) supplemented with 10 % fetal bovine serum (Gibco, 10 % FBS), the F9 teratocarcinoma cell line in DMEM (Gibco) containing 10 % FBS. The MC38 cell line was grown in advanced DMEM (Gibco) with 10 % FBS and 1 % Ultraglutamine (Lonza). CTLL2 cells were cultivated in RPMI1640 (Gibco) supplemented with 10% FBS, 1 % Ultraglutamine, 25 mM Hepes (Gibco), 0.05 mM  $\beta$ -Mercaptoethanol (Sigma Aldrich) and 60 Units/ mL human Interleukin-2 (Roche Diagnostics). Authentication of the cell line included check of post-freeze viability, growth properties, morphology, test for mycoplasma contamination, isoenzyme assay, and sterility testing and were performed by the cell bank before shipment. Seven- to eight-week-old female BALB/c mice were purchased from Charles River (Germany). Eight-week-old female 129/Sv and C57BL/6JRj mice were purchased from Janvier (France). On the day of tumor cell injection, exponentially growing F9 teratocarcinoma, CT26 colon carcinoma or MC38 cells were harvested, repeatedly washed, and resuspended in saline prior to injection. CT26 colon carcinoma cells ( $2 \times 10^6$  cells per mouse, using BALB/c mice), MC38 cells ( $1 \times 10^6$  cells per mouse, using C57BL/6JRj) or F9 teratocarcinoma cells ( $12 \times 10^7$  cells per mouse, using 129/Sv mice) were implanted subcutaneously in the right flank. Mice were monitored daily and tumor volume was measured with a caliper. Tumor volume was calculated as follows: (length [mm] x width [mm] x width [mm])/2. Animals were euthanized when tumor volumes reached a maximum of 2000 mm<sup>3</sup>, weight loss exceeded 15 %, tumors were ulcerated or 24 hours

after the last injection for the biodistribution and the multiplex flow cytometry analysis (on day 13 after tumor cell injection). Tumors, draining lymph nodes and spleen were harvested for flow cytometry analysis. To assess the biodistribution of the fusion protein, tumor, liver, lung, spleen, heart, kidney, intestine and blood was collected.

All experiments were performed under a project license granted by the Veterinäramt des Kanton Zürichs, Switzerland (27/2015) in agreement with Swiss regulations. Animals were maintained in pathogen-free facilities at the Swiss Federal Institute of Technology (ETH Zurich) and procedures were approved by the ETH Zurich Institutional Animal Care and Use Committee.

#### 8.1.2. Antibodies for therapy experiments

The F8-IL2 immunocytokine was produced as previously described [115]. In brief, a stable CHO-S cell line (Invitrogen) was incubated for 6 days in a shaking incubator at 31°C. F8-IL2 was purified from the culture medium by a protein A affinity column (Protein A agarose beads, Sino Biologicals Inc.). The commercial anti-PD-1 (clone 29F.1A12), anti-PD-L1 (clone 10F.9G2), anti-CTLA-4 (clone 9D9) were purchased from BioXCell. The products had previously been extensively studied in immunocompetent models of cancer [338,359]. Rat anti-CD4 (clone GK1.5, BioXCell), rat anti-CD8 (clone YTS169.4, BioXCell) and rabbit anti-Asialo GM1 (Wako Chemicals) antibodies were used for *in vivo* depletion, as described below.

#### 8.1.3. *In vitro* characterization of F8-IL2

F8-IL2 was analyzed using SDS-PAGE in non-reducing and reducing conditions, size exclusion chromatography (Superdex 200 Increase, 10/300 GL, GE Healthcare), and surface plasmon resonance analysis (BIAcore S200, GE Healthcare) on an EDA antigen-coated CM5 BIAcore sensor chip (GE Healthcare). The biological activity of F8-IL2 and IL2 (Proleukin, Roche) was determined as described before [115]. Briefly,  $10 \times 10^6$  cultured CTLL-2 cells were starved in CTLL2 culture medium (RPMI1640 (Gibco) supplemented with 10% FBS, 1 % Ultraglutamine, 25 mM Hepes (Gibco), 0.05 mM  $\beta$ -Mercaptoethanol (Sigma Aldrich)) without IL2 for 24 hours. Starved CTLL-2 cells ( $2 \times 10^4$ / well) were seeded in 96-well plates in CTLL2 culture medium containing varying concentrations ( $5 \times 10^{-12}$  –  $10^{-9}$  M IL2 equivalents) of IL2 equivalents (F8-IL2 or as positive control purchased human IL2 (Roche Diagnostics) in triplicates. After 48 hours

at 37°C, cell proliferation was determined with the Cell Titer 96® Aqueous One Solution (Promega) according to the manufacturer's instructions by measuring the OD at 490 nm and 620 nm. Percent proliferation was calculated as follows: % proliferation =  $(OD_{490-620}^{\text{treated}} - OD_{490-620}^{\text{medium}}) / (OD_{490-620}^{\text{untreated}} - OD_{490-620}^{\text{medium}}) \times 100 \%$ .

#### 8.1.4. Quantitative biodistribution study

Quantitative biodistribution was used to assess the *in vivo* targeting performance of F8-IL2 (n = 4) as described previously [335]. Purified F8-IL2 was radiolabeled with iodine 125 (Perkin Elmer) using the Iodogen method. Immunocompetent 129/Sv mice (n = 3) were injected with  $12 \times 10^7$  F9 teratocarcinoma cells subcutaneously into the right flank. Mice were monitored daily, and tumor volume was measured with a caliper. Tumor volume was calculated as follows:  $(\text{length [mm]} \times \text{width [mm]} \times \text{width [mm]}) / 2$ . When the tumors reach approx. 350 mm<sup>3</sup>, 0.86 µg of radio-iodinated F8-IL2 was injected intravenously into the lateral tail veins. After 24 hours, mice were sacrificed, tumor, liver, lung, spleen, heart, kidney, intestine and blood collected, weighed, and the radioactivity was counted using a Cobra γ counter (Packard, Meriden, CT, USA). The radioactivity of tumors and organs was expressed as percentage of injected dose per gram of tissue (% ID/ g ± SD).

#### 8.1.5. Therapy study and *in vivo* depletion of NK cells and CD4+ and CD8+ T cells

On the day of tumor cell injection, exponentially growing CT26 colon carcinoma or MC38 cells were harvested, repeatedly washed, and resuspended in saline prior to injection. CT26 colon carcinoma cells were implanted subcutaneously in the right flank of BALB/c mice using  $2 \times 10^6$  cells per mouse. MC38 cells were implanted subcutaneously in the right flank of C57BL/6JRj mice using  $1 \times 10^6$  cells per mouse. Mice were monitored daily and tumor volume was measured with a caliper. Tumor volume was calculated as described before. When tumors reached a suitable volume (approx. 80 mm<sup>3</sup>), mice were randomly divided into different treatment groups and injected into the lateral tail vein. Mice received three injections of 30 or 45 µg F8-IL2 or 200 µg of a checkpoint inhibitor (anti-PD-1, anti-PD-L1, or anti-CTLA-4), phosphate-buffered saline, or the combination of F8-IL2 and a checkpoint inhibitor at intervals of 72 hours. In the combination group, mice received F8-IL2 followed by a checkpoint inhibitor after 24 hours. For the *in vivo* depletion of NK, CD4<sup>+</sup>, and CD8<sup>+</sup> cells, CT26 colon carcinoma-bearing mice (n= 5 per group) were repeatedly injected intraperitoneally with 30



$\mu\text{L}$  anti-Asialo GM1 (day 2, 5, and 8 after tumor implantation), 250  $\mu\text{g}$  anti-CD4 or 250  $\mu\text{g}$  anti-CD8 antibodies (day 2, 5, 8 and 11 after tumor implantation). An additional group ( $n = 5$ ) was injected with an anti-CD4 on day -1, 2, 4, and 8 after tumor injection. A saline group ( $n = 5$ ) and a treatment group ( $n = 5$ ) without depletion were included as controls. Animals were euthanized when tumors reached a maximum of 2000  $\text{mm}^3$ . Flow cytometry of the spleen was used to verify the successful depletion of the specific leukocyte population.

#### 8.1.6. Tumor re-challenge

Mice that cleared tumors were injected subcutaneously with  $2 \times 10^6$  CT26 colon carcinoma or  $1 \times 10^6$  MC38 cells on day 62 and day 60, respectively, after the first injection of tumor cells. As controls, naïve BALB/c mice ( $n = 5$ ) and naïve C57BL/6JRj ( $n = 6$ ) were injected with the same tumor cells to monitor tumor growth and cell viability after injection.

#### 8.1.7. Immunohistochemical analysis of EDA expression in CT26 and MC38 tumors

CT26 and MC38 tumors were excised and immediately embedded in frozen section medium (Thermo Scientific). Staining was performed on 10 mm cryosections fixed in ice-cold acetone. Primary antibodies in small immunoprotein format (F8 and KSF, kindly provided by Dr. Rémy Gebleux) were detected with a rabbit anti-human IgE (1:1000, Dako Agilent) and in a second step with Alexa Fluor 488–coupled anti-rabbit (1: 200, Invitrogen). An anti-CD31 (1:100, MEC 13.3, BD Biosciences) was detected with an Alexa Fluor 594–coupled anti-rat antibody (1:200, Invitrogen). Sections were counterstained with DAPI (SigmaAldrich) and mounted with fluorescent mounting medium (Dako Agilent). Slides were then analyzed with an Axioskop2 mot plus microscope (with a 20x/0.5 objective lense, Zeiss) and documented with an AxioCam color camera (Zeiss), using the AxioVision software (4.7.2. Release, Zeiss).

#### 8.1.8. Flow cytometry

For a multiparameter flow cytometry analysis, mice were sacrificed and tumor, spleen, and draining inguinal lymph nodes were excised 24 hours after the last injection. Tumors were transferred into gentleMACS C tubes (Miltenyi) in RPMI and digested with DNase (30  $\mu\text{L}$ / tumor, Sigma) and liberase (60  $\mu\text{L}$ / tumor, Roche) for 40 minutes at 37°C using the

gentleMACS Dissociator according to the manufacturer's instruction (program 37C\_m\_TDK\_1). After centrifugation, the pellet was resuspended in 40% Percoll (GE Healthcare) and the solution was filtered using a 100 µm cell strainer (Greiner-bio-one). Percoll 75 % (10 ml for each 10 ml cell suspension) was slowly poured onto the Percoll 40 %- cell suspension. After Percoll gradient centrifugation, the buffy coat was collected. Cells were washed twice and stained (**Suppl. Table 1**). Spleen were digested as described for the tumors (using program 37C\_m\_SDK\_1). After the digestion, the erythrocytes were lysed using RBC lysis buffer (BioLegend TM). The cells were spun down and resuspended in PBS to yield a concentration of  $4 \times 10^6$  cells/ mL. Single-cell suspensions were directly used for flow cytometry staining (**Suppl. Table 1**). Lymph nodes were smashed using the plunger of a 1 mL syringe and filtered into a polystyrene tube with a cell strainer cap (StemCell Technologies). After centrifugation, cell pellets were resuspended in RPMI complemented with 10% FBS. Non-specific binding was blocked using anti-CD32/CD16 (BioLegend TM) followed by the flow cytometry antibody panel described in **Suppl. Table 1**. For intracellular staining, cells were fixed and permeabilized with fixation/ permeabilization solution (Thermo Scientific), according to the manufacturer's instructions. Cells were acquired on a Symphony flow cytometer (BD Biosciences). Data was analyzed using FlowJo (version 10.0.8, TreeStar Inc.). For an unbiased analysis, we reduced the high-dimensional dataset into two dimensions through t-distributed stochastic neighbor embedding (t-SNE) in combination with FlowSOM meta-clustering as described [376].

#### 8.1.9. Statistical analysis of murine tumor, lymph node, and spleen datasets

Data were analyzed using Prism 6.0 (GraphPad Software, Inc.). Statistical significance of *in vivo* experiments was determined with a regular two-way ANOVA test with the Bonferroni post-test. We utilized unsupervised validated clustering approaches (FlowSOM, CellCNN, Citrus) to discern between different cell populations. For FlowSOM metaclustering, flow cytometer data were compensated, exported with FlowJo software (version 10.0.8, TreeStar Inc.) and normalized using Cyt MATLAB (version 2017b). An unbiased analysis was performed as described [376].

## 8.2. Development of a novel fully-human anti-CD123 antibody to target acute myeloid leukemia

This chapter has recently been submitted for publication:

Hutmacher et al., **Development of a novel fully-human anti-CD123 antibody to target acute myeloid leukemia**, *submitted*

### 8.2.1. Cell lines

The TF-1 (CRL-2003) and the Kasumi-1 (CRL-2724) cell lines were obtained from the American Type Culture Collection (ATTC) and CHO-S cells from Invitrogen. The OCI-AML3 cell line (ACC-247) was obtained from the DSMZ. Cell lines were expanded, and stored as cryopreserved aliquots in liquid nitrogen. Cells were grown according the supplier's protocol and kept in culture for no longer than 2 weeks. Authentication of the cell line also included check of post-freeze viability, growth properties, morphology, test for mycoplasma contamination, isoenzyme assay, and sterility test were performed by the cell bank before shipment. The Kasumi-1 cell line was stably transfected with a lentivirus containing the vector with the GFP sequence (lentilab.unige.ch)[377].

### 8.2.2. Cloning and expression of recombinant CD123

The cDNA of the extracellular domains of human CD123 were obtained from Genscript and cloned into the pcDNA3.1(+) expression vector with a C-terminal 6-His tag (CD123-His) or a Fragment crystallizable (Fc) tag (CD123-Fc). The extracellular domains 2 and 3 of CD123 was cloned into the pcDNA3.1 vector with an Fc tag. Fusion proteins were expressed using polyethyleneimine (PEI)-mediated transient gene expression in CHO-S cells as described [378]. The proteins were purified from the culture medium via protein A affinity chromatography or a Ni-NTA agarose resin (ThermoFisher) and analyzed using SDS-PAGE and size exclusion chromatography (Superdex 200 Increase, 10/300, GE Healthcare).

### 8.2.3. Generation of a stable CD123 monoclonal cell line

CHO-S cells were stably transfected with a gene coding for the whole CD123 and a second gene conferring antibiotic resistance against neomycin. After antibiotic selection and limiting

dilution to generate monoclonal cell lines, the cells were screened for expression of CD123 by flow cytometry using an anti-human CD123 antibody (clone 6H6, BioLegend).

#### 8.2.4. Selection of antibodies from the ETH-2 Gold library by phage display and affinity maturation

Human monoclonal antibodies specific to the CD123 antigen were isolated by three rounds of biopanning from the ETH-2 Gold antibody phage display library as described [345]. Bacterial supernatants containing recombinant scFv antibody fragments were screened by ELISA. Those with positive signal in ELISA were analyzed using a BIAcore 200 instrument (GE Healthcare) and sequenced. The affinity maturation library was cloned by introducing sequence variability in the CDR1 of both heavy and light chain of the best clone using partially degenerate primers as already shown in [78]. The library was electroporated into fresh electrocompetent TG-1 cells. Bacterial supernatants of individual colonies were screened by ELISA and BIAcore. The best clone was sequenced and reformatted into the fully-human IgG format by cloning VH and VL into pcDNA3.1 (+) resulting in the H9 antibody.

#### 8.2.5. Cloning of BiTE(H9/OKT3), BiTE (CSL362/OKT3) and the CSL362 antibody

The sequence of CSL362 and the OKT3 was retrieved from the corresponding patents (US 8,569,461 B2 and US 7, 635, 472 B2). Vectors containing the heavy (without the ADCC engineered mutations) or light chain sequence and the OKT3 sequence were ordered from Genscript. BiTE(H9/OKT3) was assembled by PCR in the following format using specific primers: N-terminus- signal peptide-variable light chain of the H9-variable heavy chain of the H9- variable heavy chain of OKT3- variable light of OKT3- C-terminus. BiTE(CSL263/OKT3) was assembled in the same format, but a His-tag was added at the C-terminus.

#### 8.2.6. Expression of antibodies and antibody fragments

The vectors containing the antibody, antibody fragment and BiTE sequences were used for transient gene expression using polyethyleneimine as described before. The proteins were purified by protein A affinity chromatography or an Ni-NTA agarose resin (ThermoFisher).

#### 8.2.7. Epitope mapping using peptide array

In order to characterize the binding of the H9 antibody, we identified the epitope on CD123 extracellular domain using a peptide array (PepSpot, JPT). The synthesis of the target antigen

as an overlapping linear series of peptides covalently attached to a cellulose support was performed by SPOT technique at JPT. A consecutive series of 15-mer with 3 residues shift each resulted in 92 peptides, spanning the 287 amino acid sequence of CD123. The assay was performed according to manufacturer's instructions and the binding spots were detected by a chemiluminescence imager (Agfa Curix 60, Agfa Healthcare) after the incubation of the membrane with IgG(H9) and then with protein A-HRP (GE Healthcare).

#### 8.2.8. Flow cytometry-based binding of H9 and CSL362 to stable CD123 monoclonal cell line

Stably transfected CD123 expressing CHO-S cells were centrifuged and washed in FACS buffer (2 % FBS in PBS). Cells were stained with primary antibodies H9, CSL362 and a negative control antibody L19 (targeting the extracellular domain A of fibronectin). After washing, an AF647 goat anti human IgG (ThermoFisher) was used to detect the primary antibodies. The cells were washed again and analyzed on a 2-L CytoFLEX Flow Cytometer (Beckman Coulter).

#### 8.2.9. Surface Plasmon Resonance

CD123-Fc was immobilized on a CM-5 sensor chip with a density of 1600 RU using a BIAcore 200 system. Serial dilutions of antibody fractions or bacterial supernatants were investigated. The binding curves were analyzed with the BIAevaluation 3.2 software.

#### 8.2.10. ADCC potentiation

To enhance the antibody dependent cellular cytotoxicity of the antibody, two amino-acid mutations S293D and I332E were introduced into the Fc region by PCR as it has been done for other antibodies including the CSL362 antibody [326,347]. This yielded the IgG1<sup>pot</sup>(H9) and the IgG1<sup>pot</sup>(CSL362) antibody which were expressed by transient gene expression as described before.

#### 8.2.11. Isolation of human peripheral blood mononuclear cells (PBMCs)

Peripheral blood samples were obtained from healthy donors from the Blutspendedienst SRK, Zurich. Peripheral blood mononuclear cells (PBMCs) were isolated by density gradient centrifugation on Ficoll Paque Plus (GE Healthcare) according to the manufacturer's instructions. The peripheral blood was three-fold diluted in PBS solution containing 2 mM

EDTA. Then, 30 ml of diluted peripheral blood were layered on 12.9 ml Ficoll and centrifuged at 400 x g for 40 min at room temperature. PBMCs were collected, and then washed 2 times with PBS/EDTA. After washing, the cells were immediately subjected to the *in vitro* killing assay.

#### 8.2.12. ADCC assay on human cell lines

Antibody-dependent cellular cytotoxicity was analyzed using flow cytometry as described [379]. For this, target cells were labelled with CFSE (Invitrogen) according to the manufacturer's instructions and cultured with PBMC at an effector to target cell ratio (E:T) of 50:1 and the antibodies for 16 hours at 37°C in RPMI supplemented with 5% or 10% FBS. The cells were harvested, and stained with Fixable Viability Dye (Invitrogen) which labels dead cells. After 30 min of incubation, the cells were washed with PBS containing 2 % FBS and then subjected to FACS analysis using a 2-L CytoFLEX cytometer (Beckman Coulter), and data were processed using FlowJo (v.10, Tree Star). The percentage of specific lysis was calculated as follows:  $(1 - \text{number of alive target cells} / \text{number of alive target cells without antibody}) * 100$ .

#### 8.2.13. ADCC assay on AML blasts

The primary human cells used in this study were selected from the biobank of the department of Medical Oncology and Hematology, University Hospital Zurich, Zurich, Switzerland. All AML patient bone marrow and blood samples were obtained with written informed consent. The study was approved by the Ethics Board of the Canton of Zurich (2009-0062). CD3/CD19 depleted AML patient bone marrow cells were thawed and incubated for 4 days in IMDM medium supplemented with 20% FBS and 1% penicillin/streptomycin (GIBCO, Thermo Fischer Scientific) as well as 50 uM mercaptoethanol, 10 ng/mL recombinant SCF, 50 ng/mL recombinant TPO and 10 ng/mL FLT3 ligand (Peprotech). To determine CD123 expression on leukemic blast surface, CD33-BV711 (Biolegend), CD34-PE (Thermo Fischer), CD45-e450/PB (Biolegend) were co-stained with CD123-APC (Biolegend). Dead cells were excluded from analysis by staining cells with Aqua Live/Dead cell viability dye (Biolegend). After the isolation of healthy PBMCs by Ficoll centrifugation (GE Healthcare), NK cells were enriched by EasySep™ Human NK cell Isolation Kit (STEMCELL) following the manufacturer's instructions. Allogeneic NK cells and cultured CD3/CD19 depleted AML patient bone marrow cells were mixed at an effector to target ratio of 10:1 in IMDM medium supplemented with 20% FBS and

1% penicillin/streptomycin. A dilution series of IgG(L19), IgG<sup>pot</sup>(CSL362) and IgG<sup>pot</sup>(H9) was subsequently added to the cell culture which was then incubated for 24 hours at 37°C. The specific lysis was analyzed by flow cytometry using a LSR II Fortessa cell analyzer (BD Biosciences) and quantified using the formula described before.

#### 8.2.14. *In vitro* BiTE-mediated T-cell killing of primary AML blast

T cells were thawed 1 day before the assay and cultured overnight in advanced RPMI supplemented with 1x Glutamax (Gibco), 10% FBS and 1% penicillin/streptomycin (T cell medium). Effector and target cells were co-cultured in T cell medium (E:T= 10:1). A dilution series of BiTE was added to the cell solution and incubated for 24 hours at 37°C. The specific lysis of AML blasts (CD45<sup>dim</sup>) was analyzed by flow cytometry using a LSR II Fortessa cell analyzer (BD Biosciences) and quantified using the formula described before.

## 10. Copyright

Parts of this thesis have been adapted from the published or submitted articles listed below and are reproduced with permission and in accordance with the copyright guidelines of the corresponding journals.

Hutmacher and Neri, **Antibody-cytokine fusion proteins: Biopharmaceuticals with immunomodulatory properties for cancer therapy**, *Advanced Drug Delivery Reviews* (2018), *in press*

Hutmacher and Neri, **Targeted Interleukin 2 and synergy with immune check-point inhibitors** [abstract]; *Cancer Res* (2018),78(13 Suppl): Abstract nr 3811

Hutmacher and Nuñez et al, **Targeted Delivery of IL2 to the Tumor Stroma Potentiates the Action of Immune Checkpoint Inhibitors by Preferential Activation of NK and CD8+ T Cells**, *Cancer Immunol Res* (2019), *In Press*

Hutmacher et al, **Development of a novel fully-human anti-CD123 antibody to target acute myeloid leukemia**, *submitted*



## 11. List of abbreviations

ADC	Antibody-drug conjugate
ADCC	Antibody-dependent cellular cytotoxicity
ALL	Acute lymphoblastic leukemia
allo-HSCT	allogeneic hematopoietic stem cell transplantation
AML	Acute myeloid leukemia
ARC	Antibody Radionuclides conjugates
BiTE	Bi-specific T cell engager
BM	Bone marrow
CAR-T cell	Chimeric antigen receptor T cell
CDC	Complement-dependent cytotoxicity
CDR	Complementarity-determining region
CEA	Carcinoembryonic antigen
CFSE	Carboxyfluorescein succinimidyl ester
CH	Constant heavy chain
CHO	Chinese hamster ovary cell line
CL	Constant light chain
CLL	Chronic lymphoid leukemia
CML	Chronic myeloid leukemia
CTLA-4	Cytotoxic T-lymphocyte-associated protein 4
CR	Complete response
DMEM	Dulbecco's Modified Eagle Medium
DNA	Deoxyribonucleic acid
ECM	Extracellular matrix
EDA	Extra-domain A of fibronectin
EDB	Extra-domain B of fibroectin
EDTA	Ethylendiaminetetra acetic acid
EGFR	Epidermal growth factor receptor
ELISA	Enzyme-linked immunosorbent assay
EpCAM	Epithelial cell adhesion molecule
FACS	Fluorescence-activated cell sorting
FAB	French-American-British
Fab	Fragment antigen-binding portion of an antibody
FAP	Fibroblast activation protein
FBS	Fetal bovine serum
Fc	Fragment crystallizable
FcγR	Fc gamma receptor
FcRn	Neonatal Fc receptor
FDA	Food and Drug Administration
FLT3	Fms like tyrosine kinase 3
FPLC	Fast protein liquid chromatography
Fv	Fragment variable

G-CSF	Granulocyte colony-stimulating factor
GM-CSF	Granulocyte-macrophage colony-stimulating factor
GZMB	Granzyme B
HAMA	Human-anti-mouse antibodies
HER	Human epidermal growth factor receptor
HiDAC	High-dose cytarabine
HSC	Haematopoietic stem cells
IFN $\alpha/\beta/\gamma$	Interferon alpha/beta/gamma
Ig	Immunoglobulin
IL	Interleukin
IMDM	Iscove's Modified Dulbecco's Medium
i.p.	Intraperitoneal
IU	International units
i.v.	Intravenous
KD	Dissociation constant
kDa	Kilodalton
mAb	Monoclonal antibody
MHC	Major histocompatibility complex
MTD	Maximum tolerated dose
MW	Molecular Weight
NHL	Non-Hodgkin lymphoma
NK cell	Natural killer cell
NSLC	Non-small cell lung carcinoma
PBMC	Peripheral blood mononuclear cell
PBS	Phosphate buffered saline
PCR	Polymerase chain reaction
PD-1	Programmed cell death protein 1
PD-L1	Programmed cell death 1 ligand 1
PEG	Polyethylene glycol
PSMA	Prostate-specific membrane antigen
R&D	Research and development
rpm	Rotations per minute
RPMI	Roswell Park Memorial Institute
RT	Room temperature
RU	Resonance units
SEM	Standard error of the mean
s.c.	Subcutaneous
scFv	Single-chain variable fragment
SDS	Sodium dodecyl sulfate
SDS-PAGE	Sodium dodecyl sulfate polyacrylamide gel electrophoresis
SEC	Size-exclusion chromatography
SIP	Small immunoprotein

SMDC	Small molecule drug conjugates
TCR	T cell receptor
TEA	Triethylamine
Th1/2	T helper cell type 1/2
TNF	Tumor necrosis factor alpha
TnC A1	A1 domain of Teascin-C
TRAIL	TNF-related apoptosis-inducing ligand
Treg	regulatory T cell
t-SNE	t-distributed stochastic neighbor embedding
VEGF	Vascular endothelial growth factor
VH	Variable heavy chain
VL	Variable light chain
WHO	World Health Organization

## 12. References

- [1] G. Walsh, Biopharmaceutical benchmarks 2014, *Nat. Biotechnol.* 32 (2014) 992–1000.
- [2] F.M. Brodsky, Monoclonal Antibodies as Magic Bullets, *Pharm. Res.* 5 (1988) 1–9.
- [3] G. Köhler, C. Milstein, Continuous cultures of fused cells secreting antibody of predefined specificity, *Nature.* 256 (1975) 495–497.
- [4] O.H. Brekke, I. Sandlie, Therapeutic antibodies for human diseases at the dawn of the twenty-first century, *Nat. Rev. Drug Discov.* 2 (2003) 52–62. doi:10.1038/nrd984.
- [5] M. Khazaelli, R. Conry, A. LoBuglio, Human immune response to monoclonal antibodies, *J. Immunother.* 15 (1994) 42–52.
- [6] A.S. Schmid, D. Neri, Advances in antibody engineering for rheumatic diseases, *Nat. Rev. Rheumatol.* (n.d.). doi:10.1038/s41584-019-0188-8.
- [7] P. Bruhns, Properties of mouse and human IgG receptors and their contribution to disease models, *Blood.* 119 (2012) 5640–5649. doi:10.1182/blood-2012-01-380121.5640.
- [8] S.L. Morrison, M.J. Johnson, L.A. Herzenberg, V.T. Oi, Chimeric human antibody molecules: mouse antigen-binding domains with human constant region domains., *Proc. Natl. Acad. Sci.* 81 (1984) 6851–6855. doi:10.1073/pnas.81.21.6851.
- [9] S. Bell, M. Kamm, the clinical role of anti-TNFalpha antibody treatment in Crohn’s, *Aliment. Pharmacol. Ther.* 14 (2000) 501–514.
- [10] F. Baert, G. D’Haens, S. Vermeire, A. Carbonez, G. Van Assche, M. Noman, P. Rutgeerts, Influence of Immunogenicity on the Long-Term Efficacy of Infliximab in Crohn’s Disease, *N. Engl. J. Med.* 348 (2003) 601–608. doi:10.1056/nejmoa020888.
- [11] G. Bartelds, C.L.M. Krieckaert, M. Nurmohamed, P. van Schouwenburg, W.F. Lems, J. Twisk, B. Dijkmans, L. Aarden, G. Wolbink, Development of Antidrug Antibodies Against Adalimumab and Association With Disease Activity and Treatment Failure During Long-term Follow-up, *JAMA Oncol.* 305 (2011) 1460–1468.
- [12] G. Winter, P.T. Jones, P.H. Dear, M.S. Neuberger, J. Foote, Replacing the complementarity-determining regions in a human antibody with those from a mouse, *Nature.* 321 (2004) 522–525. doi:10.1038/321522a0.
- [13] C.T. Scott, Mice with a human touch, *Nat. Biotechnol.* 25 (2007) 1075–1077.
- [14] A. Jakobovits, R. Amado, X. Yang, L. Roskos, G. Schwab, From XenoMouse technology

- to panitumumab, the first fully human antibody product from transgenic mice, *Nat. Biotechnol.* 25 (2007) 1134–1143.
- [15] A.L. Nelson, E. Dhimolea, J.M. Reichert, Development trends for human monoclonal antibody therapeutics, *Nat. Rev. Drug Discov.* 9 (2010) 767–774. doi:10.1038/nrd3229.
- [16] J. McCafferty, A.D. Griffiths, G. Winter, D.J. Chiswell, Phage antibodies: filamentous phage displaying antibody variable domains, *Nature.* 348 (1990) 552–554. doi:10.1038/348552a0.
- [17] G. Winter, A.D. Griffiths, R.E. Hawkins, H.R. Hoogenboom, Making Antibodies By Phage, *Annu. Rev. Immunol.* 12 (1994) 433–455.
- [18] K. Murphy, C. Janeway, P. Travers, M. Walport, *Janeway’s Immunobiology*, 8th ed., Garland Science, 2012.
- [19] R.P. Junghans, C.L. Anderson, The protection receptor for IgG catabolism is the beta2-microglobulin-containing neonatal intestinal transport receptor., *Proc. Natl. Acad. Sci.* 93 (1996) 5512–5516. doi:10.1073/pnas.93.11.5512.
- [20] M.M. Schmidt, K.D. Wittrup, A modeling analysis of the effects of molecular size and binding affinity on tumor targeting, *Mol. Cancer Ther.* 8 (2009) 2861–2871. doi:10.1158/1535-7163.mct-09-0195.
- [21] T. Yokota, D.E. Milenic, M. Whitlow, J. Schlom, Rapid Tumor Penetration of a Single-Chain Fv and Comparison with Other Immunoglobulin Forms, *Cancer Res.* 52 (1992) 3402–3408.
- [22] K.R. Rodgers, R.C. Chou, Therapeutic monoclonal antibodies and derivatives: Historical perspectives and future directions, *Biotechnol. Adv.* 34 (2016) 1149–1158. doi:10.1016/j.biotechadv.2016.07.004.
- [23] A. Hoos, R. Ibrahim, A. Korman, K. Abdallah, D. Berman, V. Shahabi, K. Chin, R. Canzetta, R. Humphrey, Development of Ipilimumab: Contribution to a New Paradigm for Cancer Immunotherapy, *Semin. Oncol.* 37 (2010).
- [24] D. Schrama, R.A. Reisfeld, J.C. Becker, Antibody targeted drugs as cancer therapeutics, *Nat. Rev. Drug Discov.* 5 (2006) 147–159. doi:10.1038/nrd1957.
- [25] M.R. Smith, Rituximab (monoclonal anti-CD20 antibody): Mechanisms of action and resistance, *Oncogene.* 22 (2003) 7359–7368. doi:10.1038/sj.onc.1206939.
- [26] F. Kraeber-Bodéré, C. Bodet-Milin, C. Rousseau, T. Eugene, A. Pallardy, M. Chérel,

- Radioimmunoconjugates for the Treatment of Cancer, *Semin. Oncol.* 41 (2014) 613–622.
- [27] D.M. Goldenberg, Targeted therapy of cancer with radiolabeled antibodies., *J. Nucl. Med.* 43 (2002) 693–713. <http://www.ncbi.nlm.nih.gov/pubmed/11994535>.
- [28] M. Jain, G. Venkatraman, S.K. Batra, Optimization of radioimmunotherapy of solid tumors: Biological impediments and their modulation, *Clin. Cancer Res.* 13 (2007) 1374–1382. doi:10.1158/1078-0432.CCR-06-2436.
- [29] D.M. Goldenberg, R. Sharkey, G. Paganelli, J. Barbet, J. Chatal, Antibody Pretargeting Advances Cancer Radioimmunodetection and Radioimmunotherapy, *J. Clin. Oncol.* 24 (2006) 823–834. doi:10.1200/jco.2005.03.8471.
- [30] F. Kraeber-Bodéré, P.Y. Salaun, A. Oudoux, D.M. Goldenberg, J.F. Chatal, J. Barbet, Pretargeted radioimmunotherapy in rapidly progressing, metastatic, medullary thyroid cancer, *Cancer.* 116 (2010) 1118–1125. doi:10.1002/cncr.24800.
- [31] P. Polakis, Monoclonal Antibody Drug Conjugates for Cancer Therapy, *Pharmacol. Rev.* 68 (2016). doi:10.1007/978-0-387-49785-3\_14.
- [32] F.S. Lichtenegger, C. Krupka, S. Haubner, T. Köhnke, M. Subklewe, Recent developments in immunotherapy of acute myeloid leukemia Ahmed Tarhini; Timothy Burns; Rahul Parikh; Guarvel Goel; Annie im, *J. Hematol. Oncol.* 10 (2017) 1–20. doi:10.1186/s13045-017-0505-0.
- [33] P.P. Release, Pfizer receives FDA approval for Mylotarg (Gemtuzumab Ozogamicin), (2017). [https://www.pfizer.com/news/press-release/press-release-detail/pfizer\\_receives\\_fda\\_approval\\_for\\_mylotarg\\_gemtuzumab\\_ozogamicin](https://www.pfizer.com/news/press-release/press-release-detail/pfizer_receives_fda_approval_for_mylotarg_gemtuzumab_ozogamicin) (accessed March 18, 2019).
- [34] R. Hills, S. Castaigne, F. Appelbaum, M. Delaunay, M. Petersdorf, M. Othus, E. Estey, Addition of gemtuzumab ozogamicin to induction chemotherapy in adult patients with acute myeloid leukaemia: a meta-analysis of individual patient data from randomised controlled trials, *Lancet Oncol.* 15 (2014) 913–14.
- [35] BusinessWire, Seattle Genetics Discontinues Phase 3 CASCADE Trial of Vadastuximab Talirine (SGN-CD33A) in Frontline Acute Myeloid Leukemia, (2017). <https://www.businesswire.com/news/home/20170619005466/en/Seattle-Genetics-Discontinues-Phase-3-CASCADE-Trial> (accessed March 28, 2019).
- [36] S.E. Sedykh, V. V. Prinz, V.N. Buneva, G.A. Nevinsky, Bispecific antibodies : design ,

- therapy , perspectives, *Drug Des. Devel. Ther.* 12 (2018) 195–208.
- [37] K. Baker, J. Isaacs, Novel therapies for immune-mediated inflammatory diseases: what can we learn from their use in rheumatoid arthritis, spondyloarthritis, systemic lupus erythematosus, psoriasis, Cron’s disease and ulcerative colitis?, *Ann. Rheum. Dis.* 77 (2017).
- [38] Neovii, Neovii completes marketing authorisation withdrawal of Removab in the European Union, (n.d.). <https://neovii.com/neovii-completes-marketing-authorisation-withdrawal-of-removab-in-the-european-union/> (accessed March 22, 2019).
- [39] J. Couzin-Frankel, Cancer immunotherapy, *Science* (80-. ). 342 (2013) 1432–1433. doi:10.1126/science.342.6165.1432.
- [40] K. Spiekermann, J. Roesler, A. Emmendoerffer, J. Elsner, K. Welte, Functional features of neutrophils induced by G-CSF and GM-CSF treatment: differential effects and clinical implications, *Leukemia*. 11 (1997) 466–478. doi:10.1038/sj.leu.2400607.
- [41] M. Atkins, M. Lotze, J. Dutcher, R. Fisher, G. Weiss, K. Margolin, J. Abrams, M. Sznol, D. Parkinson, M. Hawkins, C. Paradise, L. Kunkel, S. Rosenberg, High-dose recombinant interleukin 2 therapy for patients with metastatic melanoma: analysis of 270 patients treated between 1985 and 1993, *J. Clin. Oncol.* 17 (1999) 2105–2116.
- [42] G. Fyfe, R. Fisher, S.A. Rosenberg, M. Sznol, D.R. Parkinson, A. Louie, Results of treatment of 255 patients with metastatic renal cell carcinoma who received high-dose recombinant interleukin-2 therapy, *J. Clin. Oncol.* 13 (1995) 688–696.
- [43] R. Fisher, S. Rosenberg, G. Fyfe, Long-term survival update for high-dose recombinant interleukin-2 in patients with renal cell carcinoma, *Cancer J. Sci. Am.* 6 Suppl 1 (2000) 55–7.
- [44] G. Spitaleri, R. Berardi, C. Pierantoni, T. De Pas, C. Noberasco, C. Libbra, R. González-Iglesias, L. Giovannoni, a Tasciotti, D. Neri, H.D. Menssen, F. de Braud, Phase I/II study of the tumour-targeting human monoclonal antibody-cytokine fusion protein L19-TNF in patients with advanced solid tumours., *J. Cancer Res. Clin. Oncol.* 139 (2013) 447–55. doi:10.1007/s00432-012-1327-7.
- [45] F. Papadia, V. Basso, R. Patuzzo, A. Maurichi, A.D.I. Florio, L. Zardi, E. Ventura, V. Lovato, L. Giovannoni, R. Gonza, Isolated Limb Perfusion With the Tumor-Targeting Human Monoclonal Antibody – Cytokine Fusion Protein L19-TNF Plus Melphalan and

- Mild Hyperthermia in Patients with Locally Advanced Extremity Melanoma, 2 (2013) 173–179. doi:10.1002/jso.23168.
- [46] T. Aoki, K. Tashiro, S. Miyatake, T. Kinashi, T. Nakano, Y. Oda, H. Kikuchi, T. Honjo, Expression of murine interleukin 7 in a murine glioma cell line results in reduced tumorigenicity in vivo., *Proc. Natl. Acad. Sci. U. S. A.* 89 (1992) 3850–4. doi:10.1073/pnas.89.9.3850.
- [47] S.E. Barker, S.M. Grosse, E.K. Siapati, A. Kritz, C. Kinnon, A.J. Thrasher, S.L. Hart, Immunotherapy for neuroblastoma using syngeneic fibroblasts transfected with IL-2 and IL-12, *Br. J. Cancer.* 97 (2007) 210–217. doi:10.1038/sj.bjc.6603857.
- [48] C. Jackaman, C.S. Bundell, B.F. Kinnear, A.M. Smith, P. Filion, D. van Hagen, B.W.S. Robinson, D.J. Nelson, IL-2 intratumoral immunotherapy enhances CD8+ T cells that mediate destruction of tumor cells and tumor-associated vasculature: a novel mechanism for IL-2., *J. Immunol.* 171 (2003) 5051–5063. doi:10.4049/jimmunol.171.10.5051.
- [49] Y. Koshita, Y. Lu, S. Fujii, H. Neda, T. Matsuyama, Y. Satoh, Y. Itoah, M. Takahashi, J. Kato, S. Sakamaki, N. Watanabe, Y. Kohigo, Y. Niitsu, Efficacy of TNF- $\alpha$  gene transduced tumor cells in treatment of established in vivo tumor, *Int. J. Cancer.* 63 (1995) 130–135.
- [50] P.W. Miller, S. Sharma, M. Stolina, L.H. Butterfield, J. Luo, Y. Lin, M. Dohadwala, R.K. Batra, L. Wu, J.S. Economou, S.M. Dubinett, Intratumoral administration of adenoviral interleukin 7 gene-modified dendritic cells augments specific antitumor immunity and achieves tumor eradication., *Hum. Gene Ther.* 11 (2000) 53–65. doi:10.1089/10430340050016157.
- [51] J.C. Becker, J.D. Pancook, S.D. Gillies, K. Furukawa, R.A. Reisfeld, T cell-mediated eradication of murine metastatic melanoma induced by targeted interleukin 2 therapy., *J. Exp. Med.* 183 (1996) 2361–6. doi:10.1084/jem.183.5.2361.
- [52] H.N. Lode, R. Xiang, T. Dreier, N.M. Varki, S.D. Gillies, R.A. Reisfeld, Natural killer cell-mediated eradication of neuroblastoma metastases to bone marrow by targeted interleukin-2 therapy., *Blood.* 91 (1998) 1706–1715.
- [53] C. Halin, S. Rondini, F. Nilsson, a Berndt, H. Kosmehl, L. Zardi, D. Neri, Enhancement of the antitumor activity of interleukin-12 by targeted delivery to neovasculature., *Nat. Biotechnol.* 20 (2002) 264–269. doi:10.1038/nbt0302-264.



- [54] R.E. Kontermann, Antibody-cytokine fusion proteins, *Arch. Biochem. Biophys.* 526 (2012) 194–205. doi:10.1016/j.abb.2012.03.001.
- [55] E.A. Rossi, D.M. Goldenberg, T.M. Cardillo, R. Stein, C.H. Chang, CD20-targeted tetrameric interferon- $\alpha$ , a novel and potent immunocytokine for the therapy of B-cell lymphomas, *Blood*. 114 (2009) 3864–3871. doi:10.1182/blood-2009-06-228890.
- [56] E.A. Rossi, D.M. Goldenberg, T.M. Cardillo, R. Stein, C. Chang, Hexavalent bispecific antibodies represent a new class of anticancer therapeutics: 1. Properties of anti-CD20/CD22 antibodies in lymphoma, *Blood*. 113 (2010) 6161–6171. doi:10.1182/blood-2008-10-187138.
- [57] E.A. Rossi, D.L. Rossi, T.M. Cardillo, R. Stein, D.M. Goldenberg, C.H. Chang, Preclinical studies on targeted delivery of multiple IFN $\alpha$ 2b to HLA-DR in diverse hematologic cancers, *Blood*. 118 (2011) 1877–1884. doi:10.1182/blood-2011-03-343145.
- [58] R.K. Jain, L.T. Baxter, Mechanisms of heterogeneous distribution of monoclonal antibodies and other macromolecules in tumors: Significance of elevated interstitial pressure, *Cancer Res.* 48 (1988) 7022–7032.
- [59] T.T. Kuo, V.G. Aveson, Neonatal Fc receptor and IgG-based therapeutics, *MAbs*. 3 (2011) 422–430. doi:10.4161/mabs.3.5.16983.
- [60] E.S. Ward, M. Cruz, C. Vaccaro, J. Zhou, Q. Tang, R. Ober, From Sorting Endosomes to Exocytosis: Association of Rab4 and Rab11 GTPases with the Fc Receptor, FcRn, during Recycling, *Mol. Biol. Cell*. 16 (2005) 2028–2038. doi:10.1091/mbc.E04.
- [61] S.D. Gillies, V. Lan, K.M. Lo, M. Super, J. Wesolowski, Improving the efficacy of antibody-interleukin 2 fusion proteins by reducing their interaction with Fc receptors, *Cancer Res.* 59 (1999) 2159–2166.
- [62] S.D. Gillies, K.M. Lo, Y. Lan, T. Dahl, W.K. Wong, C. Burger, Improved circulating half-life and efficacy of an antibody-interleukin 2 immunocytokine based on reduced intracellular proteolysis, *Clin. Cancer Res.* 8 (2002) 210–216.
- [63] T. Shinkawa, K. Nakamura, N. Yamane, E. Shoji-Hosaka, Y. Kanda, M. Sakurada, K. Uchida, H. Anazawa, M. Satoh, M. Yamasaki, N. Hanai, K. Shitara, The absence of fucose but not the presence of galactose or bisecting N-acetylglucosamine of human IgG1 complex-type oligosaccharides shows the critical role of enhancing antibody-dependent cellular cytotoxicity, *J. Biol. Chem.* 278 (2003) 3466–3473. doi:10.1074/jbc.M210665200.

- [64] P. Umana, J. Jean-Mairet, J. Bailey, Glycosylation engineering of antibodies for improving antibody-dependent cellular cytotoxicity, US 6,602,684 B1, 2003.
- [65] L. Borsi, E. Balza, M. Bestagno, P. Castellani, B. Carnemolla, A. Biro, A. Leprini, J. Sepulveda, O. Burrone, D. Neri, L. Zardi, Selective targeting of tumoral vasculature: comparison of different formats of an antibody (L19) to the ED-B domain of fibronectin., *Int. J. Cancer*. 102 (2002) 75–85. doi:10.1002/ijc.10662.
- [66] P. Holliger, P. Hudson, Engineered antibody fragments and the rise of single domains, *Nat. Biotechnol.* 23 (2005) 1126–1136.
- [67] A. Wu, W. Chen, A. Raubitschek, L. Williams, M. Neumaier, R. Fischer, S. Hu, T. Odom-Maryon, J. Wong, J. Shively, Tumor localization of anti-CEA single-chain Fvs: Improved targeting by non-covalent dimers, *Immunotechnology*. 2 (1996) 21–36.
- [68] F. Bootz, D. Neri, Immunocytokines: A novel class of products for the treatment of chronic inflammation and autoimmune conditions, *Drug Discov. Today*. 21 (2016) 180–189. doi:10.1016/j.drudis.2015.10.012.
- [69] S.D. Gillies, A new platform for constructing antibody-cytokine fusion proteins (immunocytokines) with improved biological properties and adaptable cytokine activity, *Protein Eng. Des. Sel.* 26 (2013) 561–569. doi:10.1093/protein/gzt045.
- [70] D. Neri, C.T. Supuran, Interfering with pH regulation in tumours as a therapeutic strategy, *Nat. Rev. Drug Discov.* 10 (2011) 767–777. doi:10.1038/nrd3554.
- [71] D. Neri, R. Bicknell, Tumour vascular targeting., *Nat. Rev. Cancer*. 5 (2005) 436–46. doi:10.1038/nrc1627.
- [72] C. Schliemann, A. Palumbo, K. Zuberbu, A. Villa, M. Kaspar, E. Trachsel, W. Klapper, H.D. Messen, D. Neri, Complete eradication of human B-cell lymphoma xenografts using rituximab in combination with the immunocytokine L19-IL2, *Blood*. 113 (2009) 2275–2284. doi:10.1182/blood-2008-05-160747.An.
- [73] C. Schliemann, A. Wiedmer, M. Pedretti, M. Szczepanowski, W. Klapper, D. Neri, Three clinical-stage tumor targeting antibodies reveal differential expression of oncofetal fibronectin and tenascin-C isoforms in human lymphoma, *Leuk. Res.* 33 (2009) 1718–1722. doi:10.1016/j.leukres.2009.06.025.
- [74] K. Schwager, A. Villa, C. Rösli, D. Neri, M. Rösli-Khabas, G. Moser, A comparative immunofluorescence analysis of three clinical-stage antibodies in head and neck cancer, *Head Neck Oncol.* 3 (2011) 1–6. doi:10.1186/1758-3284-3-25.

- [75] D. Neri, B. Carnemolla, A. Nissim, A. Leprini, G. Querze, E. Balza, A. Pini, L. Tarli, C. Halin, P. Neri, L. Zardi, G. Winter, Targeting by affinity-matured recombinant antibody fragments of an angiogenesis associated fibronectin isoform, *Nat. Biotechnol.* 15 (1997) 1271–1275. doi:10.1038/nm0798-822.
- [76] M. Santimaria, G. Moscatelli, G.L. Viale, L. Giovannoni, G. Neri, F. Viti, A. Leprini, L. Borsi, P. Castellani, L. Zardi, D. Neri, P. Riva, Immunoscintigraphic detection of the ED-B domain of fibronectin, a marker of angiogenesis, in patients with cancer, *Clin. Cancer Res.* 9 (2003) 571–579. doi:10.1038/nrc1627.
- [77] L. Tarli, E. Balza, F. Viti, L. Borsi, P. Castellani, D. Berndorff, L. Dinkelborg, D. Neri, L. Zardi, A high-affinity human antibody that targets tumoral blood vessels, *Blood.* 94 (1999) 192–198. doi:10.1038/nm0195-27.
- [78] A. Villa, E. Trachsel, M. Kaspar, C. Schliemann, R. Sommovilla, J.-N. Rybak, C. Rösli, L. Borsi, D. Neri, A high-affinity human monoclonal antibody specific to the alternatively spliced EDA domain of fibronectin efficiently targets tumor neo-vasculature in vivo., *Int. J. Cancer.* 122 (2008) 2405–13. doi:10.1002/ijc.23408.
- [79] F. Viti, L. Tarli, L. Giovannoni, L. Zardi, D. Neri, Increased Binding Affinity and Valence of Recombinant Antibody Fragments Lead to Improved Targeting of Tumoral Angiogenesis Increased Binding Affinity and Valence of Recombinant Antibody Fragments Lead to Improved Targeting of Tumoral Angiogenesis 1, (1999) 347–352.
- [80] G.L. Poli, C. Bianchi, G. Virota, A. Bettini, R. Moretti, E. Trachsel, G. Elia, L. Giovannoni, D. Neri, A. Bruno, Radretumab Radioimmunotherapy in Patients with Brain Metastasis: A 124I-L19SIP Dosimetric PET Study, *Cancer Immunol. Res.* 1 (2013) 134–143. doi:10.1158/2326-6066.CIR-13-0007.
- [81] B.Y.P. Gold, S.O. Freedman, Demonstration of tumor-specific antigens in human colonic carcinomata by immunological tolerance and absorption techniques, *J. Exp. Med.* 121 (1965) 439–462.
- [82] D.M. Goldenberg, H. Goldenberg, R.M. Sharkey, E. Higginbotham-Ford, R.E. Lee, L.C. Swayne, K. a Burger, D. Tsai, J. a Horowitz, T.C. Hall, Clinical studies of cancer radioimmunodetection with carcinoembryonic antigen monoclonal antibody fragments labeled with 123I or 99mTc., *Cancer Res.* 50 (1990) 909s–921s.
- [83] J.-P. Mach, F. Buchegger, M. Forni, J. Ritschard, C. Berche, J.-D. Lumbroso, M. Schreyer, C. Girardet, R. Accolla, S. Carrel, Use of radiolabelled monoclonal anti-CEA

- antibodies for the detection of human carcinomas by external photoscanning and tomoscintigraphy, *Immunol. Today*. 2 (1981) 239–249.
- [84] M.E. Ackerman, C. Chalouni, M.M. Schmidt, V. V. Raman, G. Ritter, L.J. Old, I. Mellman, K.D. Wittrup, A33 antigen displays persistent surface expression, *Cancer Immunol. Immunother.* 57 (2008) 1017–1027. doi:10.1007/s00262-007-0433-x.
- [85] P. Garinchesa, J. Sakamoto, S. Welt, F. Real, W. Rettig, L. Old, Organ-specific expression of the colon cancer antigen A33, a cell surface target for antibody-based therapy, *Int. J. Oncol.* 9 (1996) 465–471.
- [86] A.B. Stillebroer, P.F.A. Mulders, O.C. Boerman, W.J.G. Oyen, E. Oosterwijk, Carbonic Anhydrase IX in Renal Cell Carcinoma: Implications for Prognosis, Diagnosis, and Therapy, *Eur. Urol.* 58 (2010) 75–83. doi:10.1016/j.eururo.2010.03.015.
- [87] M. Munz, P.A. Baeuerle, O. Gires, The emerging role of EpCAM in cancer and stem cell signaling, *Cancer Res.* 69 (2009) 5627–5629. doi:10.1158/0008-5472.CAN-09-0654.
- [88] A.L. Yu, M.M. Uttenreuther-Fischer, C.S. Huang, C.C. Tsui, S.D. Gillies, R.A. Reisfeld, F.H. Kung, Phase I trial of a human-mouse chimeric anti-disialoganglioside monoclonal antibody ch14.18 in patients with refractory neuroblastoma and osteosarcoma, *J. Clin. Oncol.* 16 (1998) 2169–2180. doi:10.1200/JCO.1998.16.6.2169.
- [89] R. Kalluri, M. Zeisberg, Fibroblasts in cancer, *Nat. Rev. Cancer.* 6 (2006) 392–401. doi:10.1038/nrc1877.
- [90] J.A.A. Gubbels, B. Gadbaw, I.N. Buhtoiarov, S. Horibata, A.K. Kapur, D. Patel, J.A. Hank, S.D. Gillies, P.M. Sondel, M.S. Patankar, J. Connor, Ab-IL2 fusion proteins mediate NK cell immune synapse formation by polarizing CD25 to the target cell-effector cell interface, *Cancer Immunol. Immunother.* 60 (2011) 1789–1800. doi:10.1007/s00262-011-1072-9.
- [91] H. Lode, R. Xiang, S.D. Gillies, R.A. Reisfeld, Amplification of T-cell mediated immune responses by antibody-cytokine fusion proteins, *Immunol Invest.* 29 (2000) 117–120.
- [92] C. Halin, S. Rondini, F. Nilsson, A. Berndt, H. Kosmehl, L. Zardi, D. Neri, Enhancement of the antitumor activity of interleukin-12 by targeted delivery to neovasculature, *Nat. Biotechnol.* 20 (2002) 264–269.
- [93] T. Hemmerle, D. Neri, The antibody-based targeted delivery of interleukin-4 and 12 to the tumor neovasculature eradicates tumors in three mouse models of cancer., *Int. J.*

- Cancer. 134 (2014) 467–77. doi:10.1002/ijc.28359.
- [94] B. Carnemolla, L. Borsi, E. Balza, P. Castellani, R. Meazza, A. Berndt, S. Ferrini, H. Kosmehl, D. Neri, L. Zardi, Enhancement of the antitumor properties of interleukin-2 by its targeted delivery to the tumor blood vessel extracellular matrix, *Blood*. 99 (2002) 1659–1665. doi:10.1182/blood.V99.5.1659.
- [95] C. Halin, V. Gafner, M.E. Villani, L. Borsi, A. Berndt, H. Kosmehl, L. Zardi, D. Neri, Synergistic Therapeutic Effects of a Tumor Targeting Antibody Fragment , Fused to Interleukin 12 and to Tumor Necrosis Factor  $\alpha$ , *Cancer Res*. 63 (2003) 3202–3210.
- [96] S. Folli, A. Pelegrin, Y. Chalandon, X. Yao, F. Buchegger, D. Lienard, F. Lejeune, J.-P. Mach, Tumor-necrosis factor can enhance radio-antibody uptake in human colon carcinoma xenografts by increasing vascular permeability, *Int. J. Cancer*. 53 (1993) 829–836.
- [97] L. Khawli, G. Miller, A. Epstein, Effect of seven new vasoactive immunoconjugates on the enhancement of monoclonal antibody uptake in tumors, *Cancer*. 73 (1994) 824–831.
- [98] O. Boyman, J. Sprent, The role of interleukin-2 during homeostasis and activation of the immune system, *Nat. Rev. Immunol*. 12 (2012) 180–190. doi:10.1038/nri3156.
- [99] Z.C. Neal, J.C. Yang, A.L. Rakhmievich, I.N. Buhtoiarov, H.E. Lum, M. Imboden, J.A. Hank, H.N. Lode, R.A. Reisfeld, S.D. Gillies, P.M. Sondel, Enhanced Activity of Hu14 . 18-IL2 Immunocytokine against Murine NXS2 Neuroblastoma when Combined with Interleukin 2 Therapy, *Clin. Cancer Res*. 10 (2004) 4839–4847.
- [100] K. Schwager, T. Hemmerle, D. Aebischer, D. Neri, The immunocytokine L19-IL2 eradicates cancer when used in combination with CTLA-4 blockade or with L19-TNF., *J. Invest. Dermatol*. 133 (2013) 751–8. doi:10.1038/jid.2012.376.
- [101] K.L. Gutbrodt, C. Schliemann, L. Giovannoni, K. Frey, T. Pabst, W. Klapper, W.E. Berdel, D. Neri, Antibody-based delivery of interleukin-2 to neovasculature has potent activity against acute myeloid leukemia., *Sci. Transl. Med*. 5 (2013) 201ra118. doi:10.1126/scitranslmed.3006221.
- [102] P. Probst, J. Kopp, A. Oxenius, M.P. Colombo, D. Ritz, T. Fugmann, D. Neri, Sarcoma eradication by doxorubicin and targeted TNF relies upon CD8+ T cell recognition of a retroviral antigen, *Cancer Res*. (2017) canres.2946.2016. doi:10.1158/0008-5472.CAN-16-2946.

- [103] M.A. Palladino, F.R. Bahjat, E.A. Theodorakis, L.L. Moldawer, Anti-TNF- $\alpha$  therapies: the next generation, *Nat. Rev. Drug Discov.* 2 (2003) 736–746. doi:10.1038/nrd1175.
- [104] E.R. Manusama, P.T.G.A. Nooijen, T.L.M. Ten Hagen, A.H. Van Der Veen, M.W.R. De Vries, J.H.W. De Wilt, M.G. Van Ijken, R.L. Marquet, A.M.M. Eggermont, Tumor necrosis factor-alpha in isolated perfusion systems in the treatment of cancer: The Rotterdam preclinical-clinical program, *Semin. Surg. Oncol.* 14 (1998) 232–237. doi:10.1002/(SICI)1098-2388(199804/05)14:3<232::AID-SSU7>3.0.CO;2-9.
- [105] E.E. Voest, B.M. Kenyon, M.S. O’Reilly, G. Truitt, R.J. D’Amato, J. Folkman, Inhibition of angiogenesis in vivo by interleukin 12, *J. Natl. Cancer Inst.* 87 (1995) 581–586. [http://www.ncbi.nlm.nih.gov/entrez/query.fcgi?cmd=Retrieve&db=PubMed&dopt=Citation&list\\_uids=7538593](http://www.ncbi.nlm.nih.gov/entrez/query.fcgi?cmd=Retrieve&db=PubMed&dopt= Citation&list_uids=7538593).
- [106] J. Magram, S.E. Connaughton, R.R. Warriar, D.M. Carvajal, C.Y. Wu, J. Ferrante, C. Stewart, U. Sarmiento, D.A. Faherty, M.K. Gately, IL-12-deficient mice are defective in IFN-gamma production and type 1 cytokine responses., *Immunity.* 4 (1996) 471–481. doi:10.1016/S1074-7613(00)80413-6.
- [107] S.A. Quezada, T.R. Simpson, K.S. Peggs, T. Merghoub, J. Vider, X. Fan, R. Blasberg, H. Yagita, P. Muranski, P.A. Antony, N.P. Restifo, J.P. Allison, Tumor-reactive CD4<sup>+</sup> T cells develop cytotoxic activity and eradicate large established melanoma after transfer into lymphopenic hosts, *J. Exp. Med.* 207 (2010) 637–650. doi:10.1084/jem.20091918.
- [108] S.A. Quezada, K.S. Peggs, T.R. Simpson, J.P. Allison, Shifting the equilibrium in cancer immunoediting: From tumor tolerance to eradication, *Immunol. Rev.* 241 (2011) 104–118. doi:10.1111/j.1600-065X.2011.01007.x.
- [109] N. Pasche, S. Wulhfard, F. Pretto, E. Carugati, D. Neri, The antibody-based delivery of interleukin-12 to the tumor neovasculature eradicates murine models of cancer in combination with paclitaxel, *Clin. Cancer Res.* 18 (2012) 4092–4103. doi:10.1158/1078-0432.CCR-12-0282.
- [110] K.M. Lo, Y. Lan, S. Lauder, J. Zhang, B. Brunkhorst, G. Qin, R. Verma, N. Courtenay-Luck, S.D. Gillies, huBC1-IL12, an immunocytokine which targets EDB-containing oncofetal fibronectin in tumors and tumor vasculature, shows potent anti-tumor activity in human tumor models, *Cancer Immunol. Immunother.* 56 (2007) 447–457. doi:10.1007/s00262-006-0203-1.

- [111] X. Xu, P. Clarke, G. Szalai, J.E. Shively, L.E. Williams, Y. Shyr, E. Shi, F.J. Primus, Targeting and therapy of carcinoembryonic antigen-expressing tumors in transgenic mice with an antibody-interleukin 2 fusion protein, *Cancer Res.* 60 (2000) 4475–4484.
- [112] C. Klein, I. Waldhauer, V.G. Nicolini, A. Freimoser-grundschober, T. Nayak, T. Hofer, E. Van Puijenbroek, D. Wittig, S. Moser, O. Ast, P. Br, S. Neumann, M. Cristina, D.V. Mudry, H. Hinton, F. Cramer, J. Saro, S. Evers, C. Gerdes, M. Bacac, G. Van Dongen, E. Moessner, P. Uma, Cergutuzumab amunaleukin ( CEA-IL2v ), a CEA-targeted IL-2 variant-based immunocytokine for combination cancer immunotherapy : Overcoming limitations of aldesleukin and conventional IL-2-based immunocytokines, *Oncoimmunology.* 6 (2017). doi:10.1080/2162402X.2016.1277306.
- [113] H.N. Lode, R. Xiang, N.M. Varki, C.S. Dolman, S.D. Gillies, R.A. Reisfeld, Targeted interleukin-2 therapy for spontaneous neuroblastoma metastases to bone marrow, *J. Natl. Cancer Inst.* 89 (1997) 1586–1594. doi:10.1093/jnci/89.21.1586.
- [114] J.L. Hornick, L. a Khawli, P. Hu, M. Lynch, P.M. Anderson, a L. Epstein, Chimeric CLL-1 antibody fusion proteins containing granulocyte-macrophage colony-stimulating factor or interleukin-2 with specificity for B-cell malignancies exhibit enhanced effector functions while retaining tumor targeting properties., *Blood.* 89 (1997) 4437–47. <http://www.ncbi.nlm.nih.gov/pubmed/9192768>.
- [115] K. Frey, C. Schliemann, K. Schwager, R. Giavazzi, M. Johannsen, D. Neri, The immunocytokine F8-IL2 improves the therapeutic performance of sunitinib in a mouse model of renal cell carcinoma, *J. Urol.* 184 (2010) 2540–2548. doi:10.1016/j.juro.2010.07.030.
- [116] J. Mårilind, M. Kaspar, E. Trachsel, R. Somavilla, S. Hindle, C. Bacci, L. Giovannon, D. Neri, Antibody-mediated delivery of interleukin-2 to the stroma of breast cancer strongly enhances the potency of chemotherapy, *Clin. Cancer Res.* 14 (2008) 6515–6524. doi:10.1158/1078-0432.CCR-07-5041.
- [117] M. Pedretti, C. Verpelli, J. Mårilind, G. Bertani, C. Sala, D. Neri, L. Bello, Combination of temozolomide with immunocytokine F16-IL2 for the treatment of glioblastoma, *Br. J. Cancer.* 103 (2010) 827–836. doi:10.1038/sj.bjc.6605832.
- [118] H. Matsumoto, S. Liao, F. Arakawa, A. Ueno, H. Abe, A. Awasthi, M. Kuroki, Targeting of interleukin-2 to human MK-1-expressing carcinoma by fusion with a single-chain Fv of anti-MK-1 antibody, *Anticancer Res.* 4 (2002) 2001–7.

- [119] O. Christ, S. Seiter, S. Matzku, C. Burger, M. Zo, Efficacy of Local versus Systemic Application of Antibody-Cytokine Fusion Proteins in Tumor Therapy 1, *Clin. Cancer Res.* 7 (2001) 985–998.
- [120] C. Molimi, M. Figini, D. Nicosia, E. Luisãñ, V. Ramakrishna, G. Parmiani, Z. Eshhar, S. Canevari, M.P. Colombo, G. Casorati, Targeting of Interleukin 2 to Human Ovarian Carcinoma by Fusion with a Single- Chain Fv of Antifolate Receptor Antibody, *Cancer Res.* 58 (1998) 4146–4154.
- [121] R. Xiang, H.N. Lode, C.S. Dolman, T. Dreier, N.M. Varki, X. Qian, K. Lo, Y. Lan, M. Super, S.D. Gillies, R.A. Reisfeld, Elimination of Established Murine Colon Carcinoma Metastases by Antibody Interleukin 2 Fusion Protein Therapy ', (1997).
- [122] F. Pretto, G. Elia, N. Castioni, D. Neri, Preclinical evaluation of IL2-based immunocytokines supports their use in combination with dacarbazine, paclitaxel and TNF-based immunotherapy, *Cancer Immunol. Immunother.* 63 (2014) 901–910. doi:10.1007/s00262-014-1562-7.
- [123] S.D. Gillies, Y. Lan, T. Hettmann, B. Brunkhorst, Y. Sun, S.O. Mueller, K. Lo, A Low-Toxicity IL-2 – Based Immunocytokine Retains Antitumor Activity Despite Its High Degree of IL-2 Receptor Selectivity, *Clin. Cancer Res.* 17 (2011) 3673–3685. doi:10.1158/1078-0432.CCR-10-2921.
- [124] A. Tzeng, B.H. Kwan, C.F. Opel, T. Navaratna, K.D. Wittrup, Antigen specificity can be irrelevant to immunocytokine efficacy and biodistribution, *Proc. Natl. Acad. Sci.* 112 (2015) 3320–3325. doi:10.1073/pnas.1416159112.
- [125] J. Li, P. Hu, L.A. Khawli, A. Yun, A.L. Epstein, chTNT-3 / hu IL-12 Fusion Protein for the Immunotherapy of Experimental Solid Tumors, *Hybrid. Hybridomics.* 23 (2004).
- [126] V. Gafner, E. Trachsel, D. Neri, An engineered antibody – interleukin-12 fusion protein with enhanced tumor vascular targeting properties, *Int. J. Cancer.* 119 (2006) 2205. doi:10.1002/ijc.22101.
- [127] R. Somavilla, N. Pasche, E. Trachsel, L. Giovannoni, C. Roesli, A. Villa, D. Neri, Expression, engineering and characterization of the tumor-targeting heterodimeric immunocytokine, *Protein Eng. Des. Sel.* 23 (2010) 653–661. doi:10.1093/protein/gzq038.
- [128] T. Jahn, M. Zuther, B. Friedrichs, C. Heuser, S. Guhlke, H. Abken, A.A. Hombach, An IL12-IL2-Antibody Fusion Protein Targeting Hodgkin's Lymphoma Cells Potentiates



- Activation Of Nk And T Cells For An Anti-Tumor Attack, *PLoS One*. 7 (2012).  
doi:10.1371/journal.pone.0044482.
- [129] T. Hemmerle, P. Probst, L. Giovannoni, a J. Green, T. Meyer, D. Neri, The antibody-based targeted delivery of TNF in combination with doxorubicin eradicates sarcomas in mice and confers protective immunity, *Br. J. Cancer*. 109 (2013) 1206–1213.  
doi:10.1038/bjc.2013.421.
- [130] S. Bauer, J.C. Oosterwijk-Wakka, N. Adrian, E. Oosterwijk, E. Fischer, T. Wüest, F. Stenner, A. Perani, L. Cohen, A. Knuth, C. Divgi, D. Jäger, A.M. Scott, G. Ritter, L.J. Old, C. Renner, Targeted therapy of renal cell carcinoma: Synergistic activity of cG250-TNF and IFN $\gamma$ , *Int. J. Cancer*. 125 (2009) 115–123. doi:10.1002/ijc.24359.
- [131] J. Pou, J. Martínez-González, A. Rebollo, C. Rodríguez, R. Rodríguez-Calvo, P. Martín-Fuentes, A. Cenarro, F. Civeira, J.C. Laguna, M. Alegret, Type II interleukin-1 receptor expression is reduced in monocytes/macrophages and atherosclerotic lesions., *Biochim. Biophys. Acta*. 1811 (2011) 556–63. doi:10.1016/j.bbali.2011.05.014.
- [132] Y. Liu, W. Zhang, L.H. Cheung, T. Niu, Q. Wu, C. Li, C.S. Van Pelt, M.G. Rosenblum, The Antimelanoma Immunocytokine scFvMEL/TNF Shows Reduced Toxicity and Potent Antitumor Activity against Human Tumor Xenografts, *Neoplasia*. 8 (2006) 384–393.  
doi:10.1593/neo.06121.
- [133] Y. Liu, L.H. Cheung, J.W. Marks, M.G. Rosenblum, Recombinant single-chain antibody fusion construct targeting human melanoma cells and containing tumor necrosis factor, *Int. J. Cancer*. 108 (2004) 549–557. doi:10.1002/ijc.11524.
- [134] L. Borsi, E. Balza, B. Carnemolla, F. Sassi, P. Castellani, A. Berndt, A. Siri, P. Orecchia, J. Grassi, D. Neri, L. Zardi, Selective targeted delivery of TNF $\alpha$  to tumor blood vessels, *Blood*. 102 (2003) 4384–4392. doi:10.1182/blood-2003-04-1039.Supported.
- [135] S.P. Cooke, R.B. Pedley, R. Boden, R.H.J. Begent, K. a Chester, In vivo tumor delivery of a recombinant single chain Fv::tumor necrosis factor-alpha fusion [correction of factor: a fusion] protein., *Bioconjug. Chem*. 13 (2002) 7–15.  
<http://www.ncbi.nlm.nih.gov/pubmed/11792173>.
- [136] J. Sharifi, L. a Khawli, P. Hu, J. Li, A.L. Epstein, Generation of human interferon gamma and tumor Necrosis factor alpha chimeric TNT-3 fusion proteins., *Hybrid. Hybridomics*. 21 (2002) 421–432. doi:10.1089/153685902321043954.
- [137] M.G. Rosenblum, L. Cheung, K. Mujoo, J.L. Murray, An antimelanoma immunotoxin

- containing recombinant human tumor necrosis factor: tissue disposition, pharmacokinetic, and therapeutic studies in xenograft models, *Cancer Immunol. Immunother.* 40 (1995) 322–328. doi:10.1007/BF01519633.
- [138] R. De Luca, A. Soltermann, F. Pretto, C. Pemberton-Ross, G. Pellegrini, S. Wulhfard, D. Neri, Potency-matched Dual Cytokine-Antibody Fusion Proteins for Cancer Therapy., *Mol. Cancer Ther.* 16 (2017) 2442–2451. doi:10.1158/1535-7163.MCT-17-0211.
- [139] A.S. Schmid, D. Tintor, D. Neri, Novel antibody-cytokine fusion proteins featuring granulocyte-colony stimulating factor, interleukin-3 and interleukin-4 as payloads, *J. Biotechnol.* 271 (2018) 29–36. doi:10.1016/j.jbiotec.2018.02.004.
- [140] C. Hess, D. Neri, Tumor-targeting properties of novel immunocytokines based on murine IL1 $\beta$  and IL6, *Protein Eng. Des. Sel.* 27 (2014) 207–213. doi:10.1093/protein/gzu013.
- [141] K. Schwager, M. Kaspar, F. Bootz, R. Marcolongo, E. Paresce, D. Neri, E. Trachsel, Preclinical characterization of DEKAVIL (F8-IL10), a novel clinical-stage immunocytokine which inhibits the progression of collagen-induced arthritis, *Arthritis Res. Ther.* 11 (2009) 1–15. doi:10.1186/ar2814.
- [142] C. Ebbinghaus, R. Ronca, M. Kaspar, D. Grabulovski, A. Berndt, H. Kosmehl, L. Zardi, D. Neri, Engineered vascular-targeting antibody-interferon- $\gamma$  fusion protein for cancer therapy, *Int. J. Cancer.* 116 (2005) 304–313. doi:10.1002/ijc.20952.
- [143] T. Hemmerle, D. Neri, The Dose-Dependent Tumor Targeting of Antibody-IFN Fusion Proteins Reveals an Unexpected Receptor-Trapping Mechanism In Vivo, *Cancer Immunol. Res.* 2 (2014) 559–567. doi:10.1158/2326-6066.CIR-13-0182.
- [144] N. Pasche, J. Woytschak, S. Wulhfard, A. Villa, K. Frey, D. Neri, Cloning and characterization of novel tumor-targeting immunocytokines based on murine IL7, *J. Biotechnol.* 154 (2011) 84–92. doi:10.1016/j.jbiotec.2011.04.003.
- [145] M. Kaspar, E. Trachsel, D. Neri, The antibody-mediated targeted delivery of interleukin-15 and GM-CSF to the tumor neovasculature inhibits tumor growth and metastasis, *Cancer Res.* 67 (2007) 4940–4948. doi:10.1158/0008-5472.CAN-07-0283.
- [146] S. Melkko, C. Halin, L. Borsi, L. Zardi, D. Neri, An antibody-calmodulin fusion protein reveals a functional dependence between macromolecular isoelectric point and tumor targeting performance, *Int. J. Radiat. Oncol.* 54 (2002) 1485–1490. <http://www.sciencedirect.com/science/article/pii/S0360301602039275>.

- [147] U. Niesner, C. Halin, L. Lozzi, M. Günthert, P. Neri, H. Wunderli-Allenspach, L. Zardi, D. Neri, Quantitation of the tumor-targeting properties of antibody fragments conjugated to cell-permeating HIV-1 TAT peptides, *Bioconjug. Chem.* 13 (2002) 729–736. doi:10.1021/bc025517+.
- [148] C. Halin, U. Niesner, M.E. Villani, L. Zardi, D. Neri, Tumor-targeting properties of antibody-vascular endothelial growth factor fusion proteins, *Int. J. Cancer.* 102 (2002) 109–116. doi:10.1002/ijc.10674.
- [149] T. Hemmerle, S. Wulhfard, D. Neri, A critical evaluation of the tumor-targeting properties of bispecific antibodies based on quantitative biodistribution data, *Protein Eng. Des. Sel.* 25 (2012) 851–854. doi:10.1093/protein/gzs061.
- [150] A. Liu, P. Hu, L. Khawli, A.L. Epstein, B7.1/NHS76: A New Costimulator Fusion Protein for the Immunotherapy of Solid Tumors, *Journal Immunother.* 29 (2006) 425–435.
- [151] N. Zhang, R.E. Sadun, R.S. Arias, M.L. Flanagan, S.M. Sachsman, Y.C. Nien, L.A. Khawli, P. Hu, A.L. Epstein, Targeted and untargeted CD137L fusion proteins for the immunotherapy of experimental solid tumors, *Clin. Cancer Res.* 13 (2007) 2758–2767. doi:10.1158/1078-0432.CCR-06-2343.
- [152] D. Venetz, C. Hess, C. Lin, M. Aebi, D. Neri, Glycosylation profiles determine extravasation and disease-targeting properties of armed antibodies, *Proc. Natl. Acad. Sci.* 112 (2015) 201503039. doi:10.1073/pnas.1503039112.
- [153] A. Krippner-Heidenreich, I. Grunwald, G. Zimmermann, M. Kuhnle, J. Gerspach, T. Sterns, S.D. Shnyder, J.H. Gill, D.N. Mannel, K. Pfizenmaier, P. Scheurich, Single-Chain TNF, a TNF Derivative with Enhanced Stability and Antitumoral Activity, *J. Immunol.* 180 (2008) 8176–8183. doi:10.4049/jimmunol.180.12.8176.
- [154] T. Hemmerle, P. Probst, L. Giovannoni, A.J. Green, T. Meyer, D. Neri, The antibody-based targeted delivery of TNF in combination with doxorubicin eradicates sarcomas in mice and confers protective immunity., *Br. J. Cancer.* 109 (2013) 1206–13. doi:10.1038/bjc.2013.421.
- [155] T. Hemmerle, C. Hess, D. Venetz, D. Neri, Tumor targeting properties of antibody fusion proteins based on different members of the murine tumor necrosis superfamily, *J. Biotechnol.* 172 (2014) 73–76. doi:10.1016/j.jbiotec.2013.12.010.
- [156] M. Siegemund, O. Seifert, M. Zarani, T. Džinić, V. De Leo, D. Götsch, S. Münkler, M. Hutt, K. Pfizenmaier, R.E. Kontermann, An optimized antibody-single-chain TRAIL

- fusion protein for cancer therapy, *MAbs*. 8 (2016) 879–891.  
doi:10.1080/19420862.2016.1172163.
- [157] J.S. Dela Cruz, K.R. Trinh, S.L. Morrison, M.L. Penichet, Recombinant Anti-Human HER2/neu IgG3-(GM-CSF) Fusion Protein Retains Antigen Specificity and Cytokine Function and Demonstrates Antitumor Activity, *J. Immunol.* 165 (2000) 5112–5121.  
doi:10.4049/jimmunol.165.9.5112.
- [158] J.S. Dela Cruz, K.R. Trinh, H.W. Chen, A. Ribas, S.L. Morrison, M.L. Penichet, Anti-HER2/neu IgG3-(IL-2) and anti-HER2/neu IgG3-(GM-CSF) promote HER2/neu processing and presentation by dendritic cells: Implications in immunotherapy and vaccination strategies, *Mol. Immunol.* 43 (2006) 667–676.  
doi:10.1016/j.molimm.2005.04.007.
- [159] J.S. Dela Cruz, S.L. Morrison, M.L. Penichet, Insights into the mechanism of anti-tumor immunity in mice vaccinated with the human HER2/neu extracellular domain plus anti-HER2/neu IgG3-(IL-2) or anti-HER2/neu IgG3-(GM-CSF) fusion protein, *Vaccine*. 23 (2005) 4793–4803. doi:10.1016/j.vaccine.2005.04.041.
- [160] G. Helguera, J.S. Dela Cruz, C. Lowe, P.P. Ng, R. Trinh, S.L. Morrison, M.L. Penichet, Vaccination with novel combinations of anti-HER2/neu cytokines fusion proteins and soluble protein antigen elicits a protective immune response against HER2/neu expressing tumors, *Vaccine*. 24 (2006) 304–316. doi:10.1016/j.vaccine.2005.07.073.
- [161] X. Huang, D. Ye, P.E. Thorpe, Enhancing the potency of a whole-cell breast cancer vaccine in mice with an antibody-IL-2 immunocytokine that targets exposed phosphatidylserine, *Vaccine*. 29 (2011) 4785–4793.  
doi:10.1016/j.vaccine.2011.04.082.
- [162] M. Penichet, J. Dela Cruz, S.-U. Shin, S. Morrison, A recombinant IgG3-(IL-2) fusion protein for the treatment of human HER2/neu expressing tumors, *Hum. Antibodies*. 10 (2001) 43–49.
- [163] E.T. Harvill, J.M. Fleming, S.L. Morrison, In vivo properties of an IgG3-IL-2 fusion protein. A general strategy for immune potentiation, *J. Immunol.* 157 (1996) 3165–3170.
- [164] M.L. Penichet, E.T. Harvill, S.L. Morrison, An IgG3-IL-2 fusion protein recognizing a murine B cell lymphoma exhibits effective tumor imaging and antitumor activity, *J Interf. Cytokine Res.* 18 (1998) 597–607. doi:10.1089/jir.1998.18.597.

- [165] C. Klein, S41. Novel CEA-targeted IL2 variant immunocytokine for immunotherapy of cancer, *J. Immunother. Cancer.* 2 (2014) I8. doi:10.1186/2051-1426-2-S2-I8.
- [166] J.C. Becker, J.D. Pancook, S.D. Gillies, J. Mendelsohn, R.A. Reisfeld, Eradication of human hepatic and pulmonary melanoma metastases in SCID mice by antibody-interleukin 2 fusion proteins., *Proc. Natl. Acad. Sci. U. S. A.* 93 (1996) 2702–7. doi:10.1073/pnas.93.7.2702.
- [167] H. Sabzevari, S.D. Gillies, B.M. Mueller, J.D. Pancook, R.A. Reisfeld, A recombinant antibody-interleukin 2 fusion protein suppresses growth of hepatic human neuroblastoma metastases in severe combined immunodeficiency mice., *Proc. Natl. Acad. Sci. U. S. A.* 91 (1994) 9626–30. doi:10.1073/pnas.91.20.9626.
- [168] J.C. Becker, N. Varki, S.D. Gillies, K. Furukawa, R.A. Reisfeld, Long-lived and transferable tumor immunity in mice after targeted interleukin-2 therapy, *J. Clin. Invest.* 98 (1996) 2801–2804. doi:10.1172/JCI119107.
- [169] M. Naramura, S.D. Gillies, J. Mendelsohn, R.A. Reisfeld, B.M. Mueller, Mechanisms of cellular cytotoxicity mediated by a recombinant antibody- IL2 fusion protein against human melanoma cells, *Immunol.Lett.* 39 (1993) 91–99.
- [170] S.D. Gillies, Y. Lan, S. Williams, F. Carr, S. Forman, A. Raubitschek, K. Lo, An anti-CD20 – IL-2 immunocytokine is highly efficacious in a SCID mouse model of established human B lymphoma, *Proteins.* 105 (2005) 3972–3978. doi:10.1182/blood-2004-09-3533.Several.
- [171] K.L. Gutbrodt, G. Casi, D. Neri, Antibody-based delivery of IL2 and cytotoxics eradicates tumors in immunocompetent mice., *Mol. Cancer Ther.* 13 (2014) 1772–6. doi:10.1158/1535-7163.MCT-14-0105.
- [172] M. Moschetta, F. Pretto, A. Berndt, K. Galler, P. Richter, A. Bassi, P. Oliva, E. Micotti, G. Valbusa, K. Schwager, M. Kaspar, E. Trachsel, H. Kosmehl, M.R. Bani, D. Neri, R. Giavazzi, Paclitaxel Enhances Therapeutic Efficacy of the F8-IL2 Immunocytokine to EDA-Fibronectin – Positive Metastatic Human Melanoma Xenografts, *Cancer Res.* 72 (2012) 1814–24. doi:10.1158/0008-5472.CAN-11-1919.
- [173] B. Ziffels, F. Pretto, D. Neri, Intratumoral administration of IL2- and TNF-based fusion proteins cures cancer without establishing protective immunity, *Immunotherapy.* 10 (2018) 177–188.
- [174] C. Klein, I. Waldhauer, V. Nicolini, C. Dunn, A. Freimoser-Grundschober, S. Herter, E.

- Geven, O. Boerman, T. Nayak, E. van Puijenbroek, D. Wittig, S. Moser, O. Ast, P. Bruenker, R. Hosse, S. Lang, S. Neumann, H. Kettenberger, A. Grossmann, I. Gorr, S. Evers, P. Pisa, J. Fretland, V. Levitsky, C. Gerdes, M. Bacac, E. Moessner, P. Umaña, Abstract 486: Tumor-targeted, engineered IL-2 variant (IL-2v)-based immunocytokines for the immunotherapy of cancer., *Cancer Res.* 73 (2013) 486 LP-486. [http://cancerres.aacrjournals.org/content/73/8\\_Supplement/486.abstract](http://cancerres.aacrjournals.org/content/73/8_Supplement/486.abstract).
- [175] V. Nicolini, I. Waldhauer, A. Freimoser-Grundschober, S. Evers, J. Saro, M. Bacac, C. Gerdes, P. Umana, C. Klein, Abstract 2217: Combining CEA-IL2v and FAP-IL2v immunocytokines with PD-L1 checkpoint blockade, *Cancer Res.* 76 (2016) 2217 LP-2217. [http://cancerres.aacrjournals.org/content/76/14\\_Supplement/2217.abstract](http://cancerres.aacrjournals.org/content/76/14_Supplement/2217.abstract).
- [176] S.A. Holden, Y. Lan, A.M. Pardo, J.S. Wesolowski, S.D. Gillies, Augmentation of Antitumor Activity of an Antibody-Interleukin 2 Immunocytokine with Chemotherapeutic Agents, *Clin. Cancer Res.* 7 (2001) 2862–2869.
- [177] S. Dolman, D. Gillies, G. Ca-, Combined of Human Immunodeficient Therapy ' Prostate Mice Carcinoma Metastases in Severe by Interleukin, *Clin. Cancer Res.* 4 (1998) 2551–2557.
- [178] K. Schwager, T. Hemmerle, D. Aebischer, D. Neri, The Immunocytokine L19–IL2 Eradicates Cancer When Used in Combination with CTLA-4 Blockade or with L19-TNF, *J. Invest. Dermatol.* 133 (2013) 751–758. doi:10.1038/jid.2012.376.
- [179] E. Balza, B. Carnemolla, L. Mortara, P. Castellani, D. Soncini, R.S. Accolla, L. Borsi, Therapy-induced antitumor vaccination in neuroblastomas by the combined targeting of IL-2 and TNFalpha., *Int. J. Cancer.* 127 (2010) 101–10. doi:10.1002/ijc.25018.
- [180] H.D. Menssen, U. Harnack, U. Erben, D. Neri, B. Hirsch, H. Dürkop, Antibody-based delivery of tumor necrosis factor (L19-TNF $\alpha$ ) and interleukin-2 (L19-IL2) to tumor-associated blood vessels has potent immunological and anticancer activity in the syngeneic J558L BALB/c myeloma model, *J. Cancer Res. Clin. Oncol.* 144 (2018) 499–507. doi:10.1007/s00432-017-2564-6.
- [181] K. Wagner, P. Schulz, A. Scholz, B. Wiedenmann, A. Menrad, The targeted immunocytokine L19-IL2 efficiently inhibits the growth of orthotopic pancreatic cancer, *Clin. Cancer Res.* 14 (2008) 4951. doi:10.1158/1078-0432.CCR-08-0157.
- [182] G. Mariani, A. Lasku, E. Balza, B. Gaggero, C. Motta, L. Di Luca, A. Dorcaratto, G. Viale, D. Neri, L. Zardi, Tumor targeting potential of the monoclonal antibody BC-1 against

- oncofetal fibronectin in nude mice bearing human tumor implants, *Cancer*. 87 (1997) 2378–84.
- [183] J. Fallon, R. Tighe, G. Kradjian, W. Guzman, A. Bernhardt, B. Neuteboom, Y. Lan, H. Sabzevari, J. Schlom, J.W. Greiner, The immunocytokine NHS-IL12 as a potential cancer therapeutic., *Oncotarget*. 5 (2014) 1869–84. doi:10.18632/oncotarget.1853.
- [184] J.K. Fallon, A.J. Vandever, J. Schlom, J.W. Greiner, Enhanced antitumor effects by combining an IL-12/anti-DNA fusion protein with avelumab, an anti-PD-L1 antibody, *Oncotarget*. 8 (2017) 20558–20571. doi:10.18632/oncotarget.16137.
- [185] S.D. Gillies, Y. Lan, J.S. Wesolowski, X. Qian, R.A. Reisfeld, S. Holden, M. Super, Antibody-IL-12 Fusion Proteins Are Effective in SCID Mouse Models of Prostate and Colon Carcinoma Metastases, *J. Immunol*. 160 (1998) 6195–6203.
- [186] L.S. Peng, M.L. Penichet, S.L. Morrison, E. Alerts, A Single-Chain IL-12 IgG3 Antibody Fusion Protein Retains Antibody Specificity and IL-12 Bioactivity and Demonstrates Antitumor Activity, *J. Immunol*. 163 (1999) 250–258.
- [187] L.S. Peng, M.L. Penichet, J.S. Dela Cruz, S.L. Sampogna, S.L. Morrison, Mechanism of antitumor activity of a single-chain interleukin-12 IgG3 antibody fusion protein (mScIL-12.her2.IgG3)., *J. Interf. Cytokine Res*. 21 (2001) 709–20. doi:10.1089/107999001753124444.
- [188] H. Kim, W. Gao, M. Ho, Novel Immunocytokine IL12-SS1 ( Fv ) Inhibits Mesothelioma Tumor Growth in Nude Mice, *PLoS One*. 8 (2013) 1–11. doi:10.1371/journal.pone.0081919.
- [189] C. Hess, D. Neri, The antibody-mediated targeted delivery of interleukin-13 to syngeneic murine tumors mediates a potent anticancer activity, *Cancer Immunol. Immunother*. 64 (2015) 635–644. doi:10.1007/s00262-015-1666-8.
- [190] M. Vincent, D. Cochonneau, G. Teppaz, V. Solé, M. Maillason, S. Birklé, L. Garrigue-Antar, A. Quéméner, Y. Jacques, Tumor targeting of the IL-15 superagonist RLI by an anti-GD2 antibody strongly enhances its antitumor potency, *Int. J. Cancer*. 133 (2013) 757–766. doi:10.1002/ijc.28059.
- [191] V. Kermer, V. Baum, N. Hornig, R.E. Kontermann, D. Müller, An Antibody Fusion Protein for Cancer Immunotherapy Mimicking IL-15 *trans* -Presentation at the Tumor Site, *Mol. Cancer Ther*. 11 (2012) 1279–1288. doi:10.1158/1535-7163.MCT-12-0019.
- [192] V. Kermer, N. Hornig, M. Harder, A. Bondarieva, R.E. Kontermann, D. Müller,

- Combining Antibody-Directed Presentation of IL-15 and 4-1BBL in a Trifunctional Fusion Protein for Cancer Immunotherapy, *Mol. Cancer Ther.* 13 (2014) 112–121. doi:10.1158/1535-7163.MCT-13-0282.
- [193] N. Pasche, K. Frey, D. Neri, The targeted delivery of IL17 to the mouse tumor neovasculature enhances angiogenesis but does not reduce tumor growth rate, *17* (2012) 165–169. doi:10.1007/s10456-011-9239-8.
- [194] N. Pasche, D. Neri, Immunocytokines: a novel class of potent armed antibodies., *Drug Discov. Today.* 17 (2012) 583–90. doi:10.1016/j.drudis.2012.01.007.
- [195] S. Bhatt, S. Parvin, Y. Zhang, H. Cho, K. Kunkalla, F. Vega, J.M. Timmerman, S. Shin, J.D. Rosenblatt, I.S. Lossos, Anti-CD20-interleukin-21 fusokine targets malignant B cells via direct apoptosis and NK-cell – dependent cytotoxicity, *Blood.* 129 (2017) 2246–2257. doi:10.1182/blood-2016-09-738211.
- [196] S. Bhatt, D. Zhu, X. Jiang, S. Shin, J.M. Timmerman, J.D. Rosenblatt, I.S. Lossos, Targeting B-Cell Malignancies With Anti-CD20-Interleukin-21 Fusokine, *Blood.* 122 (2013) 377 LP-377. <http://www.bloodjournal.org/content/122/21/377.abstract>.
- [197] K. Frey, A. Zivanovic, S. Kathrin, D. Neri, Antibody-based targeting of interferon-alpha to the tumor neovasculature : a critical evaluation, *Integr. Biol.* 3 (2011) 468–478. doi:10.1039/c0ib00099j.
- [198] C. Xuan, K.K. Steward, J.M. Timmerman, S.L. Morrison, Targeted delivery of interferon-alpha via fusion to anti-CD20 results in potent antitumor activity against B-cell lymphoma, *Lymphoid Neoplasia.* 115 (2010) 2864–2872. doi:10.1182/blood-2009-10-250555.The.
- [199] T.-H. Huang, K.R. Chintalacharuvu, S.L. Morrison, Targeting IFN-alpha to B Cell Lymphoma by a Tumor-Specific Antibody Elicits Potent Antitumor Activities, *J. Immunol.* 179 (2007) 6881–6888. doi:10.4049/jimmunol.179.10.6881.
- [200] E.A. Rossi, D.L. Rossi, T.M. Cardillo, R. Stein, D.M. Goldenberg, C.H. Chang, Preclinical studies on targeted delivery of multiple IFN $\alpha$ 2b to HLA-DR in diverse hematologic cancers, *Blood.* 118 (2011) 1877–1884. doi:10.1182/blood-2011-03-343145.
- [201] M.M. Mizokami, P. Hu, L.A. Khawli, J. Li, A.L. Epstein, Chimeric TNT-3 antibody/murine interferon-gamma fusion protein for the immunotherapy of solid malignancies., *Hybrid. Hybridomics.* 22 (2003) 197–207. doi:10.1089/153685903322328929.
- [202] S. Bauer, N. Adrian, B. Williamson, C. Panousis, N. Fadle, J. Smerd, I. Fettah, A.M.



- Scott, M. Pfreundschuh, C. Renner, Targeted bioactivity of membrane-anchored TNF by an antibody-derived TNF fusion protein., *J. Immunol.* 172 (2004) 3930–3939. doi:10.4049/jimmunol.172.6.3930.
- [203] E. Balza, L. Mortara, F. Sassi, S. Monteghirfo, B. Carnemolla, P. Castellani, D. Neri, R.S. Accolla, L. Zardi, L. Borsi, Targeted delivery of tumor necrosis factor-alpha to tumor vessels induces a therapeutic T cell-mediated immune response that protects the host against syngeneic tumors of different histologic origin., *Clin. Cancer Res.* 12 (2006) 2575–82. doi:10.1158/1078-0432.CCR-05-2448.
- [204] U. Scherf, I. Benhar, K.O. Webber, I. Pastan, U. Brinkmann, Cytotoxic and Antitumor Activity of a Recombinant Tumor Necrosis Factor-B1 (Fv) Fusion Protein on LeY Antigen-expressing Human Cancer Cells, *Clin. Cancer Res.* 2 (1996) 1523–1531.
- [205] S.D. Gillies, Y. Lan, B. Brunkhorst, W.-K. Wong, Y. Li, K.-M. Lo, Bi-functional cytokine fusion proteins for gene therapy and antibody-targeted treatment of cancer, *Cancer Immunol. Immunother.* 51 (2002) 449–460. doi:10.1007/s00262-002-0302-6.
- [206] C. Hess, D. Neri, Evaluation of antibody-chemokine fusion proteins for tumor-targeting applications, *Exp. Biol. Med.* 239 (2014) 842–852. doi:10.1177/1535370214536667.
- [207] N. Hornig, K. Reinhardt, V. Kermer, R.E. Kontermann, D. Müller, Evaluating combinations of costimulatory antibody-ligand fusion proteins for targeted cancer immunotherapy, *Cancer Immunol. Immunother.* 62 (2013) 1369–1380. doi:10.1007/s00262-013-1441-7.
- [208] D. Müller, K. Frey, E. Kontermann, A Novel Antibody-4-1BBL Fusion Protein for Targeted Costimulation in Cancer Immunotherapy, *J. Immunother.* 8 (2008).
- [209] N. Hornig, V. Kermer, K. Frey, P. Diebolder, R. Kontermann, D. Müller, Combination of a Bispecific Antibody and Costimulatory Antibody-Ligand Fusion Proteins for Targeted Cancer Immunotherapy, *J. Immunother.* 35 (2012) 418–429.
- [210] F. Nilsson, H. Kosmehl, L. Zardi, Targeted Delivery of Tissue Factor to the ED-B Domain of Fibronectin , a Marker of Angiogenesis , Mediates the Infarction of Solid Tumors in Mice Targeted Delivery of Tissue Factor to the ED-B Domain of Fibronectin , a Marker of Angiogenesis , Mediates th, (2001) 711–716.
- [211] X. Huang, D. Ye, P.E. Thorpe, Enhancing the potency of a whole-cell breast cancer vaccine in mice with an antibody-IL-2 immunocytokine that targets exposed

- phosphatidylserine  $\alpha$ ,  $\alpha\alpha$ , *Vaccine*. 29 (2011) 4785–4793.  
doi:10.1016/j.vaccine.2011.04.082.
- [212] J.D. Pancook, C. Becker, S.D. Gillies, R.A. Reisfeld, Eradication of established hepatic human neuroblastoma metastases in mice with severe combined immunodeficiency by antibody-targeted interleukin-2, *Cancer Immunol. Immunother.* 42 (1996) 88–92.
- [213] S.D. Gillies, Y. Lan, S. Williams, F. Carr, S. Forman, A. Raubitschek, K. Lo, An anti-CD20 – IL-2 immunocytokine is highly efficacious in a SCID mouse model of established human B lymphoma, *Blood*. 105 (2005) 3972–3979. doi:10.1182/blood-2004-09-3533.Several.
- [214] K.L. Gutbrodt, G. Casi, D. Neri, Antibody-based delivery of IL2 and cytotoxics eradicates tumors in immunocompetent mice., *Mol. Cancer Ther.* 13 (2014) 1772–6. doi:10.1158/1535-7163.MCT-14-0105.
- [215] S.A. Holden, Y. Lan, A.M. Pardo, J.S. Wesolowski, S.D. Gillies, Augmentation of Antitumor Activity of an Antibody-Interleukin 2 Immunocytokine with Chemotherapeutic Agents Augmentation of Antitumor Activity of an Antibody-Interleukin 2 Immunocytokine with Chemotherapeutic Agents, 7 (2001) 2862–2869.
- [216] C. Schliemann, A. Palumbo, K. Zuberbu, A. Villa, M. Kaspar, E. Trachsel, W. Klapper, H.D. Menssen, D. Neri, Complete eradication of human B-cell lymphoma xenografts using rituximab in combination with the immunocytokine L19-IL2, 113 (2009) 2275–2283. doi:10.1182/blood-2008-05-160747.An.
- [217] E. Balza, L. Mortara, F. Sassi, S. Monteghirfo, B. Carnemolla, P. Castellani, D. Neri, R.S. Accolla, L. Zardi, L. Borsi, Targeted delivery of tumor necrosis factor- $\alpha$  to tumor vessels induces a therapeutic T cell-mediated immune response that protects the host against syngeneic tumors of different histologic origin, *Clin. Cancer Res.* 12 (2006) 2575–2582. doi:10.1158/1078-0432.CCR-05-2448.
- [218] E.E. Johnson, B.H. Yamane, I.N. Buhtoiarov, H.D. Lum, A.L. Rakhmievich, D.M. Mahvi, S.D. Gillies, P.M. Sondel, Radiofrequency ablation combined with KS-IL2 immunocytokine (EMD 273066) results in an enhanced antitumor effect against murine colon adenocarcinoma, *Clin. Cancer Res.* 15 (2009) 4875–4884. doi:10.1158/1078-0432.CCR-09-0110.
- [219] Z.C. Neal, M. Imboden, A.L. Rakhmievich, K.M. Kim, J.A. Hank, J. Surfus, J.R. Dixon,

- H.N. Lode, R.A. Reisfeld, S.D. Gillies, P.M. Sondel, NXS2 murine neuroblastomas express increased levels of MHC class I antigens upon recurrence following NK-dependent immunotherapy, *Cancer Immunol. Immunother.* 53 (2004) 41–52. doi:10.1007/s00262-003-0435-2.
- [220] E. Harvill, J. Fleming, S. Morrison, In vivo properties of an IgG3-IL-2 fusion protein. A general strategy for immune potentiation, *J. Immunol.* 157 (1996) 3165–3170.
- [221] L. Peng, M. Penichet, J. Dela Cruz, S.L. Sampogna, S. Morrison, Mechanism of Antitumor Activity of a Single-Chain Interleukin-12 IgG3 Antibody Fusion Protein (mscIL-12.her2.IgG3), *J. Interf. Cytokine Res.* 21 (2004).
- [222] S. Dubois, J. Mariner, T.A. Waldmann, Y. Tagaya, IL-15R $\alpha$  recycles and presents IL-15 in trans to neighboring cells, *Immunity.* 17 (2002) 537–547. doi:10.1016/S1074-7613(02)00429-6.
- [223] S.K. Olsen, N. Ota, S. Kishishita, M. Kukimoto-Niino, K. Murayama, H. Uchiyama, M. Toyama, T. Terada, M. Shirouzu, O. Kanagawa, S. Yokoyama, Crystal structure of the interleukin-15-interleukin-15 receptor  $\alpha$  complex: Insights into trans and cis presentation, *J. Biol. Chem.* 282 (2007) 37191–37204. doi:10.1074/jbc.M706150200.
- [224] B. Robert, J.-P. Mach, J.-C. Mani, M. Ychou, S. Folli, J.-C. Artus, A. Pèlerin, Cytokine targeting in tumors using a bispecific antibody directed against carcinoembryonic antigen and tumor necrosis factor  $\alpha$ , *Cancer Res.* 56 (1996) 4758–4765. <http://www.embase.com/search/results?subaction=viewrecord&from=export&id=L26338081%5Cnhttp://sfx.library.uu.nl/utrecht?sid=EMBASE&issn=00085472&id=doi:&atitle=Cytokine+targeting+in+tumors+using+a+bispecific+antibody+directed+against+carcinoembryonic+antig>.
- [225] S. Cazzamalli, B. Ziffels, F. Widmayer, P. Murer, G. Pellegrini, F. Pretto, S. Wulhfard, D. Neri, Enhanced Therapeutic Activity of Non-Internalizing Small Molecule-Drug Conjugates Targeting Carbonic Anhydrase IX in Combination With Targeted Interleukin-2, *Clin. Cancer Res.* (2018). <http://clincancerres.aacrjournals.org/content/early/2018/04/24/1078-0432.CCR-17-3457.abstract>.
- [226] M.M. Van Den Heuvel, M. Verheij, R. Boshuizen, J. Belderbos, A.C. Dingemans, D. De Ruyscher, J. Laurent, R. Tighe, J. Haanen, S. Quarantino, NHS-IL2 combined with radiotherapy : preclinical rationale and phase Ib trial results in metastatic non-small

- cell lung cancer following first-line chemotherapy, (2015) 1–13. doi:10.1186/s12967-015-0397-0.
- [227] C.M.L. Zegers, N.H. Rekers, D.H.F. Quaden, N.G. Lieuwes, A. Yaromina, W.T. V Germeraad, L. Wieten, E. a L. Biessen, L. Boon, D. Neri, E.G.C. Troost, L.J. Dubois, P. Lambin, Radiotherapy combined with the immunocytokine L19-IL2 provides long-lasting antitumor effects., *Clin. Cancer Res.* 21 (2015) 1151–60. doi:10.1158/1078-0432.CCR-14-2676.
- [228] F. Eckert, J. Schmitt, D. Zips, M.A. Krueger, B.J. Pichler, S.D. Gillies, W. Strittmatter, R. Handgretinger, K. Schilbach, Enhanced binding of necrosis-targeting immunocytokine NHS-IL12 after local tumour irradiation in murine xenograft models, *Cancer Immunol. Immunother.* 65 (2016) 1003–1013. doi:10.1007/s00262-016-1863-0.
- [229] K. Schwager, T. Hemmerle, D. Aebischer, D. Neri, The Immunocytokine L19 – IL2 Eradicates Cancer When Used in Combination with CTLA-4 Blockade or with L19-TNF, *J. Invest. Dermatol.* 133 (2013) 751–758. doi:10.1038/jid.2012.376.
- [230] T. List, G. Casi, D. Neri, A Chemically Defined Trifunctional Antibody – Cytokine – Drug Conjugate with Potent Antitumor Activity, *Mol. Cancer Ther.* 13 (2014) 2641–2653. doi:10.1158/1535-7163.MCT-14-0599.
- [231] F. Yuan, M. Dellian, D. Fukumura, M. Leunig, D. a Berk, V.P. Torchilin, R.K. Jain, Vascular Permeability in a Human Tumor Xenograft : Molecular Size Dependence and Cutoff Size, *Cancer Res.* 55 (1995) 3752–3756. doi:10.1038/nature02924.
- [232] X. Liu, J. Guo, S. Han, L. Yao, A. Chen, Q. Yang, H. Bo, P. Xu, J. Yin, Z. Zhang, Enhanced immune response induced by a potential influenza A vaccine based on branched M2e polypeptides linked to tuftsin, *Vaccine.* 30 (2012) 6527–6533. doi:10.1016/j.vaccine.2012.08.054.
- [233] M.A. Firer, G. Gellerman, Targeted drug delivery for cancer therapy: the other side of antibodies, *J. Hematol. Oncol.* 5 (2012) 70. doi:10.1186/1756-8722-5-70.
- [234] R. Danielli, R. Patuzzo, A.M. Di Giacomo, G. Gallino, A. Maurichi, A. Di Florio, O. Cutaia, A. Lazzeri, C. Fazio, C. Miracco, L. Giovannoni, G. Elia, D. Neri, M. Maio, M. Santinami, Intralesional administration of L19-IL2/L19-TNF in stage III or stage IVM1a melanoma patients: results of a phase II study, *Cancer Immunol. Immunother.* 64 (2015) 999–1009. doi:10.1007/s00262-015-1704-6.
- [235] E. Balza, B. Carnemolla, L. Mortara, P. Castellani, D. Soncini, R.S. Accolla, L. Borsi,

- Therapy-induced antitumor vaccination in neuroblastomas by the combined targeting of IL-2 and TNF, *Int. J. Cancer*. 127 (2010) 101–110. doi:10.1002/ijc.25018.
- [236] D.M. Pardoll, The blockade of immune checkpoints in cancer immunotherapy, *Nat. Rev. Cancer*. 12 (2016) 252–264. doi:10.1038/nrc3239.The.
- [237] D.H. Charych, U. Hoch, J.L. Langowski, S.R. Lee, M.K. Addepalli, P.B. Kirk, D. Sheng, X. Liu, P.W. Sims, L.A. VanderVeen, C.F. Ali, T.K. Chang, M. Konakova, R.L. Pena, R.S. Kanhere, Y.M. Kirksey, C. Ji, Y. Wang, J. Huang, T.D. Sweeney, S.S. Kantak, S.K. Doberstein, NKTR-214, an Engineered Cytokine with Biased IL2 Receptor Binding, Increased Tumor Exposure, and Marked Efficacy in Mouse Tumor Models, *Clin. Cancer Res*. 22 (2016) 680–690. doi:10.1158/1078-0432.CCR-15-1631.
- [238] C. Bernatchez, C. Haymaker, N.M. Tannir, H. Kluger, M. Tetzlaff, S.E. Bentebibel, N. Jackson, I. Gergel, M. Tagliaferri, J. Zalevsky, U. Hoch, M. Imperiale, S. Aung, P. Hwu, M. Sznol, M. Hurwitz, A. Diab, A CD122-biased agonist increases CD8 T cells and natural killer cells in the tumor microenvironment ; making cold tumors hot with NKTR-214, *J. Immunother. Cancer*. 2 (2014) 1. doi:10.1200/JCO.2016.67.2477.2.
- [239] S. Shusterman, W.B. London, S.D. Gillies, J.A. Hank, S.D. Voss, R.C. Seeger, C.P. Reynolds, J. Kimball, M.R. Albertini, B. Wagner, J. Gan, J. Eickhoff, K.B. Desantes, S.L. Cohn, T. Hecht, B. Gadbar, R.A. Reisfeld, J.M. Maris, P.M. Sondel, Antitumor Activity of Hu14.18-IL2 in Patients With Relapsed / Refractory Neuroblastoma : A Children ' s Oncology Group (COG) Phase II Study, *J. Clin. Oncol*. 28 (2010) 4969–4975. doi:10.1200/JCO.2009.27.8861.
- [240] A. Ribas, J.M. Kirkwood, M.B. Atkins, T.L. Whiteside, W. Gooding, A. Kovar, S.D. Gillies, O. Kashala, M.A. Morse, Phase I/II open-label study of the biologic effects of the interleukin-2 immunocytokine EMD 273063 (hu14.18-IL2) in patients with metastatic malignant melanoma, *J. Transl. Med*. 7 (2009) 1–11. doi:10.1186/1479-5876-7-68.
- [241] S. Shusterman, W. London, J. Hank, M. Parisi, B. Shulkin, S. Servaes, A. Naranjo, H. Shimada, J. Gan, S. Gillies, J. Maris, J. Park, P. Sondel, A feasibility and phase II study of the hu14.18-IL2 immunocytokine in combination with GM-CSF and isotretinoin in patients with recurrent or refractory neuroblastoma: A Children's Oncology Group study, *J. Clin. Oncol*. 22 (2015).
- [242] S. Gillessen, U.S. Gnad-Vogt, E. Gallerani, J. Beck, C. Sessa, A. Omlin, M.R. Mattiacci, B. Liedert, D. Kramer, J. Laurent, D.E. Speiser, R. Stupp, A phase i dose-escalation study

- of the immunocytokine EMD 521873 (Selectikine) in patients with advanced solid tumours, *Eur. J. Cancer.* 49 (2013) 35–44. doi:10.1016/j.ejca.2012.07.015.
- [243] J.P. Connor, M.C. Cristea, N.L. Lewis, L.D. Lewis, P.B. Komarnitsky, M.R. Mattiacci, M. Felder, S. Stewart, J. Harter, J. Henslee-downey, D. Kramer, R. Neugebauer, R. Stupp, A phase 1b study of humanized KS-interleukin-2 ( huKS-IL2 ) immunocytokine with cyclophosphamide in patients with EpCAM-positive advanced solid tumors, (2013) 1–12.
- [244] Y.-J. Ko, G.J. Bublely, R. Weber, C. Redfern, D. Gold, L. Finke, A. Kovar, T. Dahl, S.D. Gillies, Safety, Pharmacokinetics, and Biological Pharmacodynamics of the Immunocytokine EMD273066 (huKS-IL2): Results of a Phase I Trial in Patients with Prostate Cancer, *J. Immunother.* 27 (2004) 232–239.
- [245] J. Connor, M. Cristea, N. Lewis, L. Lewis, M. Mattiacci, M. Felder, S. Stewart, J. Henslee-Downey, R. Neugebauer, Komarnitsky, Phase IB trial of EMD 273066 (huKS-IL2) with cyclophosphamide in patients with EpCAM-positive advanced solid tumors, *J. Clin. Oncol.* 29 (2011) 2556.
- [246] O. Gladkov, R. Ramlau, P. Serwatowski, J. Milanowski, J. Tomeczko, P. Komarnitsky, D. Kramer, M. Krzakowski, Cyclophosphamide and tucotuzumab (huKS-IL2) following first-line chemotherapy in responding patients with extensive-disease small-cell lung cancer, *Anticancer. Drugs.* 26 (2015) 1061–1068.
- [247] V. Bachanova, F. Lansigan, D.P. Quick, D. Vlock, S. Gillies, R. Nakamura, Remission Induction in a Phase I/II Study of an Anti-CD20-Interleukin-2 Immunocytokine DI-Leu16-IL2 in Patients with Relapsed B-Cell Lymphoma, *Blood.* 126 (2015) 1533 LP-1533. <http://www.bloodjournal.org/content/126/23/1533.abstract>.
- [248] F. Lansigan, R. Nakamura, D.P. Quick, D. Vlock, A. Raubitschek, S.D. Gillies, V. Bachanova, DI-Leu16-IL2, an Anti-CD20-Interleukin-2 Immunocytokine, Is Safe and Active in Patients with Relapsed and Refractory B-Cell Lymphoma: A Report of Maximum Tolerated Dose, Optimal Biologic Dose, and Recommended Phase 2 Dose, *Blood.* 128 (2016) 620 LP-620. <http://www.bloodjournal.org/content/128/22/620.abstract>.
- [249] F. Lansigan, R. Nakamura, D. Quick, D. Vlock, A. Raubitschek, S. Gillies, V. Bachanova, Phase I/II study of an anti-CD20-interleukin-2 immunocytokine DI-Leu16-IL2 in patients with relapsed b-cell lymphoma (NHL), *J. Clin. Oncol.* 34 (2016).

- [250] M. Johannsen, G. Spitaleri, G. Curigliano, J. Roigas, S. Weikert, C. Kempkensteffen, A. Roemer, C. Kloeters, P. Rogalla, G. Pecher, K. Miller, A. Berndt, H. Kosmehl, E. Trachsel, M. Kaspar, V. Lovato, R. González-Iglesias, L. Giovannoni, H.D. Menssen, D. Neri, F. de Braud, The tumour-targeting human L19-IL2 immunocytokine: preclinical safety studies, phase I clinical trial in patients with solid tumours and expansion into patients with advanced renal cell carcinoma., *Eur. J. Cancer.* 46 (2010) 2926–35. doi:10.1016/j.ejca.2010.07.033.
- [251] T.K. Eigentler, B. Weide, F. De Braud, G. Spitaleri, A. Romanini, A. Pflugfelder, R. González-Iglesias, A. Tasciotti, L. Giovannoni, K. Schwager, V. Lovato, M. Kaspar, E. Trachsel, H.D. Menssen, D. Neri, C. Garbe, A dose-escalation and signal-generating study of the immunocytokine L19-IL2 in combination with dacarbazine for the therapy of patients with metastatic melanoma, *Clin. Cancer Res.* 17 (2011) 7732–7742. doi:10.1158/1078-0432.CCR-11-1203.
- [252] B. Weide, T.K. Eigentler, A. Pflugfelder, H. Zelba, A. Martens, G. Pawelec, L. Giovannoni, P.A. Ruffini, G. Elia, D. Neri, R. Gutzmer, J.C. Becker, C. Garbe, Intralesional Treatment of Stage III Metastatic Melanoma Patients with L19-IL2 Results in Sustained Clinical and Systemic Immunologic Responses, *Cancer Immunol. Res.* 2 (2014) 668–678. doi:10.1158/2326-6066.CIR-13-0206.
- [253] H. Kaplon, J.M. Reichert, Antibodies to watch in 2018, *MAbs.* 10 (2018) 183–203. doi:10.1080/19420862.2018.1415671.
- [254] B. Weide, D. Neri, G. Elia, Intralesional treatment of metastatic melanoma: a review of therapeutic options, *Cancer Immunol. Immunother.* 66 (2017) 647–656. doi:10.1007/s00262-016-1952-0.
- [255] Philogen, Philogen Pipeline, (n.d.). [http://www.philogen.com/en/products/pipeline\\_16.html](http://www.philogen.com/en/products/pipeline_16.html) (accessed May 24, 2018).
- [256] C. Catania, M. Maur, R. Berardi, A. Rocca, A.M. Di Giacomo, G. Spitaleri, C. Masini, C. Pierantoni, R. González-Iglesias, G. Zigon, A. Tasciotti, L. Giovannoni, V. Lovato, G. Elia, H.D. Menssen, D. Neri, S. Cascinu, P.F. Conte, F. De Braud, The tumor-targeting immunocytokine F16-IL2 in combination with doxorubicin: Dose escalation in patients with advanced solid tumors and expansion into patients with metastatic breast cancer, *Cell Adhes. Migr.* 9 (2015) 14–21. doi:10.4161/19336918.2014.983785.
- [257] C. Schliemann, K.L. Gutbrodt, A. Kerkhoff, M. Pohlen, S. Wiebe, G. Silling, L.

- Angenenendt, T. Kessler, R.M. Mesters, L. Giovannoni, M. Schaefers, B. Altvater, C. Rossig, I. Gruenewald, E. Wardelmann, G. Koehler, D. Neri, M. Stelljes, W.E. Berdel, Targeting Interleukin-2 to the Bone Marrow Stroma for Therapy of Acute Myeloid Leukemia Relapsing After Allogeneic Hematopoietic Stem Cell Transplantation, *Cancer Immunol Res.* 3 (2015) 547–557. doi:10.1158/2326-6066.CIR-14-0179.
- [258] F.. Braud, C. Catania, A. Onofri, C. Pierantoni, S. Cascinu, M. Maur, C. Masini, P.. Conte, L. Giovannoni, A. Tasciotti, V. Lovato, D. Neri, H.D. Menssen, Combination of the immunocytokine F16-IL2 with doxorubicin or paclitaxel in patients with solid tumors: Results from two phase Ib trials, *J. Clin. Oncol.* 29 (2011) 2595.
- [259] F.G. De Braud, C. Catania, C. Masini, M. Maur, S. Cascinu, R. Berardi, L. Giovannoni, G. Spitaleri, S. Boselli, D. Neri, Combinations of the immunocytokine F16-IL2 with doxorubicin or with paclitaxel investigated in phase Ib studies in patients with advanced solid tumors, *J. Clin. Oncol.* 28 (2010).
- [260] J. Schellens, J. Tabernero, U. Lassen, I. Melero, K. Homicsko, G. Argiles, J. Gracia, M. Sorensen, G. Coukos, E. Angevin, H. Joensuu, E. Van Brummelen, C. Menke, T. Nayak, S. Romagnoli, B. Reis, S. Brossard, S. Evers, J. Suarez, H. Verheul, CEA-targeting engineered IL2: Clinical confirmation of tumor targeting and evidence of intra-tumoral immune activation, *J. Clin. Oncol.* 33 (2015) 3016.
- [261] B. Ribba, C. Boetsch, T. Nayak, Z.-X. Xu, H.-P. Grimm, H. Silber-Baumann, J. Saro, S. Evers, V. Teichgräber, Schedule optimization of a novel tumor-targeted IL-2 variant immunocytokine by integration of human in vivo immune cell kinetics and functional imaging, *Ann. Oncol.* 27 (2016).
- [262] E. van Brummelen, U. Lassen, I. Melero, J. Tabernero, K. Homicsko, E. Angevin, V. Teichgräber, L. Jukofsky, E. Rossmann, G. Babitzki, P. Silva, M. Canamero, C. Boetsch, S. Evers, J. Charo, G. Argiles, Pharmacokinetics (PK) and Pharmacodynamics (PD) of cergutuzumab amunaleukin (CA), a carcinoembryonic antigen (CEA)-targeted interleukin 2 variant (IL2v) with abolished binding to CD25, *Ann. Oncol.* 28 (2017) 2017. doi:10.1093/annonc/mdx376.
- [263] E. van Brummelen, Early clinical development of targeted anticancer agents, Utrecht University, 2017.
- [264] M. van der Houven van Oordt, E. van Brummelen, T. Nayak, M. Huisman, L. de Wit-van der Veen, E. Mulder, O. Hoekstra, M. Stokkel, G. van Dongen, H. Verheul, M.



- Feilke, C. Guizani, E. Guarin, S. Evers, J. Saro, J. Schellens, 89Zr-labeled CEA-targeted IL-2 variant immunocytokine in patients with solid tumors: CEA-mediated tumor accumulation in a dose-dependent manner and role of IL-2 receptor binding, *Ann. Oncol.* (2016).
- [265] J.W. Kim, C.R. Heery, M. Bilusic, N. Singh, R. Madan, H. Sabzevari, J. Schlom, J. Gulley, First-in-human phase I trial of NHS-IL12 in advanced solid tumors, *J. Clin. Oncol.* 30 (2012) TPS2617.
- [266] S.M. Rudman, M.B. Jameson, M.J. Mckeage, P. Savage, D.I. Jodrell, M. Harries, G. Acton, F. Erlandsson, J.F. Spicer, A Phase 1 Study of AS1409 , a Novel Antibody-Cytokine Fusion Protein , in Patients with Malignant Melanoma or Renal Cell Carcinoma, *Clin. Cancer Res.* 17 (2011) 1998–2006. doi:10.1158/1078-0432.CCR-10-2490.
- [267] J.. Spicer, M.. Jameson, P. Savage, D. Jodrell, S. Rudman, F. Erlandsson, G. Acton, M. McKeage, A phase I study of AS1409, a novel antibody-cytokine fusion protein, in patients with malignant melanoma (MM) or renal cell carcinoma (RCC), *J. Clin. Oncol.* 27 (2009) 3024.
- [268] G. Mariani, A. Lasku, A. Pau, G. Villa, C. Motta, G. Calcagno, G. Taddei, P. Castellani, K. Syrigos, A. Dorcaratto, A. Epenetos, L. Zardi, G. Viale, A pilot pharmacokinetic and immunoscintigraphic study with the technetium-99m-labeled monoclonal antibody BC-1 directed against oncofetal fibronectin in patients with brain tumors, *Cancer.* 80 (1997).
- [269] F. Papadia, V. Basso, R. Patuzzo, A. Maurichi, A. Di Florio, L. Zardi, E. Ventura, R. González-Iglesias, V. Lovato, L. Giovannoni, A. Tasciotti, D. Neri, M. Santinami, H.D. Menssen, F. De Cian, Isolated limb perfusion with the tumor-targeting human monoclonal antibody-cytokine fusion protein L19-TNF plus melphalan and mild hyperthermia in patients with locally advanced extremity melanoma, *J. Surg. Oncol.* 107 (2013) 173–179. doi:10.1002/jso.23168.
- [270] D. Lienard, P. Ewalenko, J. Delmotte, N. Renard, F. Lejeune, High-dose recombinant tumor necrosis factor alpha in combination with interferon gamma and melphalan in isolation perfusion of the limbs for melanoma and sarcoma, *J. Clin. Oncol.* 10 (1992) 52–60.
- [271] C.O. Starnes, Coley's toxins in perspective, *Nature.* 357 (1992) 11–12.

- [272] E. Balada, J. Ordi-Ros, M. Vilardell-Tarres, Molecular mechanisms mediated by Human Endogenous Retroviruses (HERVs) in autoimmunity, *Rev. Med. Virol.* 19 (2009) 273–286. doi:10.1002/rmv.
- [273] L. Baudino, K. Yoshinobu, N. Morito, M.L. Santiago-Raber, S. Izui, Role of endogenous retroviruses in murine SLE, *Autoimmun. Rev.* 10 (2010) 27–34. doi:10.1016/j.autrev.2010.07.012.
- [274] A. Perl, Pathogenic mechanisms in systemic lupus erythematosus, *Autoimmunity.* 43 (2010) 1–6. doi:10.3109/08916930903374741.
- [275] R.F. Downey, F.J. Sullivan, F. Wang-Johanning, S. Ambs, F.J. Giles, S.A. Glynn, Human endogenous retrovirus K and cancer: Innocent bystander or tumorigenic accomplice?, *Int. J. Cancer.* 137 (2015) 1249–1257. doi:10.1002/ijc.29003.
- [276] G. Kassiotis, Endogenous Retroviruses and the Development of Cancer, *J. Immunol.* 192 (2014) 1343–1349. doi:10.4049/jimmunol.1302972.
- [277] F. Schiavetti, J. Thonnard, D. Colau, T. Boon, P.G. Coulie, A Human Endogenous Retroviral Sequence Encoding an Antigen Recognized on Melanoma by Cytolytic T Lymphocytes A Human Endogenous Retroviral Sequence Encoding an Antigen Recognized on Melanoma by Cytolytic T Lymphocytes 1, (2002) 5510–5516.
- [278] I. Waldhauer, V. Nicolini, A. Freimoser-Grundschober, L. Codarri-Deak, T. Nayak, O. Boerman, F. Cavallo, M. Bacac, C. Gerdes, P. Umana, C. Klein, FAP-IL2v (RG7461), a novel targeted immunocytokine for cancer immunotherapy, *Eur. J. Cancer* 55S2. (2016).
- [279] K. Matsuoka, J. Koreth, H.T. Kim, G. Bascug, S. McDonough, Y. Kawano, K. Murase, C. Cutler, V.T. Ho, E.P. Alyea, P. Armand, B.R. Blazar, J.H. Antin, R.J. Soiffer, J. Ritz, Low-Dose Interleukin-2 Therapy Restores Regulatory T Cell Homeostasis in Patients with Chronic Graft-Versus-Host Disease, *Sci. Transl. Med.* 5 (2013). <http://stm.sciencemag.org/content/5/179/179ra43.abstract>.
- [280] J.B.B. Ridgway, L.G. Presta, P. Carter, “Knobs-into-holes” engineering of antibody CH3 domains for heavy chain heterodimerization, *Protein Eng.* 9 (1996) 617–621. doi:10.1016/1380-2933(96)80685-3.
- [281] R. Baluna, J. Rizo, B.E. Gordon, V. Ghetie, E.S. Vitetta, Evidence for a structural motif in toxins and interleukin-2 that may be responsible for binding to endothelial cells and initiating vascular leak syndrome., *Proc. Natl. Acad. Sci. U. S. A.* 96 (1999) 3957–

62. doi:10.1073/pnas.96.7.3957.
- [282] J. Sharifi, L.A. Khawli, P. Hu, S. King, A. Epstein, Characterization of a Phage Display-Derived Human Monoclonal Antibody (NHS76) counterpart to chimeric TNT-1 Directed Against Necrotic Regions of Solid Tumors, *Hybrid. Hybridomics*. 20 (2004).
- [283] P.A. Erba, M. Sollini, E. Orciuolo, C. Traino, M. Petrini, G. Paganelli, E. Bombardieri, C. Grana, L. Giovannoni, D. Neri, H.D. Menssen, G. Mariani, Radioimmunotherapy with Radretumab in Patients with Relapsed Hematologic Malignancies, *J. Nucl. Med.* 53 (2012) 922–927. doi:10.2967/jnumed.111.101006.
- [284] S.S. Brack, M. Silacci, M. Birchler, D. Neri, Tumor-targeting properties of novel antibodies specific to the large isoform of tenascin-C, *Clin. Cancer Res.* 12 (2006) 3200–3208. doi:10.1158/1078-0432.CCR-05-2804.
- [285] L. Borsi, B. Carnemolla, G. Nicolo, B. Spinaz, T. Giorgio, L. Zardi, Expression of different tenascin isoforms in normal, hyperplastic and neoplastic human breast tissues, *Int. J. Cancer*. 52 (1992) 688–692.
- [286] D. a Heuveling, R. de Bree, D.J. Vugts, M.C. Huisman, L. Giovannoni, O.S. Hoekstra, C.R. Leemans, D. Neri, G. a M.S. van Dongen, Phase 0 microdosing PET study using the human mini antibody F16SIP in head and neck cancer patients., *J. Nucl. Med.* 54 (2013) 397–401. doi:10.2967/jnumed.112.111310.
- [287] M. Midulla, R. Verma, M. Pignatelli, B. Tumor, E. Cells, M.A. Ritter, N.S. Courtenay-luck, A.J.T. George, Source of Oncofetal ED-B-containing Fibronectin : Implications of Production by Both Tumor and Endothelial Cells Source of Oncofetal ED-B-containing Fibronectin : Implications of Production by, (2000) 164–169.
- [288] M.M. Van Den Heuvel, M. Verheij, R. Boshuizen, J. Belderbos, A.C. Dingemans, D. De Ruyscher, J. Laurent, R. Tighe, J. Haanen, S. Quarantino, NHS-IL2 combined with radiotherapy : preclinical rationale and phase Ib trial results in metastatic non-small cell lung cancer following first-line chemotherapy, *J. Transl. Med.* (2015) 1–13. doi:10.1186/s12967-015-0397-0.
- [289] J.C. Yang, R.M. Sherry, S.M. Steinberg, S. Topalian, D.J. Schwartzentruber, P. Hwu, C. Seipp, L. Rogers-Freezer, K. Morton, D. White, D. Liewehr, M. Merino, S. Rosenberg, Randomized Study of High-Dose and Low-Dose Inertleukin-2 in Patients with Metastatic Renal Cancer, *J. Clin. Oncol.* 21 (2003) 3127–3132. doi:10.1016/j.atherosclerosis.2009.05.009.Effect.

- [290] S.A. Rosenberg, J.C. Yang, D.E. White, S.M. Steinberg, Durability of Complete Responses in Patients With Metastatic Cancer Treated With High-Dose Interleukin-2. Identification of the Antigens Mediating Response, *Ann. Surg.* 228 (1998) 307–319. [https://ac-els-cdn-com.sire.ub.edu/S0022534705686697/1-s2.0-S0022534705686697-main.pdf?\\_tid=c0c25770-0942-4419-8e79-5fd3c8823e54&acdnat=1534950890\\_b69aa439208d5ecefdd10d18e8a9229](https://ac-els-cdn-com.sire.ub.edu/S0022534705686697/1-s2.0-S0022534705686697-main.pdf?_tid=c0c25770-0942-4419-8e79-5fd3c8823e54&acdnat=1534950890_b69aa439208d5ecefdd10d18e8a9229).
- [291] G. Spitaleri, R. Berardi, C. Pierantoni, T. De Pas, C. Noberasco, C. Libbra, R. González-Iglesias, L. Giovannoni, A. Tasciotti, D. Neri, H.D. Menssen, F. De Braud, Phase I/II study of the tumour-targeting human monoclonal antibody-cytokine fusion protein L19-TNF in patients with advanced solid tumours, *J. Cancer Res. Clin. Oncol.* 139 (2013) 447–455. doi:10.1007/s00432-012-1327-7.
- [292] J.A. Hank, J. Gan, H. Ryu, A. Ostendorf, M.C. Stauder, A. Sternberg, M. Albertini, K.M. Lo, S.D. Gillies, J. Eickhoff, P.M. Sondel, Immunogenicity of the Hu14.18-IL2 immunocytokine molecule in adults with melanoma and children with neuroblastoma, *Clin. Cancer Res.* 15 (2009) 5923–5930. doi:10.1158/1078-0432.CCR-08-2963.
- [293] D. Venetz, D. Koovely, B. Weder, D. Neri, Targeted reconstitution of cytokine activity upon antigen binding using split cytokine antibody fusion proteins, *J. Biol. Chem.* 291 (2016) 18139–18147. doi:10.1074/jbc.M116.737734.
- [294] Definition of leukemia, Natl. Cancer Inst. (n.d.). <https://web.archive.org/web/20140527085758/http://www.cancer.gov/cancertopics/types/leukemia> (accessed December 17, 2018).
- [295] R.L.K. Virchow, *Weisses Blut* (1845), *Gesammelte Abhandlungen zur wissenschaftlichen medicin*, Meidinger Sohn Comp. 1856 (n.d.) 149–154.
- [296] L. Bullinger, H. Dohner, J.R. Pollack, *Genomics in Leukemias*, First Edit, Elsevier Inc., 2010. doi:10.1016/B978-0-12-374934-5.00033-7.
- [297] PDQ Pediatric Treatment Editorial Board. PDQ Childhood Acute Lymphoblastic Leukemia Treatment, Natl. Cancer Inst. (2019). <https://www.cancer.gov/types/leukemia/patient/child-all-treatment-pdq> (accessed March 8, 2019).
- [298] SEER Stat Fact Sheets: Acute Myeloid Leukemia (AML): [seer.cancer.gov](http://seer.cancer.gov), (2019). <https://seer.cancer.gov/statfacts/html/amyl.html> (accessed February 21, 2019).

- [299] A.B. Mariotto, R.L. Siegel, C.C. Lin, R. Alteri, K.D. Stein, C.E. DeSantis, A. Jemal, J.L. Kramer, A.S. Robbins, Cancer treatment and survivorship statistics, 2014, CA. Cancer J. Clin. 64 (2014) 252–271. doi:10.3322/caac.21235.
- [300] G. Tamamyian, T. Kadia, F. Ravandi, G. Borthakur, J. Cortes, E. Jabbour, N. Daver, M. Ohanian, H. Kantarjian, M. Konopleva, Critical Reviews in Oncology / Hematology Frontline treatment of acute myeloid leukemia in adults, Crit. Rev. Oncol. / Hematol. 110 (2017) 20–34. doi:10.1016/j.critrevonc.2016.12.004.
- [301] C. Bennet, J. M., Catovsky, D., Daniel, M. T., Flandrin, G., Galton, D. A. G., Gralnick, H. T., & Sultan, Proposals for the classification of the acute leukemias, Br. J. Haematol. 33.4 (1976) 451–8.
- [302] J.W. Vardiman, J. Thiele, D.A. Arber, R.D. Brunning, M.J. Borowitz, A. Porwit, N.L. Harris, M.M. Le Beau, E. Hellström-Lindberg, A. Tefferi, C.D. Bloomfield, The 2008 revision of the World Health Organization (WHO) classification of myeloid neoplasms and acute leukemia: Rationale and important changes, Blood. 114 (2009) 937–951. doi:10.1182/blood-2009-03-209262.
- [303] National Cancer Institute. Physician Data Query. Adult Acute Myeloid Leukemia Treatment, (2019). [www.cancer.gov/types/leukemia/hp/adult-aml-treatment-pdq](http://www.cancer.gov/types/leukemia/hp/adult-aml-treatment-pdq) (accessed February 28, 2019).
- [304] H. Döhner, E.H. Estey, S. Amadori, F.R. Appelbaum, T. Büchner, A.K. Burnett, H. Dombret, P. Fenaux, D. Grimwade, R.A. Larson, F. Lo-Coco, T. Naoe, D. Niederwieser, G.J. Ossenkoppele, M.A. Sanz, J. Sierra, M.S. Tallman, B. Löwenberg, C.D. Bloomfield, Diagnosis and management of acute myeloid leukemia in adults: Recommendations from an international expert panel, on behalf of the European LeukemiaNet, Blood. 115 (2010) 453–474. doi:10.1182/blood-2009-07-235358.
- [305] Signs and Symptoms of Acute Myeloid Leukemia (AML), Am. Cancer Soc. (2018). <https://www.cancer.org/cancer/acute-myeloid-leukemia/detection-diagnosis-staging/signs-symptoms.html#references> (accessed March 6, 2019).
- [306] J. Yates, H. Wallace, R. Ellison, J. Holland, Cytosine arabinoside (NSC-63878) and daunorubicin (NSC-83142) therapy in acute nonlymphocytic leukemia, Cancer Chemother. Rep. 57 (1973) 485–8.
- [307] H.F. Fernandez, Z. Sun, X. Yao, S.M. Luger, J. Racevskis, E.M. Paietta, G.W. Dewald, J.M. Rowe, M.R. Litzow, M.S. Tallman, Anthracycline Dose Intensification in Acute

- Myeloid Leukemia, *N. Engl. J. Med.* 361 (2009) 1249–1259.  
doi:10.1056/nejmoa0904544.
- [308] B. Löwenberg, G. Ossenkoppele, W. van Putten, C. Graux, A. Ferrant, P. Sonneveld, J. Maertens, M. Jongen-lavrencic, M. Von Lilienfeld-toal, B.J. Biemond, E. Vellenga, M.V.M. Kooy, L.F. Verdonck, J. Beck, H. Döhner, A. Gratwohl, T. Pabst, G. Verhoef, High-Dose Daunorubicin in Older Patients with Acute Myeloid Leukemia, *N. Engl. J. Med.* 361 (2009) 1235–1248.
- [309] M.A. Sekeres, R.M. Stone, D. Zahrieh, D. Neuberg, V. Morrison, D.J. De Angelo, I. Galinsky, S.J. Lee, Decision-making and quality of life in older adults with acute myeloid leukemia or advanced myelodysplastic syndrome, *Leukemia*. 18 (2004) 809–816. doi:10.1038/sj.leu.2403289.
- [310] A.K. Burnett, D. Milligan, A. Prentice, A.H. Goldstone, R.K. Hills, M.F. McMullin, A.G. Prentice, D. Milligan, K. Wheatley, A comparison of low-dose cytarabine and hydroxyurea with or without all-trans retinoic acid for acute myeloid leukemia and high-risk myelodysplastic syndrome in patients not considered fit for intensive treatment, *Cancer*. 109 (2007) 1114–1124. doi:10.1002/cncr.22496.
- [311] J. Saultz, R. Garzon, Acute Myeloid Leukemia: A Concise Review, *J. Clin. Med.* 5 (2016) 33. doi:10.3390/jcm5030033.
- [312] G. Roboz, Current treatment of acute myeloid leukemia, *Curr. Opin. Oncol.* 24 (2012) 711–719.
- [313] T.M. Kadia, F. Ravandi, J. Cortes, H. Kantarjian, Toward Individualized Therapy in Acute Myeloid Leukemia, *JAMA Oncol.* 1 (2015) 820.  
doi:10.1001/jamaoncol.2015.0617.
- [314] C.M. Schürch, Therapeutic Antibodies for Myeloid Neoplasms—Current Developments and Future Directions, *Front. Oncol.* 8 (2018).  
doi:10.3389/fonc.2018.00152.
- [315] U. Testa, E. Pelosi, A. Frankel, CD 123 is a membrane biomarker and a therapeutic target in hematologic malignancies., *Biomark. Res.* 2 (2014) 4. doi:10.1186/2050-7771-2-4.
- [316] C.T. Jordan, D. Upchurch, S.J. Szilvassy, M.L. Guzman, D.S. Howard, A.L. Pettigrew, T. Meyerrose, R. Rossi, B. Grimes, D.A. Rizzieri, S.M. Luger, G.L. Phillips, The interleukin-3 receptor alpha chain is a unique marker for human acute myelogenous leukemia

- stem cells, *Leukemia*. 14 (2000) 1777–1784. doi:10.1038/sj.leu.2401903.
- [317] M.G. Manz, T. Miyamoto, K. Akashi, I.L. Weissman, Prospective isolation of human clonogenic common myeloid progenitors, *Proc. Natl. Acad. Sci.* 99 (2002) 11872–11877. doi:10.1073/pnas.172384399.
- [318] L. Munoz, J.F. Nomdedeu, O. Lopez, M.J. Carnicer, M. Bellido, A. Aventin, S. Brunet, J. Sierra, D.M. Pardoll, Interleukin-3 receptor alpha chain (CD123) is widely expressed in hematologic malignancies, *Haematologica*. 86 (2001) 1261–1269. doi:10.1007/978-94-007-0304-9.
- [319] F. Vergez, A.S. Green, J. Tamburini, J.-E. Sarry, B. Gaillard, P. Cornillet-Lefebvre, M. Pannetier, A. Neyret, N. Chapuis, N. Ifrah, F. Dreyfus, S. Manenti, C. Demur, E. Delabesse, C. Lacombe, P. Mayeux, D. Bouscary, C. Recher, V. Bardet, High levels of CD34+CD38low/–CD123+ blasts are predictive of an adverse outcome in acute myeloid leukemia, *Haematologica*. 96 (2011) 1792–1798. doi:10.3324/haematol.2011.047894.
- [320] U. Testa, R. Riccioni, S. Militi, E. Coccia, E. Stellacci, P. Samoggia, G. Mariani, A. Rossini, A. Battistini, F. Lo-coco, C. Peschle, U. Testa, R. Riccioni, S. Militi, E. Coccia, E. Stellacci, P. Samoggia, R. Latagliata, G. Mariani, Elevated expression of IL-3R $\alpha$  in acute myelogenous leukemia is associated with enhanced blast proliferation, increased cellularity, and poor prognosis, 100 (2011) 2980–2988. doi:10.1182/blood-2002-03-0852.
- [321] S.Y. Chu, E. Pong, H. Chen, S. Phung, E.W. Chan, N.A. Endo, R. Rashid, C. Bonzon, I.W.L. Leung, U.S. Muchhal, G.L. Moore, M.J. Bennett, D.E. Szymkowski, J.R. Desjarlais, Immunotherapy with Long-Lived Anti-CD123  $\times$  Anti-CD3 Bispecific Antibodies Stimulates Potent T Cell-Mediated Killing of Human AML Cell Lines and of CD123+ Cells in Monkeys: A Potential Therapy for Acute Myelogenous Leukemia, *Blood*. 124 (2014). <http://www.bloodjournal.org/content/124/21/2316?sso-checked=true>.
- [322] D. Karpova, L. Collins, E. Bonvini, M.P. Rettig, W.C. Eades, L.G. Eissenberg, J.K. Ritchey, F. Gao, S. Johnson, P.A. Moore, M. Al-Hussaini, J.F. DiPersio, G.R. Chichili, G.L. Uy, Targeting CD123 in acute myeloid leukemia using a T-cell-directed dual-affinity retargeting platform, *Blood*. 127 (2015) 122–131. doi:10.1182/blood-2014-05-575704.
- [323] F. Gaudet, J.F. Nemeth, R. McDaid, Y. Li, B. Harman, H. Millar, A. Teplyakov, J.

- Wheeler, J. Luo, S. Tam, S.-J. Wu, E. Chen, S. Rudnick, G. Chu, A. Hughes, L. Luistro, D. Chin, A. Babich, A. Kalota, I. Singh, M. Salvati, Y. Elsayed, R.M. Attar, Development of a CD123xCD3 Bispecific Antibody (JNJ-63709178) for the Treatment of Acute Myeloid Leukemia (AML), *Blood*. 128 (2016) 2824 LP-2824.  
<http://www.bloodjournal.org/content/128/22/2824.abstract>.
- [324] A. Mardiros, C. Dos Santos, T cells expressing CD123-specific chimeric antigen receptors exhibit specific cytolytic effector functions and antitumor effects against human acute myeloid leukemia, *Blood*. 122 (2013) 3138–3148. doi:10.1182/blood-2012-12-474056.The.
- [325] T. Cai, R. Galetto, A. Gouble, J. Smith, A. Cavazos, S. Konoplev, A.A. Lane, M.L. Guzman, H.M. Kantarjian, N. Pemmaraju, M. Konopleva, Pre-Clinical Studies of Anti-CD123 CAR-T Cells for the Treatment of Blastic Plasmacytoid Dendritic Cell Neoplasm (BPDCN), *Blood*. 128 (2016) 4039 LP-4039.  
<http://www.bloodjournal.org/content/128/22/4039.abstract>.
- [326] S.J. Busfield, M. Biondo, M. Wong, H. Ramshaw, E. Lee, S. Ghosh, H. Braley, C. Panousis, A. Roberts, S. He, D. Thomas, L. Fabri, G. Vairo, R. Lock, A. Lopez, A. Nash, Targeting of acute myeloid leukemia in vitro and in vivo with an anti-CD123 mAb engineered for optimal ADCC, (2014) 2213–2221.
- [327] E. Court, Johnson and Johnson Discards Two Hoped-for Billion-Dollar Drugs, (n.d.).  
<https://www.marketwatch.com/story/johnson-johnson-discards-two-hoped-for-billion-dollar-drugs-2017-10-17> (accessed November 29, 2018).
- [328] R.N. Schwartz, L. Stover, J. Dutcher, Managing toxicities of high-dose interleukin-2., *Oncology*. 16 (2002) 11–20.
- [329] G. Phan, P. Attia, S. Steinberg, D. White, S. Rosenberg, Factors Associated With Response to High-Dose Interleukin-2 in Patients With Metastatic Melanoma, *J. Clin. Oncol.* 19 (2001) 3477–3482.
- [330] P. Lui, R. Cashin, M. Machado, M. Hemels, P.K. Corey-Lisle, T.R. Einarson, Treatments for metastatic melanoma: Synthesis of evidence from randomized trials, *Cancer Treat. Rev.* 33 (2007) 665–680. doi:10.1016/j.ctrv.2007.06.004.
- [331] C. Robert, L. Thomas, I. Bondarenko, S. O’Day, J. Weber, C. Garbe, C. Lebbe, J.-F. Baurain, A. Testori, J.-J. Grob, N. Davidson, J. Richards, M. Maio, A. Hauschild, W.H. Miller, P. Gascon, M. Lotem, K. Harmankaya, R. Ibrahim, S. Francis, T.-T. Chen, R.



- Humphrey, A. Hoos, J.D. Wolchok, Ipilimumab plus Dacarbazine for Previously Untreated Metastatic Melanoma, *N. Engl. J. Med.* 364 (2011) 2517–2526. doi:10.1056/NEJMoa1104621.
- [332] S.F. Hodi, S. O’Day, D.F. McDermott, W.J. Urba, Improved Survival with Ipilimumab in Patients with Metastatic Melanoma, *N. Engl. J. Med.* 363 (2010) 711–723.
- [333] P. Castellani, G.L. Viale, A. Dorcaratto, G. Nicolo, J. Kaczmarek, G. Querze, L. Zardi, The fibronectin isoform containing the ED-B oncofetal domain: a marker of angiogenesis, *Int. J. Cancer.* 59 (1994) 612–618.
- [334] J.N. Rybak, C. Roesli, M. Kaspar, A. Villa, D. Neri, The extra-domain A of fibronectin is a vascular marker of solid tumors and metastases, *Cancer Res.* 67 (2007) 10948–10957. doi:10.1158/0008-5472.CAN-07-1436.
- [335] B.M. Tjink, L.R. Perk, M. Budde, M. Stigter-Van Walsum, G.W.M. Visser, R.W. Kloet, L.M. Dinkelborg, C.R. Leemans, D. Neri, G.A.M.S. Van Dongen, 124I-L19-SIP for immuno-PET imaging of tumour vasculature and guidance of 131I-L19-SIP radioimmunotherapy, *Eur. J. Nucl. Med. Mol. Imaging.* 36 (2009) 1235–1244. doi:10.1007/s00259-009-1096-y.
- [336] A. Burnett, M. Wetzler, B. Löwenberg, Therapeutic advances in acute myeloid leukemia, *J. Clin. Oncol.* 29 (2011) 487–494. doi:10.1200/JCO.2010.30.1820.
- [337] V. Strassberger, K.L. Gutbrodt, N. Krall, C. Roesli, H. Takizawa, M.G. Manz, T. Fugmann, D. Neri, ScienceDirect A comprehensive surface proteome analysis of myeloid leukemia cell lines for therapeutic antibody development, *J. Proteomics.* 99 (2014) 138–151. doi:10.1016/j.jprot.2014.01.022.
- [338] S.I.S. Mosely, J.E. Prime, R.C.A. Sainson, J.-O. Koopmann, D.Y.Q. Wang, D.M. Greenawalt, M.J. Ahdesmaki, R. Leyland, S. Mullins, L. Pacelli, D. Marcus, J. Anderton, A. Watkins, J. Coates Ulrichsen, P. Brohawn, B.W. Higgs, M. McCourt, H. Jones, J.A. Harper, M. Morrow, V. Valge-Archer, R. Stewart, S.J. Dovedi, R.W. Wilkinson, Rational selection of syngeneic preclinical tumor models for immunotherapeutic drug discovery, *Cancer Immunol. Res.* 5 (2016) 29–42. doi:10.1158/2326-6066.CIR-16-0114.
- [339] J. Duraiswamy, K.M. Kaluza, G.J. Freeman, G. Coukos, Dual blockade of PD-1 and CTLA-4 combined with tumor vaccine effectively restores T-cell rejection function in tumors, *Cancer Res.* 73 (2013) 3591–3603. doi:10.1158/0008-5472.CAN-12-4100.

- [340] A. Huang, P. Gulden, A. Woods, M. Thomas, C. Tong, W.E.I. Wang, V.H. Engelhardt, G. Pasternack, R. Corrieri, D. Hunt, D.M. Pardoll, E.M. Jaffee, The immunodominant major histocompatibility complex class I-restricted antigen of a murine colon tumor derives from an endogenous retroviral gene product, *Proc. Natl. Acad. Sci.* 93 (1996) 9730–9735.
- [341] C. Becker, H. Pohla, B. Frankenberger, T. Schöler, M. Assenmacher, D.J. Schendel, T. Blankenstein, Adoptive tumor therapy with T lymphocytes enriched through an IFN- $\gamma$  capture assay, *Nat. Med.* 7 (2001) 1159–1162. doi:10.1038/nm1001-1159.
- [342] M.J. Selby, J.J. Engelhardt, R.J. Johnston, L.S. Lu, M. Han, K. Thudium, D. Yao, M. Quigley, J. Valle, C. Wang, B. Chen, P.M. Cardarelli, D. Blanset, A.J. Korman, Preclinical development of ipilimumab and nivolumab combination immunotherapy: Mouse tumor models, In vitro functional studies, and cynomolgus macaque toxicology, *PLoS One.* 11 (2016) 1–19. doi:10.1371/journal.pone.0161779.
- [343] P. Probst, J. Kopp, A. Oxenius, M.P. Colombo, D. Ritz, T. Fugmann, D. Neri, Sarcoma eradication by doxorubicin and targeted TNF relies upon CD8+T-cell recognition of a retroviral antigen, *Cancer Res.* 77 (2017) 3644–3654. doi:10.1158/0008-5472.CAN-16-2946.
- [344] N.D. Huntington, H. Tabarias, K. Fairfax, J. Brady, Y. Hayakawa, M.A. Degli-Esposti, M.J. Smyth, D.M. Tarlinton, S.L. Nutt, NK Cell Maturation and Peripheral Homeostasis Is Associated with KLRG1 Up-Regulation, *J. Immunol.* 178 (2007) 4764–4770. doi:10.4049/jimmunol.178.8.4764.
- [345] M. Silacci, S. Brack, G. Schirru, A. Ettore, A. Merlo, F. Viti, D. Neri, Design , construction , and characterization of a large synthetic human antibody phage display library, (2005) 2340–2350. doi:10.1002/pmic.200401273.
- [346] A. Villa, E. Trachsel, M. Kaspar, C. Schliemann, R. Somavilla, J.N. Rybak, C. R??sli, L. Borsi, D. Neri, A high-affinity human monoclonal antibody specific to the alternatively spliced EDA domain of fibronectin efficiently targets tumor neo-vasculature in vivo, *Int. J. Cancer.* 122 (2008) 2405–2413. doi:10.1002/ijc.23408.
- [347] G.A. Lazar, W. Dang, S. Karki, O. Vafa, J.S. Peng, L. Hyun, C. Chan, H.S. Chung, A. Eivazi, S.C. Yoder, J. Vielmetter, D.F. Carmichael, R.J. Hayes, B.I. Dahiyat, Engineered antibody Fc variants with enhanced effector function, *Proc. Natl. Acad. Sci.* 103 (2006) 4005–4010. doi:10.1073/pnas.0508123103.

- [348] A. Pini, F. Viti, A. Santucci, B. Carnemolla, L. Zardi, P. Neri, D. Neri, Design and Use of a Phage Display Library, *J. Biol. Chem.* 273 (1998) 21769–21776.
- [349] S.E. Broughton, T.R. Hercus, M.P. Hardy, B.J. McClure, T.L. Nero, M. Dottore, H. Huynh, H. Braley, E.F. Barry, W.L. Kan, U. Dhagat, P. Scotney, D. Hartman, S.J. Busfield, C.M. Owczarek, A.D. Nash, N.J. Wilson, M.W. Parker, A.F. Lopez, Dual Mechanism of Interleukin-3 Receptor Blockade by an Anti-Cancer Antibody, *Cell Rep.* 8 (2014) 410–419. doi:10.1016/j.celrep.2014.06.038.
- [350] R. Frank, The SPOT-synthesis technique: Synthetic peptide arrays on membrane supports - Principles and applications, *J. Immunol. Methods.* 267 (2002) 13–26. doi:10.1016/S0022-1759(02)00137-0.
- [351] S.E. Broughton, T.R. Hercus, T.L. Nero, W.L. Kan, E.F. Barry, M. Dottore, K.S. Cheung Tung Shing, C.J. Morton, U. Dhagat, M.P. Hardy, N.J. Wilson, M.T. Downton, C. Schieber, T.P. Hughes, A.F. Lopez, M.W. Parker, A dual role for the N-terminal domain of the IL-3 receptor in cell signalling, *Nat. Commun.* 9 (2018) 1–15. doi:10.1038/s41467-017-02633-7.
- [352] P.A. Prieto, J.C. Yang, R.M. Sherry, M.S. Hughes, U.S. Kammula, D.E. White, C.L. Levy, S.A. Rosenberg, G.Q. Phan, CTLA-4 blockade with ipilimumab: Long-term follow-up of 177 patients with metastatic melanoma, *Clin. Cancer Res.* 18 (2012) 2039–2047. doi:10.1158/1078-0432.CCR-11-1823.
- [353] A. Maker, G. Phan, P. Attia, J. Yang, S.A. Rosenberg, Tumor Regression and Autoimmunity in Patients Treated With Cytotoxic T Lymphocyte-Associated Antigen 4 Blockade and Interleukin 2: A Phase I/ II Study, *Ann. Surg. Oncol.* 12 (2005) 1005–1016.
- [354] S.A. Quezada, K.S. Peggs, M.A. Curran, J.P. Allison, CTLA4 blockade and GM-CSF combination immunotherapy alters the intratumor balance of effector and regulatory T cells, *J. Clin. Invest.* 116 (2006) 1935–1945. doi:10.1172/JCI27745.
- [355] T.R. Simpson, F. Li, W. Montalvo-ortiz, M.A. Sepulveda, K. Bergerhoff, F. Arce, C. Roddie, J.Y. Henry, H. Yagita, J.D. Wolchok, K.S. Peggs, V. Jeffrey, J.P. Allison, S.A. Quezada, Fc-dependent depletion of tumor-infiltrating regulatory T cells co-defines the efficacy of anti – CTLA-4 therapy against melanoma, *J. Clin. Invest.* 123 (2013) 1695–1710. doi:10.1084/jem.20130579.
- [356] F. Arce Vargas, A.J.S. Furness, K. Litchfield, K. Joshi, R. Rosenthal, E. Ghorani, I.

Solomon, M.H. Lesko, N. Ruef, C. Roddie, J.Y. Henry, L. Spain, A. Ben Aissa, A. Georgiou, Y.N.S. Wong, M. Smith, D. Strauss, A. Hayes, D. Nicol, T. O'Brien, L. Mårtensson, A. Ljungars, I. Teige, B. Freundés, K. Harrington, A. Melcher, A. Wotherspoon, N. Francis, B. Challacombe, A. Fernando, S. Hazell, A. Chandra, L. Pickering, J. Lynch, S. Rudman, S. Chowdhury, K. Harrison-Phipps, M. Varia, C. Horsfield, A. Polson, G. Stamp, M. O'Donnell, W. Drake, P. Hill, D. Hrouda, E. Mayer, J. Olsburgh, G. Kooiman, K. O'Connor, G. Stewart, M. Aitchison, M. Tran, N. Fotiadis, H. Verma, J. Lopez, J. Lester, F. Morgan, M. Kornaszewska, R. Attanoos, H. Adams, H. Davies, D. Fennell, J. Shaw, J. Le Quesne, A. Nakas, S. Rathinam, W. Monteiro, H. Marshall, L. Nelson, J. Bennett, J. Riley, L. Primrose, L. Martinson, G. Anand, S. Khan, M. Nicolson, K. Kerr, S. Palmer, H. Remmen, J. Miller, K. Buchan, M. Chetty, L. Gomersall, S. Lock, B. Naidu, G. Langman, S. Trotter, M. Bellamy, H. Bancroft, A. Kerr, S. Kadiri, J. Webb, G. Middleton, M. Djearaman, Y. Summers, R. Califano, P. Taylor, R. Shah, P. Krysiak, K. Rammohan, E. Fontaine, R. Booton, M. Evison, P. Crosbie, S. Moss, F. Idries, J. Novasio, L. Joseph, P. Bishop, A. Chaturvedi, A. Marie Quinn, H. Doran, A. leek, P. Harrison, K. Moore, R. Waddington, F. Blackhall, J. Rogan, E. Smith, C. Dive, G. Brady, D. Rothwell, S. Gulati, F. Chemie, J. Tugwood, J. Pierce, D. Lawrence, M. Hayward, N. Panagiotopoulos, R. George, D. Patrini, M. Falzon, E. Borg, R. Khiroya, M. Jamal-Hanjani, G. Wilson, N. Juul Birkbak, T. Watkins, N. McGranahan, C. Abbosh, S. Horswell, R. Mitter, M. Escudero, A. Stewart, A. Rowan, C. Hiley, J. Goldman, A. Ahmed, M. Taylor, J. Choudhary, P. Shaw, R. Veeriah, J. Czyzewska-Khan, D. Johnson, J. Laycock, R. Hynds, M. Werner Sunderland, J. Reading, M. Novelli, D. Oukrif, S. Janes, M. Forster, T. Ahmad, S. Ming Lee, P. van Loo, J. Herrero, J. Hartley, R. Kevin Stone, T. Denner, M. Costa, S. Begum, B. Phillimore, T. Chambers, E. Nye, S. Ward, G. Elgar, M. Al-Bakir, D. Carnell, R. Mendes, J. George, N. Navani, D. Papadatos-Pastos, M. Scarci, P. Gorman, H. Lowe, L. Ensell, D. Moore, M. MacKenzie, M. Wilcox, H. Bell, A. Hackshaw, Y. Ngai, S. Smith, N. Gower, C. Ottensmeier, S. Chee, B. Johnson, A. Alzetani, E. Shaw, E. Lim, P. De Sousa, M. Tavares Barbosa, A. Nicholson, A. Bowman, S. Jordan, A. Rice, H. Raubenheimer, C. Proli, M. Elena Cufari, J. Carlo Ronquillo, A. Kwayie, H. Bhayani, M. Hamilton, Y. Bakar, N. Mensah, L. Ambrose, A. Devaraj, S. Buder, J. Finch, L. Azcarate, H. Chavan, S. Green, H. Mashinga, K. Lau, M. Sheaff, P. Schmid, J. Conibear, V. Ezhil, V. Prakash, S. Danson, J. Bury, J. Edwards, J. Hill, S.

- Matthews, Y. Kitsanta, K. Suvarna, M. Shackcloth, J. Gosney, P. Postmus, S. Feeney, J. Asante-Siaw, P. Russell, T. Light, T. Horey, K. Blyth, C. Dick, A. Kirk, M. Pule, T. Marafioti, M. Gore, J. Larkin, S. Turajlic, C. Swanton, K.S. Peggs, S.A. Quezada, Fc Effector Function Contributes to the Activity of Human Anti-CTLA-4 Antibodies, *Cancer Cell*. 33 (2018) 649–663.e4. doi:10.1016/j.ccell.2018.02.010.
- [357] M.J. Selby, J.J. Engelhardt, M. Quigley, K.A. Henning, T. Chen, M. Srinivasan, A.J. Korman, Anti-CTLA-4 Antibodies of IgG2a Isotype Enhance Antitumor Activity through Reduction of Intratumoral Regulatory T Cells, *Cancer Immunol. Res.* 1 (2013) 32–42. doi:10.1158/2326-6066.CIR-13-0013.
- [358] J. Schachter, A. Ribas, G. V. Long, A. Arance, J.J. Grob, L. Mortier, A. Daud, M.S. Carlino, C. McNeil, M. Lotem, J. Larkin, P. Lorigan, B. Neyns, C. Blank, T.M. Petrella, O. Hamid, H. Zhou, S. Ebbinghaus, N. Ibrahim, C. Robert, Pembrolizumab versus ipilimumab for advanced melanoma: final overall survival results of a multicentre, randomised, open-label phase 3 study (KEYNOTE-006), *Lancet*. 390 (2017) 1853–1862. doi:10.1016/S0140-6736(17)31601-X.
- [359] J. Duraiswamy, K.M. Kaluza, G.J. Freeman, G. Coukos, Dual Blockade of PD-1 and CTLA-4 Combined with Tumor Vaccine Effectively Restores T-Cell Rejection Function in Tumors, *Cancer Res.* 73 (2013) 3591–3603. doi:10.1158/0008-5472.CAN-12-4100.
- [360] D. Neri, P.M. Sondel, ScienceDirect Immunocytokines for cancer treatment : past , present and future, *Curr. Opin. Immunol.* 40 (2016) 96–102. doi:10.1016/j.coi.2016.03.006.
- [361] B. Weide, E. Derhovanessian, A. Pflugfelder, T.K. Eigentler, P. Radny, H. Zelba, C. Pföhler, G. Pawelec, C. Garbe, High response rate after intratumoral treatment with interleukin-2: results from a phase 2 study in 51 patients with metastasized melanoma., *Cancer*. 116 (2010) 4139–46. doi:10.1002/cncr.25156.
- [362] S. Bobisse, R. Genolet, A. Roberti, J.L. Tanyi, J. Racle, B.J. Stevenson, C. Iseli, A. Michel, M.A. Le Bitoux, P. Guillaume, J. Schmidt, V. Bianchi, D. Dangaj, C. Fenwick, L. Derré, I. Xenarios, O. Michielin, P. Romero, D.S. Monos, V. Zoete, D. Gfeller, L.E. Kandalaft, G. Coukos, A. Harari, Sensitive and frequent identification of high avidity neo-epitope specific CD8+T cells in immunotherapy-naïve ovarian cancer, *Nat. Commun.* 9 (2018) 1–10. doi:10.1038/s41467-018-03301-0.
- [363] D.A. Wick, J.R. Webb, J.S. Nielsen, S.D. Martin, D.R. Kroeger, K. Milne, M. Castellarin,

- K. Twumasi-Boateng, P.H. Watson, R.A. Holt, B.H. Nelson, Surveillance of the tumor mutanome by T cells during progression from primary to recurrent ovarian cancer, *Clin. Cancer Res.* 20 (2014) 1125–1134. doi:10.1158/1078-0432.CCR-13-2147.
- [364] F. Perna, S.H. Berman, R.K. Soni, J. Mansilla-Soto, J. Eyquem, M. Hamieh, R.C. Hendrickson, C.W. Brennan, M. Sadelain, Integrating Proteomics and Transcriptomics for Systematic Combinatorial Chimeric Antigen Receptor Therapy of AML, *Cancer Cell.* 32 (2017) 506–519.e5. doi:10.1016/j.ccell.2017.09.004.
- [365] V. Strassberger, K.L. Gutbrodt, N. Krall, C. Roesli, H. Takizawa, M.G. Manz, T. Fugmann, D. Neri, A comprehensive surface proteome analysis of myeloid leukemia cell lines for therapeutic antibody development, *J. Proteomics.* 99 (2014) 138–151. doi:10.1016/j.jprot.2014.01.022.
- [366] A. Hofmann, B. Gerrits, A. Schmidt, T. Bock, D. Bausch-Fluck, R. Aebersold, B. Wollscheid, Proteomic cell surface phenotyping of differentiating acute myeloid leukemia cells, *Blood.* 116 (2010) 1–3. doi:10.1182/blood-2010-02-271270.
- [367] D.M. Schewe, A. Alsadeq, C. Sattler, L. Lenk, F. Vogiatzi, G. Cario, S. Vieth, T. Valerius, S. Roskopf, F. Meyersieck, J. Alten, M. Schrappe, M. Gramatzki, M. Peipp, C. Kellner, An Fc-engineered CD19 antibody eradicates MRD in patient-derived MLL-rearranged acute lymphoblastic leukemia xenografts, *Blood.* 130 (2017) 1543–1552. doi:10.1182/blood-2017-01-764316.
- [368] L. Bologna, M. Introna, C. Ferrara, A. Rambaldi, F. Da Roit, J.H. Leusen, J. Golay, C. Klein, Glycoengineered CD20 antibody obinutuzumab activates neutrophils and mediates phagocytosis through CD16B more efficiently than rituximab, *Blood.* 122 (2013) 3482–3491. doi:10.1182/blood-2013-05-504043.
- [369] J. Li, N.J. Stagg, J. Johnston, M.J. Harris, S.A. Menzies, D. DiCara, V. Clark, M. Hristopoulos, R. Cook, D. Slaga, R. Nakamura, L. McCarty, S. Sukumaran, E. Luis, Z. Ye, T.D. Wu, T. Sumiyoshi, D. Danilenko, G.Y. Lee, K. Totpal, D. Ellerman, I. Hötzel, J.R. James, T.T. Junttila, Membrane-Proximal Epitope Facilitates Efficient T Cell Synapse Formation by Anti-FcRH5/CD3 and Is a Requirement for Myeloma Cell Killing, *Cancer Cell.* 31 (2017) 383–395. doi:10.1016/j.ccell.2017.02.001.
- [370] R.E. Kontermann, U. Brinkmann, Bispecific Antibodies, *Drug Discov. Today.* 1–4 (2015) 265–310. doi:10.1002/9783527682423.ch11.
- [371] A. Manuscript, P. Onlinefirst, Antibody-based delivery of TNF to the tumor neo-

- vasculature potentiates the therapeutic activity of a peptide anti-cancer vaccine  
Philipp Probst, (2018) 1–28. doi:10.1158/1078-0432.CCR-18-1728.
- [372] F. Li, M.K. Sutherland, C. Yu, R.B. Walter, L. Westendorf, J. Valliere-Douglass, L. Pan, A. Cronkite, D. Sussman, K. Klussman, M. Ulrich, M.E. Anderson, I.J. Stone, W. Zeng, M. Jonas, T.S. Lewis, M. Goswami, S.A. Wang, P.D. Senter, C.-L. Law, E.J. Feldman, D.R. Benjamin, Characterization of SGN-CD123A, A Potent CD123-Directed Antibody–Drug Conjugate for Acute Myeloid Leukemia, *Mol. Cancer Ther.* 17 (2018) 554–564. doi:10.1158/1535-7163.MCT-17-0742.
- [373] R.E. Kontermann, Half-life extended biotherapeutics, *Expert Opin. Biol. Ther.* 16 (2016) 903–915. doi:10.1517/14712598.2016.1165661.
- [374] M. Schlapschy, U. Binder, C. Börger, I. Theobald, K. Wachinger, S. Kisling, D. Haller, A. Skerra, PASylation: A biological alternative to PEGylation for extending the plasma half-life of pharmaceutically active proteins, *Protein Eng. Des. Sel.* 26 (2013) 489–501. doi:10.1093/protein/gzt023.
- [375] V. Schellenberger, C.W. Wang, N.C. Geething, B.J. Spink, A. Campbell, W. To, M.D. Scholle, Y. Yin, Y. Yao, O. Bogin, J.L. Cleland, J. Silverman, W.P.C. Stemmer, A recombinant polypeptide extends the in vivo half-life of peptides and proteins in a tunable manner, *Nat. Biotechnol.* 27 (2009) 1186–1190. doi:10.1038/nbt.1588.
- [376] M. Nowicka, C. Krieg, L.M. Weber, F.J. Hartmann, S. Guglietta, B. Becher, M.P. Levesque, M.D. Robinson, CyTOF workflow: differential discovery in high-throughput high-dimensional cytometry datasets, *F1000Research.* 6 (2017) 748. doi:10.12688/f1000research.11622.1.
- [377] R. Myburgh, O. Cherpin, E. Schlaepfer, H. Rehrauer, R.F. Speck, K.H. Krause, P. Salmon, Optimization of critical hairpin features allows miRNA-based gene knockdown upon single-copy transduction, *Mol. Ther. - Nucleic Acids.* 3 (2014) e207. doi:10.1038/mtna.2014.58.
- [378] D.L. Hacker, D. Kiseljak, Y. Rajendra, S. Thurnheer, L. Baldi, F.M. Wurm, Polyethyleneimine-based transient gene expression processes for suspension-adapted HEK-293E and CHO-DG44 cells, *Protein Expr. Purif.* 92 (2013) 67–76. doi:10.1016/j.pep.2013.09.001.
- [379] M. Yamashita, S. Kitano, H. Aikawa, A. Kuchiba, M. Hayashi, N. Yamamoto, K. Tamura, A. Hamada, A novel method for evaluating antibody-dependent cell-mediated

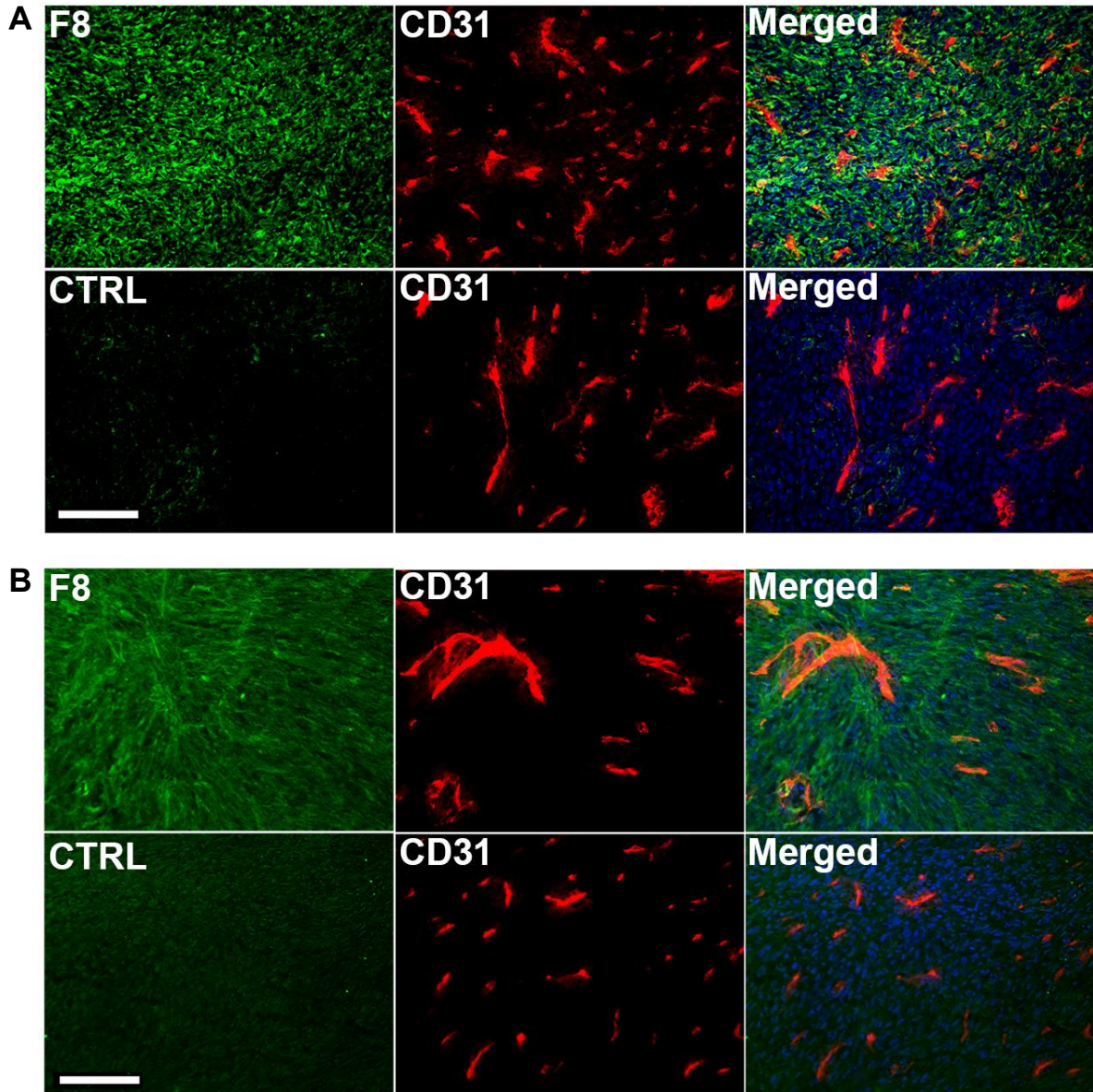
cytotoxicity by flowcytometry using cryopreserved human peripheral blood mononuclear cells, *Sci. Rep.* 6 (2016) 1–10. doi:10.1038/srep19772.



## 13. Supplementary Information

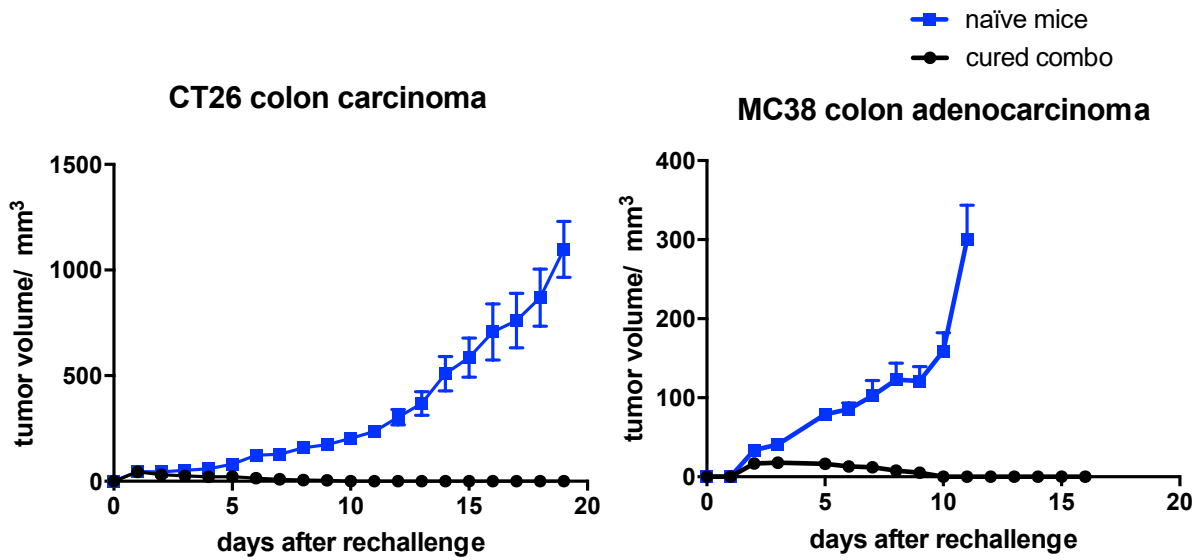
### 13.1. F8-IL2 in combination with immune check-point inhibitors

#### 13.1.1. Microscopic analysis of EDA expression (green) on CT26 colon carcinoma



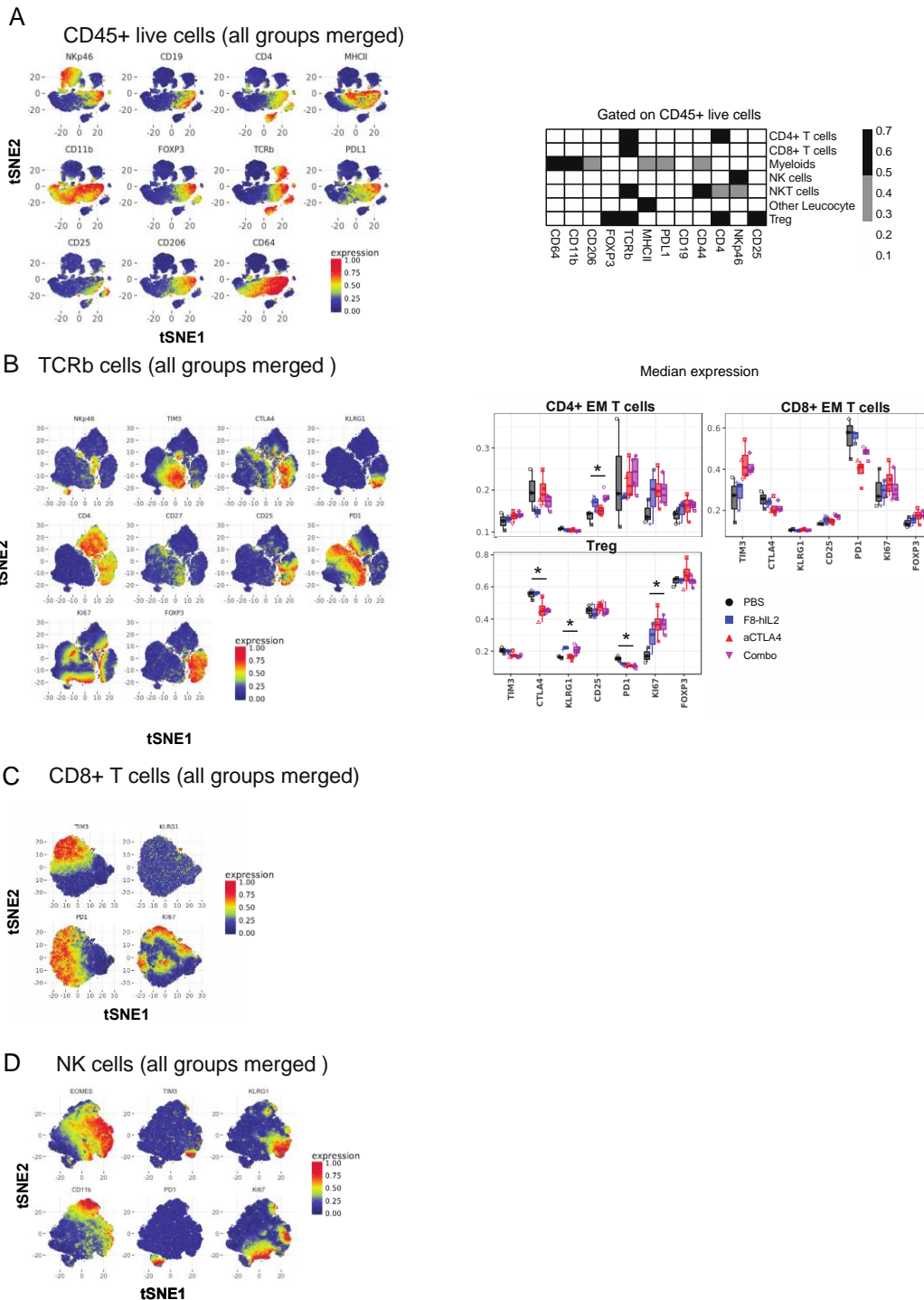
**Suppl. Figure 1:** (A) and MC38 colon carcinoma (B) using the F8 antibody. The KSF antibody (directed against an irrelevant antigen) was used as negative control (CTRL). An anti CD31 antibody was used to stain tumor vessels (red). Scale bar = 100  $\mu\text{m}$ .

### 13.1.2. Rechallenge tumor studies



**Suppl. Figure 2:** All cured mice from the therapy studies were rechallenged with either  $2 \times 10^6$  CT26 colon carcinoma cells or  $1 \times 10^6$  MC38 cells on day 0 and monitored for tumor growth (black curve). Naïve mice were used as control group (blue curve). All cured mice were able to reject the tumor cells whereas in naïve mice, the tumors grew steadily.

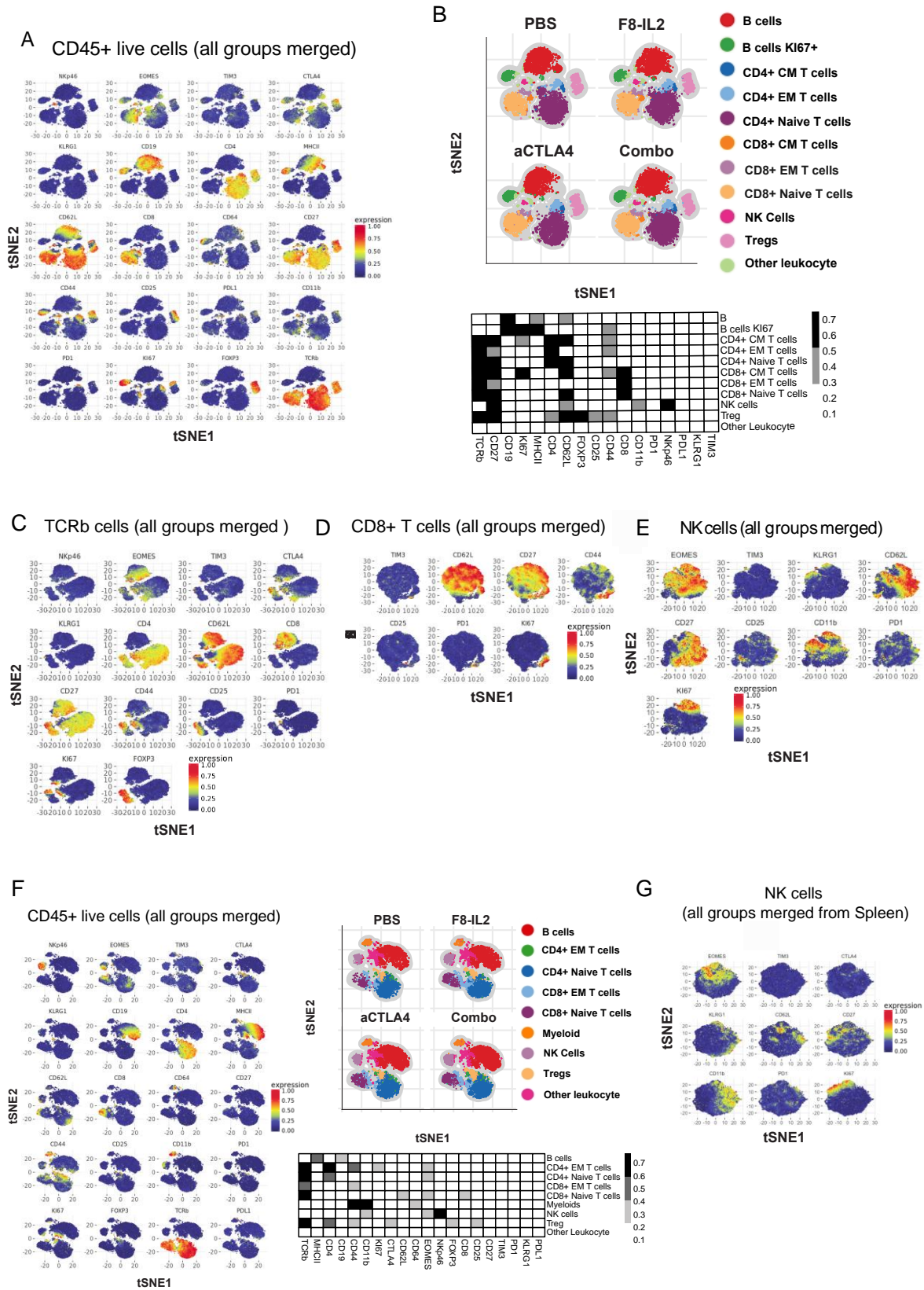
### 13.1.3. Multiparameter flowcytometric analysis of CT26 tumor immune cell infiltrates



**Suppl. Figure 3:** CT26 tumors were stained with fluorochrome-conjugated antibodies. (A) t-SNE map displaying stochastically selected live CD45+ cells (left) and heat map showing the median marker expression (value range: 0-1, black and white) for each defined population of **Figure 13A** from all conditions. (B) t-SNE map displaying stochastically selected TCRb+ cells (left) and median expression of selected cell markers shown for T cell subpopulations in each treatment (right). (C) t-SNE map displaying stochastically selected CD8+ T cells from all conditions. (D) t-SNE map displaying stochastically selected NK+ cells from all conditions. \*,  $p < 0.05$ , \*\*,  $p < 0.01$ , \*\*\*,  $p < 0.001$

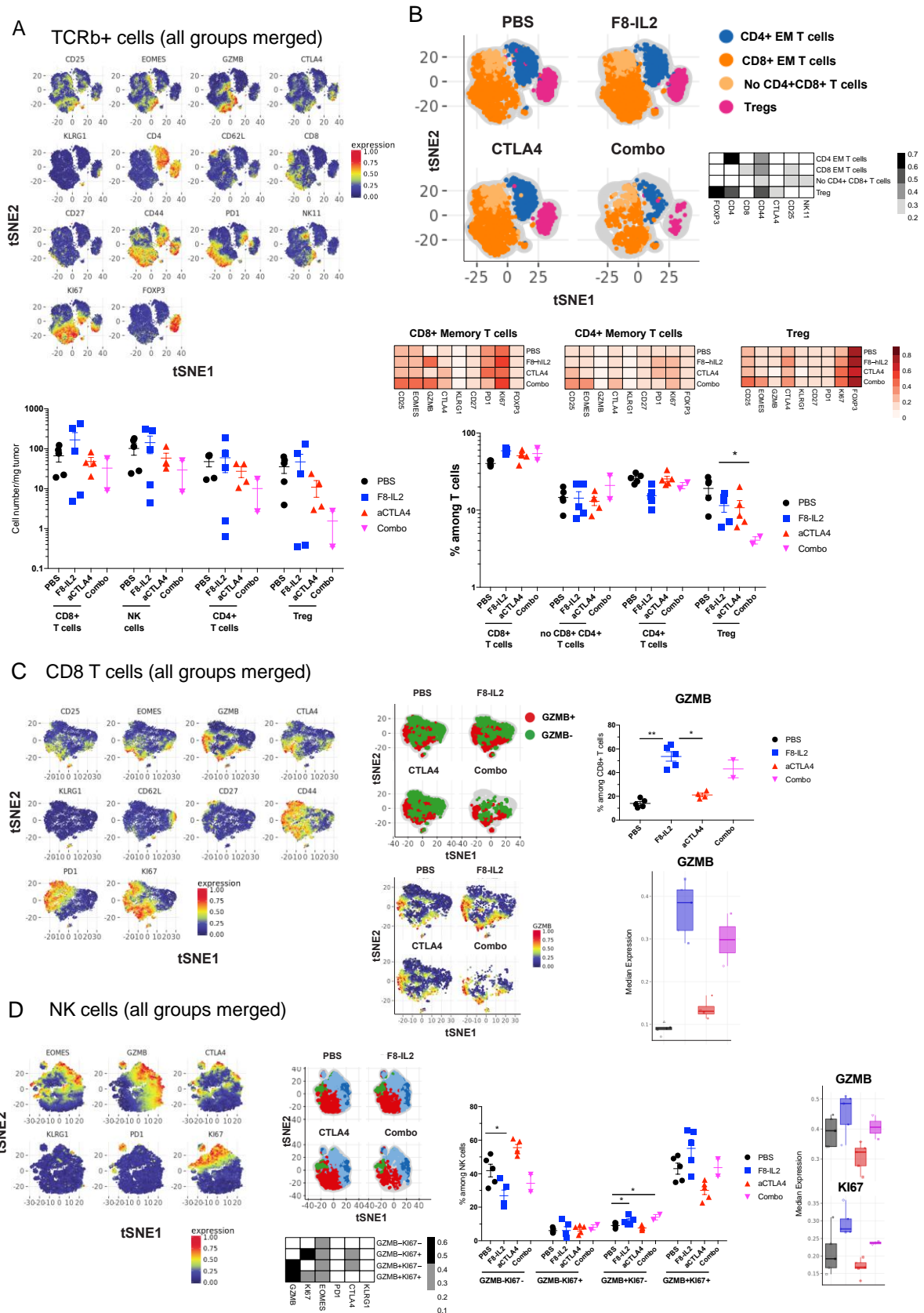


13.1.4. Multiparameter flowcytometric analysis of lymph nodes and intrasplenic immune cell infiltrates of CT26 colon carcinoma bearing mice.



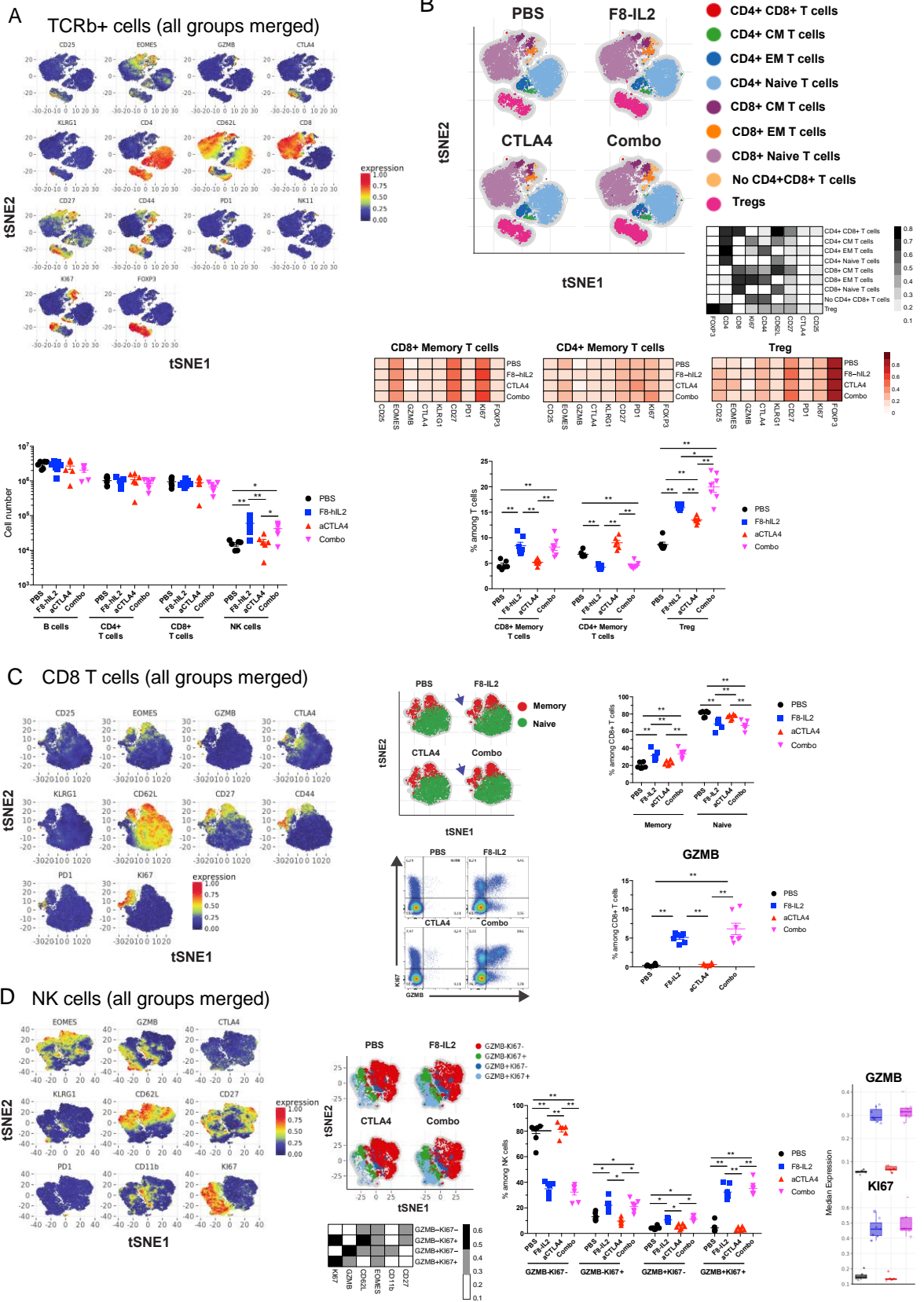
**Suppl. Figure 4:** CT26 tumor draining lymph nodes were stained with fluorochrome-conjugated antibodies. (A) t-SNE map displaying stochastically selected live CD45+ cells from all lymph nodes. (B) t-SNE map showing the FlowSOM-guided meta-clustering gated on CD45+ cells (upper panel) and heat map showing the median marker expression (value range: 0-1, black and white) for each defined population from the lymph node (lower panel). (C) t-SNE map displaying stochastically selected TCRb+ cells, (D) selected CD8+ T cells and (E) selected NK cells from all lymph nodes. (F-G) Splenocytes from mice bearing CT26 tumors were stained with fluorochrome-conjugated antibodies. (F) t-SNE map displaying stochastically selected live CD45+ cells from the spleen (left). (F, right) t-SNE map showing the FlowSOM-guided meta-clustering gated on CD45+ cells (upper panel) and heat map showing the median marker expression (black and white) for each defined population from the spleen (lower panel). (G) t-SNE map displaying stochastically selected NK cells from the spleen.

### 13.1.5. Multiparameter flowcytometric analysis of MC38 tumor immune cell infiltrates



**Suppl. Figure 5:** MC38 tumors were stained with fluorochrome-conjugated antibodies. (A) t-SNE map displaying stochastically selected TCRb<sup>+</sup> cells (upper panel) and frequencies of the four Tcrb<sup>+</sup> cell subclusters among total T cells within the different conditions (bottom, pooled data from 2 independent experiments). (B) t-SNE map showing the FlowSOM-guided meta-clustering of TCRb<sup>+</sup> cells in the different treatment groups (upper panel) and heat map showing the median marker expression for each defined population from all conditions (lower panel). (C) t-SNE map displaying stochastically selected CD8<sup>+</sup> T cells (left) and the FlowSOM-guided meta-clustering in the different treatment groups (middle). Frequencies (upper right) of GZMB<sup>+</sup> staining among CD8<sup>+</sup> T cells and median expression of GZMB (lower right) within the different conditions. (D) t-SNE map displaying stochastically selected NK cells (NK1.1<sup>+</sup> TCRb<sup>-</sup>, left), t-SNE map displaying the FlowSOM-guided meta-clustering of NK cells in the different treatment groups (middle left) and heat map showing the median marker expression (middle lower panel). Frequencies (middle right) of the four NK cell subclusters among total NK cells and median expression (right) of GZMB and Ki67 within the different conditions are displayed as well. \*,  $p < 0.05$ , \*\*,  $p < 0.01$ , \*\*\*,  $p < 0.001$

### 13.1.6. Multiparameter flowcytometric analysis of lymph node immune cell infiltrates of MC38 colon carcinoma bearing mice





**Suppl. Figure 6: Multiparameter flowcytometric analysis of lymph node immune cell infiltrates.** MC38 tumor draining lymph nodes were stained with fluorochrome-conjugated antibodies. (A) t-SNE map displaying stochastically selected TCRb+ cells (upper panel) and quantification (cell number) of live intratumoral CD45+ cell clusters in the different treatment groups (lower panel). (B) t-SNE map showing the FlowSOM-guided metaclustering of TCRb+ cells in the different treatment groups (upper panel), heat map (middle panel) showing the median marker expression and frequency (lower panel) for selected population from all conditions. (C) t-SNE map displaying stochastically selected CD8+ T cells (left), the FlowSOM-guided meta-clustering in the different treatment groups (middle) and frequencies of each defined population within the treatment group (right upper panel). Representative flow cytometric analysis of GZMB and Ki67 frequencies of GZMB+ staining among CD8+ T cells within the different conditions (right lower panel). (D) t-SNE map displaying stochastically selected NK cells (NK1.1+ TCRb-, left), t-SNE map displaying the FlowSOM-guided meta-clustering of NK cells in the different treatment groups (middle left) and heat map showing the median marker expression (middle lower panel). Frequencies (middle right) the four NK cell subclusters among total NK cells and median expression (right) of GZMB and Ki67 within the different conditions are displayed as well. n= 6 mice per group, \*, p < 0.05, \*\*, p < 0.01, \*\*\*, p < 0.001

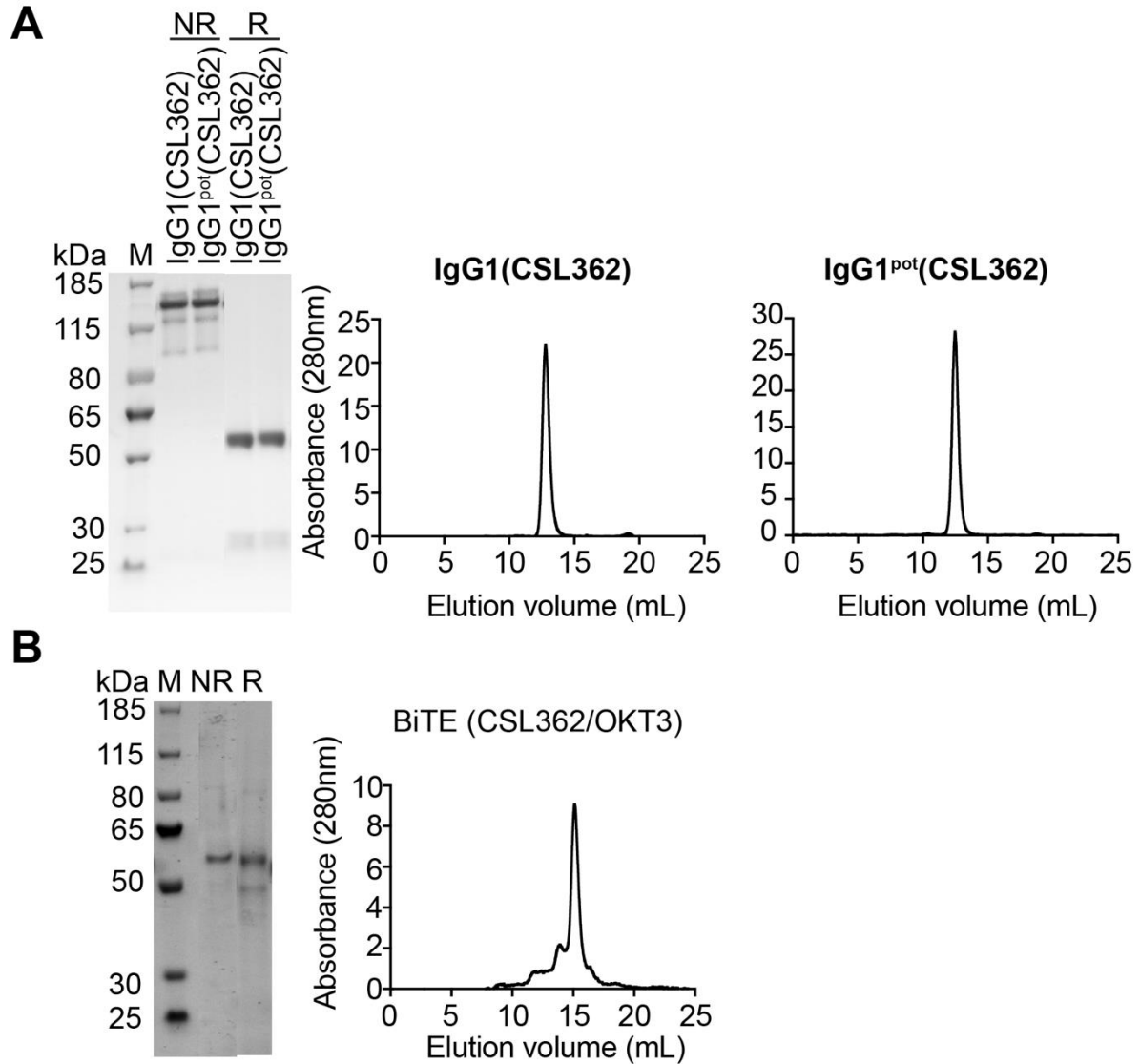
13.1.7. Antibody clone list

**Suppl. Table 1:** Clone list of all antibodies that were used for the single cell analysis

Antigens	Clones	Fluorochromes	Isotypes	Manufacturers
CD19	6D5	Biotin	rat IgG2a	BD PharmingenTM
CD45	30-F11	BUV 395	rat IgG2b	BD PharmingenTM
CD8	53-6.7	BUV 805	rat IgG2a	BD PharmingenTM
CD4	GK1.5	BUV 496	rat IgG2b	BD PharmingenTM
I-A/I-E	M5/114.15.2	BUV 661	rat IgG2b	BD PharmingenTM
CD62L	MEL-14	BUV 737	rat IgG2a	BD PharmingenTM
NKp46	29A1.4	FITC	rat IgG2a	Thermo Fisher Scientific
NK1.1	PK136	BV785	mouse IgG2a	BioLegendTM
CD64	X54-5/7.1	BV 421	mouse IgG1	BioLegendTM
CD27	LG3A10	BV 480	armenian hamster IgG1	BD PharmingenTM
CD44	IM7	BV 570	rat IgG2b	BioLegendTM
CD25	PC61	AlexaFlour 488	rat IgG1	BioLegendTM
CD206	C068C2	BV 650	rat IgG2a	BioLegendTM
CD11B	M1/70	BV 711	rat IgG2b	BioLegendTM
PD-1	29F.1A12	BV 785	rat IgG2a	BD PharmingenTM
PD-1	J43	BV 605	armenian hamster IgG2	BD PharmingenTM
TCRb	H57-597	PE-Cy5	armenian hamster IgG1	BioLegendTM
PD-L1	MIH5	PE-Cy7	rat IgG2a	Thermo Fisher Scientific
KLRG1	2F1/KLRG1	APC-C7	armenian hamster IgG1	BioLegendTM
TIM3	B8.2C12	AlexaFlour 647	rat IgG1	BioLegendTM
Streptavidin		BUV395		BD PharmingenTM
Streptavidin		BUV563		BD PharmingenTM
<b>INTRACELLULAR</b>				
Antigens	Clones	Fluorochromes	Isotypes	Manufacturers
KI-67	B56	PE	mouse IgG1	BioLegendTM
EOMES	Dan11mag	PerCP-eFlour710	rat IgG2a	Thermo Fisher Scientific
FOXP3	FJK-16s	PE-eFlour610	rat IgG2a	Thermo Fisher Scientific
GZMB	GB11	AlexaFlour 647	mouse IgG1	BD PharmingenTM
CTLA4	UC10-4F10-11	APC-AR700	armenian hamster IgG1	BD PharmingenTM
LIVE/DEAD Fixable Aqua				Life TechnologiesTM

13.2. Development of a novel fully-human anti-CD123 antibody to target acute myeloid leukemia

13.2.1. Expression and characterization of IgG1(CSL362), IgG1<sup>pot</sup>(CSL362) and BiTE(CSL362/OKT3)



**Suppl. Figure 7:** (A) SDS-PAGE and size exclusion chromatography profile of IgG1(CSL362) and IgG1<sup>pot</sup>(CSL362). (B) SDS-PAGE and size exclusion chromatography profile of BiTE(CSL362/OKT3). M= Marker, NR= non-reducing, R= reducing conditions.

13.2.2. Sequences of the parental anti CD123 scFv with the highest ELISA signal derived from phage display, the affinity matured scFv(H9), the IgG1(H9) and the IgG1<sup>pot</sup>(H9) heavy and light chains

**Parental scFv**

EVQLLESGGGLVQPGGSLRLSCAASGFTFSSYAMSWVRQAPGKGLEWVSAISGSGGSTYYADSVKGRFTI  
ISRDNSKNTLYLQMNSLRAEDTAVYYCAKTWQFFDYWGQGLTVTVSSGGGGSGGGGSGGGGGEIVLTQ  
SPGTLSPGERATLSCRASQSVSSHLAWYQQKPGQAPRLLIYGASSRATGIPDRFSGSGSGTDFTLTISR  
LEPEDFAVYYCQQSGKRPTFGQGTKVEIKAAAEQKLISEEDL

**Affinity matured scFv(H9)**

EVQLLESGGGLVQPGGSLRLSCAASGFTFSLYSMSWVRQAPGKGLEWVSAISGSGGSTYYADSVKGRFTI  
SRDNSKNTLYLQMNSLRAEDTAVYYCAKTWQFFDYWGQGLTVTVSSGGGGSGGGGSGGGGGEIVLTQS  
PGTSLSPGERATLSCRASQSVPERLAWYQQKPGQAPRLLIYGASSRATGIPDRFSGSGSGTDFTLTISR  
EPEDFAVYYCQQSGKRPTFGQGTKVEIKAAAEQKLISEEDL

**IgG1(H9) heavy chain**

EVQLLESGGGLVQPGGSLRLSCAASGFTFSLYSMSWVRQAPGKGLEWVSAISGSGGSTYYADSVKGRFTI  
SRDNSKNTLYLQMNSLRAEDTAVYYCAKTWQFFDYWGQGLTVTVSSASTKGPSVFPLAPSSKSTSGGTA  
ALGCLVKDYFPEPVTVSWNSGALTSGVHTFPAVLQSSGLYSLSSVTVPSSSLGTQTYICNVNHKPSNTKV  
DKKVEPKSCDKTHTCPPCPAPELLGGPSVFLFPPKPKDTLMISRTPEVTCVVDVSHEDPEVKFNWYVDG  
VEVHNAKTKPREEQYNSTYRVVSVLTVLHQDWLNGKEYKCKVSNKALPAPIEKTISKAKGQPREPQVYTL  
PPSRDELTKNQVSLTCLVKGFYPSDIAVEWESNGQPENNYKTPPVLDSDGSFFLYSKLTVDKSRWQQG  
NVFSCSVMH~~EA~~LHNHYTQKSLSLSPGK

**IgG1(H9) and IgG1<sup>pot</sup>(H9) light chain**

EIVLTQSPGTLSPGERATLSCRASQSVPERLAWYQQKPGQAPRLLIYGASSRATGIPDRFSGSGSGTDF  
TLTISRLEPEDFAVYYCQQSGKRPTFGQGTKVEIKRTVAAPSVFIFPPSDEQLKSGTASVCLLNNFYPRE  
AKVQWKVDNALQSGNSQESVTEQDSKDYSLSTLTLSKADYEKHKVYACEVTHQGLSSPVTKSFNRG  
EC

**IgG1<sup>pot</sup>(H9) heavy chain**

EVQLLESGGGLVQPGGSLRLSCAASGFTFSLYSMSWVRQAPGKGLEWVSAISGSGGSTYYADSVKGRFTI  
SRDNSKNTLYLQMNSLRAEDTAVYYCAKTWQFFDYWGQGLTVTVSSASTKGPSVFPLAPSSKSTSGGTA  
ALGCLVKDYFPEPVTVSWNSGALTSGVHTFPAVLQSSGLYSLSSVTVPSSSLGTQTYICNVNHKPSNTKV  
DKKVEPKSCDKTHTCPPCPAPELLGGPDVFLFPPKPKDTLMISRTPEVTCVVDVSHEDPEVKFNWYVD  
GVEVHNAKTKPREEQYNSTYRVVSVLTVLHQDWLNGKEYKCKVSNKALPAPEEKISKAKGQPREPQVY  
TLPPSRDELTKNQVSLTCLVKGFYPSDIAVEWESNGQPENNYKTPPVLDSDGSFFLYSKLTVDKSRWQQ  
GNVFC~~SV~~MHEALHNHYTQKSLSLSPGK

**BiTE (H9/OKT3)**

EIVLTQSPGTLSPGERATLSCRASQSVPERLAWYQQKPGQAPRLLIYGASSRATGIPDRFSGSGSGTDF  
TLTISRLEPEDFAVYYCQQSGKRPTFGQGTKVEIK  
GGGGSGGGGSGGGGSEVQLLESGGGLVQPGGSLRLSCAASGFTFSLYSMSWVRQAPGKGLEWVSAIS  
GSGGSTYYADSVKGRFTISRDNKNTLYLQMNSLRAEDTAVYYCAKTWQFFDYWGQGLTVTVSSGGGG  
SDIKLQQSGAELARPGASVKMSCKTSGYTFTRYTMHWVKQRPQGQGLEWIGYINPSRGYTNYNQKFKDK  
ATLTTDKSSSTAYMQLSSLTSEDSAVYYCARYYDDHYCLDYWGQGTTLTVSSVEGGSGGGSGGGSGGGV

DDIQLTQSPAIMSASPGEKVTMTCRASSSVSYMNWYQQKSGTSPKRWIYDTSKVASGVPYRFSGSGSG  
TSYSLTISSMEAEDAATYYCQQWSSNPLTFGAGTKLELK

**Suppl. Figure 8:** *Underlined amino acids, also presented in italics, correspond to key residues within the CDR1 loops of the heavy chains. Underlined amino acids correspond to key residues in the CDR1 of the light chain, while amino acids displayed in boldface correspond to the mutations used to potentiate ADCC.*

## 14. Acknowledgments

First of all, I would like to express my gratitude to Prof. Dr. Dario Neri for giving me the chance to perform my PhD under his supervision. I am very grateful for all his support, his trust and all the instructive discussions.

I also thank Prof. Dr. Cornelia Halin for all her good advice and who kindly accepted to be my co-examiner.

A special thanks belong to Prof. Dr. Burkhard Becher, Dr. Nicolas Nuñez, and Dr. Anna Rita Liuzzi for the excellent collaboration. Moreover, I would like to thank Prof. Markus Manz and Dr. Renier Myburgh for their help and support. Additionally, I would like to thank Laura Volta and Patrizia Murer for the good coworking. More than that, I would like to thank Francesco Rinaldi, Jacqueline Mock and Simon Eitzinger. I had the privilege to supervise them and they have contributed to this thesis. I would like to thank Dr. Mattia Matasci for his help with the generation of the stable CD123 cell line. Many thanks go also to all the former and current members of the group for the great atmosphere and their support. A special thanks goes to Dr. Anja Schmid, for all our discussions and the good time we had within and outside the lab.

Finally, my deepest thanks go to my parents for their unconditional love and support. I am especially thankful for the all the time that they were looking after my daughter when I was preparing the thesis. I like to thank my husband, Simon, for all his love and encouragement. Also, I thank my sister for being the best sister in the world. Without the support of my family, this would have never been possible. Also, my thanks go to my beautiful little daughter, who supported me with her wonderful first smiles while writing the thesis.

## 15. Curriculum vitae

### Personal Information

Name: Cornelia Hutmacher-Berndt  
Adress: Dammstrasse 8, 8610 Uster  
Mobile Phone: +41 76 331 88 17  
E-Mail: cornelia.hutmacher@pharma.ethz.ch  
Date of Birth: 12.03.1991  
Nationality: Swiss

### Education

2015- present PhD student in the group of Prof. Dr. Dario Neri, Institute of Pharmaceutical Sciences, Departement of Chemistry and Applied Biosciences, ETH Zurich  
2018-2019 Maternity leave  
2015 Swiss Federal Pharmacist Exam  
2013- 2015 MSc Pharmaceutical Sciences ETH Zurich  
2010- 2013 BSc Pharmaceutical Sciences ETH Zurich  
2003- 2009 Grammar School Zürcher Oberland, specialised in classical languages (Greek and Latin), Wetzikon

### Work Experience

2015- 2019 PhD student in the group of Prof. Dr. Dario Neri, Institute of Pharmaceutical Sciences, Department of Chemistry and Applied Biosciences, ETH Zurich  
Thesis: Innovative strategies for the immunotherapy of liquid and solid tumors  
2015- 2019 Pharmacist at Bahnhofapotheke P.Bolliger AG, Schaffhausen  
2014- 2019 Pharmacist in training at at Bahnhofapotheke P.Bolliger AG, Schaffhausen

2014 Master thesis in the group of Prof. Dr. Michael Detmar, Institute of Pharmaceutical Sciences, Department of Chemistry and Applied Biosciences, ETH Zurich  
Thesis: The role of the lymphatic endothelium in anti-tumor immune responses

2009- 2010 Internship at the Interdisciplinary Surgery and Maternité Station in the clinic Hirslanden, Zurich, Switzerland

### **Extracurricular activities**

2018 Poster presentation at the American Association for Cancer Research Annual Meeting 2018, Chicago, IL. Philadelphia  
Title: Targeted Interleukin 2 and synergy with immune check-point inhibitors

### **Languages**

German Native speaker  
English Fluent in spoken and written (Certificate in advanced English)  
French Good in spoken and written

### **Awards**

2013- 2015 Winner of the ETH Excellence Scholarship and Opportunity Award – Novartis Scholarship for the degree program Master of Science in Pharmaceutical Sciences 2013-2015 at the ETH Zurich

### **Publications**

Hutmacher and Neri, Targeted Interleukin 2 and synergy with immune check-point inhibitors [abstract]; *Cancer Res*, 2018, 78(13 Suppl): Abstract nr 3811

Hutmacher and Nuñez et al., Targeted Delivery of IL2 to the Tumor Stroma Potentiates the Action of Immune Checkpoint Inhibitors by Preferential Activation of NK and CD8+ T Cells, *Cancer Immunol Res*, 2019, *In Press*



Hutmacher et al., Development of a novel fully-human anti-CD123 antibody to target acute myeloid leukemia, *submitted*

Hutmacher and Neri, Antibody-cytokine fusion proteins: Biopharmaceuticals with immunomodulatory properties for cancer therapy, *Advanced Drug Delivery Reviews*, 2018, *in press*

Dieterich C., Ikenberg K., Cetintas T., Kapaklikaya K., Hutmacher C., and Detmar M., Tumor-Associated Lymphatic Vessels Upregulate PDL1 to Inhibit T-Cell Activation, *Frontiers in Immunology*, 2017, 8, doi: <https://doi.org/10.3389/fimmu.2017.00066>